

DOTTORATO DI RICERCA IN INGEGNERIA DELL' INFORMAZIONE E
DELLA COMUNICAZIONE

DIPARTIMENTO DI SCIENZA E TECNICA DELL INFORMAZIONE E
DELLA COMUNICAZIONE – INFOCOM-

UNIVERSITA' DI ROMA "SAPIENZA"

MODELING AND SYNTHESIS OF CIRCUITS
ANALOGUE TO GENERALIZED ONDULATORY
PHENOMENA GIROSCOPICALLY COUPLED

MAURIZIO PASCHERO

DOCENTI ESAMINATORI:

PROF. P. BURRASCANO (Università di Perugia)
PROF. S. GIORDANO (Università di Pisa)
PROF. F. SANTUCCI (Università dell'Aquila)

COORDINATORE DEL DOTTORATO : PROF. S. BARBAROSSA
(Università degli studi di Roma "Sapienza")

TUTORE SCIENTIFICO : PROF. F.M. FRATTALE MASCIOLI
(Università degli studi di Roma "Sapienza")

“Lo scienziato non studia la Natura perché è utile farlo, la studia perché ne trae diletto, e ne trae diletto perché la Natura é bella. Se non fosse bella non varrebbe la pena di conoscerla, e se non valesse la pena di conoscere la Natura, la vita non sarebbe degna di essere vissuta”

*Henri Poincaré (1854-1912)
Ingegnere minerario e illustre matematico*

Acknowledgements

The most of the people I'm going to acknowledge in this note are Italians so I finally chose to write it in my first language that probably allow me to express my feeling in a more appropriate way.

Prima di tutto desidero ringraziare la mia famiglia per avermi sempre sostenuto nelle mie scelte. Dedico questo lavoro alla memoria di mio padre che probabilmente oggi sarebbe felice e stupito di vedere che quel ragazzo discolo e svogliato che ero qualche anno fa ha deciso di avventurarsi in questa difficile e meravigliosa esperienza che è la ricerca. Gli sarò sempre grato per avermi insegnato in rispetto per gli altri e la tenacia nel perseguire gli obiettivi.

Voglio ringraziare il Prof. F.M. Frattale Mascioli per avermi sempre dato la possibilità di esprimere le mie idee umane e scientifiche in piena autonomia, per avermi dato l'opportunità di confrontarmi con la didattica e infine per avermi concesso la serenità necessaria a scrivere questo lavoro proteggendomi negli ultimi mesi da ogni altra incombenza.

Desidero ricordare i colleghi e amici Antonello Rizzi, Francesco Barcellona, Gabriele Allegria, Gianluca Grisanti e Guido Del Vescovo che con la loro energica vitalità hanno reso le mie giornate a INFOCOM estremamente piacevoli. Un ringraziamento speciale va a Massimo Panella il quale mi ha dimostrato continua stima e amicizia offrendomi sempre il suo valido aiuto sia in ambito accademico che umano.

Il ringraziamento più sincero e sentito va a Francesco dell'Isola e Maurizio Porfiri per l'entusiasmo per la ricerca che mi hanno trasmesso in quegli indimenticabili pomeriggi dell'autunno del 2000. Non c'è dubbio che questo mio lavoro sia in qualche modo figlio di quell'entusiasmo.

Desidero inoltre ringraziare Andrea Campus, Corrado Maurini, Davide Spinello, Pier Mario Pollina e Silvio Alessandrini con i quali ho avuto il piacere di dividere parte del mio cammino. Ogni discussione con ognuno di loro è sempre stata (e spero sarà) fonte di nuove idee stimolanti.

Desidero inoltre ringraziare il Prof. Giuseppe Martinelli per la prontezza con la quale ha chiarito alcuni miei dubbi nati durante la stesura di questo lavoro, Mauro Vincenti per la paziente ricerca bibliografica che ho utilizzato per la stesura del sesto capitolo, Il Prof. Giovanni Jacovitti, il Prof. Gaetano Scarano e il Prof. Raffaele Parisi per i loro consigli e i loro suggerimenti tesi al miglioramento della fruibilità di questo lavoro.

Trovo infine doveroso menzionare l'elevata qualità dei corsi che ho avuto la fortuna di seguire presso il dipartimento "Engineering Science and Mechanics" del "Virginia Polytechnic Institute and State University", devo a quei corsi una considerevole parte della mia preparazione.

Alla luce di ciò che è successo pochi giorni fa qui a Blacksburg mi sembra doveroso ringraziare tutti gli amici e parenti che mi hanno chiamato....mi avete quasi fuso il computer....grazie per il vostro affetto.

Contents

1	Introduction	8
1.1	Why this work?	8
1.2	Overview	10
2	Derivation of a circuit analogue of a generalized undulatory phenomena	13
2.1	Introduction	13
2.2	Discrete formulation	14
2.3	Derivation of a generalized analogue lumped circuit	16
2.3.1	Blackbox approach	16
2.3.2	Constitutive relation	17
2.3.3	Impedance and admittance	22
2.3.4	Same example of components identification	23
2.3.5	One node to one port mapping	25
2.3.6	A variational approach	34
2.3.7	one node to n-port mapping	36
2.4	External characterization of the network	53
2.4.1	Introduction	53
2.4.2	One node to n ports mapping	53
2.4.3	One node to one port mapping	59
3	External characterization of a transducer	64
3.1	Introduction	64
3.2	Unidirectional ideal transducers	65

3.2.1	Introduction	65
3.2.2	Y-configuration	65
3.2.3	Z-configuration	66
3.2.4	G-configuration	66
3.2.5	H-Configuration	67
3.3	Bidirectional ideal transducers	67
3.3.1	Introduction	67
3.3.2	Y-configuration	68
3.3.3	Z-configuration	68
3.3.4	G-configuration	69
3.3.5	H-Configuration	70
3.4	Bidirectional real transducers	70
3.4.1	Introduction	70
3.4.2	Y-configuration	71
3.4.3	Z-configuration	71
3.4.4	G-configuration	72
3.4.5	H-Configuration	72
3.5	Constitutive symmetry of real transducers	73
3.5.1	Introduction	73
3.5.2	Y-symmetrization	73
3.5.3	Z-symmetrization	74
3.5.4	G-symmetrization	74
3.5.5	H-symmetrization	75
3.6	Examples	76
3.6.1	A pinned rigid link	76
3.6.2	Balanced force to couple transducers	78
3.6.3	Piezoelectric transducers	79
4	Derivation of some applications.	87
4.1	Introduction	87
4.2	Derivation of the zero order networks.	87

4.3	Some example of zero order networks	88
4.3.1	Mass-spring oscillator.	88
4.3.2	Torsional pendulum.	90
4.4	Derivation of the second order networks.	93
4.4.1	One node to n ports synthesis	94
4.4.2	One node to one port synthesis	99
4.5	An example of second order network	103
4.5.1	Extensional vibration on a beam.	103
4.5.2	One node to n port mapping	105
4.5.3	One node to one port mapping	106
4.6	Derivation of the fourth order networks.	107
4.6.1	One node to n port synthesis	108
4.6.2	One node to one port synthesis	116
4.7	An example of fourth order network	122
4.7.1	The Euler beam.	122
4.7.2	One node to n port mapping	123
4.7.3	One node to one port mapping	126
5	Hybrid systems gyroscopically coupled	129
5.1	Introduction	129
5.2	One dimensional coupling	130
5.2.1	Introduction	130
5.2.2	The case of ideal transducers	130
5.2.3	Uncoupled system VS gyroscopically coupled system	133
5.2.4	The case of real transducers	144
5.3	M-dimensional coupling	148
5.3.1	Introduction	148
5.3.2	The case of ideal transducers	148
5.3.3	Uncouple system VS gyroscopically Coupled system	152
5.3.4	same example of hybrid coupled system	157

6	RC Active Synthesis of the analogue electrical network	165
6.1	Introduction	165
6.2	Straight Forward synthesis	166
6.2.1	A brief overview on classical synthesis Technique	166
6.2.2	RC-Active synthesis of a gyrator inductors and a NIC.	169
6.2.3	Some new strategies of synthesis	174
7	Concluding remarks	187
7.1	Conclusions	187
7.2	Recommendations for future works	188

Chapter 1

Introduction

1.1 Why this work?

In the recent years there was an increasing interest in smart structures. This general definition include all those systems able to detect their own state and to change it in order to satisfy some given specifications. A large number of devices characterized by a huge set of physical phenomena can be classified as smart structure. A typical example, widely studied in the literature in the last few years, is represented by those systems able to automatically damp vibration phenomena acting on them. The majoriry of those systems are realized by using piezoelectric transducers coupled with suitable electric network.[Lesieutre (1998)]. During the past years a large number of solution has been proposed in this direction. Among them we'd like to highlight the strategy used in the piezoelectromechanical (PEM) structures, where a given structure is connected to an electrical network through an array of piezoelectric transducers. It is required to this network to achieving the most efficient multimodal energy transduction from the given structure to the electrical network itself. In [Vidoli et al.(2000)], there was heuristically proven that in order to guarantee the maximum energy transfer between the given structure and the electrical network they must be governed by the same differential operator. This requirement can be expressed more precisely by saying that the electrical network must be the analogue of the hosting structure, meaning that the two must share the same spectral properties and, cosequently, their evolutions must be governed by the beam equation. The problem of design a circuit analogue to an Euler beam has been initially solved in [Alessandrioni et al. (2002)]

where it has been proposed a circuital network able to impose the same differential equation governing the evolution of the beam, between the adjacent nodes of the circuit. By the way the problem of finding suitable termination analogue to a general boundary conditions (BC) has been only partially addressed. A different solution which take into account for the most general BC has been proposed in [Andreas et al. (2004)] and [Porfiri et al. (2004)], however those works don't offer a physical interpretation of each components of the circuit but stands same relations that must be fulfilled among their nominal values. The basic feature of this approach is in the possibility to establish a multimodal resonance between the hosting beam and electrical circuit connected to it. This property can be summarized by saying that, using this methodology, it is possible to realize a complete energy transfer from the hosting beam to the electrical network.

The basic idea of the present work can be summarized in the following question-It is possible to apply this methodology to a larger number of systems?- More precisely :- it is possible to design a circuit able to absorb the whole energy of a given system connected to it trough an array of transducers?- It is quite easy to understand that this kind of systems could be fruitfully used for a large set of applications. Among them we had cited the vibration damping but we can imaging application like the harvesting the insonorizzation or even application more oriented to the elaborations as the damage detection. By the way the main purpose of this work is the development of a theory able to describe those systems and to give a precise methodology in order to design a circuit analogue to a given physical system rather than the investigation of a particular application.

In this work we will show how it is possible generalize the result obtained in multimodal vibration damping to a huge class of problems described by means of a single partial differential equation (PDE) depending on an integer index n . This PDE is given below.

$$K \frac{\partial^n F(x, t)}{\partial x^n} + (-1)^n \rho \frac{\partial^2 F(x, t)}{\partial x^2} \quad (1.1)$$

where $F(x, t)$ is a generic scalar field defined over the domain $[0, L] \times \mathbb{R}^+$, where the scalar $x \in [0, L]$ represents the space variable and it is measured in $[m]$ and scalar $t \in \mathbb{R}^+$ represents the time variable and it is measured in $[s]$. K and ρ are generic scalar quantities whose ratio

K/ρ must assume the physical dimensions of $[m^{2n}/s^2]$. Looking at eq. (1.1) it can be easily realized that it assumes a well known form for some special values of n . For example when $n = 0$ it becomes, for a specified values of the space variable x , the well known equation of an harmonic oscillator able to describe a huge number of problem once the parameters F, K and ρ assume an actual meaning different, in general, for each particular system. Moreover the ratio ρ/K measured in $[s^{-2}]$ assumes the meaning of the natural oscillation frequency of the system. Another class of problems can be obtained by choosing $n = 1$, in this case eq. (1.1) becomes the well known wave equation able to describe a very large number of physical phenomena once the parameters F, K and ρ assume an actual meaning different, in general, for each particular application. Moreover the ratio ρ/K measured in $[m^2/s^{-2}]$ assumes the meaning of the velocity of propagation of the wave. Similarly for $n = 2$ eq. (1.1) becomes after a suitable specification of the parameters F, K and ρ the well known Elastica equation describing the transversal vibration on a shear undeformable beam. All the given examples are related with an oscillating behavior so that we will call the whole set of physical phenomena described by eq. (1.1) generalized ondulatory phenomena.

In this work will be described how it is possible to design a circuit analogue to a generic system whose evolution is described by eq. (1.1) and how it is possible to connect it to the given physical system through an array of transducers in order to absorb from it the energy associate with the oscillations. The complete system obtained in this way will include the given physical system the array of transducer and the analogue circuit and will be called hybrid coupled system. This hybrid system will be described in this work by means of a generalized version of the notions used by the classical circuit theory. This methodology of analysis will result in an algebraical description of the system very suitable for digital elaborations purpose.

1.2 Overview

In this section we will give some information about the structure of this work. The whole work is constituted by seven chapters, being this introduction the first of them and the last one a report of the conclusion and an opportunity to list some possible ideas for future work on this subject. The remaining five chapters must be splitted in two subcategories. The first of them,

including chapters two to five, must to be considered the main core of this work and include the modelling of some circuits analogue of eq. (1.1) (chapter 2 and 4), the circuital modelling of the transducers (chapter 3) and the circuital model of a whole hybrid gyroscopically coupled systems (chapter 5). The second subcategory including the sixth chapter only is devoted to the RC-active synthesis of the electric circuit analogue of eq. (1.1).

More precisely this work has the following structure:

Chapter 1: This introduction.

Chapter 2: First of all it is performed a discretization of the spatial domain and it is defined over it a finite difference equation approximating eq. (1.1). Then it is given a brief recall on a generalized version of some basic notion of the classical circuit theory in order to define the notion of lumped circuit in a general contest. This recall wants to point out on the fact that the analogue circuit derived has no be restricted to the electrical case only. A first synthesis technique, based on the algebrical manipulation of the finite difference equation, it is given. It is put in evidence as this simple technique is not able to give any information about the circuital implementation of the BC prescribed at the border of the domain. A variational approach it is used in order to derive the BCs consistent with eq. (1.1). A more sophisticated synthesis technique, based on the structure of those BCs it is given. This technique has to be considered general and it seems reasonable to successfully apply it to the circuital synthesis of different differential operator. A new technique devoted to the design of suitable termination networks able to reproduce the most general BCs for the first kind of synthesis is introduced. This new technique is based on the external characterization of the system.

Chapter 3: The circuital modelling of a transducer is treated. Based on the general circuital notions given in the second chapter the generic transducers is thought as an hybrid two ports network, where the word hybrid want to describe the different physical nature of the two port. The notion of monodirectional ideal transducers and bidirectional ideal transducers are introduced. A bidirectional real transducers is modeled as an ideal bidirectional transducers having some parasitic constitutive effect on each port. Finally some examples is proposed. In this contest it is given a circuital model of an extensional a bending and

a torsional piezoelectric transducer.

Chapter 4: Here we apply the theory developed in the second chapter in order to derive some examples. We point out on the fact that the derivation of a circuit analogue of a generalized oscillatory phenomena is independent from the actual meaning of the parameters F, K and ρ that effect only the nominal value on the components and the physical interpretation of the quantities defining the circuit. This chapter has been positioned after the transducers modelling in order to highlight the opportunity to recognize in a system of order $2n$ (for $n \geq 2$) $n - 1$ arrays of ideal transducers embedded in the system itself.

Chapter 5: Here we give a precise definition of hybrid gyroscopically coupled system. First of all we define a one dimensional hybrid coupled system and we study its properties in both the frequency and the time domain showing how it is possible to completely transfer the energy from a part of the hybrid system to the other part. Then we study how the complications rising from the use of a real transducer can be solved. Then those results are extended to the M dimensional case. Finally it is given an example for systems of order zero two and four.

Chapter 6: First of all we give a brief overview on the classical solution historically proposed in the circuit theory in order to design synthetic floating positive and negative inductor negative impedance and ideal transformers. This research is restricted to the use of operational amplifiers (OPA) capacitors and resistor. Based on those notions it is given a valuation on the number of OPAs needed to design an analogue circuit of order $2n$. Some new strategy of synthesis it is proposed. It is shown how it is possible to realize an analogue circuit of order $2n$ by using two OPAs only for each module. Finally it is proposed a stability analysis of those circuits when the ideal OPAs are replaced with a more realistic model including some not ideal features of those components.

Chapter 7: Here we get the conclusion of our work and give some possible ideas for future work on this subject.

Chapter 2

Derivation of a circuit analogue of a generalized ondulatory phenomena

2.1 Introduction

In the previous chapter we have introduced a general PDE able to describe a large number of problems by giving an actual meaning to some parameters. In this chapter we will introduce a discretization of the spacial domain in order to derive a finite difference equation approximating the differential operator. Then we will introduce a generalized version of some basic notions of the circuit theory, those notions will be used to design a lumped circuit analogue to the discrete differential operator governing a generalized ondulatory phenomena. First of all we will describe a synthesis technique based on the algebraical manipulation of differential operator. Then we will put in evidence the lack of a clear methodology to impose the most general BC at the edge of the domain for this simple kind of synthesis. In order to overpass this problem we will introduce a more sophisticated synthesis technique. Based on this novel technique we will derive a methodology to impose the most general BC for the first synthesis technique too. It should be noted that this sophisticated synthesis technique is general and can be applied in order to obtain the synthesis of different differential operators.

2.2 Discrete formulation

As we have said before, we want to derive a lumped circuit analogue of the PDE formulated by eq. (1.1). The first step we need to walk is to project the continuous space domain $[0, L]$ in a finite dimensional space. So it is needed to introduce a mesh of M nodes uniformly separated by an incremental step $\Delta = \frac{L}{M}$ approximating the spacial domain $[0..L]$.

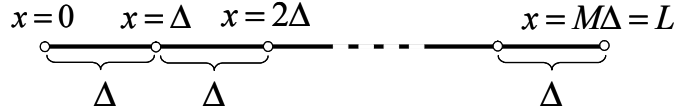


Figure 2-1: Discretization of the spacial domain.

Once we have introduced the mesh shown in fig. (2-1) the scalar field $F(x, t)$ will be described by its samples $F(0, t), F(\Delta, t), \dots, F(M\Delta, t)$. More precisely we want to derive a lumped circuit governed by the following equation¹:

$$KF_k^{(2n)}(t) + (-1)^n \rho \frac{d^2 F_k(t)}{dt^2} = 0 \tag{2.1}$$

Now in order to express the discrete space derivatives of the scalar field $F(x, t)$ we need to introduce a finite difference scheme. Many choices can be made, however in order to obtain a symmetric discrete equation it is useful to introduce a centered finite difference scheme as shown in fig.(2-2).

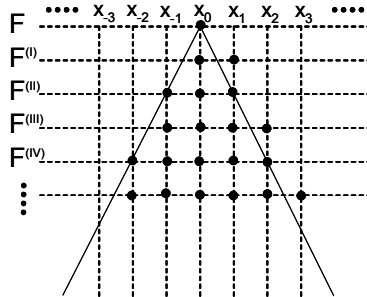


Figure 2-2: Cenetered finite difference scheme.

¹in this work the expression $\square_k^{(j)}$ has the meaning of a discrete version of the quantity $\frac{\partial^j \square}{\partial x^j} \Big|_{x=k\Delta}$. Moreover the expressions $\square_k^{(0)}$ and \square_k must be thought as equivalent.

Looking at fig. (2-2) it is clear that we need to add a new sample for each order of derivation so that the derivative or order zero (i.e. a sample of the function it self) at the k^{th} node is defined by means of a single sample, the discrete derivative of order one is defined by means of a linear combination of two samples and so on. In general the derivative of order j at a generic node k will be a linear combination of $j + 1$ samples centered around the k^{th} node. The weight of this linear combination can be found by using the simple rule offered by the Tartaglia triangle², with alternate minus signs. This scheme is shown below:

$$\begin{array}{ccccccc}
 & & & & & & 1 \\
 & & & & & & 1 & -1 \\
 & & & & & & 1 & -2 & 1 \\
 & & & & & & 1 & -3 & 3 & -1 \\
 & & & & & & 1 & -4 & 6 & -4 & 1 \\
 & & & & & & & & & & \vdots
 \end{array}$$

a general expression of the m^{th} discrete spatial derivative at $x = x_k$ can be derived combining the Tartaglia scheme with the one shown in fig. (2-2). This rule is given by the following equation:

$$F_k^{(j)}(t) = \frac{1}{\Delta^j} \sum_{i=-\lceil \frac{j}{2} \rceil}^{\lfloor \frac{j}{2} \rfloor} (-1)^{(i+\lceil \frac{j}{2} \rceil)} \binom{j}{i+\lceil \frac{j}{2} \rceil} F_{k+i}(t) \quad \text{where } j > 0 \quad (2.2)$$

substituting the rule formulated by eq.(2.2) into eq. (2.1) we obtain:

$$\sum_{i=-n}^n (-1)^{i+n} \binom{2n}{i+n} F_{k+i}(t) + (-1)^n \beta^{2n} \frac{d^2 F_k(t)}{dt^2} = 0 \quad (2.3)$$

where

$$\beta = \Delta \sqrt[2n]{\frac{\rho}{K}}$$

²Some author refer to this scheme as "Pascal triangle" by the way for patriotic reasons in those note we will use the Italian reference.

it can be noted that the constant β has the physical unit of $[s]^{\frac{1}{n}}$ regardless of the physical dimension of the scalar field $F(x, t)$.

2.3 Derivation of a generalized analogue lumped circuit

2.3.1 Blackbox approach

First of all we need to introduce the concept of port. A port is a set of two access points characterized by means of two quantities an intensive one we will label in the following with the symbol Π and an extensive one we will label in the following with the symbol Φ ³. It is crucial for the definition of port that the quantity Φ going into the first access point is equal and opposite to the one going out from the second access point as shown in fig (2-3 a). Moreover it is important that the pair (Φ, Π) is complementary in power i.e. the product of the physical dimension of those two quantities must have the physical dimension of a power $[W]$. For example we can chose Φ equal to the force "flowing through" the access point and Π equal to the difference of velocity between the two access points⁴. A natural generalization of this concept leads to the definition of a n ports system. There are two different ways to define a n ports system. The first possibility is to define each of the n ports by mean of a pair of access point. In this case the system will be characterized by $2n$ access points as shown in fig. (2-3 b) and will be referred as usual as balanced configuration. Alternatively we can refer the definition of each port to a common access point, in this case the system will be characterized by $n + 1$ access points and the Φ quantity flowing out from the common access point will be equal to the sum of all the Φ quantities flowing in the remaining n terminals⁵. This situation shown in fig.(2-3 c) will be referred as usual as unbalanced configuration. We'd like to remark that our definition of a n ports system does not require to the pair (Φ_i, Π_i) characterizing the i^{th} port of the system to have the same physical dimension to the pair (Φ_j, Π_j) characterizing the j^{th} port of the system.

³An intensive quantity is a physical scalar quantity whose value does not depend on the amount of the substance for which it is measured. It is the counterpart of an extensive quantity that conversely depend on the amount of the substance for which it is measured. Moreover each intensive quantity is complementary to an extensive one. i.e. the product of the phisical dimension of the two quantitties has the phisical dimension of a power $[W]$.

⁴It must be noted that the force and the velocity are vectorial quantities so they must be projected in a given direction in order to use them as extensive and intesive quantity associated with a port.

⁵In the following we will refer to an access point as a terminal or vice versa.

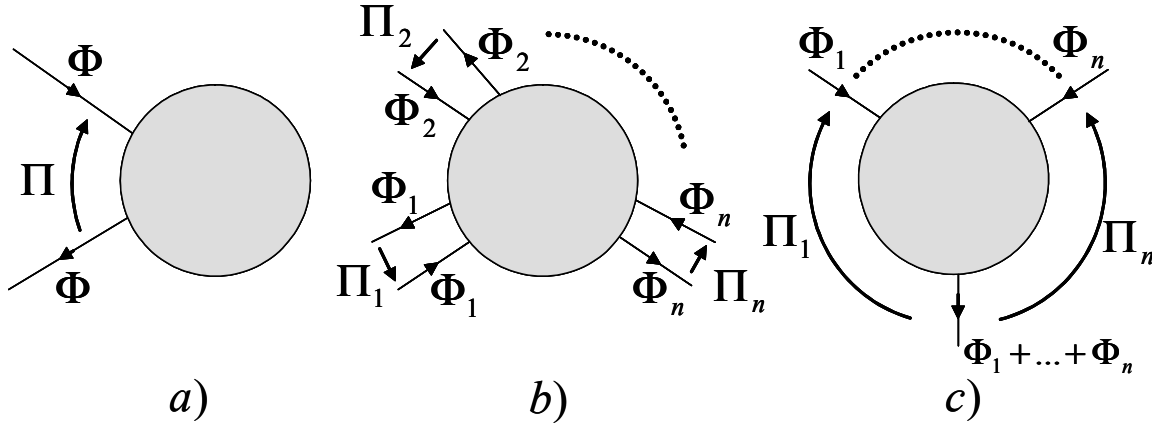


Figure 2-3: a) One port system b) Balanced n ports system c) Unbalanced n ports system.

For example we can think a two port system in which a port will be characterized by the pair (current, voltage) and the other port will be characterized by the pair (force, velocity) and so on. This freedom in the choice of the physical nature of the ports compel us to precise that if the unbalanced conflagration is used we need to assume the existence of a different reference terminal for each different nature of the ports of the system.

2.3.2 Constitutive relation

Once we have introduced the concept of port we need to give a physical relation between the two quantities related to the port, i.e. a constitutive equation. In order to give a constitutive equation we need to chose one of the variables as independent and give a rule to express the remaining dependent variable as a function of the independent one.

One port element

(α, β) element The most general linear constitutive equation it can be given [Chua (2003)] states a proportional relation between the α^{th} time derivative of the intensive quantity and the β^{th} time derivative of the extensive quantity. It is given for the linear case by the following relation:

$$\frac{d^\alpha \Pi}{dt^\alpha} = R \frac{d^\beta \Phi}{dt^\beta} \quad \text{where } \alpha, \beta \in \mathbb{N} \text{ and } R \in \mathbb{R} \quad (2.4)$$

The circuitual symbol it has been chosen to be the one proposed in [Chua (2003)]. A thick black band is needed at the bottom of the symbol in Fig. (2-4) in order to distinguish the intensive quantity index α from the extensive quantity index β .

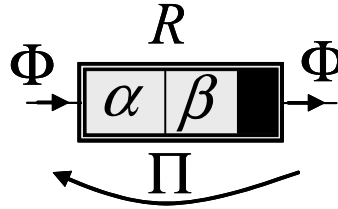


Figure 2-4: Circuitual symbol for an (α, β) element.

A different kind of constitutive equation can be obtained specifying the value of the intensive quantity and leaving the extensive quantity not specified or vice versa.

Generalized independent Π source

$$\begin{cases} \Pi = \Pi_0 \\ \Phi \text{ not specified} \end{cases}$$

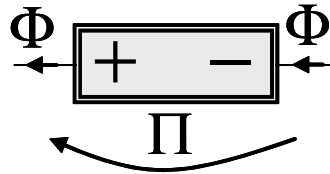


Figure 2-5: Circuitual symbol for a generalized independent Π source.

Generalized independent Φ source

$$\begin{cases} \Phi = \Phi_0 \\ \Pi \text{ not specified} \end{cases}$$

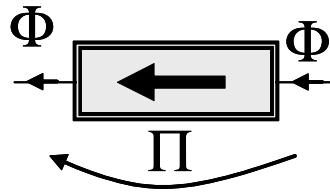


Figure 2-6: Circuitual symbol for a generalized independent Φ source.

A special kind of independent source can be obtained choosing $\Pi_0 = 0$ and $\Phi_0 = 0$

Generalized short circuit

$$\begin{cases} \Pi = 0 \\ \Phi \text{ not specified} \end{cases}$$

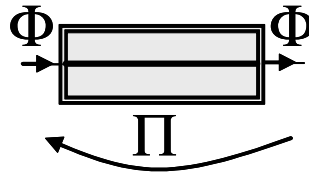


Figure 2-7: Circuitual symbol for a generalized short circuit.

Generalized open circuit

$$\begin{cases} \Phi = 0 \\ \Pi \text{ not specified} \end{cases}$$

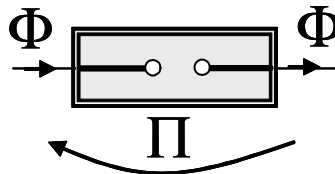


Figure 2-8: Circuitual symbol for a generalized open circuit.

Two ports element

Similarly we can define a two ports network by means of two constitutive equations relating two dependant variables to the two remaining variables chosen as independent ones.

There exist a lot of admissible constitutive equations for two ports network, by the way we will introduce only the ones that will be used in the following sections.

Generalized $\Pi C\Pi S$

$$\begin{cases} \Pi_2 = G_{\Pi\Pi}\Pi_1 \\ \Phi_1 = 0 \\ \Phi_2 \text{ not specified} \end{cases} \quad (2.5)$$

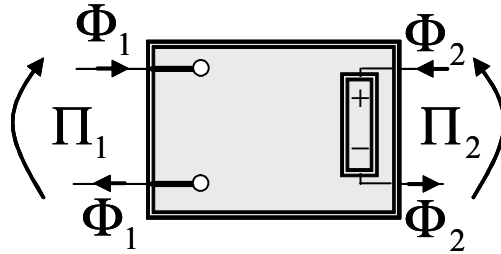


Figure 2-9: Circuitual symbol for a generalized Π controlled Π source.

Generalized $\Pi C\Phi S$

$$\begin{cases} \Phi_2 = G_{\Pi\Phi}\Pi_1 \\ \Phi_1 = 0 \\ \Pi_2 \text{ not specified} \end{cases} \quad (2.6)$$

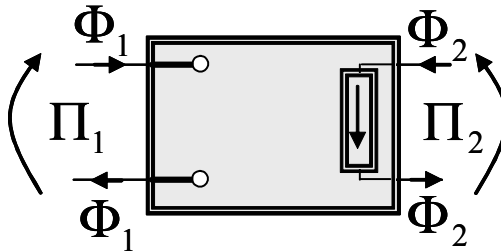


Figure 2-10: Circuitual symbol for a generalized Π controlled Φ source.

Generalized $\Phi C\Phi S$

$$\begin{cases} \Phi_2 = G_{\Phi\Phi}\Phi_1 \\ \Pi_1 = 0 \\ \Pi_2 \text{ not specified} \end{cases} \quad (2.7)$$

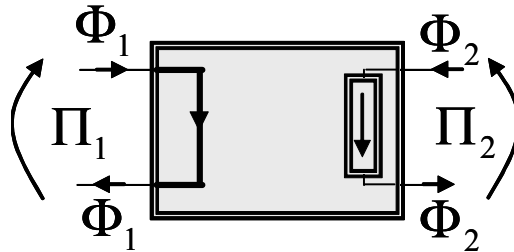


Figure 2-11: Circuit symbol for a generalized Φ controlled Φ source.

Generalized $\Phi C\Pi S$

$$\begin{cases} \Pi_2 = G_{\Phi\Pi}\Phi_1 \\ \Pi_1 = 0 \\ \Phi_2 \text{ not specified} \end{cases} \quad (2.8)$$

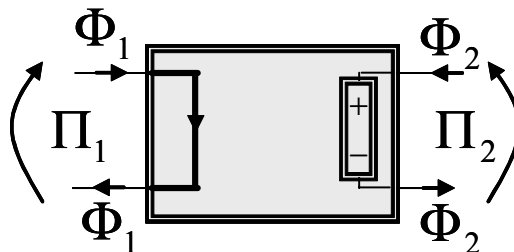


Figure 2-12: Circuit symbol for a generalized Φ controlled Π source.

Generalized lever

$$\begin{cases} \Pi_1 = n\Pi_2 \\ \Phi_1 = -\frac{1}{n}\Phi_2 \end{cases} \quad (2.9)$$

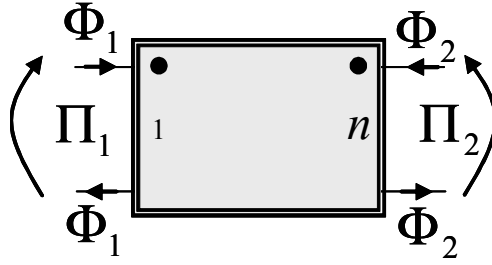


Figure 2-13: Circuitual symbol for a non inverting generalized lever.

$$\begin{cases} \Pi_1 = -n\Pi_2 \\ \Phi_1 = \frac{1}{n}\Phi_2 \end{cases} \quad (2.10)$$

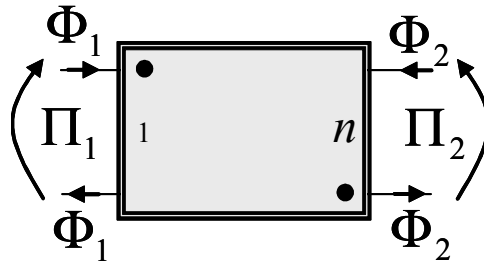


Figure 2-14: Circuitual symbol for an inverting generalized lever.

2.3.3 Impedance and admittance

We will define the impedance of a port by the ratio between the Laplace transform of the Π quantity imposed through the terminal of a port and the Laplace transform of the Φ quantity flowing through the same terminals when all the remaining ports are connected to a generalized open circuit. As usual, we will refer to this quantity with the symbol $Z(s)$ where s is the Laplace variable. Similarly we will define the admittance of a port by the ratio between the Φ quantity flowing through the terminal of a port and the Laplace transform of the Π quantity between the same terminals when all the remaining ports are connected to a generalized short

circuit. As usual we will refer to this quantity with the symbol $Y(s)$. As an example we will explicitly give the impedance $Z(s)$ and the admittance $Y(s)$ for an (α, β) element.

$$Z(s) = \frac{\Pi(s)}{\Phi(s)} = R s^{\beta-\alpha} \quad (2.11)$$

$$Y(s) = \frac{\Phi(s)}{\Pi(s)} = \frac{s^{\alpha-\beta}}{R} \quad (2.12)$$

Similarly it is possible to define a cross-impedance $Z_{ij}(s)$ (cross-admittance) as the ratio between the Laplace transform of the Π quantity read at the port i and the Laplace transform of the Φ quantity imposed at the port j when all the remaining ports are connected to a generalized open circuit (as the ratio between the Laplace transform of the Φ quantity read at the port i and the Laplace transform of the Π quantity imposed at the port j when all the remaining ports are connected to a generalized short circuit).

2.3.4 Same example of components identification

In this subsection we will introduce an identification for some of the basic elements introduced above, when the pair (Π, Φ) assume an actual meaning. In the following we will give some possible choices for the pair (Π, Φ) and we will indicate some special circuital symbols in order to identify the same component for a different choice of the pair (Π, Φ) . For example once we have fixed a given direction we can consider the projection of a force F along this direction as an extensive quantity defining a port. It is quite easy to understand that the complementary intensive quantity can be identified by the difference of the velocity v (along the same direction of the force) between the two access points defining the port. Similarly we can choose as extensive quantity the moment M along a given direction consequently we will obtain the difference of the angular velocity ω between the two access points defining the port as a complementary intensive quantity. A third possible example is obtained by choosing the Voltage V as intensive quantity and the current I as its complementary extensive quantity. In the following of this chapter we will show that the analogue circuit of eq. (2.3) can be obtained by a suitable connection of $(1, 0)$ elements, $(0, 1)$ elements and generalized lever, so, in the following table, we will give an interpretation of those components for the three possible pairs described above.

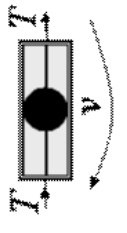
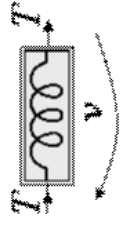
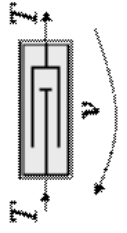
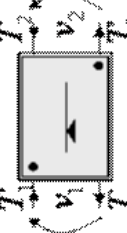
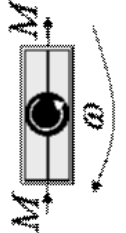
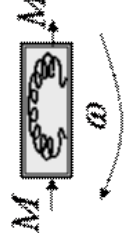
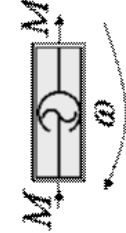
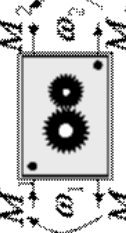
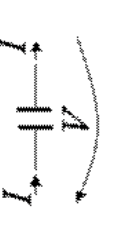
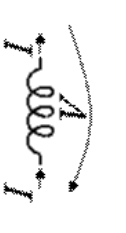

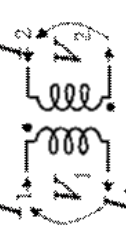
Intensive quantity	v	Force	T							
Extensive quantity	Velocity			(1,0)element	(0,1)element	(0,0)element	Generalized lever			
				 Mass	 Extensional spring	 Extensional damper	 Lever			
				 Rotational mass	 Bending spring	 Bending damper	 Gear box			
				 Capacitor	 Inductor	 Resistor	 Transformer			

Table 2-1: Interpretation of same basic component for different specification of the pair (Π, Φ) .

2.3.5 One node to one port mapping

In order to design a circuit analogue to the discrete differential problem described by eq. (2.1) we can initially associate a node of the mesh with a port of the analogue circuit as shown in fig. (2-15). The basic idea we want to implement is to obtain a relation between the quantities defining the ports of the system to be equal to the relation between the samples of the scalar field $F(x, t)$ i.e. eq. (2.1). For a reason that will appear more clear in the following sections we will take the time derivative of eq.(2.1). There exist two different ways to associate a sample with a port. We can choose to describe the samples $\frac{dF_k(t)}{dt}$ of the time derivative of the scalar field $F(x, t)$ either by means of the intensive quantity Π or by means of the extensive quantity Φ characterizing the port.

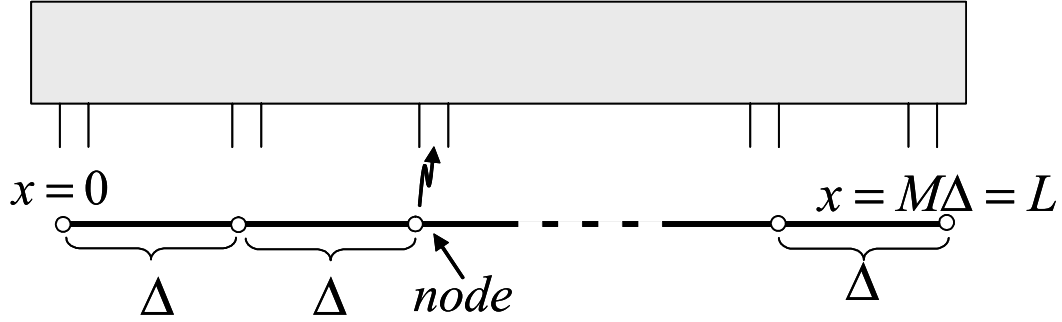


Figure 2-15: One node to one port mapping.

It should be noted that, depending on the physical nature of the scalar field $F(x, t)$ (i.e. it is intensive or extensive) just one of the two possible analogies could be coherent with the definition of port we have introduced in the previous section. This issue will be developed in the following.

$\frac{dF}{dt} \rightarrow \Pi$ **analogy** The purpose of this section is to design a circuit governed, in the Laplace domain, by the following equation (i.e. eq. (2.3) where the symbol $\frac{dF_k}{dt}$ has been replaced with the symbol Π_k representing an intensive quantity):

$$\sum_{i=-n}^n (-1)^i \binom{2n}{i+n} \frac{1}{s} \Pi_{k+i}(t) + \Delta^{2n} \frac{\rho}{K} s \Pi_k(t) = 0 \quad (2.13)$$

First of all we note that when $n = 0$ eq. (2.13) assumes the following simplified form:

$$\frac{1}{s}\Pi_k(t) + \frac{\rho}{K}s\Pi_k(t) = 0 \quad (2.14)$$

eq. (2.14) can be rearranged as follows:

$$\left(Ks^{\alpha_1-\beta_1} + \rho s^{\alpha_2-\beta_2}\right)\Pi_k(t) = 0 \quad (2.15)$$

where $\alpha_2 - \beta_2 - \alpha_1 + \beta_1 = 2$. Eq. (2.15) can be interpreted from a circuital point of view as the shunt of an (α_1, β_1) element of nominal value $1/K$ and an (α_2, β_2) element of nominal value $1/\rho$, as shown in fig. (2-16). We'd like to remark that in order to produce eq. (2.15) it is needed the interconnection one node only, by the way if we have a mesh having a larger number of nodes we can "attach" the basic circuit described above to each node.

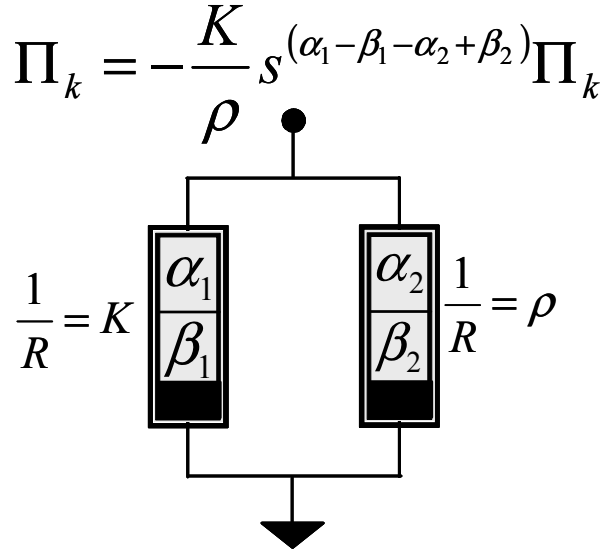


Figure 2-16: One node to one port $\frac{dF}{dt} \rightarrow \Pi$ synthesis for $n = 0$.

In order to obtain the needed circuit when $n > 0$ we can introduce a useful mathematical identity relating the coefficient of a finite difference scheme.

$$\binom{2n}{n} = - \left(\sum_{i=-n}^{-1} (-1)^i \binom{2n}{i+n} + \sum_{i=1}^n (-1)^i \binom{2n}{i+n} \right) \quad n > 0 \quad (2.16)$$

Substituting eq. (2.16) in eq. (2.13) we obtain:

$$\sum_{i=-n}^{-1} (-1)^i \binom{2n}{i+n} \frac{1}{s} (\Pi_{k+i}(t) - \Pi_k(t)) + \sum_{i=1}^n (-1)^i \binom{2n}{i+n} \frac{1}{s} (\Pi_{k+i}(t) - \Pi_k(t)) + \quad (2.17)$$

$$+ (-1)^n \Delta^{2n} \frac{\rho}{K} s \Pi_k(t) = 0$$

equation (2.17) can be rearranged in the following form:

$$\left(\sum_{\substack{i=-n \\ i \neq 0}}^n \left[-\frac{K}{\Delta^{2n-1}} (-1)^i \binom{2n}{i+n} \right] s^{\alpha_1 - \beta_1} (\Pi_k(t) - \Pi_{k+i}(t)) \right) + [\Delta \rho] s^{\alpha_2 - \beta_2} (\Pi_k(t) - 0) = 0 \quad n > 0 \quad (2.18)$$

where $\alpha_2 - \beta_2 - \alpha_1 + \beta_1 = 2$. Eq. (2.18) can be interpreted as a balance of extensive quantities flowing out from the k^{th} node. A straight forward synthesis of eq. (2.18) can be obtained by the interconnection of the k^{th} nodes of the mesh with the previous n nodes and with the subsequent n nodes by means of (α_1, β_1) elements. The nominal value of the component connecting the k^{th} node of the mesh with node $k \pm j$ is given by the coefficients of eq. 2.18. This connection produce the terms in the summation of eq. (2.18).

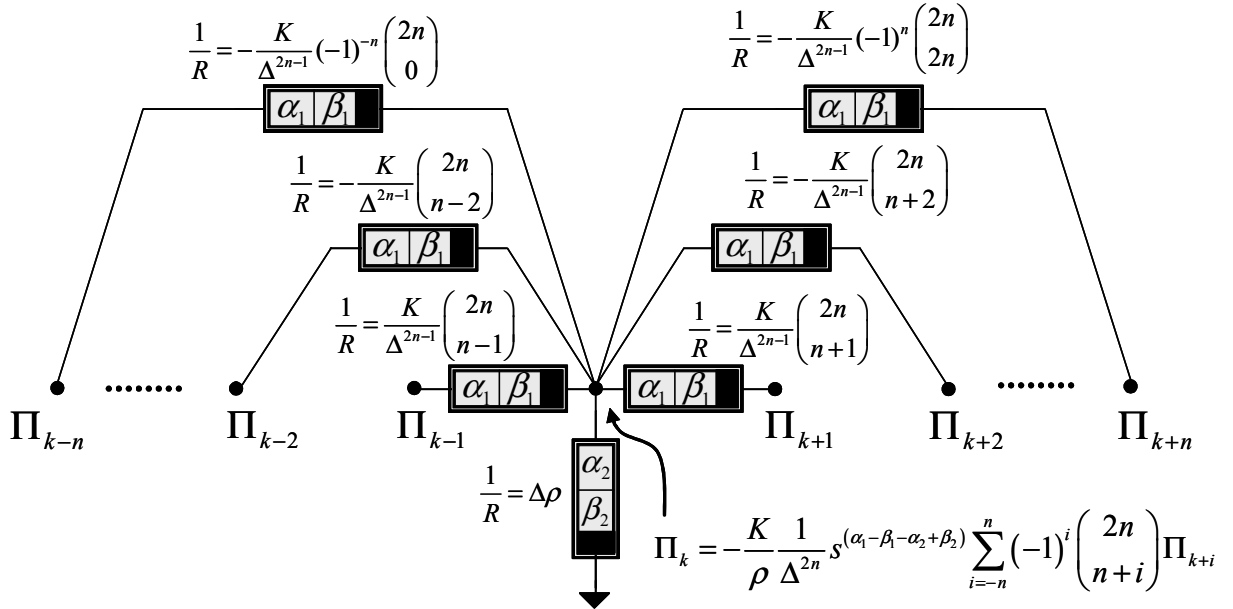


Figure 2-17: Basic circuit of the one node to one port $\frac{dF}{dt} \rightarrow \Pi$ synthesis.

The extra term out of the summation sign can be obtained by interconnecting an (α_2, β_2) element of nominal value $1/\Delta\rho$ between the k^{th} node and the reference node. The basic circuitual scheme described above is shown in fig. (2-17) The complete circuitual scheme can be obtained by "attaching" the basic circuit shown in fig. (2-17) to each node taking care of avoiding components doubling. This procedure will result in the circuit shown in fig. (2-18) for the case of $n = 6$. It should be noted that this circuit assumes the form of the network proposed in [Alessandroni et al. (2002)] when $n = 2, \alpha_2 = 1, \beta_2 = 0, \alpha_1 = 0, \beta_1 = 1$ and $(\Pi, \Phi) = (V, I)$.

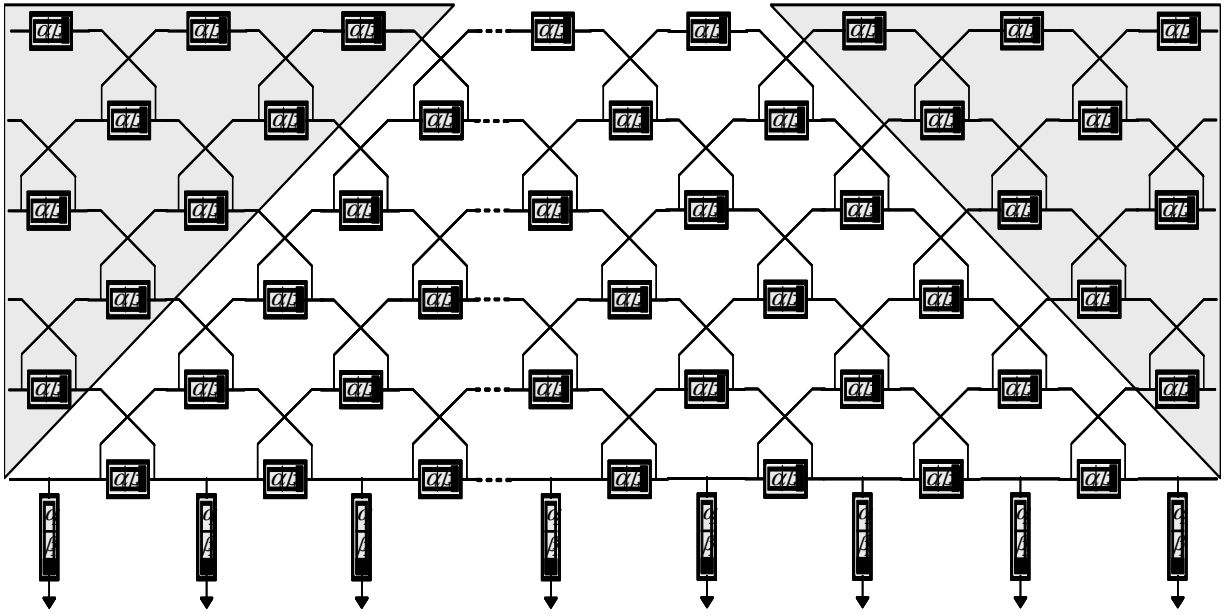


Figure 2-18: Complete circuit for the one node to one port $\frac{dF}{dt} \rightarrow \Pi$ synthesis for $n = 6$.

In the figure are drawn two gray triangles. The components inside those triangles don't belong to the circuit, by the way they are been plotted in order to highlight the structure of the network. More precisely we will see in the subsequent section how it is possible to substitute the subnetwork in the gray triangle with a suitable termination subnetwork taking in count for the most general BC. The circuit shown in fig.(2-18) can be tough as the chain connection of a proper number of the 12 ports ($2n$ for the general case) basic section shown in fig. (2-19). In this figure is put in evidence the opportunity to divide the not symmetric basic section in the chain connection of two symmetric subnetworks; the first one containing an (α_2, β_2) element and all (α_1, β_1) elements with negative nominal value and the other one containing all the (α_1, β_1)

elements with positive nominal value.

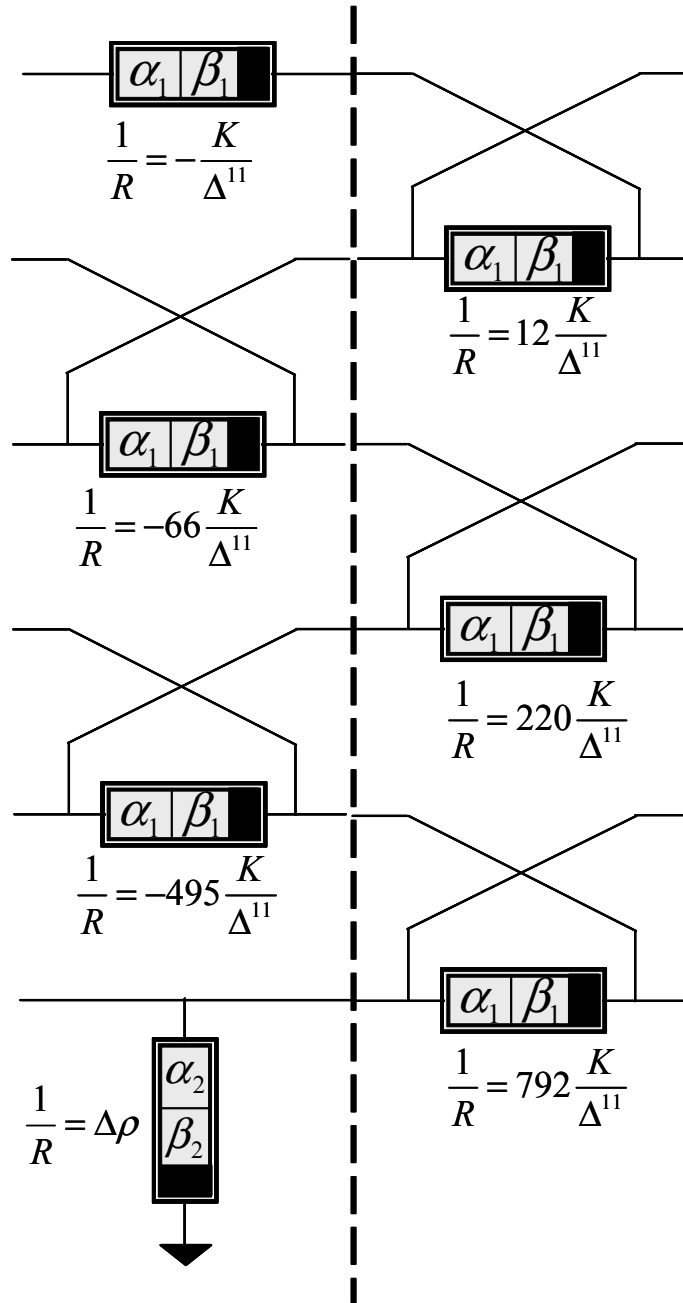


Figure 2-19: Basic section for the one node to one port $\frac{dF}{dt} \rightarrow \Pi$ synthesis.

It should be noted that using this simple synthesis technique it is needed to use components of negative values, moreover it is not clear how the circuit should be modified in order to take care of the BC present at the edge of the spatial domain. In the following section it will be

shown how this problem can be overpassed.

$\frac{dF}{dt} \rightarrow \Phi$ **analogy** The purpose of this section is to design a circuit governed, in the Laplace domain, by the following equation (i.e. eq. (2.1) where the symbol $\frac{dF_k}{dt}$ is replaced with the symbol Φ_k representing an extensive quantity):

$$\sum_{i=-n}^n (-1)^i \binom{2n}{i+n} \frac{1}{s} \Phi_{k+i}(t) + \Delta^{2n} \frac{\rho}{K} s \Phi_k(t) = 0 \quad (2.19)$$

First of all we note that when $n = 0$ eq. (2.13) assume the following simplified form:

$$\frac{1}{s} \Phi_k(t) + \frac{\rho}{K} s \Phi_k(t) = 0 \quad (2.20)$$

eq. (2.20) can be rearranged as follows:

$$K s^{\beta_2 - \alpha_2} \Phi_k(t) + \rho s^{\beta_1 - \alpha_1} \Phi_k(t) = 0 \quad (2.21)$$

where $\alpha_2 - \beta_2 - \alpha_1 + \beta_1 = 2$. Eq. (2.21) can be interpreted from a circuital point of view as the series of an (α_1, β_1) element of nominal value ρ and an (α_2, β_2) element of nominal value K , as shown in fig. (2-20). We'd like to remark that in order to produce eq. (2.21) it is needed to interconnect one loop only, by the way if we have a mesh having a larger number of nodes we can "attach" the basic circuit to each node.

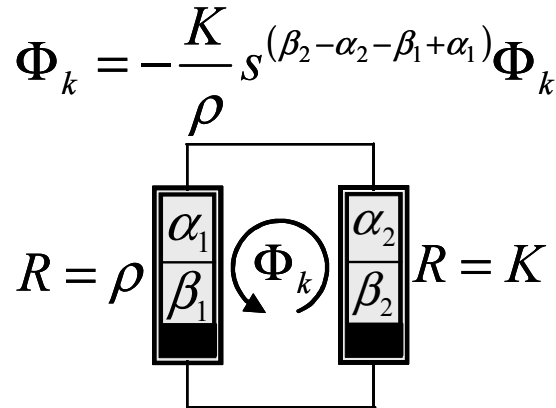


Figure 2-20: One node to one port $\frac{dF}{dt} \rightarrow \Phi$ synthesis for $n = 0$.

In order to design a circuit for $n > 0$ we can use the identity (2.16). Substituting eq. (2.19) in eq. (2.16) and rearranging we obtain:

$$\left(\sum_{\substack{i=-n \\ i \neq 0}}^n \left[-\frac{K}{\Delta^{2n-1}} (-1)^i \binom{2n}{i+n} \right] s^{\beta_2 - \alpha_2} (\Phi_k(t) - \Phi_{k+i}(t)) \right) + [\Delta\rho] s^{\beta_1 - \alpha_1} \Phi_k(t) = 0 \quad n > 0 \quad (2.22)$$

where $\alpha_2 - \beta_2 - \alpha_1 + \beta_1 = 2$. Eq. (2.22) can be interpreted as a balance of intensive quantities of a loop k . having $2n + 1$ edges. A straight forward synthesis of eq. (2.22) can be obtained by the interconnection of $2n$ (α_2, β_2) elements in common between the loop associated with the k^{th} sample and loops associated with the previous and the subsequent n samples. The nominal value of the component in common by the loop k and the loop $k \pm j$ is given by the coefficients of eq. 2.22. This connection produce the terms in the summation of eq. (2.22). The extra term out of the summation sign can be obtained by closing the loop with an (α_1, β_1) element of nominal value $\Delta\rho$. The basic circuit described above is shown in figure (2-21). The complete circuital scheme can be obtained by "attaching" the network shown in fig.(2-21) to each loop taking care of avoiding complements doubling. This procedure will result in a very complex structure that can not be represented by means of a planar graph for the general case. Consequently the circuit must be designed for each value of n . A nice inspiration can be obtained by the work of M. C. Escher on the plane partition with polygonal tiles.[Escher (2001)],[Schattschneider et al. (1990)]. For example the famous litograph named "Reptiles" shown in fig. (2-22 a)) can give us a nice idea for deriving the topological graph for $n = 3$. In this figure the reptiles going out from one side of the picture and going in from the opposite side suggests the possibility to connect two edges belonging to two different loops with a virtual tape constraining those two edges to be the same one, as remarked in fig (2-22 b)).

where the extensive quantities $\Phi_0, \dots, \Phi_{\pm 5}$ flowing in the heptagon loop are related with the samples of the scalar field $F(x, t)$. The two edges joined by the same tape must be thought as the same edge. In order to make the picture more clear all the tapes except two are been dashed.

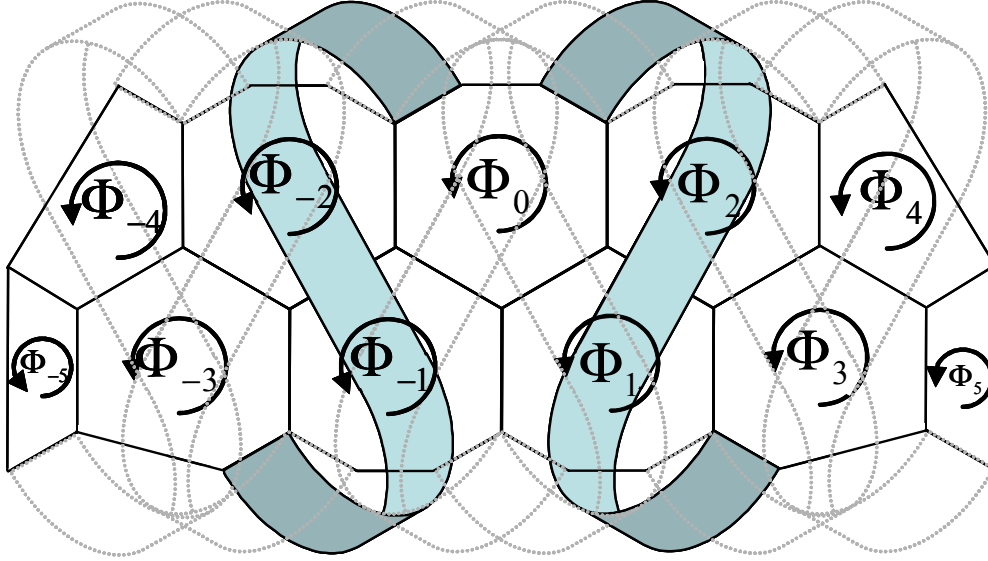


Figure 2-23: Topological graph of the one node to one port $\frac{dF}{dt} \rightarrow \Phi$ synthesis for $n = 3$ and $M = 11$.

It should be noted again that this kind of synthesis requires the use of components having negative nominal value, moreover it is not clear how to modify the network in order to produce the analogue of the most general BC at the edge of the spatial domain.

Boundary condition

As we have observed previously the synthesis technique described in the previous subsections has the advantage to be easily obtained from the algebraic manipulation of equation (2.1). However on the reverse side of the coin we had put in evidence that it is not clear how to modify the network in order to emulate the most general BC of the actual system. As known from the PDE theory the BCs are part and parcel of the spectral properties of a differential operator so their study is crucial in order to realize an incisive coupling between two systems. In the following sub section we will show how this problem can be completely solved developing a more sophisticated synthesis technique based on a variational approach.

2.3.6 A variational approach

In this section we will show how, using a variational approach, it is possible to associate to the PDE (2.1) the consistent set of BCs. Let $F(x, t)$ be a scalar field defined over the domain $x \in [0, L]$ and $t \in \mathbb{R}^+$, where the scalar x represents the space variable and it is measured in $[m]$ and scalar t represents the time variable and it is measured in $[s]$. In order to derive the PDE and the consistent set of BC we will assume the potential energy U and the kinetic energy T of the system to be both quadratic form defined as follows:

$$U = \int_0^L \frac{1}{2} K \left(\frac{\partial^n F(x, t)}{\partial x^n} \right)^2 dx \quad (2.23)$$

$$T = \int_0^L \frac{1}{2} \rho \left(\frac{\partial F(x, t)}{\partial t} \right)^2 dx \quad (2.24)$$

Assuming the dimensional unit of the scalar field $F(x, t)$ to be $[D]$, consequently the unit of the scalar K must be chosen to be $[Kg][m]^{2n+1}[s]^{-2}[D]^{-2}$; and similarly the unit of the scalar ρ must be chosen to be $[Kg][m][D]^{-2}$ in order to make the unit of U and T to be $[J]$. Once we have defined the potential energy U and the kinetic energy T we can easily define the Lagrangian of the problem \mathcal{L} as:

$$\mathcal{L} = U - T \quad (2.25)$$

and the action between the two assumed instants of time t_1 and t_2 as:

$$\mathcal{A} = \int_{t_1}^{t_2} \mathcal{L} dt \quad (2.26)$$

The Hamilton principle stands that the evolution of a dynamic system from the instant of time t_1 to the instant of time t_2 is found imposing the stationarity of the action functional. The requirement to be assumed for the instants of time t_1 and t_2 has the mathematical meaning of setting:

$$\delta F(x, t_1) = \delta F(x, t_2) = 0 \quad (2.27)$$

The needed stationary point can be obtained imposing to the first variation of the action (2.26) to be zero. Substituting the (2.23) and (2.24) in the (2.25) and then the (2.25) in the (2.26) we

obtain:

$$\mathcal{A} = \int_{t_1}^{t_2} \left(\int_0^L \frac{1}{2} K \left(\frac{\partial^n F(x, t)}{\partial x^n} \right)^2 dx - \int_0^L \frac{1}{2} \rho \left(\frac{\partial F(x, t)}{\partial t} \right)^2 dx \right) dt \quad (2.28)$$

Now evaluating the first variation of the (2.28), we obtain:

$$\delta \mathcal{A} = \int_{t_1}^{t_2} \left(\int_0^L K \left(\frac{\partial^n F(x, t)}{\partial x^n} \right) \delta \left(\frac{\partial^n F(x, t)}{\partial x^n} \right) dx - \int_0^L \rho \left(\frac{\partial F(x, t)}{\partial t} \right) \delta \left(\frac{\partial F(x, t)}{\partial t} \right) dx \right) dt = 0 \quad (2.29)$$

Using the commutative property between the $\delta(\cdot)$ and the $\partial(\cdot)$ operator we can write:

$$\delta \mathcal{A} = \int_{t_1}^{t_2} \left(\int_0^L K \left(\frac{\partial^n F(x, t)}{\partial x^n} \right) \frac{\partial^n}{\partial x^n} (\delta F(x, t)) dx - \int_0^L \rho \left(\frac{\partial F(x, t)}{\partial t} \right) \frac{\partial}{\partial t} (\delta F(x, t)) \right) dt = 0 \quad (2.30)$$

Now we need to integrate by part with respect to the space and the time variable x and t in order to move the derivative from the variation of the scalar field $F(x, t)$ to $F(x, t)$ itself. We obtain:

$$\delta \mathcal{A} = \int_{t_1}^{t_2} \left\{ K \left(\frac{\partial^n F(x, t)}{\partial x^n} \right) \delta \left(\frac{\partial^{n-1} F(x, t)}{\partial x^{n-1}} \right) \Big|_0^L - \frac{\partial}{\partial x} \left(K \left(\frac{\partial^n F(x, t)}{\partial x^n} \right) \right) \delta \left(\frac{\partial^{n-2} F(x, t)}{\partial x^{n-2}} \right) \Big|_0^L + \dots \right. \quad (2.31)$$

$$\left. \dots - \frac{\partial^{n-1}}{\partial x^{n-1}} \left(K \left(\frac{\partial^n F(x, t)}{\partial x^n} \right) \right) \delta F(x, t) \Big|_0^L + \rho \left(\frac{\partial F(x, t)}{\partial t} \right) \delta F(x, t) \Big|_{t_1}^{t_2} + \dots \right. \quad (2.32)$$

$$\left. \dots + \int_0^L \left((-1)^n \frac{\partial^n}{\partial x^n} \left(K \frac{\partial^n F(x, t)}{\partial x^n} \right) + \frac{\partial}{\partial t} \left(\rho \frac{\partial F(x, t)}{\partial t} \right) \right) \delta F(x, t) dx \right\} dt = 0 \quad (2.33)$$

Using (2.27) in (2.32) and assuming the quantities K and ρ to be constants we can write the following well posed differential problem:

$$(-1)^n K \frac{\partial^{2n} F(x, t)}{\partial x^{2n}} + \rho \frac{\partial^2 F(x, t)}{\partial t^2} = 0 \quad (2.34)$$

associated with the following boundary conditions (BCs) to be prescribed at the boundary points $x = 0$ and $x = L$.

$$K \frac{\partial^n F(x, t)}{\partial x^n} = 0 \quad \text{or} \quad \delta \left(\frac{\partial^{n-1} F(x, t)}{\partial x^{n-1}} \right) \quad \text{specified} \quad (2.35)$$

$$K \frac{\partial^{n+1} F(x, t)}{\partial x^{n+1}} = 0 \quad \text{or} \quad \delta \left(\frac{\partial^{n-2} F(x, t)}{\partial x^{n-2}} \right) \quad \text{specified} \quad (2.36)$$

\vdots

$$K \frac{\partial^{2n-1} F(x, t)}{\partial x^{2n-1}} = 0 \quad \text{or} \quad \delta F(x, t) \quad \text{specified} \quad (2.37)$$

As expected, as a result of the variational procedure, we get back the PDE governing a generalized undulatory phenomena moreover this procedure gives us the set of constant BC associated to this PDE. Now we will put in evidence some properties of the found BC. Looking at eq. (2.35)...(2.37) it can be noted that the product of the two quantities of each line has the dimension $[Kg][m]^2[s]^{-2} = [J]$. Moreover those equations shows that the two quantities that appear in each line can not be assigned simultaneously. We will call the BC on the right of each line of (2.35)...(2.37) the complementar to the BC on the left of the same line. As usual, we will call the quantities on the right of each line related to space derivative of order $[0..n - 1]$ essential boundary conditions (EBC), and the quantities on the left of each line related to the space derivatives of order $[n..2n - 1]$ natural boundary conditions (NBC). As we noted before each EBC is complementar to a NBC. Finally we want to note that in order to have a well posed differential problem, we need to assign n BCs for each edge of the spatial domain (i.e. $x = 0$ and $x = L$). Moreover, as we said before, each of those BCs must be chosen between an EBC and its complementar NBC, so there exist 2^n possible choices to constraint each edge of the spacial domain.

2.3.7 one node to n-port mapping

As we show previously in order to have a well posed problem we need to impose n BCs for each edge of the spacial domain, moreover we know that each of those n constraints must be chosen between an EBC and the complementar NBC. As we have noted before, the product of the physical dimension of an EBC with the dimension of the complementar NBC has the

physical dimension of an energy [J]. Furthermore, as we said before, a port is defined by means of an extensive and an intensive quantity with the constraint that the product of those two quantities has the physical dimension of a power [W]. As well known the power and the energy are related by a time derivative; this fact suggest the idea of mapping each pair of complementar BC on a pair defining a port. More precisely we should map one node of the mesh on n ports of the analogue circuit by imposing to each of the n pairs $(dEBC/dt, NBC)$ to be associated to a pair (Π, Φ) or with a pair (Φ, Π) defining each port, see fig.(2-24). So that once we have chosen to describe the time derivative of the EBC by means of an intensive (extensive) quantity automatically we are describing the complementar NBC with an extensive (intensive) quantity. In such a way, it will be possible to realize each of the n BCs simply avoiding at each port the intensive or the extensive quantity. More precisely we will close a port on a generalized short circuit in order to satisfy the homogeneous EBC or we will close the same port on a generalized open circuit in order to satisfy the homogeneous NBC (or vice versa). The further requirement we need to accomplish in order to design the analogue circuit of the differential operator under exam is the imposition to the port involving the EBC related to the scalar field $F(x, t)$ itself (i.e. without any space derivative) to be governed by the finite difference equation (2.1).

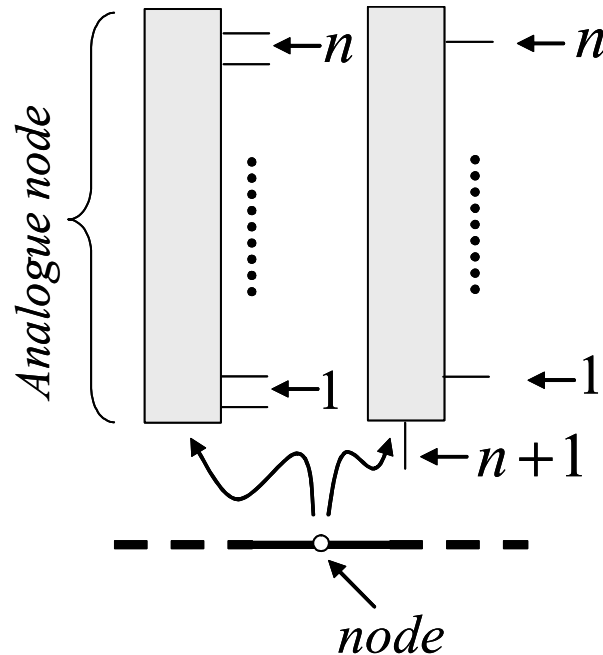


Figure 2-24: One node to n ports mapping.

This idea will allow us to produce a synthesis technique where it is clear how to realize the required BCs. We will refer to this technique as one node to n port mapping. The derivation of a lumped circuit, analogue of the differential operator described by eq.(2.34) and (2.35)..(2.37), can be done in a couple of ways. We can describe the time derivative of the scalar field $F(x, t)$ either by mean of an intensive variable Π or by mean of a extensive variable Φ . As we said before, depending on the nature of the scalar quantity $F(x, t)$, only one of those analogies will be coherent with the definition of port.

$\frac{dF}{dt} \rightarrow \Pi$ **analogy** Being the scalar field $F(x, t)$ (without any spacial derivative) associated to an EBC, once we have chosen to describe its time derivative by means of an extensive quantity we automatically choose to express all the EBCs by mean of an intensive quantity. Moreover we have shown that each EBC is complementar to a NBC; so once we have associated the quantity Π_j to the EBC $_j$ automatically we are describing the complementar NBC $_j$ with the quantity Φ_j . At this point, in order to develop a synthesis technique, we need to go into more depth in the study of the mathematical structure of the set of the consistent BC. It must be noted that each BC is related to the previous one by mean of a spacial derivative. Moreover, as we note before, the EBCs are related with the spatial derivatives between the order 0 and the order $n - 1$ while the NBC are related to the spatial derivatives between the order n and the order $2n - 1$. Furthermore it should be noted that the derivative of order $2n$ appears in the differential equation. Those considerations highlight that the basic operation we need to perform is the first discrete spatial derivative. There exists four different ways for evaluating a sample of the first discrete spatial derivative. Those four ways are related on the nature of the input and the output of the circuit, in fact both of them can be represented by means of either an extensive quantity or an intensive one. Those four circuits are described below. The circuit able to realize a Π to Π first order spacial derivative can be easily realized using a Π CIS having gain $1/\Delta$ where Δ is the step between to adjacent nodes of the mesh. This circuit is shown in fig.(2-25).

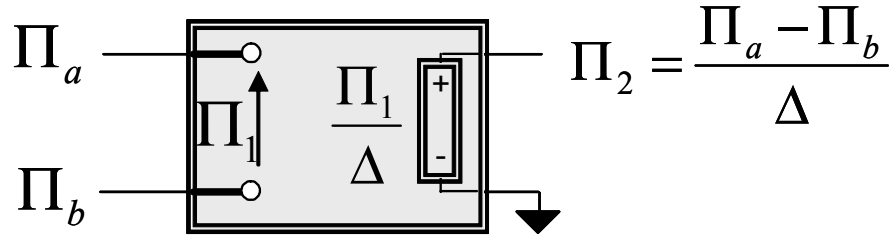


Figure 2-25: Basic circuit able to perform a Π to Π first order spatial discrete derivative.

The circuit able to realize a Π to Φ first order spatial derivative can be easily realized using a bipolar (α_1, β_1) element as shown in fig.(2-26)

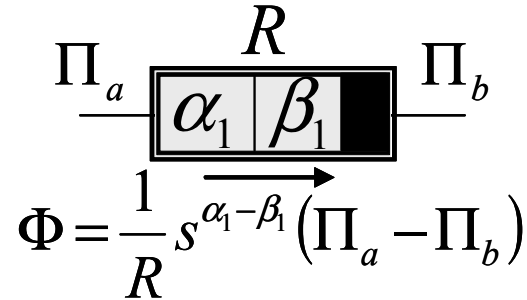


Figure 2-26: Basic circuit able to perform a Π to Φ first order spatial discrete derivative.

It should be noted that this circuit can realize a time derivative of order $\alpha_1 - \beta_1$ too. The circuit able to realize a Φ to Φ first order derivative can be easily realized using a $\Phi C\Phi S$ of gain $1/\Delta$ as shown in fig.(2-27).

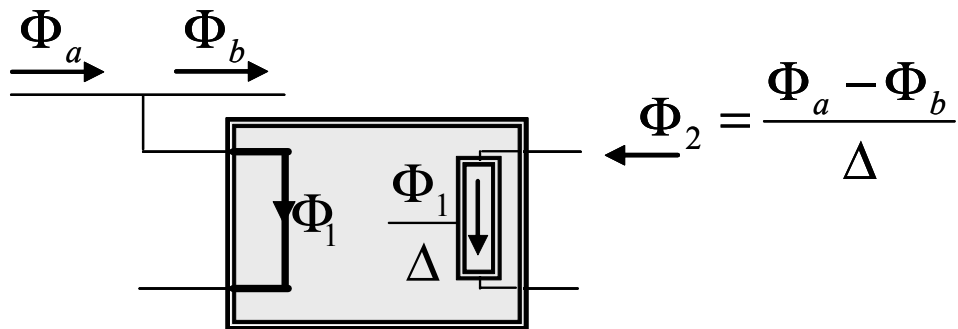


Figure 2-27: Basic circuit able to perform a Φ to Φ first order spatial discrete derivative.

The circuit able to realize a Φ to Π first order derivative can be easily realized using a bipolar

constitutive (α_2, β_2) element as shown in fig.(2-28). It should be noted that this circuit can realize a time derivative of order $\beta_2 - \alpha_2$ too. Now we need to properly connect those basic circuits in order to reproduce the mathematical structure of the BC. Consequently we need to use a suitable number of Π to Π circuit in order to evaluate the first $n - 1$ derivatives (associated with the EBCs), a Π to Φ circuit to perform the step involving the transition between the last EBC (associated with the derivative of order $n - 1$) and the first NBC (associated with the derivative of order n) and a proper number of Φ to Φ circuits to realize the derivatives between the order n and $2n - 1$ (associated with the NBCs),

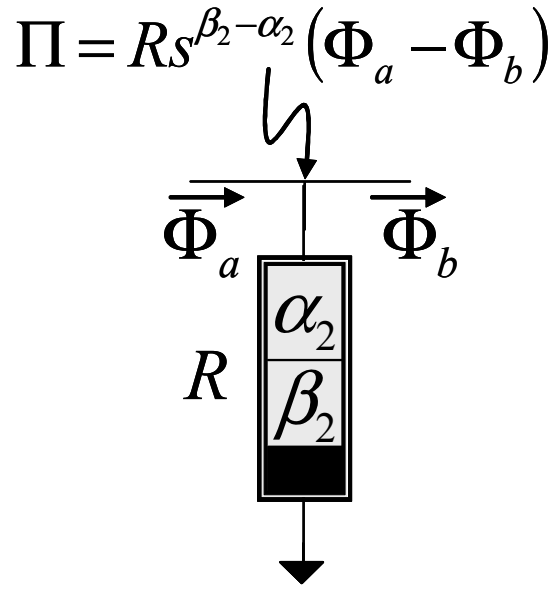


Figure 2-28: Basic circuit able to perform a Φ to Π first order spatial discrete derivative.

finally we need to use Φ to Π circuit in order to obtain the derivative of order $2n$ appearing in the finite difference equation. As we note previously we need $2n + 1$ samples in order to obtain a discrete derivative of order $2n$, so we need to connect at least $2n + 1$ nodes. Connecting those nodes using $2n$ pieces of the Π to Π circuit shown in fig.(2-25) we can produce $2n$ samples of the first spacial derivative. Connecting those $2n$ samples by means of another $2n - 1$ pieces of the Π to Π circuit we can produce $2n - 1$ samples of the second spatial derivative. We can iterate this procedure $n - 1$ times obtaining $n + 2$ samples of the $(n - 1)^{th}$ spatial derivative. This derivative is associated with the last EBC. A circuit able to realize these features is shown in fig. (2-29). It should be noted that this circuit realizes only the compatibility relation; in

fact the elaboration is done only on the intensive quantities, while a constitutive relation, as we mention before, requires a relation between a Π and a Φ quantity. The $n + 2$ samples obtained as an output of the previous circuitual scheme must be elaborated in order to produce $n + 1$ samples of the n^{th} spatial discrete derivative of the scalar field $F(x, t)$ that is associated to an NBC so it must be described by means of a Φ quantity. This means that we need to design a suitable connection of n pieces of the base circuit shown in fig. (2-26). Having $R = \Delta/K$ This connection is shown in fig. (2-30).

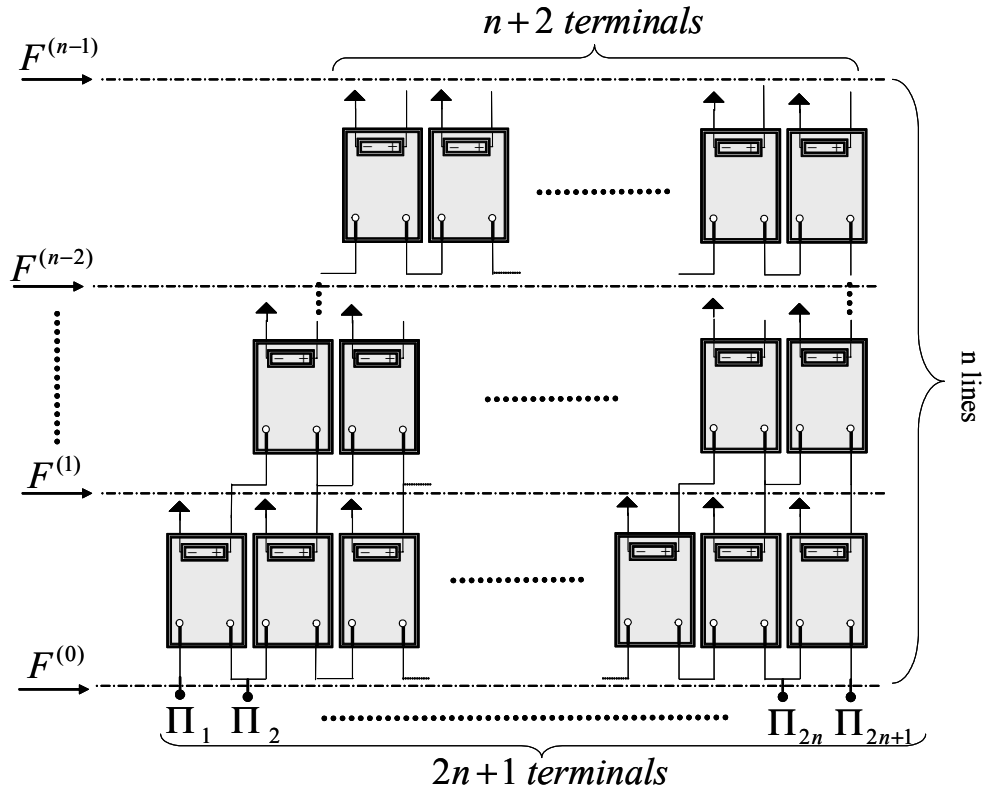


Figure 2-29: Circuit scheme able to emulate the n EBC as Π quantities on the n lines.

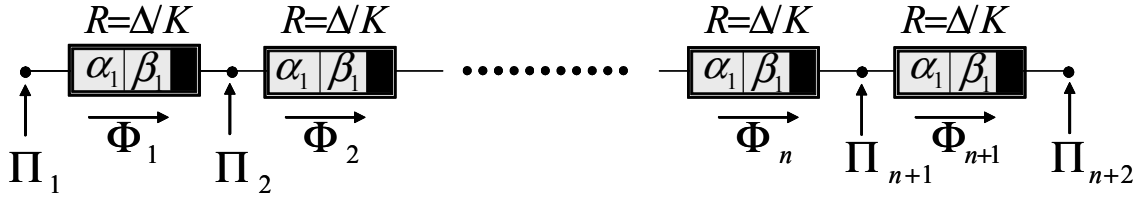


Figure 2-30: Circuit scheme able to evaluate the $n + 1$ Φ samples of the spatial derivative of order n starting from $n + 2$ Π samples of the derivative of order $n - 1$.

Now we need to realize all the NBCs. We can properly connect n pieces of the basic circuit shown in fig.(2-27) to elaborate $n + 1$ samples of the n^{th} spatial derivative in order to obtain n samples of the $(n + 1)^{th}$ spatial derivative. As we have done before we can iterate this procedure $n - 1$ times obtaining 2 samples of the $(2n - 1)^{th}$ discrete spatial derivative. A circuitual scheme able to realize the needed elaboration is shown in fig.(2-31). It can be noted that this circuit realize only the balancing relations.

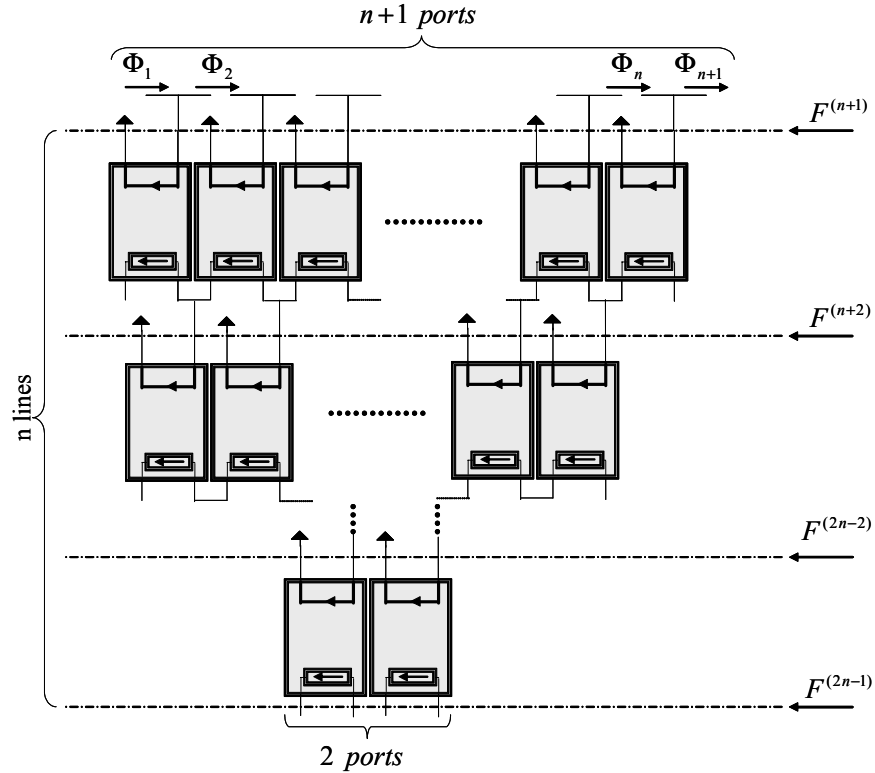


Figure 2-31 Circuit scheme able to emulate the n NBC as Φ quantities on the n lines.

Finally we need to use the two Φ quantities flowing through the two output ports of the previous circuit as the input of the circuit shown in fig.(2-28) having $R = \frac{1}{\rho\Delta}$ in order to realize the differential equation 2.1. Now we need to connect the circuital schemes shown in fig.(2-29), (2-30), (2-31) and (2-28) in such a way that each of the n terminal (each line of the fig. (2-29) and (2-31)) is associated to the Π quantity of the j^{th} derivative and the Φ quantity of the $(2n - j - 1)^{th}$ derivative. The complete scheme of connection is shown in fig. (2-30). The analogue circuit needed can be obtained repeating the circuital structure shown in fig. (2-32) for each node of the finite mesh, taking care of avoiding element doubling. Comparing the finite difference equation shown in the bottom of the figure with eq.2.1 it can be easily realized that the double time derivative can be obtained by setting $-\alpha_1 + \alpha_2 + \beta_1 - \beta_2 = 2$. There exist a lot of different choices, for example we can choose $\alpha_1 = 0, \alpha_2 = 1, \beta_1 = 1$ and $\beta_2 = 0$.

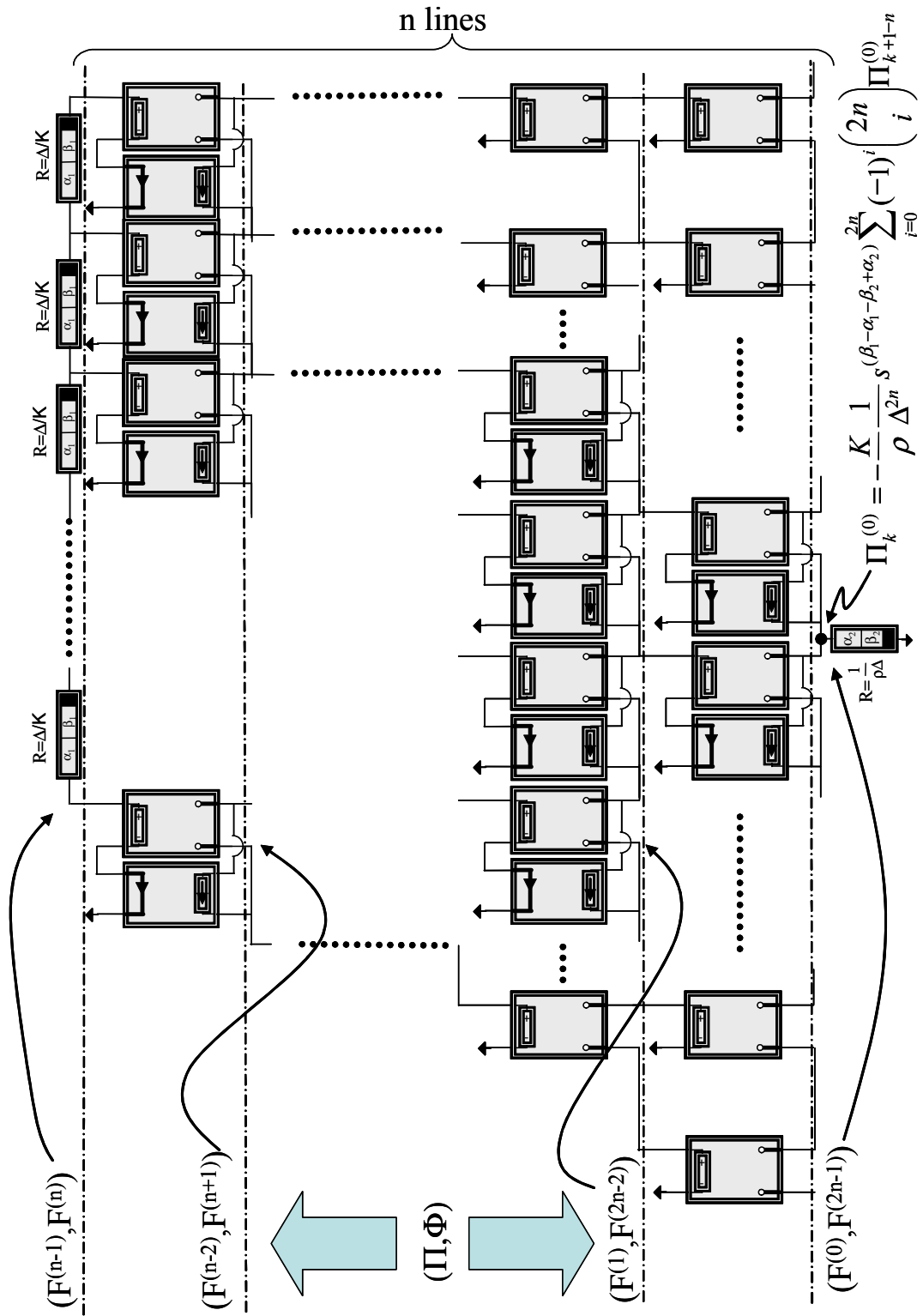


Figure 2-32: Complete scheme for the one node to n ports $\frac{\partial F}{\partial t} \rightarrow \Pi$ synthesis.

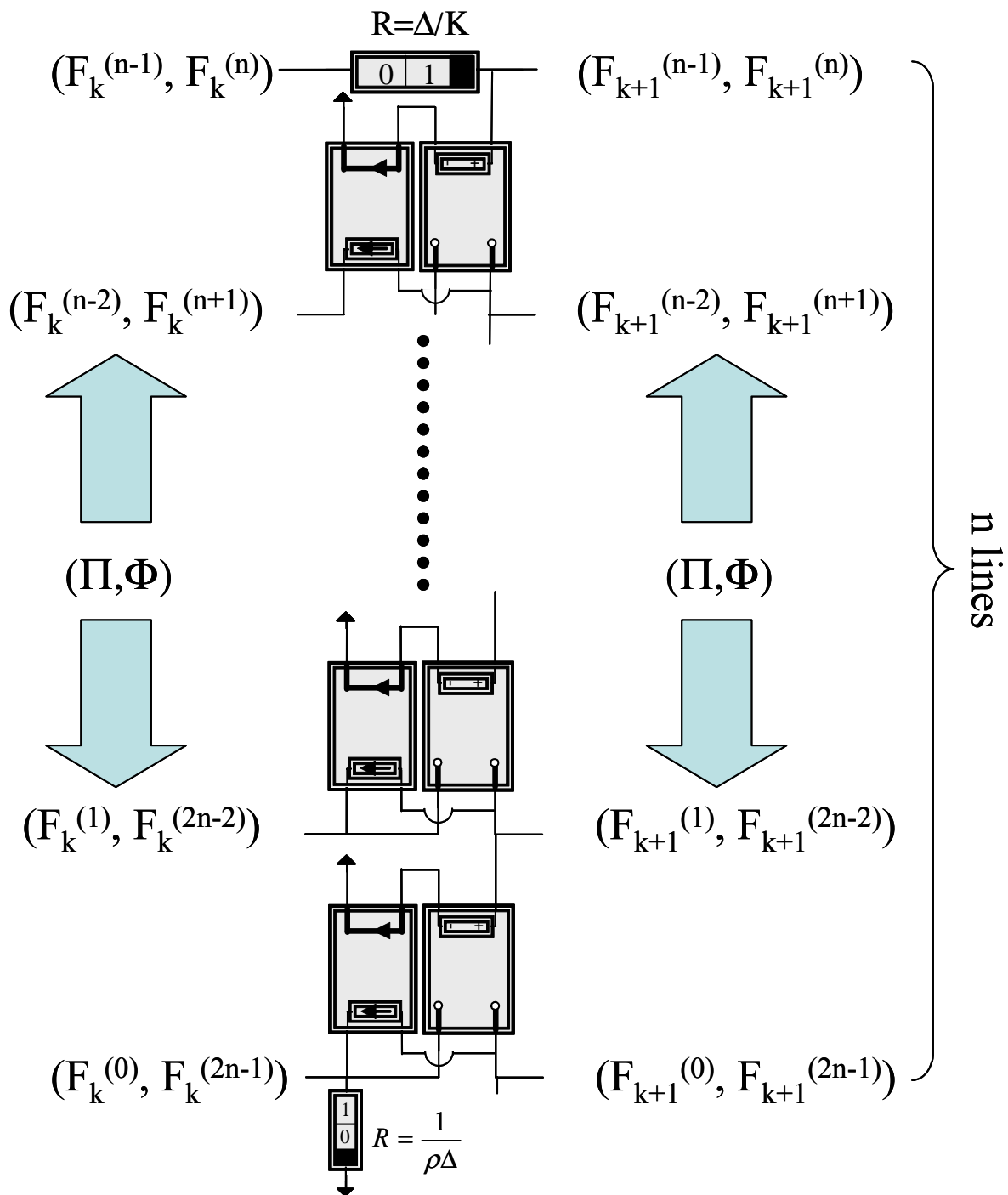


Figure 2-33: Basic section of one node to n ports $\frac{\partial F}{\partial t} \rightarrow \Pi$ synthesis.

Once we have drawn the complete scheme it is easy to recognize that it can be obtained by the cascade connection of a basic $2n + 1$ terminals network. Such a basic network is shown in fig.(2-33) where the index k and $k + 1$ refers to a couple of generic adjacent nodes of the mesh. Finally it can be noted that each of the $n - 1$ rows of the basic module is constitute by a given connection of one $\Pi C \Pi S$ and a $\Phi C \Phi S$. As shown in fig. (2-34) this scheme is equivalent to a generalized lever.

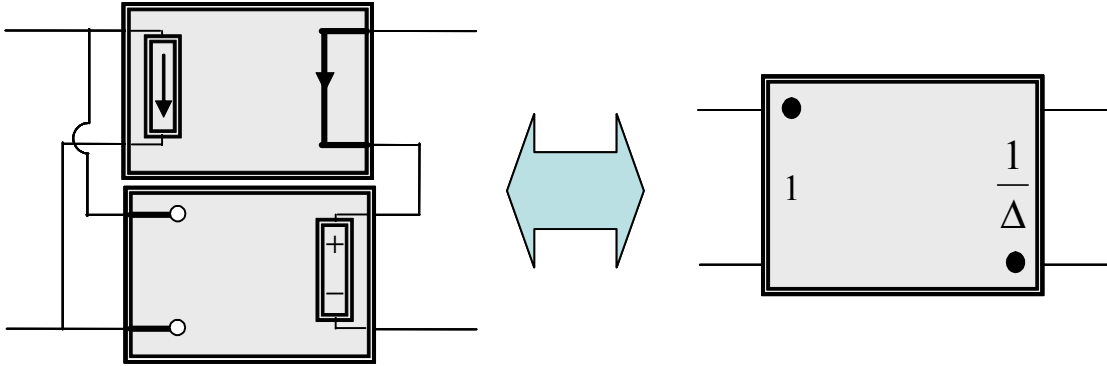


Figure 2-34: Circuitual equivalence between a given connection of a $\Pi C \Pi S$ and a $\Phi C \Phi S$ and an inverting generalized lever.

Using this circuitual equivalence it is possible to redraw the basic module using generalized levers and (α, β) elements only i.e. avoiding the use of generalized controlled source. As we did before in fig. (2-35) we put in evidence the opportunity to represent the non symmetric basic section as the cascade of two symmetric subsections. These subnetworks have a specific physical meaning, in fact one of them takes in count all the constitutive relations and we will refer to it as constitutive subnetwork; the other one groups all the generalized levers and realize all the geometric and the balancing equations and we will refer to it as geometric/balancing subnetwork. As we will show in the next section the subsection notion will be crucial in order to guarantee the symmetry of the whole circuit. It should be noted that this circuit assumes the form of the network proposed in [Andreas et al. (2004)] and [Porfiri et al. (2004)] when $n = 2, \alpha_2 = 1, \beta_2 = 0, \alpha_1 = 0, \beta_1 = 1$ and $(\Pi, \Phi) = (V, I)$.

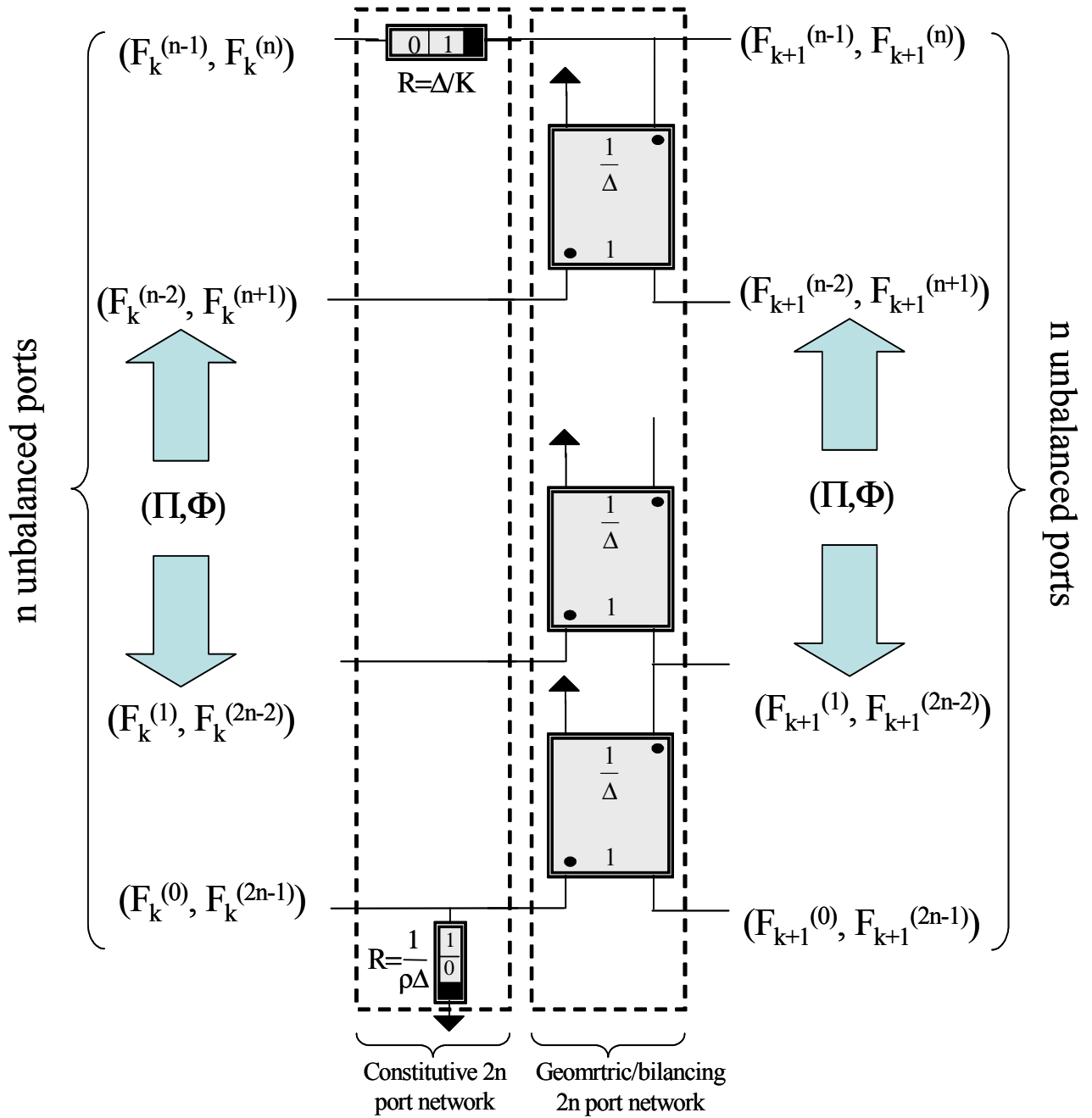


Figure 2-35: Basic section for the one node to n ports $\frac{\partial F}{\partial t} \rightarrow \Pi$ synthesis with generalized lever and (α, β) elements. The generalized levers are collected in the right subsection that takes in count for geometrical and balancing equation, while the (α, β) elements are collected in the left subsection that takes in count for the constitutive equation.

$\frac{dF}{dt} \rightarrow \Phi$ **analogy** An alternative choice is to describe the time derivative of the scalar field F by means of an extensive quantity. Being the scalar $F(x,t)$ associated to an EBC all the remaining EBCs must be described by means of an extensive quantity. Proceeding as we have done in the previous subsection, we can realize all the EBC by the circuitual scheme shown in fig.(2-36).

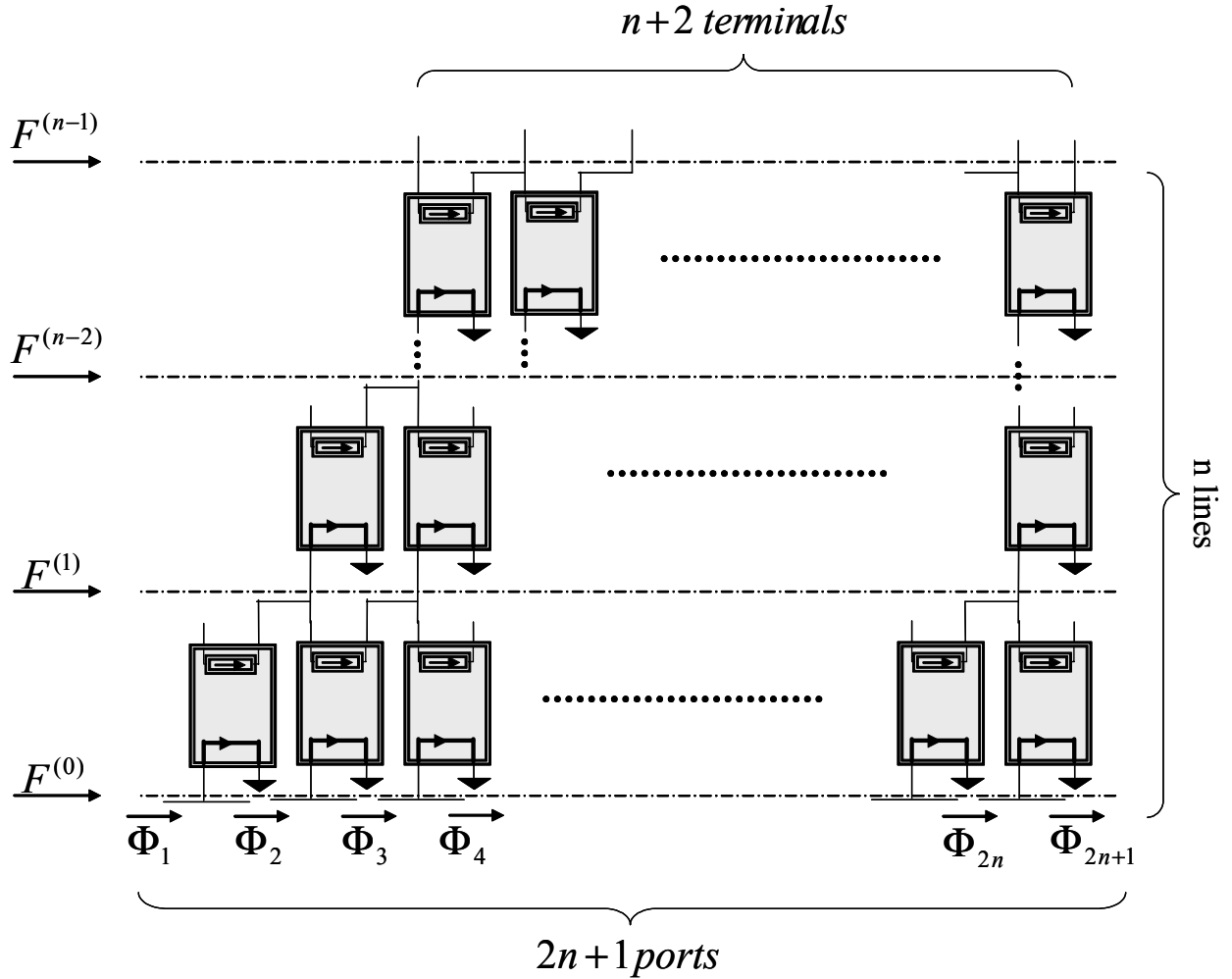


Figure 2-36: Circuit scheme able to emulate the n EBC as Φ quantities on the n lines.

The constitutive relation between the $(n-1)^{th}$ discrete spatial derivative and the n^{th} derivative can be realized by means of the scheme shown in fig.(2-37) having $R = \frac{K}{\Delta}$

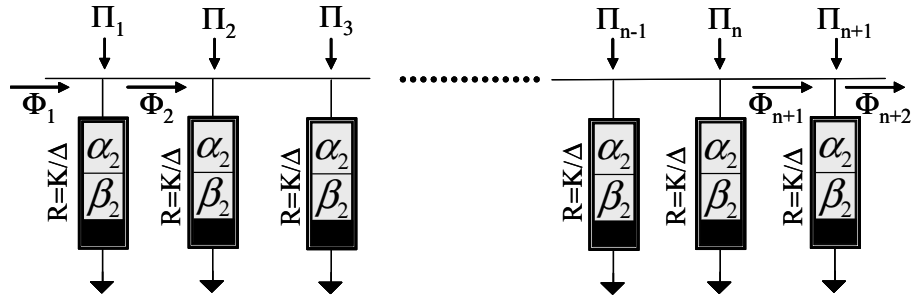


Figure 2-37: Circuit scheme able to evaluate $n + 1$ Π samples of the spacial derivative of order n starting from $n + 2$ Φ samples of the derivative of order $n - 1$.

Now we can realize the n NBC elaborating the $n + 1$ samples of the n^{th} spatial derivative by means of a proper connection of the basic circuit shown in Fig. (2-38)

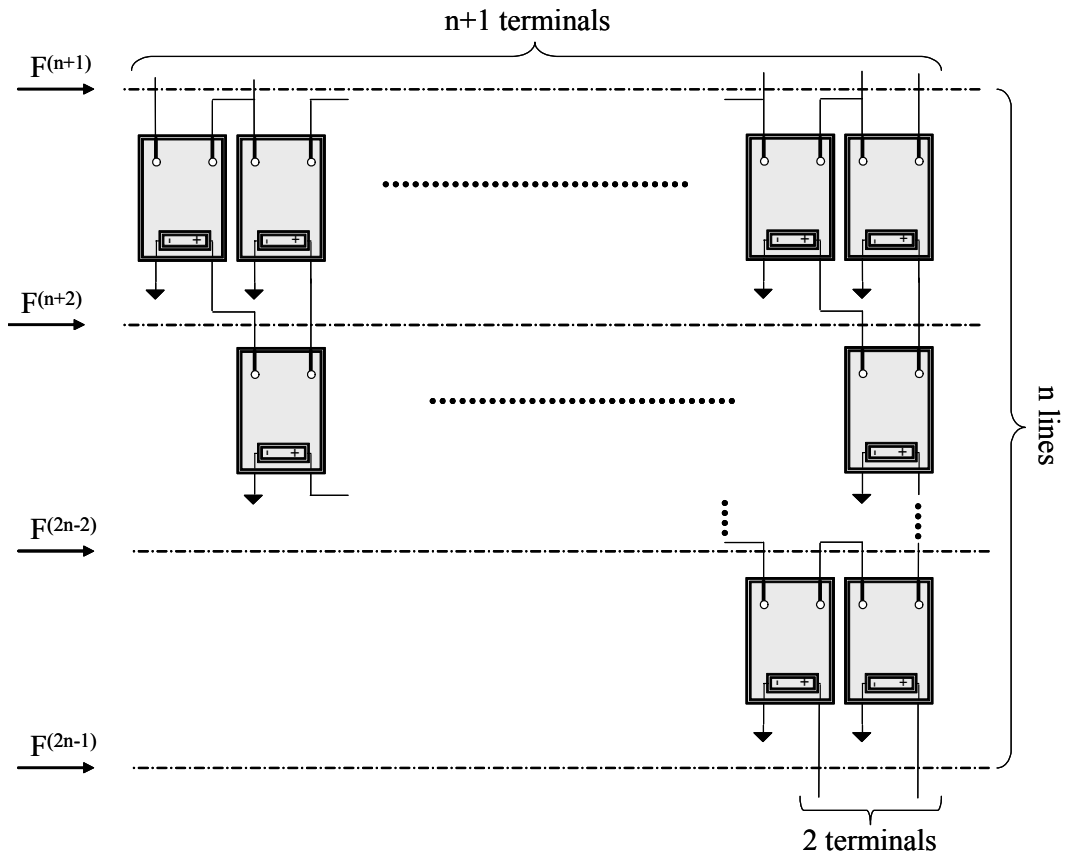


Figure 2-38: Circuit scheme able to emulate the n NBC as Φ quantities on the n lines.

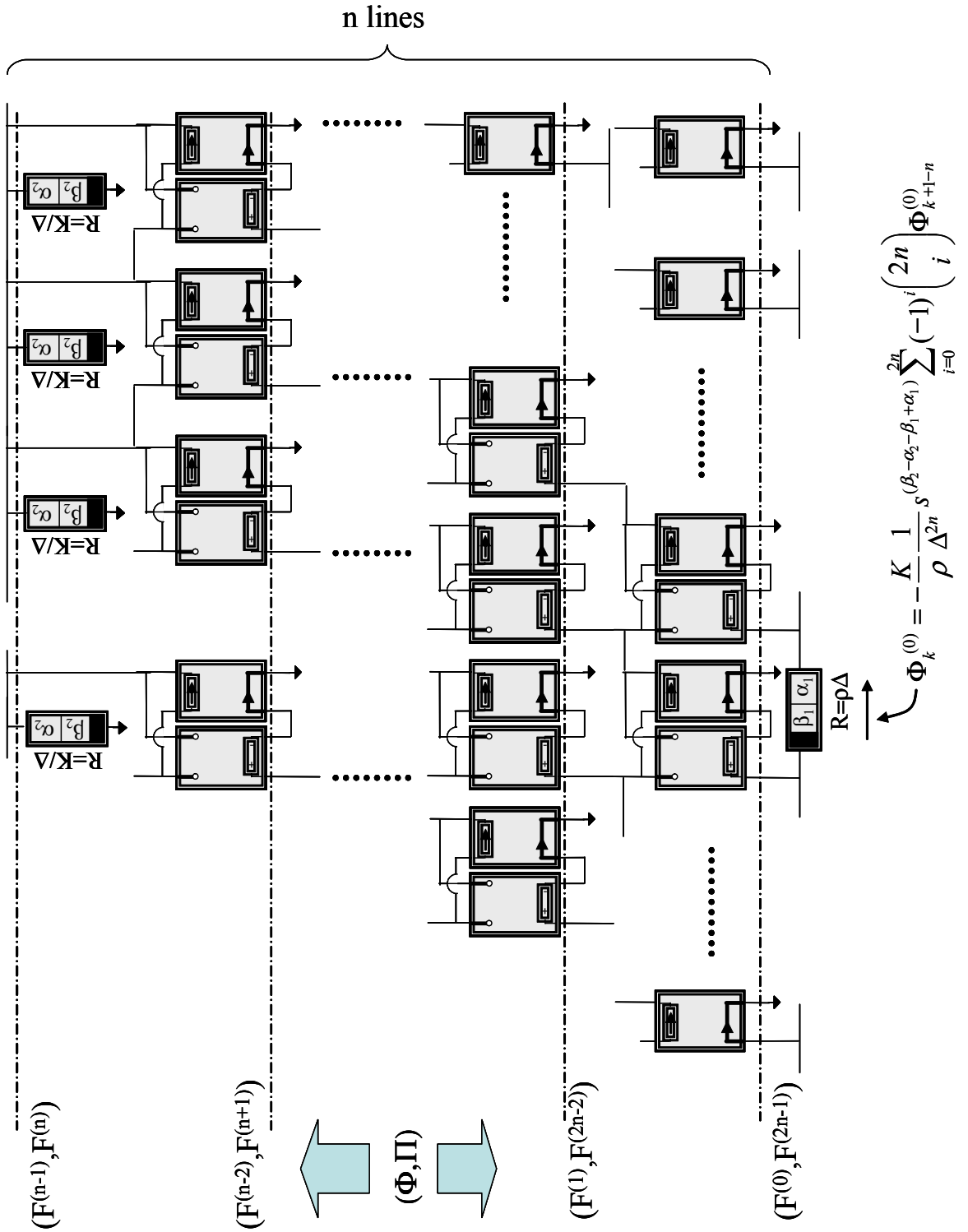


Figure 2-39: Complete scheme for the one node to n ports $\frac{\partial F}{\partial t} \rightarrow \Phi$ synthesis.

Finally we need to impose the discrete differential problem (2.1) relating the spatial derivative of order $2n^{th}$ to the spatial derivative of order zero (i.e. the function it self). The latter step can be realized by means of the circuit shown in Fig. (2-23) having $R = \Delta\rho$. In order to obtain the final scheme we need to properly connect the circuits previously described. In particular it is required that the Φ quantity describing the m^{th} derivative will be associated with the Π quantity describing the $(2n - m - 1)^{th}$ derivative. The complete scheme of connection is shown in fig. (2-39). As we have done previously it is useful to extract a basic module of the complete network. Using the circuital equivalence shown in fig. (2-33) we will derive the $2n$ port network shown in fig. (2-40). It should be noted that, as he have done in the $\frac{\partial F}{\partial t} \rightarrow \Pi$ analogy, it is possible to split the $2n$ port network in the cascade connection of two different $2n$ port networks. The first one takes in count the constitutive relations and the second one takes in count the geometrical and the balancing relations. This subdivision will be useful in order to make symmetric the analogue circuit of the differential operator over the whole spatial domain. Finally it can be easily realized that for the one node to n port mapping the $\frac{\partial F}{\partial t} \rightarrow \Pi$ analogy and the $\frac{\partial F}{\partial t} \rightarrow \Phi$ analogy brings to the same circuital scheme, except that the first one has an unbalanced representation while the second one has a balanced one. The only important difference is that while in the first case the differential problem is described by means of the Π quantity between the terminals of the (α_2, β_2) element, in the second case it is described by means of the Φ quantities flowing through the (α_1, β_1) element. The latter property is true for the one node to one port synthesis too, even if in that case the two circuits obtained for the $\frac{\partial F}{\partial t} \rightarrow \Pi$ and the $\frac{\partial F}{\partial t} \rightarrow \Phi$ identification have different structures. Summarizing our observation we can say that in both the synthesis techniques we described the samples of the samples of the scalar field $F(x, t)$ are related with the Π of the Φ quantities associated with the constitutive (α, β) elements. This property must be kept in mind, in fact it will be fundamental when in the next section in order to derive an external characterization of the circuit we will choose the access point of the circuit. Before completing this section we want to note that the BC based synthesis technique used in this section in order to derive a circuit analogue to a generalized undulatory phenomena can be used as a general synthesis technique of differential operators.

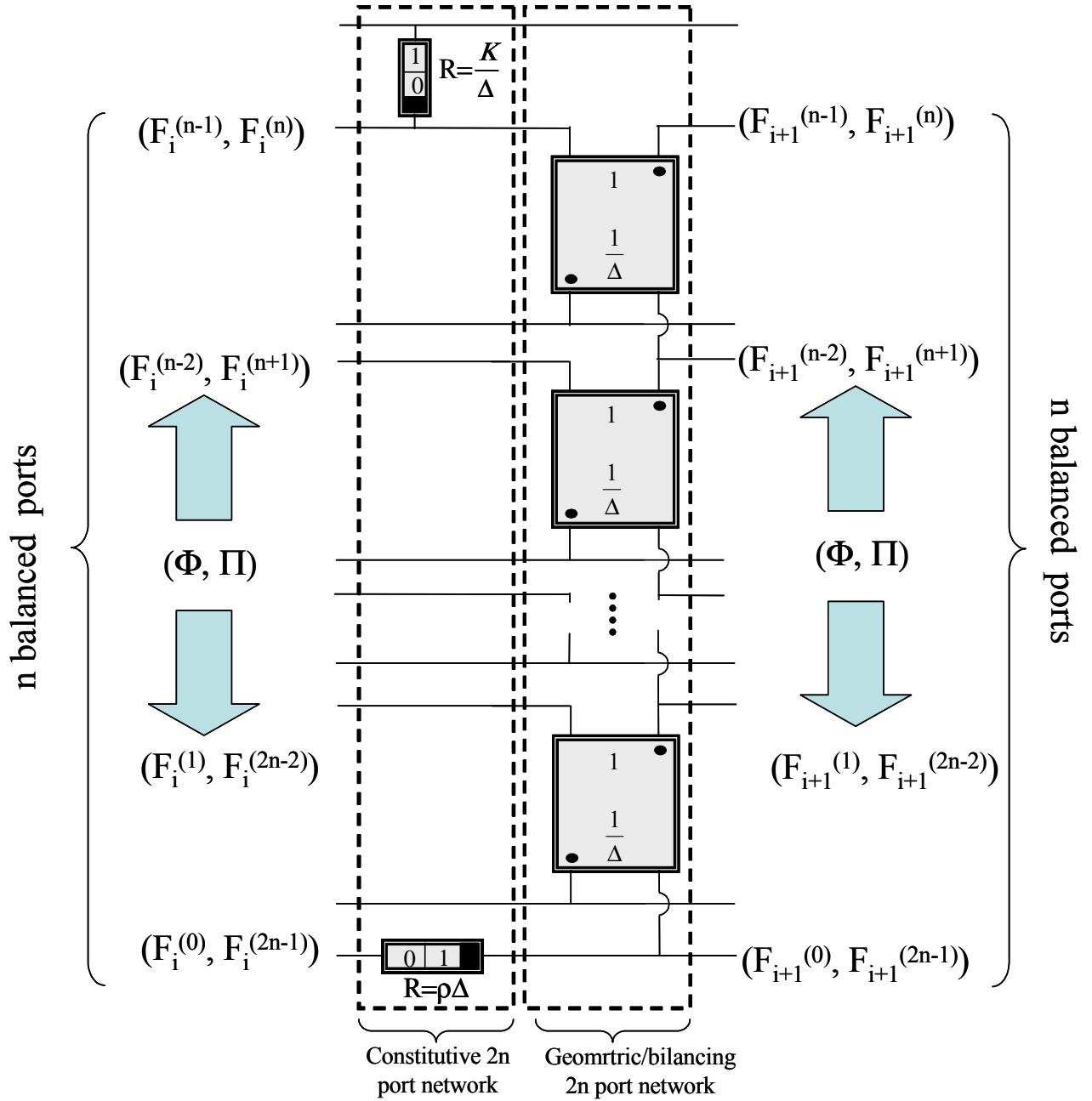


Figure 2-40: Basic section for the one node to n ports $\frac{\partial F}{\partial t} \rightarrow \Phi$ synthesis with generalized lever and (α, β) elements. The generalized levers are collected in the right subsection that takes in count for geometrical and balancing equation, while the (α, β) elements are collected in the left subsection that takes in count for the constitutive equation.

2.4 External characterization of the network

2.4.1 Introduction

The purpose of this subsection is to derive an external characterization of the network described in the previous subsection. In order to produce a blackbox characterization of the system, first of all, we need to choose the access point of the circuit. We want to describe how the samples of the scalar field $F(x, t)$, associated to each node, interact among them. In order to realize this description of the system we need to choose the port associated to each node as the access point to the system. More precisely we will use the sample of the scalar field F as external independent variable and the complementary quantity as dependent ones. This procedure will result in an admittance characterization for the $\frac{dF}{dt} \rightarrow \Pi$ analogy and in an impedance characterization for the $\frac{dF}{dt} \rightarrow \Phi$ analogy. As we noted before, for the $\frac{dF}{dt} \rightarrow \Pi$ synthesis, the samples of the scalar field $F(x, t)$ are described by means of the Π quantities between the terminal of the (α_2, β_2) elements, consequently, in this case, we should take the access ports of the system shunted with those elements. Similarly for the $\frac{dF}{dt} \rightarrow \Phi$ synthesis, the samples of the scalar field $F(x, t)$ are described by means of the Φ quantities flowing through the (α_1, β_1) elements, consequently, in this case, we should take the access ports of the system in series with those elements. In the following of this section we will derive those characterization for both the one node to n ports and the one node to one port synthesis technique. Moreover, we will show how this procedure will be used in order to derive a methodology to design the most general BC also for the one node to one port synthesis.

2.4.2 One node to n ports mapping

$\frac{\partial F}{\partial t} \rightarrow \Pi$ analogy

As we noted in the previous subsection the complete network can be obtained by the cascade connection of a number of basic networks shown in fig. (2-33) large as the number of nodes in the mesh (i.e. M) shown in fig. (2-1). This connection produces a not symmetric system. In order to obtain a symmetric system we need to connect it in cascade with a constitutive subnetwork on the right edge or a geometrical/balancioum subnetwork on the left. Once the system has been symmetrized we must apply the termination network taking in count for the

BCs As we said previously this synthesis technique map one node of the mesh in n ports of the analogue circuit in such a way that the pair (Π, Φ) of i^{th} port is associated with pair (EBC,NBC) of the i^{th} line of eq.2.37 (starting from the bottom), so that the homogeneous EBC at the i^{th} port can be simply imposed by interconnecting it on a generalized short circuit while the complementar NBC can be imposed by closing the same port on a generalized open circuit. In order to derive a general formulation of the problem (i.e. valid for each termination condition) we will close the i^{th} port (starting from the top) on a (α_1, β_1) element of nominal admittance $R = \gamma_i \frac{K}{\Delta^{2i-1}}$. This choice allows us to collect the term $\frac{K}{\Delta^{2i-1}}$ from the admittance matrix that we are evaluating⁶. This procedure can appear an unuseful complication by the way it allows us to produce a general tractation, in fact we can obtain the short cut and the open circuit conditions simply taking the limit for $\gamma_i \rightarrow 0$ or $\gamma_i \rightarrow \infty$ respectively for $i \in 1..n$. The basic section described above is shown in fig. (2-41 a) for the unbalanced case and in fig. (2-41 b) for the balanced one.

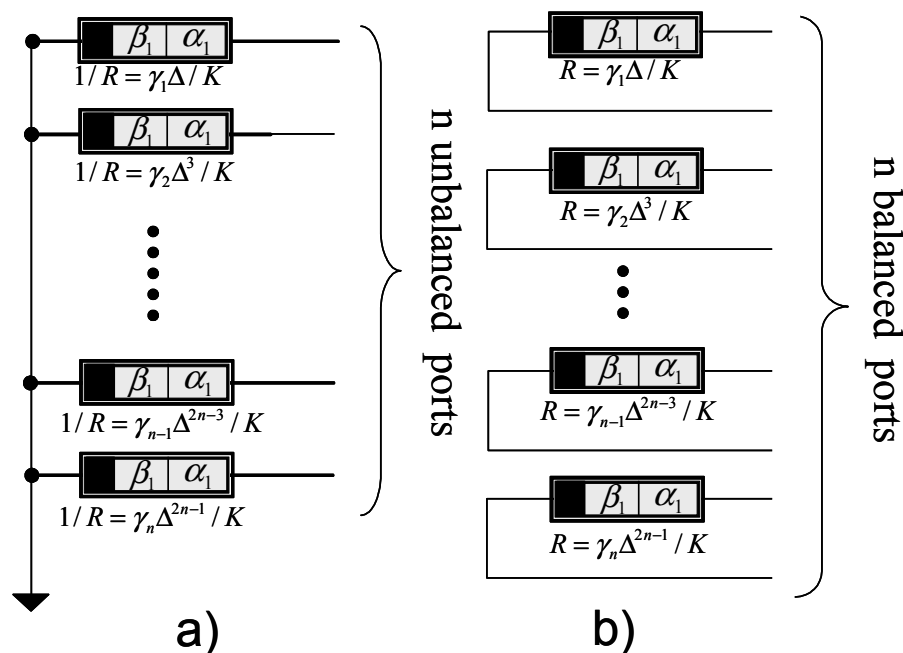


Figure 2-41: Termination section for the one node to n ports synthesis.

At this point we need to choose between the two possible symmetrization techniques. As we

⁶This fact can be easily understand if we think that each port of the circuit is connected to previous one by means of a generalized lever having $1/\Delta$ as trasformation ratio. It can be easily realized that the impedance at the first port of a generalized lever is related to the impedance at the second port by means of the quantity $1/\Delta^2$.

have said in the introduction we want to access the system shunting the ports to the (α_2, β_2) elements or taking them in series with the (α_1, β_1) elements, so if we connect a constitutive subnetwork and the termination section on the right of the whole circuit we will fall into an unsolvable circuit. In fact for some BC we should obtain a port shunted with a generalized short circuit or in series with a generalized open circuit. This observation suggests to symmetrize the circuit by connecting a geometric/balancioum subnetwork on the left of the system. The circuit described above is shown in fig. (2-42) for $n = 6$. As shown in the same figure the generic element of admittance matrix y_{ij} can be evaluated connecting a generalized Π source of nominal value Π_i at the i^{th} port and a generalized short circuit to all the remaining ports. Then we need to measure the Φ_j quantity flowing through the j^{th} port. The admittance y_{ij} will be given by the ratio:

$$y_{ij} = \frac{\Pi_i}{\Phi_j} \Bigg|_{\substack{\Phi_k=0 \\ k=1..M \\ k \neq j}} \quad (2.38)$$

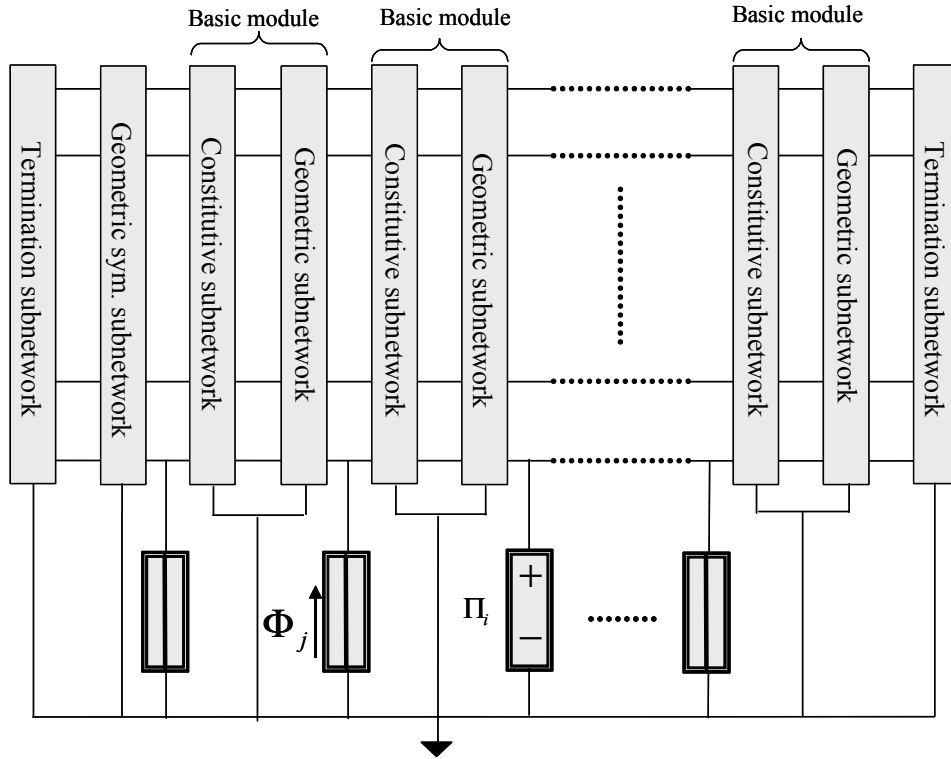


Figure 2-42: Circuital scheme for the external characterization for the one node to n port

$F \rightarrow \Pi$ synthesis.

Now we want to investigate the mathematical structure of the admittance matrix we will obtain using the procedure described above. First of all we need to understand how the access port interact among them and with the termination section taking in count for the BC. Taking in mind the synthesis procedure we had described in the previous section we can draw the scheme shown in fig.(2-43). In this scheme we will show the node of the mesh and the analogue n nodes associated to each of them.

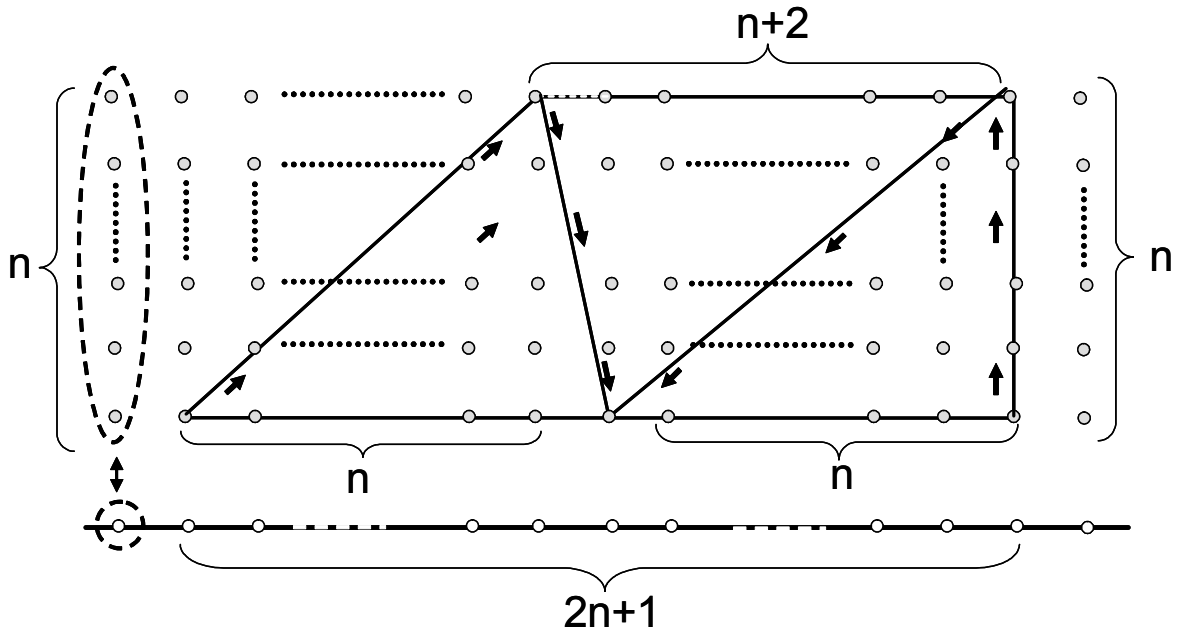


Figure 2-43: Scheme of interaction among the nodes of the mesh.

From the calculation scheme we can note that $2n + 1$ sample are used to evaluate $n + 2$ sample of the spatial derivative of order $n - 1$ than those samples are used to impose the discrete differential problem in the node in the middle. This means that each node interacts with the previous and subsequent n nodes. Consequently each row (column) of the admittance matrix will have only $2n + 1$ non trivial elements. Moreover only the first n nodes and the last n node of the mesh interacts with the boundary termination network. This property can be expressed saying that the termination network will effect the $n \times n$ submatrices at the corner of the admittance matrix (i.e. the termination condition doesn't effect any element out of those matrices). So evaluating the whole matrix \mathbb{Y} for the general case we will obtain a matrix having

the structure shown in fig. (2-44).

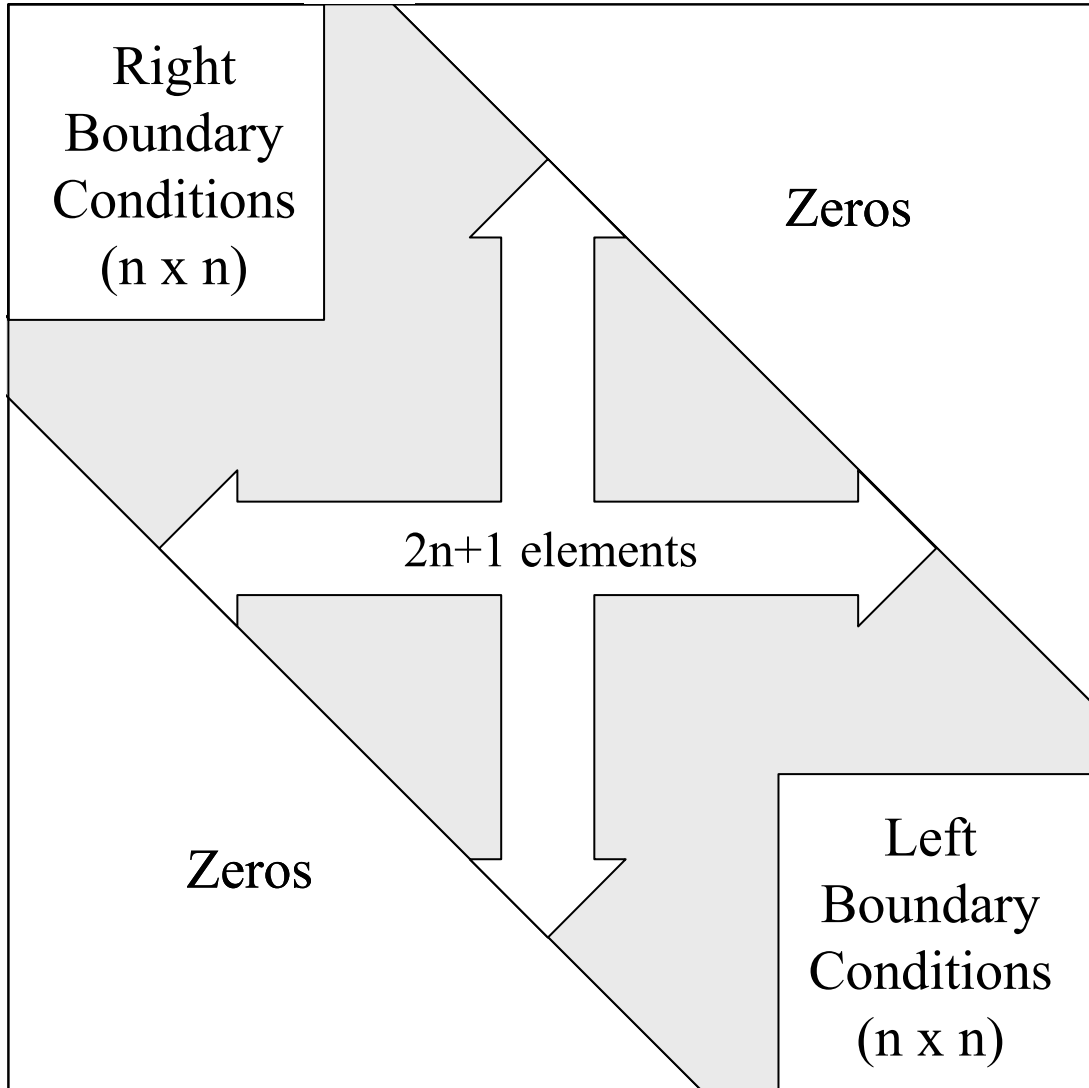


Figure 2-44: Mathematical structure of the admittance matrix.

This matrix is symmetric with respect of both the first and the second principal diagonals. Consequently the $n \times n$ corner submatrices are symmetric too therefore they have $(n + 1)\frac{n}{2}$ independent elements take in count the BCs. In particular the elements belonging to those submatrices will be rational function for which the numerator and the denominator will be

polynomial functions of the variables γ_i for $i = 1..n$. Additionally it is quite easy to realize that the $2n + 1$ elements on each of the rows and on each columns of the gray band are related to the coefficients of the difference equation 2.1.

$\frac{\partial F}{\partial t} \rightarrow \Phi$ analogy

As we note in the previous subsection the complete network can be obtained by the cascade connection of a number of $2n + 1$ terminals network shown in fig. (2-40) large as the number of node in the mesh (i.e. M) shown in fig. (2-1). In order to obtain a symmetric system we need to cascade connect a geometric/balancioum subnetwork on the left edge before applying the termination network taking in count for the BCs. As we said previously, this synthesis technique maps one node in n port in such a way that the pair (Φ, Π) of i^{th} port has the meaning of the pair (EBC, NBC) of the i^{th} line of eq.2.37 (starting from the bottom), so that the EBC at the i^{th} port can be simply imposed by closing it on a generalized open circuit while the complementar NBC can be imposed through a generalized short circuit. In order to derive a general formulation of the problem (i.e. valid for each termination condition) we will connect the i^{th} port relative to the bound node to the reference node trough an (α_1, β_1) element of nominal impedance $\gamma_i \frac{K}{\Delta^{2i-1}}$ in such a way we can obtain the short cut and the open circuit condition simply taking the limit for $\gamma_i \rightarrow 0$ or $\gamma_i \rightarrow \infty$ for $i \in 1..n$. As we said before in this case the port should be taken in series with the (α_1, β_1) elements of the constitutive subnetworks. The circuit described above is shown in fig. (2-43) for $n = 6$. As shown in the same figure the generic element of admittance matrix z_{ij} can be evaluated connecting a generalized Φ source of nominal value Φ_i at the i^{th} port and a generalized open circuit to all the remaining ports. Then we need to measure the Π_j quantity between the terminal of the j^{th} port. The impedance z_{ij} will be given by the ratio:

$$z_{ij} = \frac{\Phi_i}{\Pi_j} \Bigg|_{\substack{\Pi_k=0 \\ k=1..M \\ k \neq j}} \quad (2.39)$$

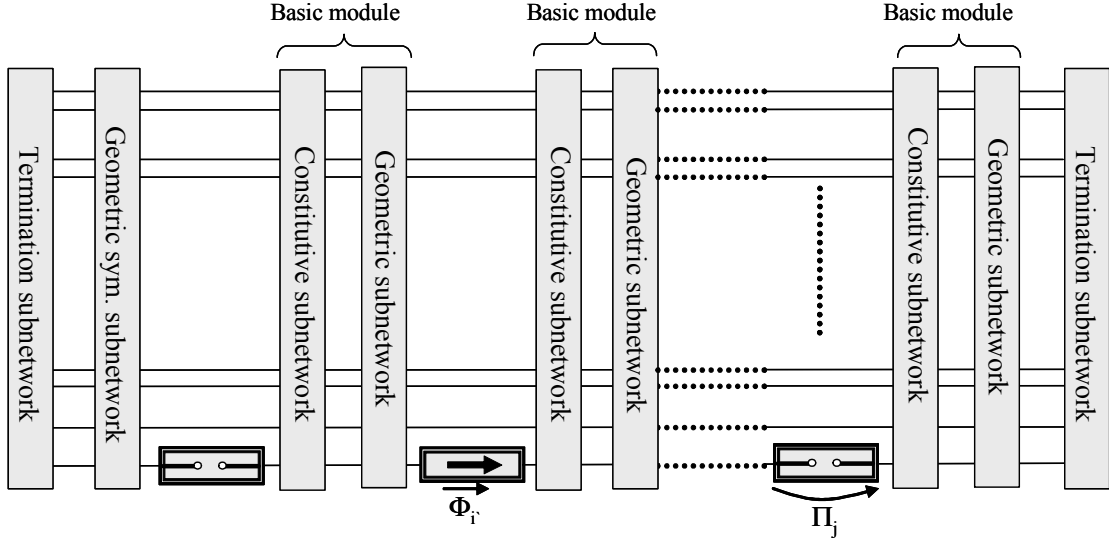


Figure 2-45: Circuitual scheme for the external characterization for the one node to n port $F \rightarrow \Phi$ synthesis.

Evaluating the whole matrix \mathbb{Z} for the general case we will obtain a matrix having exactly the same structure shown in fig.(2-43).

2.4.3 One node to one port mapping

$\frac{\partial F}{\partial t} \rightarrow \Pi$ **analogy** As we have done in the previous subsection we can derive the admittance matrix of the circuit whose basic section is shown in fig. (2-19) for $n = 6$ by considering the access ports of the network shunted with the (α_2, β_2) elements. The generic element of this matrix can be obtained using the definition given by eq. (2.38). Applying this definition we will find a matrix having the structure shown in fig. (2-44) except that for the corner submatrices taking in count for the BCs. As we have remarked previously while we have shown a clear procedure to impose BCs for the one node to n port mapping we have not a clear methodology to impose BCs for the one node to one port mapping. This obstacle can be overpassed by requiring to the admittance matrices of the two circuits to be equal. We have shown in fig. (2-44) that the BCs effect only the symmetric $n \times n$ corner submatrices, moreover we have remarked that those matrices have $(n+1)\frac{n}{2}$ independent elements. So in order to make the two admittance matrices equal we need to modify the elements belonging to the corner submatrices. We need to design a termination subnetwork having $(n+1)\frac{n}{2}$ degrees of freedom (i.e. $(n+1)\frac{n}{2}$

independent components) able to alter the values of the elements belonging to the corner $(n \times n)$ submatrices. This problem can be solved by means of the termination section shown in fig. (2-46), where the $(n + 1)\frac{n}{2}$ independent components are chosen to be proportional to $\frac{\Delta^{2n-1}}{K}$ by means of the parameter Γ_{ij} $i = 1..n$ and $j = i..n$. This choice allows us to collect the term $\frac{K}{\Delta^{2n-1}}$ from the admittance matrix that we are evaluating.

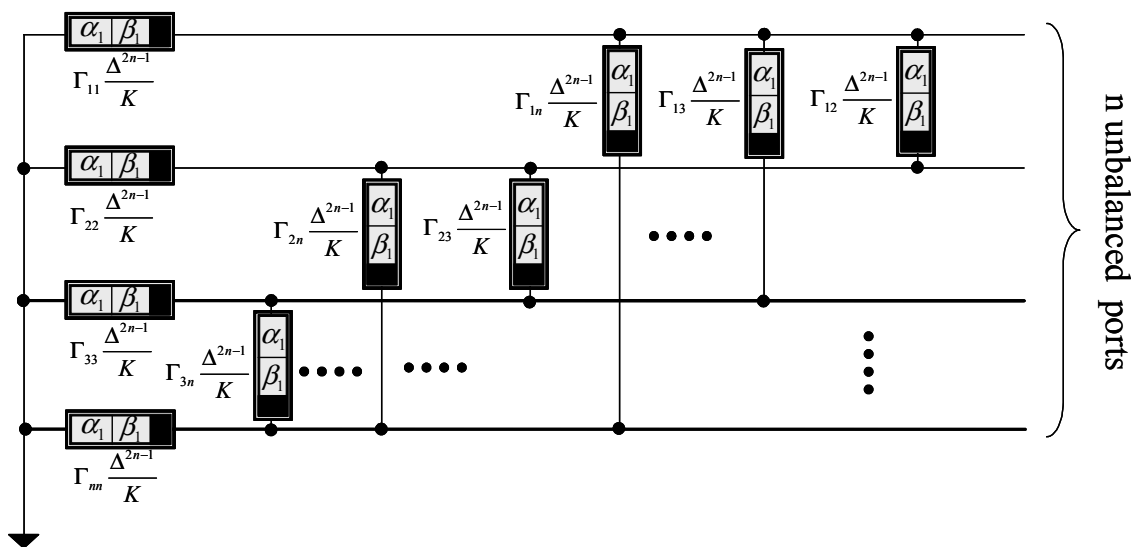


Figure 2-46: Termination section for the one node to one port $\frac{dF}{dt} \rightarrow \Pi$ synthesis.

The procedure described above gives us a methodology to evaluate all the correct BCs for the one node to one port mapping, in fact equating the elements of the two matrices one to one we obtain a well posed linear system of $(n + 1)\frac{n}{2}$ equations in $(n + 1)\frac{n}{2}$ unknowns. Now we need to properly connect the termination section shown in fig. (2-46) to the network shown in fig. (2-19) for $n = 6$. Since we are describing the circuit by means of its admittance matrix shunting the n ports of the termination network to the first and the last n port of the circuit, we will add the $(n \times n)$ admittance matrix of the termination section to the $(n \times n)$ corner submatrices of the circuit without BC. This connection scheme is shown in fig. (2-47). In particular the unknowns will be associated with the nominal values of the elements (i.e. Γ_{ij} $i = 1..n$ and $j = i..n$) while the note terms of the system will be the $(n + 1)\frac{n}{2}$ rational function of the parameters γ_i for $i = 1..n$ introduced in the previous subsection.

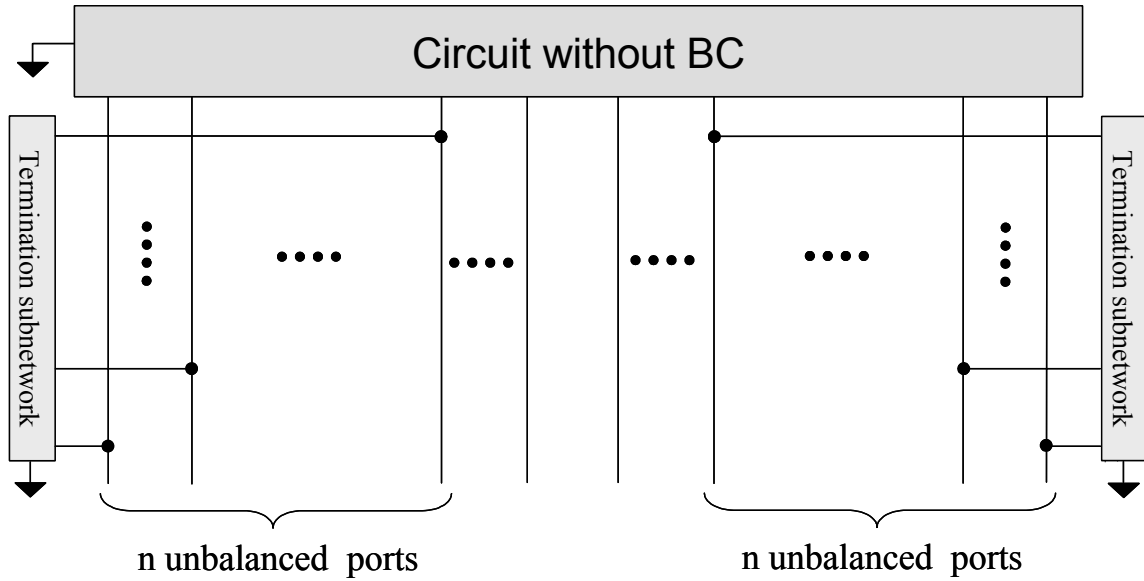


Figure 2-47: Connection of the termination sections for the one node to one port $\frac{dF}{dt} \rightarrow \Pi$ synthesis.

This means that solving the linear system we will find the most general values for the needed components as a function of the parameter γ_i for $i = 1..n$. The actual values for each particular BC will be obtained by taking the limit for $\gamma_i \rightarrow 0$ or $\gamma_i \rightarrow \infty$ for $i = 1..n$. Some examples of this procedure will be given in the following chapter.

$\frac{\partial F}{\partial t} \rightarrow \Phi$ **analogy** As we have done in the previous subsection we can derive the impedance matrix of the circuit whose basic section is shown in fig. (2-21) by considering the access ports of the network in series with the (α_1, β_1) elements. The generic element of this matrix can be obtained using the definition given by eq. (2.39). Applying this definition we will find a matrix having the structure shown in fig. (2-44) except that for the corner submatrices taking in count for the BCs. As we have remarked previously while we have shown a clear procedure to impose BCs for the one node to n port mapping we have not a clear methodology to impose BCs for the one node to one port mapping. This obstacle can be overpassed by requiring to the impedance matrices of the two circuits to be equal. We have shown in fig. (2-44) that the BCs effect only the symmetric $n \times n$ corner submatrices, moreover we have remarked that those matrices have $(n+1)\frac{n}{2}$ independent elements. So in order to make the two impedance matrices equal we need

to modify the elements belonging to the corner submatrices. We need to design a termination subnetwork having $(n + 1)\frac{n}{2}$ degrees of freedom (i.e. $(n + 1)\frac{n}{2}$ independent components) able to alter the values of the elements belonging to the corner $(n \times n)$ submatrices. This problem can be solved by means of the dual network of the termination section shown in fig. (2-46). This network can not be drawn for the general case so that we will show in fig (2-48) the circuit obtained for $n = 3$.

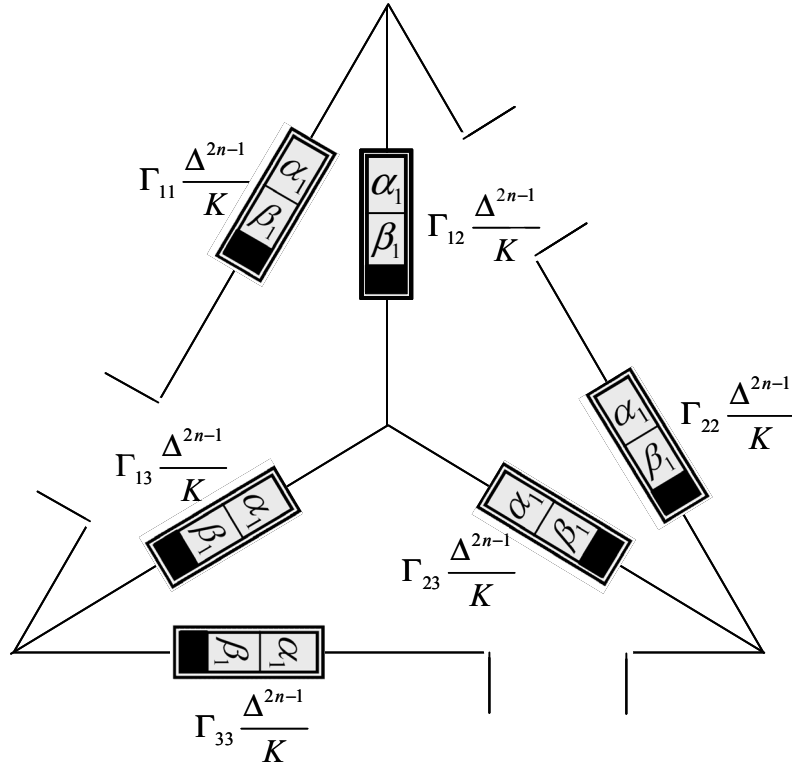


Figure 2-48: Termination section for the one node to one port $\frac{dF}{dt} \rightarrow \Phi$ synthesis when $n = 3$.

Now we need to properly connect the termination section shown in fig. (2-48) to the network whose basic section is shown in fig. (2-21). Since we are describing the circuit by means of its impedance matrix connecting the n ports of the termination network in series with the first and the last n port of the circuit, we will add the $(n \times n)$ impedance matrix of the termination section to the $(n \times n)$ corner submatrices of the circuit without BC. This connection scheme is shown in fig. (2-49).

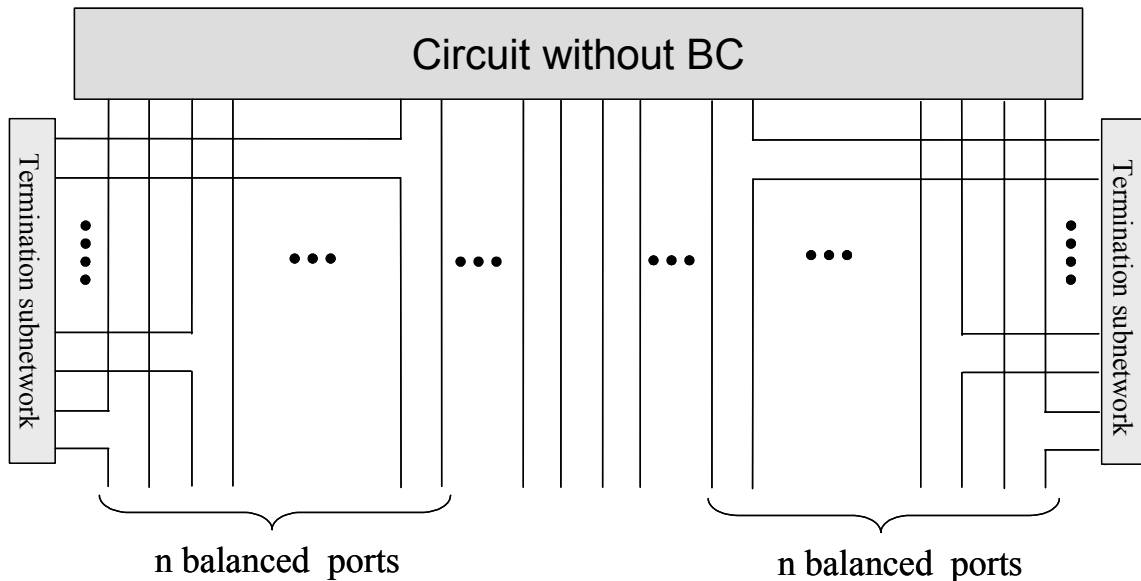


Figure 2-49: Connection of the termination sections for the one node to one port $\frac{dF}{dt} \rightarrow \Phi$ synthesis.

The procedure described above gives us a methodology to evaluate all the correct BCs for the one node to one port mapping, in fact equating the elements of the two matrices one to one we obtain a well posed linear system of $(n + 1)\frac{n}{2}$ equations in $(n + 1)\frac{n}{2}$ unknowns. In particular the unknowns will be associated with the nominal values of the elements (i.e. Γ_{ij} $i = 1..n$ and $j = i..n$) while the note terms of the system will be the $(n + 1)\frac{n}{2}$ rational function of the parameters γ_i for $i = 1..n$ introduced in the previous subsection. This means that solving the linear system we will find the most general values for the needed components as a function of the parameter γ_i for $i = 1..n$. The actual values for each particular BC will be obtained by taking the limit for $\gamma_i \rightarrow 0$ or $\gamma_i \rightarrow \infty$ for $i = 1..n$. Some examples of this procedure will be given in the following chapter.

Chapter 3

External characterization of a transducer

3.1 Introduction

In this section we will introduce a circuital model of a transducers. More precisely we will model a transducer as a device able to "read" a given signal having an assigned physical dimension from an access point of a given system and to "write" a new signal proportional to the read one but having different physical dimensions. In this chapter we will introduce different circuital models for a transducers. Each one of this models will include more characteristics than the previous one. First of all we will give a model for a unidirectional transducer as two ports hybrid network capable to modify the physical nature of a signal. Then we will describe a bidirectional ideal transducer as a two ports network able to realize a transduction in both the directions simultaneously. Then in order to produce a more realistic model of real device we will include in the model of an ideal bidirectional transducer some parasitic elements taking in count for the physical properties of the real device. Then we will dedicate some comment on the possibility to neglect the asymmetries of the real transducers. In chapter 5 we will show how this symmetrization can be fruitfully used in order to realize a coupled system. Finally we will give some example of transducer starting from the equations describing the physical phenomenon of interest and deriving from them the circuital model for the correspondent transducer

3.2 Unidirectional ideal transducers

3.2.1 Introduction

As we have said in the introduction a unidirectional transducer is a two port network able to perform a conversion from the pair (Π_1, Φ_1) having a given physical dimension to the pair (Π_2, Φ_2) having, in general, different physical dimensions. It must be noted that the read quantity could be Π_1 or the Φ_1 but not both of them. Similarly the written quantity could be Π_2 or the Φ_2 but not both of them. The previous argumentation makes clear that it will be possible to characterize a unidirectional transducer in four different ways.

3.2.2 Y-configuration

A *Y* unidirectional ideal transducer is a device able to read the quantity Π_1 without producing any side effect on the pair (Π_1, Φ_1) characterizing the port where the device is connected and to produce at the port 2 a signal Φ_2 proportional with the signal Π_1 . In fig. (3-1) is shown the equivalent circuit for this device.

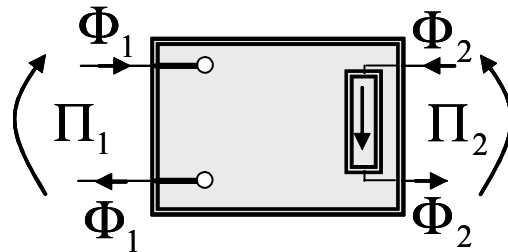


Figure 3-1: Unidirectional ideal transducer. Y-configuration.

$$\begin{cases} \Phi_2 = y_{21}\Pi_1 \\ \Phi_1 = 0 \\ \Pi_2 \text{ not specified} \end{cases} \quad (3.1)$$

3.2.3 Z-configuration

A Z unidirectional ideal transducer is a device able to read the quantity Π_1 without producing any side effect on the pair (Π_1, Φ_1) defining the port where the device is connected and to produce at the port 2 a signal Π_2 proportional with the signal Π_1 . In fig. (3-2) is shown the equivalent circuit for this device.

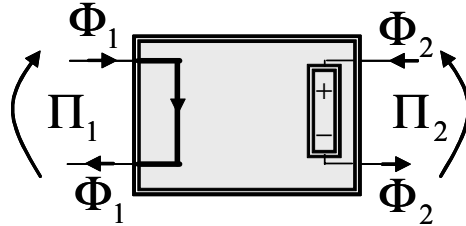


Figure 3-2: Unidirectional ideal transducer. Z-configuration.

$$\begin{cases} \Pi_2 = z_{21}\Phi_1 \\ \Pi_1 = 0 \\ \Phi_2 \text{ not specified} \end{cases} \quad (3.2)$$

3.2.4 G-configuration

A G unidirectional ideal transducer is a device able to read the quantity Φ_1 without producing any side effect on the pair (Π_1, Φ_1) characterizing the port where the device is connected and to produce at the port 2 a signal Π_2 proportional with the signal Φ_1 . In fig. (3-3) is shown the equivalent circuit for this device.

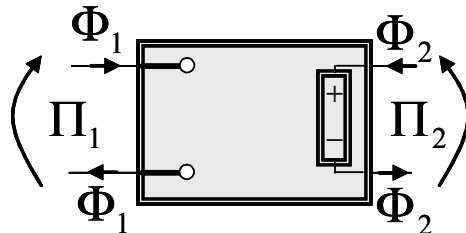


Figure 3-3: Unidirectional ideal transducer. G-configuration.

$$\begin{cases} \Pi_2 = g_{21}\Pi_1 \\ \Phi_1 = 0 \\ \Phi_2 \text{ not specified} \end{cases} \quad (3.3)$$

3.2.5 H-Configuration

A H unidirectional ideal transducer is a device able to read the quantity Φ_1 without producing any modification at the pair (Π_1, Φ_1) defining the port where the device is connected and to produce at the port 2 a signal Φ_2 proportional with the signal Φ_1 . In fig. (3-4) is shown the equivalent circuit for this device.

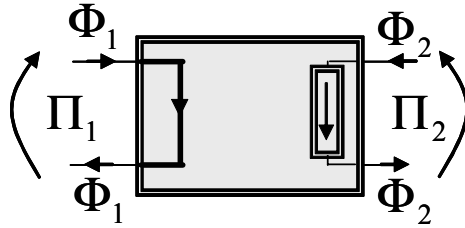


Figure 3-4: Unidirectional ideal transducer. H-configuration.

$$\begin{cases} \Phi_2 = h_{21}\Phi_1 \\ \Pi_1 = 0 \\ \Pi_2 \text{ not specified} \end{cases} \quad (3.4)$$

3.3 Bidirectional ideal transducers

3.3.1 Introduction

As we have said in the introduction a bidirectional ideal transducer is a two ports network able to perform a bidirectional communication between the two ports of the system. More precisely we can say that this device produces at a port a signal proportional to another signal read at the other port. Simultaneously it writes at the latter port the complementar signal proportional

to the signal complementary to the one written at the first port. Again we have four different representations for this device.

3.3.2 Y-configuration

A Y bidirectional ideal transducer is a device able to read the quantity Π_1 at the first port and to produce at the second port a signal Φ_2 proportional with the signal Π_1 . Simultaneously it is able to read the quantity Π_2 at the second port and to produce at the first port a signal Φ_1 proportional with the signal Π_2 . In fig. (3-5 a) is shown the equivalent circuit for this device while in fig. (3-5 b) is shown its circuitual symbol.

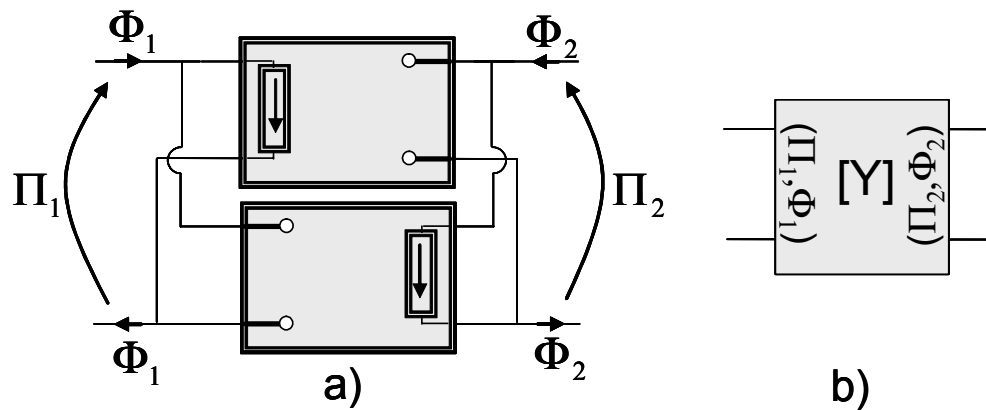


Figure 3-5: Bidirectional ideal transducer. Y -configuration. a) Complete circuitual model. b) Circuitual symbol.

$$\begin{cases} \Phi_1 = y_{12}\Pi_2 \\ \Phi_2 = y_{21}\Pi_1 \end{cases} \quad (3.5)$$

3.3.3 Z-configuration

A Z bidirectional ideal transducer is a device able to read the quantity Φ_1 at the first port and to produce at the second port a signal Π_2 proportional with the signal Φ_1 . Simultaneously it is able to read the quantity Π_2 at the second port and to produce at the first port a signal Φ_1

proportional with the signal Φ_2 . In fig. (3-6 a) is shown the equivalent circuit for this device while in fig. (3-6 b) is shown its circuital symbol.

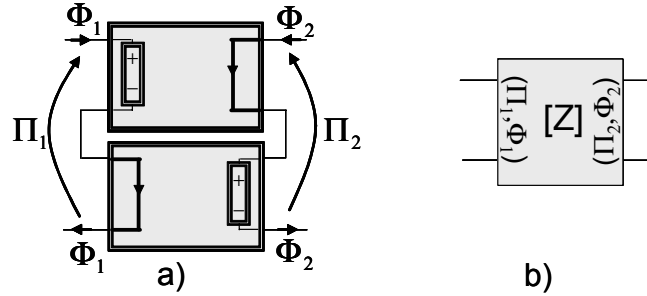


Figure 3-6: Bidirectional ideal transducer. Z -configuration. a) Complete circuital model. b) Circuital symbol.

$$\begin{cases} \Pi_1 = z_{12}\Phi_2 \\ \Pi_2 = z_{21}\Phi_1 \end{cases} \quad (3.6)$$

3.3.4 G-configuration

A G bidirectional ideal transducer is a device able to read the quantity Π_1 at the first port and to produce at the second port a signal Π_2 proportional with the signal Π_1 . Simultaneously it is able to read the quantity Φ_2 at the second port and to produce at the first port a signal Φ_1 proportional with the signal Φ_2 . In fig. (3-7 a) is shown the equivalent circuit for this device while in fig. (3-7 b) is shown its circuital symbol.

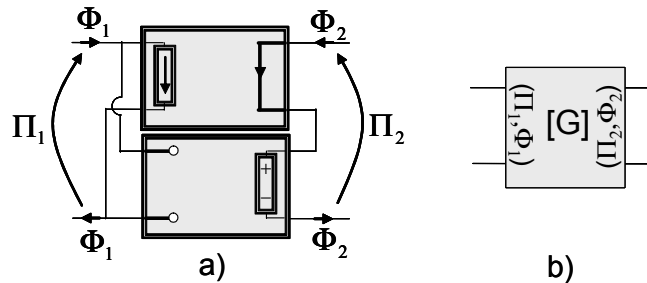


Figure 3-7: Bidirectional ideal transducer. G -configuration. a) Complete circuital model. b) Circuital symbol.

$$\begin{cases} \Phi_1 = g_{12}\Phi_2 \\ \Pi_2 = g_{21}\Pi_1 \end{cases} \quad (3.7)$$

3.3.5 H-Configuration

A H bidirectional ideal transducer is a device able to read the quantity Φ_1 at the first port and to produce at the second port a signal Φ_2 proportional with the signal Φ_1 . Simultaneously it is able to read the quantity Π_2 at the second port and to produce at the first port a signal Π_1 proportional with the signal Π_2 . In fig. (3-8 a) is shown the equivalent circuit for this device while in fig. (3-8 b) is shown its circuitual symbol.

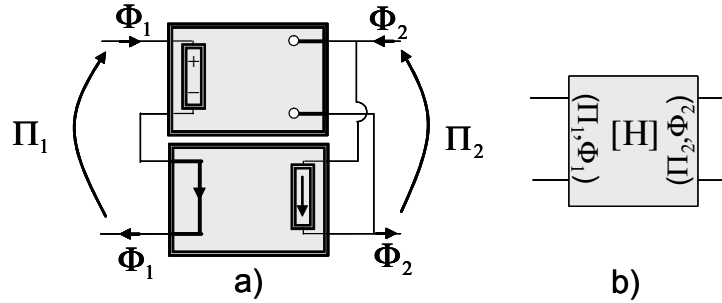


Figure 3-8: Bidirectional ideal transducer. H -configuration. a) Complete circuitual model. b) Circuitual symbol.

$$\begin{cases} \Pi_1 = h_{12}\Pi_2 \\ \Phi_2 = h_{21}\Phi_1 \end{cases} \quad (3.8)$$

3.4 Bidirectional real transducers

3.4.1 Introduction

As we have said in the introduction a bidirectional real transducer is a two port network able to provide a more detailed circuitual model of a real component. It can be obtained by connecting some parasitic element to both the ports of an ideal bidirectional transducer taking into account

for a bipolar linear constitutive relation i.e. an (α, β) element. Again we have four different representation for this device.

3.4.2 Y-configuration

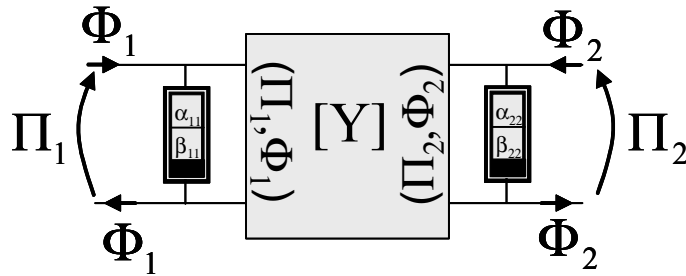


Figure 3-9: Bidirectional real transducer. Y-configuration.

$$\begin{cases} \Phi_1 = y_{11}\Pi_1 + y_{12}\Pi_2 \\ \Phi_2 = y_{21}\Pi_1 + y_{22}\Pi_2 \end{cases} \quad (3.9)$$

3.4.3 Z-configuration

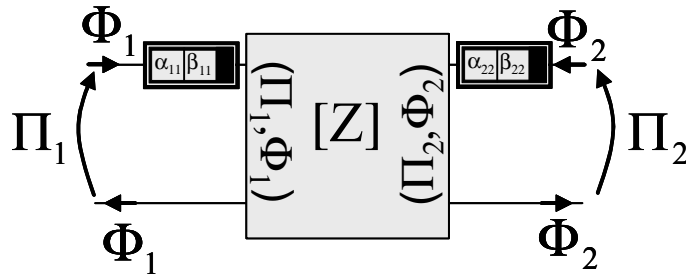


Figure 3-10: Bidirectional real transducer. Z-configuration.

$$\begin{cases} \Pi_1 = z_{11}\Phi_1 + z_{12}\Phi_2 \\ \Pi_2 = z_{21}\Phi_1 + z_{22}\Phi_2 \end{cases} \quad (3.10)$$

3.4.4 G-configuration

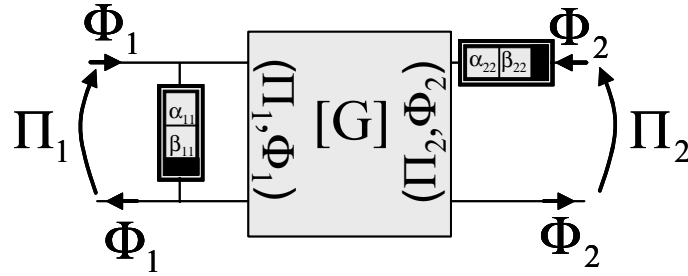


Figure 3-11: Bidirectional real transducer. *G*-configuration.

$$\begin{cases} \Phi_1 = g_{11}\Pi_1 + g_{12}\Phi_2 \\ \Pi_2 = g_{21}\Pi_1 + g_{22}\Phi_2 \end{cases} \quad (3.11)$$

3.4.5 H-Configuration

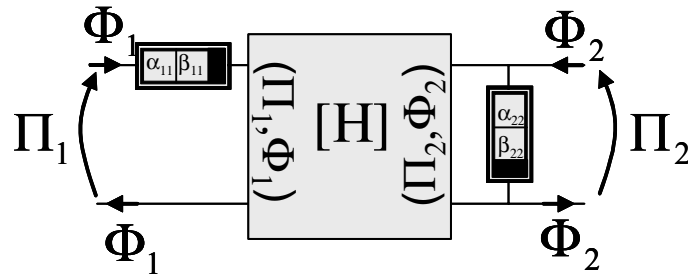


Figure 3-12: Bidirectional real transducer. *H*-configuration.

$$\begin{cases} \Pi_1 = h_{11}\Phi_1 + h_{12}\Pi_2 \\ \Phi_2 = h_{21}\Phi_1 + h_{22}\Pi_2 \end{cases} \quad (3.12)$$

3.5 Constitutive symmetry of real transducers

3.5.1 Introduction

In this subsection we will introduce a special kind of symmetry. This symmetry is needed to describe how the parasite element connected at the first port of a real transducer depends on the Laplace variable compared with the one connected at the second port. This notion is based on the idea that a real transducer is symmetrizable when the ratio between the parasite element at the first port and the one at the second port of a real transducer is independent of the Laplace variable s . When this happens it is possible to connect to the first or the second port an extra parasite element of equal constitutive nature in order to make the ratio equal to one. As usual, it is possible to put in evidence four different kinds of constitutive symmetrization.

3.5.2 Y-symmetrization

Using the idea described above the Y -symmetrization can be obtained by shunting an extra $(\alpha_{11}, \beta_{11})$ element of value \bar{R}_{11} to the first port and an extra $(\alpha_{22}, \beta_{22})$ element of value \bar{R}_{22} to the second port, as shown in fig. (3-13).

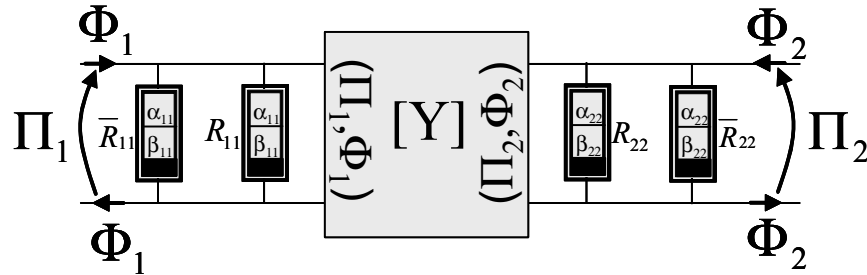


Figure 3-13: Circuitual scheme for the Y -symmetrization of a real bidirectional transducer.

The Y -symmetrization procedure requires the fulfillment of the following constraint equations:

$$\alpha_{11} - \beta_{11} - \alpha_{22} + \beta_{22} = 0 \quad (3.13)$$

$$\frac{1}{R_{11}} + \frac{1}{\bar{R}_{11}} = \frac{1}{R_{22}} + \frac{1}{\bar{R}_{22}} \quad (3.14)$$

It is quite obvious that there exist many ways to satisfy eq. (3.14) from an analytical point of view, even if in the practice it could be hard to modify the physical properties of the transducer. By the way we will show in the fifth chapter how the notion of symmetrization of a real transducer can be fruitfully used.

3.5.3 Z-symmetrization

Similarly the Z -symmetrization can be obtained by connecting an extra $(\alpha_{11}, \beta_{11})$ element of value \bar{R}_{11} in series to the first port and an extra $(\alpha_{22}, \beta_{22})$ element of value \bar{R}_{22} in series to the second port, as shown in fig. (3-14)

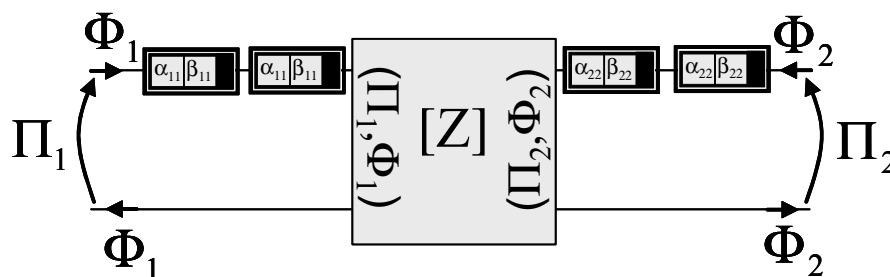


Figure 3-14: Circuital scheme for the Z -symmetrization of a real bidirectional transducer.

The Z -symmetrization procedure requires the fulfillment of the following constraint equations:

$$\alpha_{11} - \beta_{11} - \alpha_{22} + \beta_{22} = 0 \quad (3.15)$$

$$R_{11} + \bar{R}_{11} = R_{22} + \bar{R}_{22} \quad (3.16)$$

It is quite obvious that there exist many ways to satisfy eq. (3.16) for an analytical point of view, even if in the practice it could be hard to modify the physical properties of the transducer. By the way we will show in the fifth chapter how the notion of symmetrization of a real transducer can be fruitfully used.

3.5.4 G-symmetrization

Similarly the G -symmetrization can be obtained by shunting an extra $(\alpha_{11}, \beta_{11})$ element of value \bar{R}_{11} to the first port and by connecting an extra $(\alpha_{22}, \beta_{22})$ element of value \bar{R}_{22} in series

to the second port, as shown in fig. (3-15).

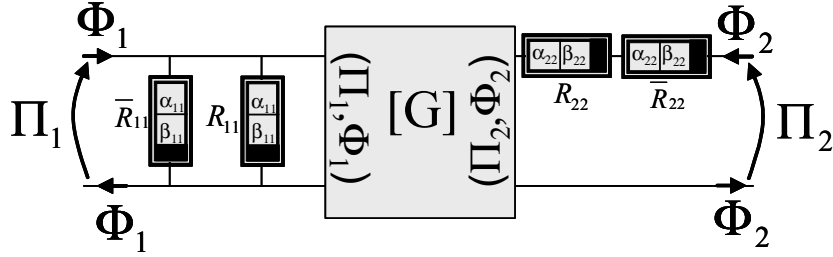


Figure 3-15: Circuitual scheme for the G -symmetrization of a real bidirectional transducer..

The G -symmetrization procedure requires the fulfillment of the following constraint equations

$$\alpha_{11} - \beta_{11} + \alpha_{22} - \beta_{22} = 0 \quad (3.17)$$

$$\frac{1}{R_{11}} + \frac{1}{\bar{R}_{11}} = R_{22} + \bar{R}_{22} \quad (3.18)$$

It is quite obvious that there exist many ways to satisfy eq. (3.18) for an analytical point of view, even if in the practice it could be hard to modify the physical properties of the transducer. By the way we will show in the fifth chapter how the notion of symmetrization of a real transducer can be fruitfully used.

3.5.5 H-symmetrization

Using the idea described above the H -symmetrization can be obtained by connecting an extra $(\alpha_{11}, \beta_{11})$ element of value \bar{R}_{11} in series to the first port and by shunting an extra $(\alpha_{22}, \beta_{22})$ element of value \bar{R}_{22} to the second port, as shown in fig. (3-16).

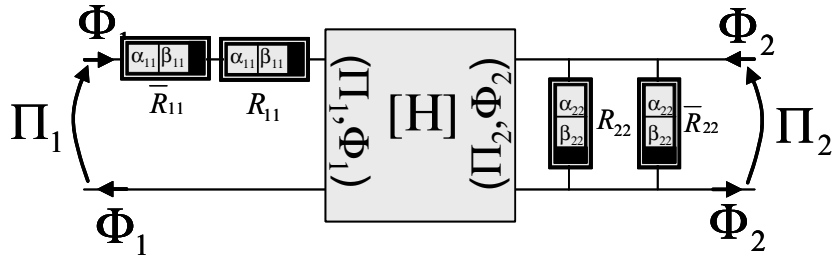


Figure 3-16: Circuitual scheme for the H -symmetrization of a real bidirectional transducer.

The H -symmetrization procedure requires the fulfillment of the following constraint equations

$$\alpha_{11} - \beta_{11} + \alpha_{22} - \beta_{22} = 0 \quad (3.19)$$

$$R_{11} + \overline{R}_{11} = \frac{1}{R_{22}} + \frac{1}{\overline{R}_{22}} \quad (3.20)$$

It is quite obvious that there exist many ways to satisfy eq. (3.20) from an analytical point of view, even if in the practice it could be very to modify the physical properties of the transducer by the way we will show in the fifth chapter how the notion of symmetrization of a real transducer can be fruitfully used.

3.6 Examples

3.6.1 A pinned rigid link

In the previous chapter we briefly discuss the constitutive relation of a two-ports system, there we gave the constitutive equations for a generalized lever. In table (2-1) we gave some example of generalized lever when its two ports are characterized by the same pair, here we give a new interpretation for a generalized lever when its two ports are characterized by different pairs. For example when the pair $(\Pi_1, \Phi_1) = (v, F)^1$ and the quantity n has the physical dimension of a length $[m]$ the second port will be characterized by the pair $(\Pi_2, \Phi_2) = (\omega, M)$ and the system will represent a rigid link pinned at one of its ends and free to slide on the other end. This simple system is shown in fig. (3-17).

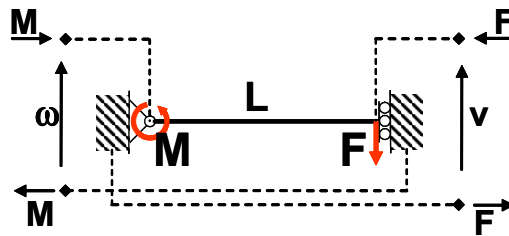


Figure 3-17: Mechanical model of a force moment transducer.

¹A Π quantity must be associated with an incremental quantity, for example the velocity v_1 of a point with respect to the velocity v_2 of a different point. So it should be correctly indicated with the notation $\Delta v = v_1 - v_2$. By the way in those notes we will omit the symbol Δ .

When we apply a force on the end free to slide, we obtain a couple proportional to the applied force on the pinned end, while the force needed for the equilibrium is supplied by the ground holding the pin which forms an unbalanced port with the slider. Similarly, if we apply a couple at the pinned end, we produce a force at the end free to slide, while the couple need for the balance is supplied by the ground holding the slider which forms an unbalanced port with the pin. Moreover the angular velocity of the rigid link around the pin is proportional to the translation velocity of the slider. The linearized constitutive equation for the physical device described above are given by:

$$\begin{cases} v = -L\omega \\ M = LF \end{cases} \quad (3.21)$$

Based on the consideration exposed in the previous sections of this chapter we will give a new interpretation of this element. In fact looking at equation (3.8) it is quite easy to realize that it behaves exactly as an ideal bidirectional H transducer, so we will represent it with the circuitual symbol shown in fig. (3-18). In the figure is put in evidence the unbalanced nature of the ports. It should be noted that as we say above, from a theoretical point of view, we need to use two different reference grounds one for the angle and one for the position. In the following subsection we will show how it is possible to design an unbalanced force to couple transducers.

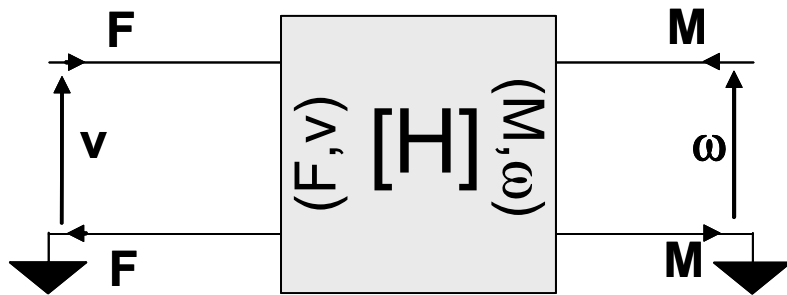


Figure 3-18: Force couple transducers, H model.

The ideality of the transducers achieve from the ideality of the pivot and of the slider. If those constraints will be not ideal we should include some parasitic element taking in count for those non idealities.

3.6.2 Balanced force to couple transducers

In this subsection we will design a balanced force to couple transducers. It can be obtained by the scheme shown in fig. (3-19) where two different unbalanced transducers are connected by means of two rigid links, one holding the two pivot and the other holding the two slider. Those links transmit the force and the couple respectively, realizing a series connection.

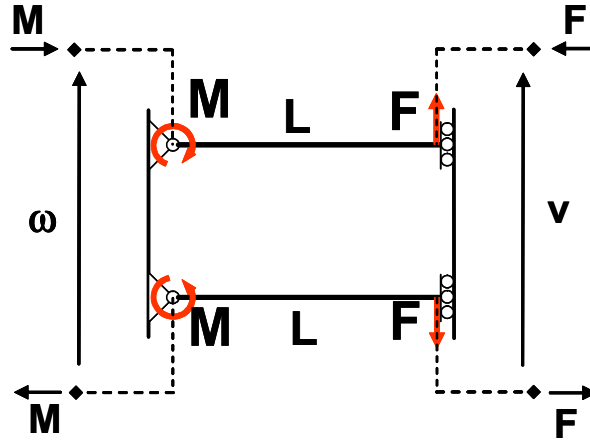


Figure 3-19: Balanced force couple transducer.

It should be noted that this system is able to transduce a balanced force into a balanced couple. The two rigid links are needed in order to "conduct" the force and the couple, by the way they are always balanced and don't need to be connected to the ground in order to work correctly. The argumentation produced above make clear why the mechanical system shown in fig. (3-19) behaves as an ideal bidirectional H transducer. the circuitual symbol of this device is shown in fig. (3-20).

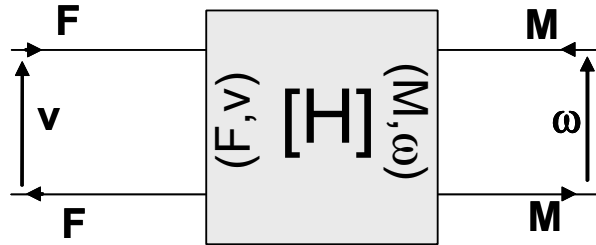


Figure 3-20: Balanced force couple transducer. H model.

3.6.3 Piezoelectric transducers

In this sub section we will introduce a huge class of transducers which functioning is based on the piezoelectric property of some materials. A complete description of a piezoelectric transducer should include an introduction to the linear piezoelectricity. By the way, the aim of this work is to give a circuital interpretation of the physical devices so that we will restrict our tractation to furnish the pointwise constitutive equation for a piezoelectric crystal without deriving them. A quite complete tractation of the phenomena can be found in [IEEE std. 246]. As usual, those equations can be given in four different forms listed below:

$$\begin{cases} T_{ij} = c_{ijkl}^E - e_{kij}E_k \\ D_i = e_{ikl}S_{kl} + \epsilon_{ij}^S E_k \end{cases} \quad (3.22)$$

$$\begin{cases} S_{ij} = s_{ijkl}^E + d_{kij}E_k \\ D_i = d_{ikl}T_{kl} + \epsilon_{ij}^T E_k \end{cases} \quad (3.23)$$

$$\begin{cases} S_{ij} = s_{ijkl}^D T_{kl} + g_{kij}D_k \\ E_i = -g_{ikl}T_{kl} + \beta_{ik}^T D_k \end{cases} \quad (3.24)$$

$$\begin{cases} T_{ij} = c_{ijkl}^D S_{kl} - h_{kij}D_k \\ E_i = -h_{ikl}S_{kl} + \beta_{ik}^S D_k \end{cases} \quad (3.25)$$

Where T and S are respectively the second order stress and strain tensors, c^D (s^D) and c^E (s^E) are fourth order elastic stiffness (compliance) tensor measured keeping respectively the electric displacement D and electric field E constant. Finally e, d, g, h represent different forms of the third order piezoelectricity tensor. Those expression of the constitutive equations, although exact, are employed in approximations which are valid under certain limiting circumstances. The utility of each pair of constitutive equations depends on the fact that certain variables on the right hand side are close to zero under some circumstances. Consequently, the proper set to use in a given problem is dependent on the actual mechanical and electrical configuration. In the case of interest described in fig. (3-21), where is shown a thin lamina of piezoelectric material having length l_p (along x_1) width w_p (along x_2).and thickness h_p (along x_3). For this system we can assume that the stress tensor and the electric field vector assumes the following form (for

more details see [Crawley et al. (1987)],[Hagood et al. (1991)],[Hanagud et al. (1992)]:

$$T = \begin{pmatrix} T_{11} & 0 & T_{13} \\ 0 & 0 & 0 \\ T_{31} & 0 & 0 \end{pmatrix}, \quad E = \begin{pmatrix} 0 \\ 0 \\ E_3 \end{pmatrix} \quad (3.26)$$

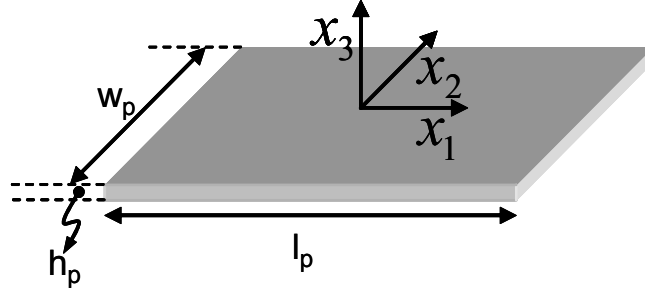


Figure 3-21: A thin lamina of a piezoelectric crystal having a metallization on the top and the bottom faces.

Once the constitutive equations (3.23) are given using the Voigth notation and the hypothesis (3.26) are assumed we obtain the following one dimensional constitutive equation:

$$\begin{cases} S_{11} = s_{11}^E T_{11} - d_{31} E_3 \\ D_3 = -d_{31} T_{11} + \epsilon_{33}^T E_3 \end{cases} \quad (3.27)$$

In the following subsection we will describe how the pointwise constitutive equation (3.27) can be used in order to design some actuators able to transduce extensional, bending and torsional vibrations.

Extensional piezo transducers

Referring to fig. (3-21) we can obtain an extensional transducer by applying metallization of negligible thickness on the top and the bottom bases of the piezoelectric lamina forming an electrical port. Similarly we can use the left and the right faces (along x_1) of the crystal as the two access points of a mechanical port as shown in fig. (3.22).

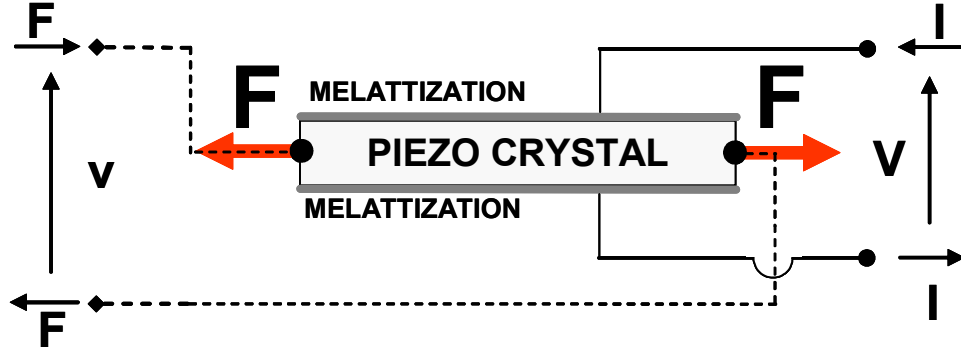


Figure 3-22: Extensional piezoelectric transducer. Physical device.

Based on the assumption (3.26) and on the geometry of the device we can derive the following relation:

$$S_{11} = \frac{x_1}{l_p}, \quad T_{11} = \frac{F}{w_p h_p}, \quad E_3 = \frac{V}{h_p} \quad \text{and} \quad D_3 = \frac{Q}{l_p w_p} \quad (3.28)$$

where, with abuse of notation, x_1 is the elongation along x_1 and F is the force applied to the mechanical port., while V and Q are the voltage and the charge at the electrical port. Substituting eq. (3.28) in eq.(3.27) and choosing F and Q as dependent variables we obtain the following integral constitutive equations:

$$\begin{cases} F = \frac{h_p w_p}{l_p s_{11}^E} x_1 + \frac{d_{31} w_p}{s_{11}^E} V \\ Q = -\frac{d_{31} w_p}{s_{11}^E} x_1 + \frac{l w_p}{h_p} \left(\frac{s_{11}^E \epsilon_{33}^T - d_{31}^2}{s_{11}^E} \right) V \end{cases} \quad (3.29)$$

Taking the Laplace transform of the equations above they can be expressed as a function of the pairs (F, v) and (I, V) by:

$$\begin{cases} F = y_{11}(s)v + y_{12}(s)V \\ I = y_{21}(s)v + y_{22}(s)V \end{cases} \quad (3.30)$$

where v is the elongation velocity along x_1 and I is the electrical current. Moreover we have:

$$y_{11}(s) = \frac{1}{s} \frac{h_p w_p}{l_p s_{11}^E}, \quad y_{12}(s) = \frac{d_{31} w_p}{s_{11}^E}, \quad y_{21}(s) = -\frac{d_{31} w_p}{s_{11}^E} \quad \text{and} \quad y_{22}(s) = s \frac{l w_p}{h_p} \left(\frac{s_{11}^E \epsilon_{33}^T - d_{31}^2}{s_{11}^E} \right) \quad (3.31)$$

Comparing equation (3.30) with eq. (3.9) it easy to understand that an extensional real transducer can be interpreted as a real bidirectional transducer having as parasitic effect an (0, 1) element at the mechanical port (i.e. an extensional spring) and a (1, 0) element at the electrical port (i.e. a capacitor), as shown in fig. (3-23).

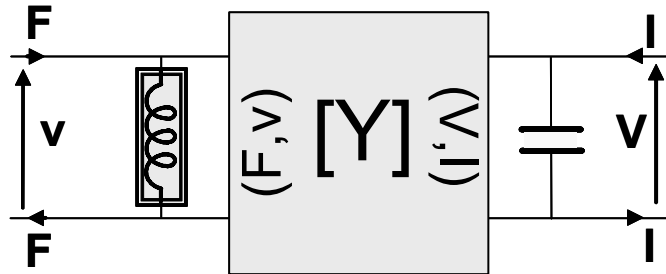


Figure 3-23: Equivalent circuit for an extensional piezoelectric transducer.

Bending piezo transducers

A bending transducer is a system able to transduce the pair $(\Delta\omega, M)$ in the pair $(\Delta V, I)$ (and vice versa). It can be obtained by means of the physical device shown in fig.(3-24).

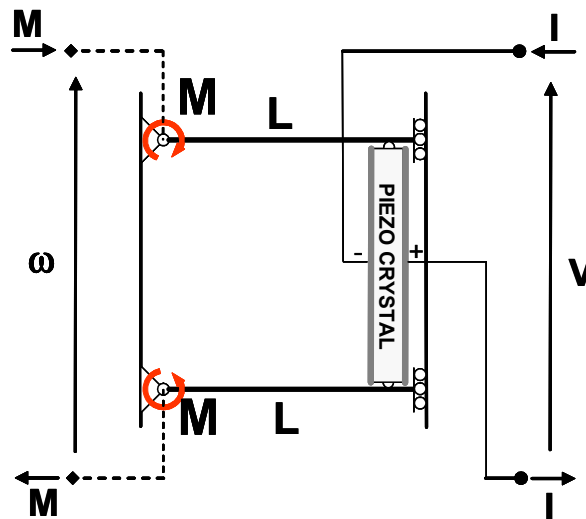


Figure 3-24: Bending piezoelectric transducers. Physical model.

Looking at figure (3-24) it can be realized that this transducer can be built by connecting an extensional piezoelectric transducer between the two sliders of a balanced force to couple transducers. In the figure is shown the polarity of the piezoelectric lamina. This quantity is related to the sign of the transduction coefficient. This connection forces the ends of the piezoelectric lamina to move together with the slider, moreover the force is transmitted from the slider to the piezo actuator. The situation described above can be interpreted as the chain connection between a balanced force to couple transducers and an extensional piezoelectric transducer as shown in fig. (3-25).

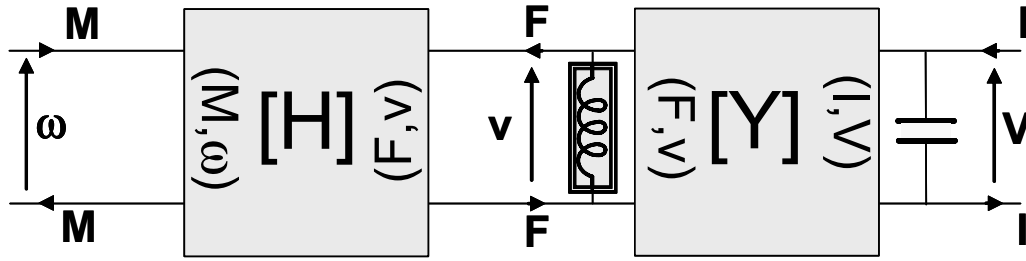


Figure 3-25: Bending piezoelectric transducers as the cascade of basic element.

Applying the classical technique of the circuit theory we can derive an external characterization of the circuit shown in fig. (3-25). For example the Y model of the circuit can be expressed by means of the following relations

$$\begin{cases} M = y_{11}(s)\Delta\omega + y_{12}(s)\Delta V \\ I = y_{21}(s)\Delta\omega + y_{22}(s)\Delta V \end{cases} \quad (3.32a)$$

where:

$$y_{11}(s) = \frac{1}{s} \frac{h^2 h_p w_p}{4 l_p s_{11}^E}, \quad y_{12}(s) = \frac{h d_{31} w_p}{2 s_{11}^E}, \quad y_{21}(s) = -\frac{h d_{31} w_p}{2 s_{11}^E} \quad (3.33)$$

$$\text{and } y_{22}(s) = s \frac{l_p w_p}{h_p} \left(\frac{s_{11}^E \epsilon_{33}^T - d_{31}^2}{s_{11}^E} \right)$$

Comparing equation (3.32a) with eq. (3.9) it is quite easy to understand that a bending transducers is a bidirectional real transducer having as parasitic component an $(0, 1)$ element on the mechanical port (i.e. an bending spring) and an $(1, 0)$ element at the electrical port (i.e.

a capacitance). The circuitual symbol for this device is shown in fig. (3-26).

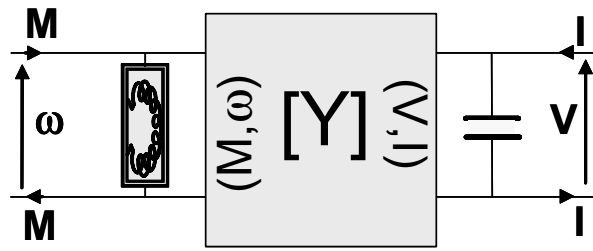


Figure 3-26: Equivalent circuit for a bending piezoelectric transducer. Y model.

The system described in this section performs as we expect, by the way its functioning requires the presence of the rigid link holding the pivots needed in order to transmit the force from one side to the other of the system. In some application it could be needed to replace this link with a deforming body. In this situation two pivots become an access port for the pair (F, v) as well as for the pair (M, ω) . Sometimes this extra transduction is not desired and must be considered as a side effect. In the following section we will show how to realize a pure bending transducer.

Pure bending piezoelectric actuator

A system able to produce a pure bending transduction can be obtained by means of the scheme shown in fig. (3-27)

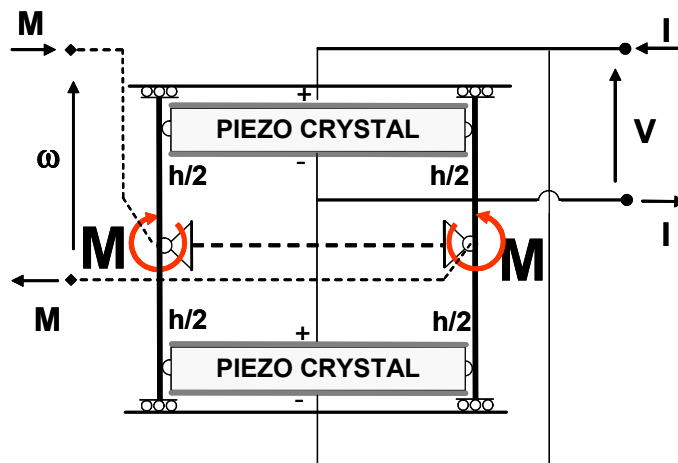


Figure 3-27: Pure bending piezoelectric transducer. Physical model.

This system can be obtained by connecting two bending transducers taking care of keeping the two piezoelectric transducers with an inverse polarity. The two actuators must be connected imposing to the rigid link of the first transducer to rotate together with the ones of the second transducers. This mechanical connection can be obtained by shunting the mechanical port of the two transducers. This connection guarantees that the rigid link holding the two pivot is stress free and consequently it can be removed. Simultaneously, it can be easily realized that by shunting the electrical ports of the two transducers we obtain a connection coherent with the polarization of the piezoelectric. The situation described above can be interpreted as the shunt between two bending piezoelectric transducers as shown in fig. (3-28).

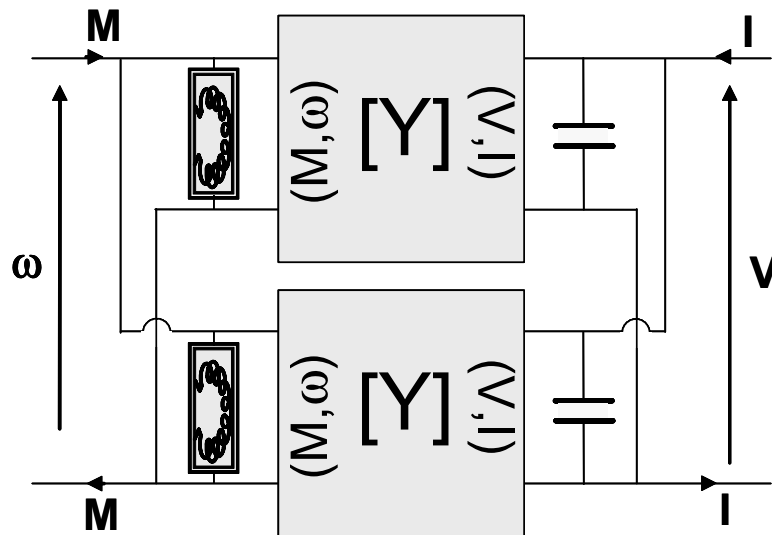


Figure 3-28: Pure bending transducers as the cascade of basic elements.

The equivalent circuit of the whole system is shown in fig. (3-26) while the parameters y_{11} , y_{12} , y_{21} and y_{22} defining the circuit can be obtained by doubling the values given in (3.33).

Torsional piezo transducers

As a last example we will describe a torsional piezoelectric transducer. It can be obtained by means of the physical device shown in fig. (3-29).

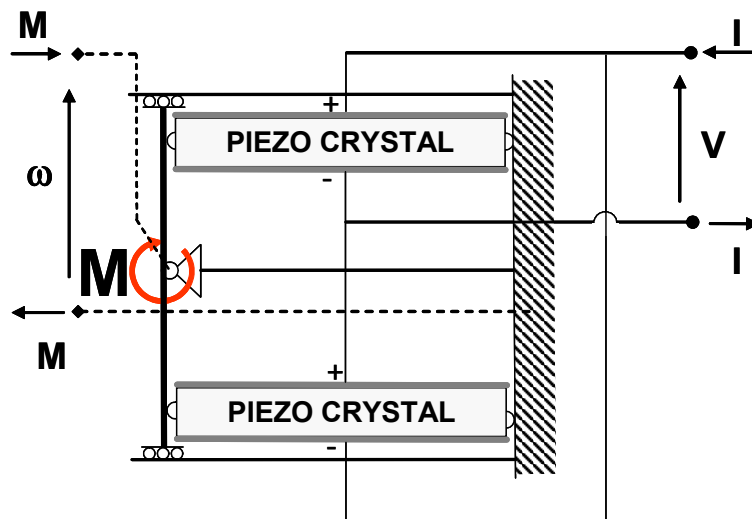


Figure 3-29: Torsional piezoelectric transducer. Physical model.

It is easy to realize that a torsional piezoelectric transducers can be obtained by referring to the ground the mechanical port of the pure bending transducer. Consequently its equivalent circuit can be obtained by referring the angular velocity ω (characterizing the mechanical port) to ground. As shown in fig. (3-30).

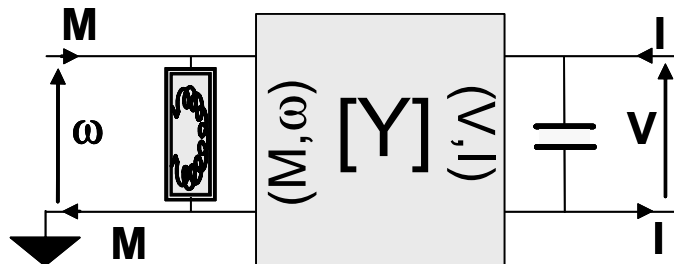


Figure 3-30: Equivalent circuit for a torsional piezoelectric transducer. Y model.

It should be noted that, from a theoretical point of view, in this case we should refer to the symbol M as the twisting moment instead of bending moment and we should interpret the parasitic element on the mechanical port as a torsion spring instead of a bending spring. By the way, this is exclusively a theoretical clarification.

Chapter 4

Derivation of some applications.

4.1 Introduction

In this chapter we will apply the theory developed in the previous chapters to some cases of interest. First of all we will derive the needed circuit including the termination subnetwork taking in count for the most general BC for the cases $n = 0$ $n = 1$ and $n = 2$ and for all the possible kind of synthesis proposed. This general derivation should remark that the circuitual scheme obtained and the nominal values of the components are still independent from the application. The only thing that changes from an application to the other is the physical meaning of the quantity characterizing the ports of the circuits and the interpretation of the components. Obviously a similar analysis can be performed for larger values of n .

4.2 Derivation of the zero order networks.

The equation governing the evolution of a discrete zero order ondulatory phenomena can be obtained by choosing $n = 0$ in eq. (2.1) that will assume the following form:

$$KF_k^{(0)}(t) + (-1)^0 \rho \frac{d^2 F_k(t)}{dt^2} = 0 \quad (4.1)$$

When $n = 0$ doesn't exist any interaction between the node of the mesh, consequently doesn't exist any special requirement (i.e. BC) for the termination node of the spatial domain. This means that in this case we can simply use the one node to one port mapping without lack of

generality. The circuit obtained for the one node to one port synthesis are been derived in the second chapter. The circuit obtained for the $\frac{dF}{dt} \rightarrow \Pi$ synthesis is shown in fig. (2-16) while the one obtained for the $\frac{dF}{dt} \rightarrow \Phi$ synthesis is shown in fig. (2-20). In fig (4-1) we will show those two synthesis when the time derivative are realized using (1,0) and (0,1) elements.

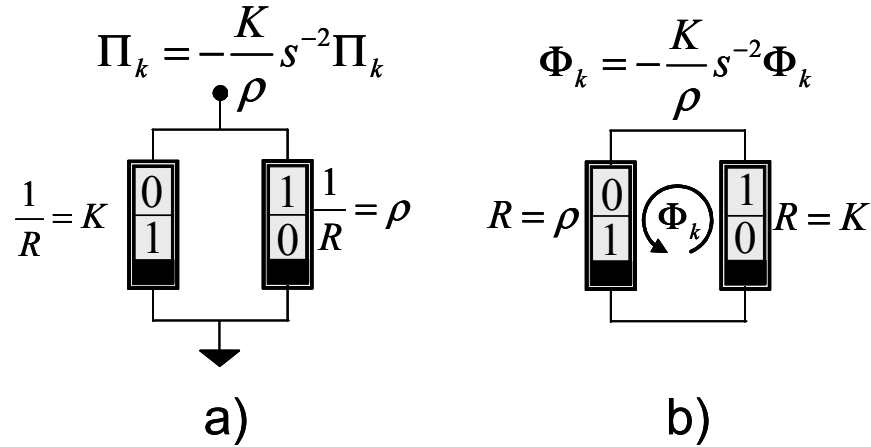


Figure 4-1: One node to one port synthesis for $n = 0$. a) $\frac{dF}{dt} \rightarrow \Pi$ b) $\frac{dF}{dt} \rightarrow \Phi$.

In the following subsection we will give some examples of zero order ondulatory phenomena (i.e. harmonic oscillators).

4.3 Some example of zero order networks

4.3.1 Mass-spring oscillator.

The Mass-spring oscillator can be derived by the general zero order theory by the following interpretation of the general parameter:

General descriptor	Actual descriptor	Physical meaning
$F(x, t)$	$u(x, t)$	displacement
K	k	stiffness
ρ	m	mass

Table 4-1

Over this condition the equation 4.1 becomes:

$$ku_k(t) + m \frac{d^2 u_k(t)}{dt^2} = 0 \quad (4.2)$$

The physical system can be represented by means of a pointwise mass m joined to the ground by means of an extensional spring k , as shown in fig. (4-2).

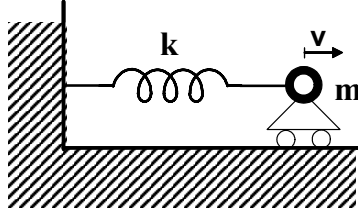


Figure 4-2: Mass-Spring hoscillator.

$\frac{dF}{dt} \rightarrow \Pi$ **synthesis**

In this section we will give an actual meaning to the components and the physical quantity governing the evolution of the general zero order circuit shown in fig. (4-1). As reported in table 4-1 the scalar field $F(x, t)$ is associated with the displacement $u(x, t)$ so that the intensive quantity Π_k of the k^{th} node will be associated with the velocity v_k . Consequently the complementar extensive quantity will be associated with the force T_k . Based on those argumentations using table 2-1 it is possible to specify the general circuit shown in fig. (4-1 a) for the case of interest as shown in fig 4-3.

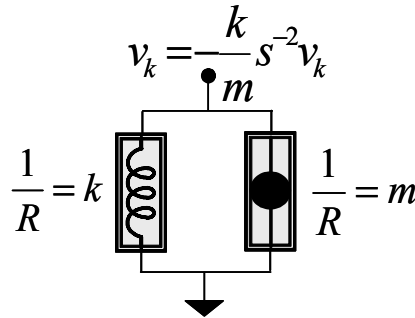


Figure 4-3: Equivalent circuit of a mass.spring hoscillator using the one node to one port

$\frac{dF}{dt} \rightarrow \Pi$ synthesis.

$\frac{dF}{dt} \rightarrow \Phi$ synthesis

In this section we will give an actual meaning to the components and the physical quantity governing the evolution of the general zero order circuit shown in fig. (4-1). As reported in table 4-1 the scalar field $F(x, t)$ is associated with the displacement $u(x, t)$ so that the extensive quantity Φ_k of the k^{th} node will be associated with the velocity v_k . Consequently the complementar intensive quantity will be associated with the force T_k . Being the velocity v_k an intensive representing it with an extensive quantity we will obtain a not coherent synthesis where the nominal value of the mass is associated with the stiffness of a spring and viceversa. Based on those argumentations using table 2-1 it is possible to specify the general circuit shown in fig. (4-1 b) for the case of interest as shown in fig 4-4.

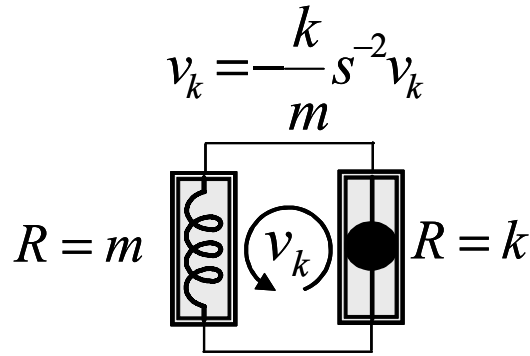


Figure 4-4: Equivalent circuit of a mass.spring hoscillator using the one node to one port

$\frac{dF}{dt} \rightarrow \Phi$ synthesis.

4.3.2 Torsional pendulum.

The Torsional pendulum can be derived by the general zero order theory by the following interpretation of the general parameter:

General descriptor	Actual descriptor	Physical meaning
$F(x, t)$	$u(x, t)$	angular displacement
K	k_T	torsional stiffness
ρ	J	rotational inertia

Table 4-2

Over this condition the equation 4.1 becomes:

$$k_T \theta_k(t) + m \frac{d^2 \theta_k(t)}{dt^2} = 0 \quad (4.3)$$

The physical system can be represented by means of a disk having a rotational inertia equal to J joined to the ceiling by means of a wire of negligible mass having a rotational stiffness equal to k_T , as shown in fig. (4-5).

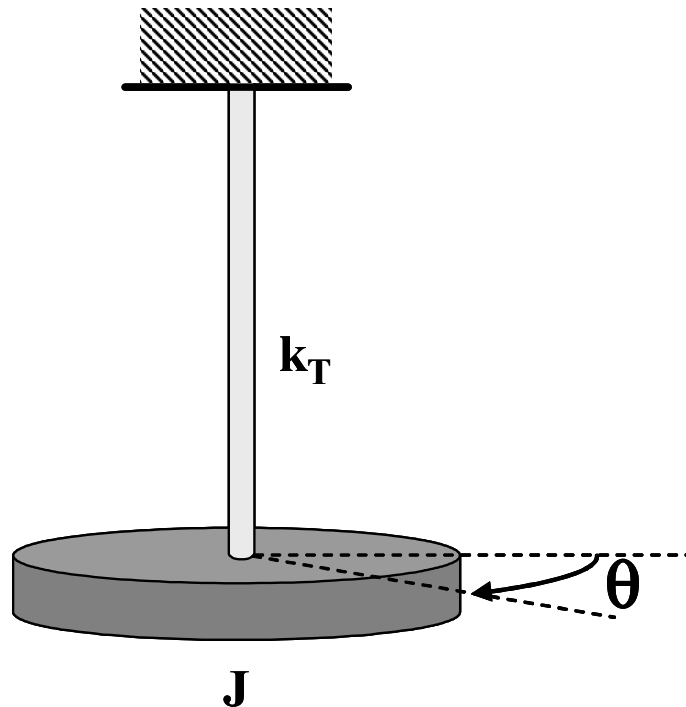


Figure 4-5: Torsional pendulum.

$\frac{dF}{dt} \rightarrow \Pi$ **synthesis**

In this section we will give an actual meaning to the components and the physical quantity governing the evolution of the general zero order circuit shown in fig. (4-1). As reported in table 4-2 the scalar field $F(x, t)$ is associated with the angular displacement $\theta(x, t)$ so that the intensive quantity Π_k of the k^{th} node will be associated with the angular velocity ω_k . Consequently the complementar extensive quantity will be associated with the torque M_k . Based on those argumentations using table 2-1, it is possible to specify the general circuit shown in fig. (4-1 a) for the case of interest as shown in fig 4-6.

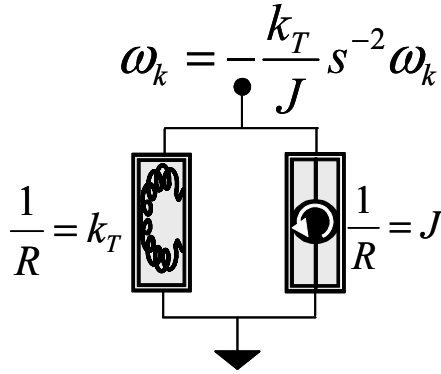


Figure 4-6: Equivalent circuit of a torsional pendulum using the one node to one port $\frac{dF}{dt} \rightarrow \Pi$ synthesis.

$\frac{dF}{dt} \rightarrow \Phi$ **synthesis**

In this section we will give an actual meaning to the components and the physical quantity governing the evolution of the general zero order circuit shown in fig. (4-1). As reported in table 4-1 the scalar field $F(x, t)$ is associated with the angular displacement $\theta(x, t)$ so that the extensive quantity Φ_k of the k^{th} node will be associated with the angular velocity ω_k . Consequently the complementar intensive quantity will be associated with the torque M_k . Being the angular velocity ω_k an intensive representing it with an extensive quantity we will obtain a not coher-

ent synthesis where the nominal value of the rotational inertia is associated with the rotational stiffness of a spring and viceversa. Based on those argumentations using table 2-1, it is possible to specify the general circuit shown in fig. (4-1 b) for the case of interest as shown in fig 4-7.

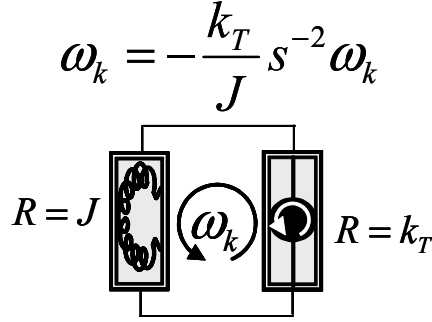


Figure 4-7: Equivalent circuit of a torsional pendulum using the one node to one port $\frac{dF}{dt} \rightarrow \Pi$ synthesis.

4.4 Derivation of the second order networks.

The equation governing the evolution of a discrete second order ondulatory phenomena can be obtained by choosing $n = 1$ in eq. (2.1) that will assume the following form:

$$\sum_{i=-1}^1 (-1)^{i+1} \binom{2}{i+1} F_{k+i}(t) + (-1)^1 \frac{K}{\rho} \Delta^2 \frac{\partial^2 F_k(t)}{\partial t^2} = 0 \quad (4.4)$$

that can be rewritten in extended form as follows:

$$F_{k-1}(t) - 2F_k(t) + F_{k+1}(t) - \frac{K}{\rho} \Delta^2 \frac{\partial^2 F_k(t)}{\partial t^2} = 0 \quad (4.5)$$

The previous equation puts in evidence that when $n = 1$ there exists an interaction between the k^{th} node of the mesh and the previous and the subsequent node, consequently the left (right) termination network taking in count for the BC will interact with the first (last) node. This means that in this case it will be needed to evaluate all the possible termination conditions using the one node to n ports network. Then, based on this synthesis, we will evaluate the

right termination section for all the possible BC for both the $\frac{dF}{dt} \rightarrow \Pi$ and $\frac{dF}{dt} \rightarrow \Phi$ synthesis. As we said before we have in general 2^n different types of BC, so in this case we will have the four (2^1) different types of BC listed in the following table:

EBC1=0	NBC1=0
type1	type2

Table 4-3: All possible types of homogeneous BCs for the second order network.

4.4.1 One node to n ports synthesis

$\frac{dF}{dt} \rightarrow \Pi$ synthesis

As we have said in the second chapter the complete circuit for the one node to n ports mapping can be obtained by the cascade connection of how many basic sections how many are the nodes of the mesh; then we need to symmetrize the system including the symmetrization subnetwork, finally we need to terminate the left and the right side of the whole circuit with two termination sections shown in fig (2-41 a) The complete network obtained is shown in fig. (4-8).

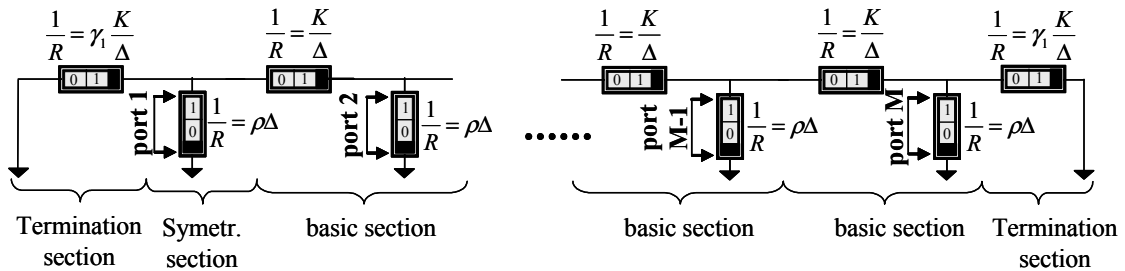


Figure 4-8: One node to n ports $\frac{dF}{dt} \rightarrow \Pi$ synthesis complete network for a second order system.

Now we want to derive an external characterization of the circuit shown in fig.(4-8) In that

figure we have explicitly shown the access port of the system. The admittance matrix \mathbb{Y} of this circuit evaluated from those ports is given below:

$$\mathbb{Y} = \mathbb{Y}_1 + \mathbb{Y}_2 \quad (4.6)$$

$$\mathbb{Y}_1 = \Delta \rho s \begin{pmatrix} 1 & 0 & 0 & \cdots & 0 & 0 & 0 \\ 0 & 1 & 0 & \cdots & 0 & 0 & 0 \\ 0 & 0 & 1 & \cdots & 0 & 0 & 0 \\ \vdots & \vdots & \vdots & \ddots & \vdots & \vdots & \vdots \\ 0 & 0 & 0 & \cdots & 1 & 0 & 0 \\ 0 & 0 & 0 & \cdots & 0 & 1 & 0 \\ 0 & 0 & 0 & \cdots & 0 & 0 & 1 \end{pmatrix} = \Delta \rho s \mathbb{I} \quad (4.7)$$

$$\mathbb{Y}_2 = \frac{K}{\Delta s} \begin{pmatrix} \psi_{11} & -1 & 0 & 0 & 0 & 0 & 0 & \cdots & 0 \\ -1 & 2 & -1 & 0 & 0 & 0 & 0 & \cdots & 0 \\ 0 & -1 & 2 & -1 & 0 & 0 & 0 & \cdots & 0 \\ 0 & 0 & -1 & 2 & -1 & 0 & 0 & \cdots & 0 \\ \vdots & \ddots & \ddots & \ddots & \ddots & \ddots & \ddots & \ddots & \vdots \\ 0 & \cdots & 0 & 0 & -1 & 2 & -1 & 0 & 0 \\ 0 & \cdots & 0 & 0 & 0 & -1 & 2 & -1 & 0 \\ 0 & \cdots & 0 & 0 & 0 & 0 & -1 & 2 & -1 \\ 0 & \cdots & 0 & 0 & 0 & 0 & 0 & -1 & \psi_{MM} \end{pmatrix} \quad (4.8)$$

where

$$\psi_{11} = \psi_{MM} = 1 + \gamma_1$$

It can be noted that the matrix \mathbb{Y}_2 takes in count the $(0, 1)$ elements while the matrix \mathbb{Y}_1 takes in count the $(1, 0)$ elements. As we said previously the 1×1 corner submatrices takes in count for the termination subnetworks emulating the most general BC. The terms ψ_{11} and ψ_{MM} can be specified in order to obtain all the needed BC. The two (2^n) possible types of homogeneous BC are listed in the following table:

	type1	type2
γ_1	$(\infty)1$	0
ψ_{11}	2	1

Table 4-4

In the previous table we wrote that the type1 condition is obtained by taking the limit for $\gamma_1 \rightarrow 1$ instead of $\gamma_1 \rightarrow \infty$ as expected from the theory we described in the second chapter. Now we try to explain this fact. When γ_1 goes to infinity the component of the termination section becomes a generalized short circuit and so the $(1,0)$ element shunted with the first port is connected between two copies of the reference node, and consequently can not be used as a port of the system. This situation requires the definition of a reduced matrix having one port less. In this situation shown in fig.(4-10) the elements in the dashed line don't give any contribution to the circuit and can be removed. The resultant circuit is equivalent to the old one if we consider the termination component equivalent to one of the $(0,1)$ element of the constitutive subnetwork (i.e. $\gamma_1 \rightarrow 1$).

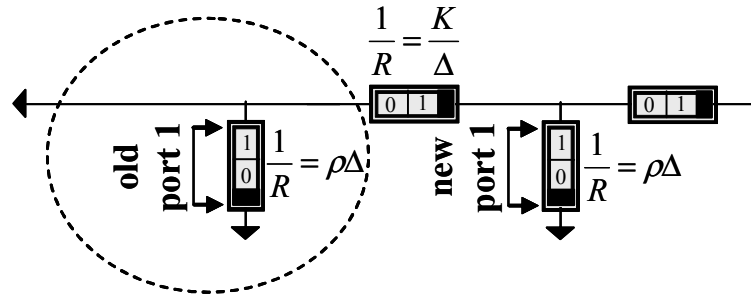


Figure 4-9: One node to n ports $\frac{dF}{dt} \rightarrow \Pi$ synthesis type1 BC for a second order system.

$\frac{dF}{dt} \rightarrow \Phi$ synthesis

As we have said in the second chapter the complete circuit for the one node to n ports mapping can be obtained by the cascade connection of how many basic sections how many are the nodes

of the mesh; then we need to symmetrize the system including the symmetrization subnetwork, finally we need to terminate the left and the right side of the whole circuit with two termination sections shown in fig. (2-41b). The complete network obtained is shown in fig. (4-10).

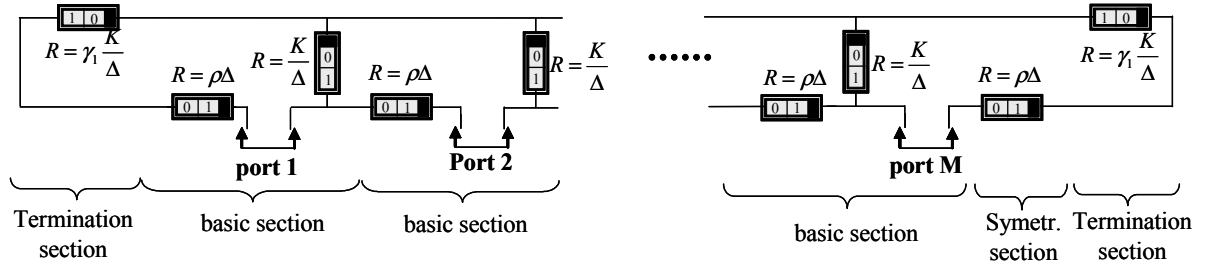


Figure 4-10: One node to n ports $\frac{dF}{dt} \rightarrow \Phi$ synthesis complete network for a second order system.

Now we want to derive an external characterization of the circuit shown in fig.(4-10). In that figure we have explicitly shown the access port of the system. The impedance matrix \mathbb{Z} of this circuit evaluated from those ports is given below:

$$\mathbb{Z} = \mathbb{Z}_1 + \mathbb{Z}_2 \quad (4.9)$$

$$\mathbb{Z}_1 = \Delta \rho s \begin{pmatrix} 1 & 0 & 0 & \cdots & 0 & 0 & 0 \\ 0 & 1 & 0 & \cdots & 0 & 0 & 0 \\ 0 & 0 & 1 & \cdots & 0 & 0 & 0 \\ \vdots & \vdots & \vdots & \ddots & \vdots & \vdots & \vdots \\ 0 & 0 & 0 & \cdots & 1 & 0 & 0 \\ 0 & 0 & 0 & \cdots & 0 & 1 & 0 \\ 0 & 0 & 0 & \cdots & 0 & 0 & 1 \end{pmatrix} = \Delta \rho s \mathbb{I} \quad (4.10)$$

$$\mathbb{Z}_2 = \frac{K}{\Delta_s} \begin{pmatrix} \xi_{11} & -1 & 0 & 0 & 0 & 0 & 0 & \dots & 0 \\ -1 & 2 & -1 & 0 & 0 & 0 & 0 & \dots & 0 \\ 0 & -1 & 2 & -1 & 0 & 0 & 0 & \dots & 0 \\ 0 & 0 & -1 & 2 & -1 & 0 & 0 & \dots & 0 \\ \vdots & \ddots & \ddots & \ddots & \ddots & \ddots & \ddots & \ddots & \vdots \\ 0 & \dots & 0 & 0 & -1 & 2 & -1 & 0 & 0 \\ 0 & \dots & 0 & 0 & 0 & -1 & 2 & -1 & 0 \\ 0 & \dots & 0 & 0 & 0 & 0 & -1 & 2 & -1 \\ 0 & \dots & 0 & 0 & 0 & 0 & 0 & -1 & \xi_{MM} \end{pmatrix} \quad (4.11)$$

where

$$\xi_{11} = \xi_{MM} = 1 + \gamma_1$$

It can be noted that the matrix \mathbb{Z}_2 takes in count the $(1,0)$ elements while the matrix \mathbb{Z}_1 takes in count the $(0,1)$ elements. As we said previously the 1×1 corner submatrices takes in count for the termination subnetwork emulating the most general BC. The terms ξ_{11} can be specified in order to obtain all the needed BC. The two (2^1) possible types of homogeneous BC are listed in the following table:

	type1	type2
γ_1	$(\infty)1$	0
ξ_{11}	2	1

Table 4-5

In the previous table we wrote that the type1 condition is obtained by taking the limit for $\gamma_1 \rightarrow 1$ instead of for $\gamma_1 \rightarrow \infty$ as expected from the theory we described in the second chapter. Now we try to explain this fact. When γ_1 goes to infinity the component of the termination section becomes a generalized open circuit and so the $(0,1)$ element connected in series with the first port is flowed by a zero Φ quantity, and consequently can not be used as a port of the

system. This situation requires the definition of a reduced matrix having one port less. In this situation shown in fig.(4-11) the elements in the dashed line don't give any contribution to the circuit and can be removed. The resultant circuit is equivalent to the old one if we consider the termination component equivalent to one of the element $(1, 0)$ element of the constitutive subnetwork (i.e. $\gamma_1 \rightarrow 1$).

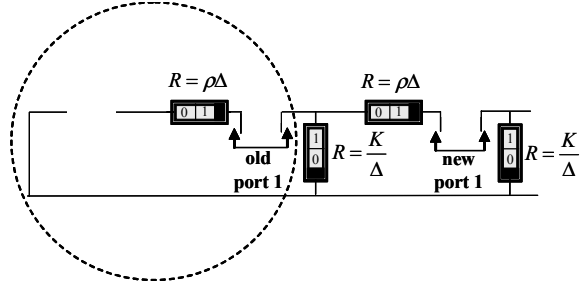


Figure 4-11: One node to n ports $\frac{dF}{dt} \rightarrow \Phi$ synthesis type 1 BC for a second order system.

4.4.2 One node to one port synthesis

$\frac{dF}{dt} \rightarrow \Pi$ synthesis

As we have said in the second chapter the needed circuit can be obtained by means of the circuit shown in fig. (2-18). Fixing $n = 1$ and satisfying the constraint $\alpha_2 - \beta_2 - \alpha_1 + \beta_1 = 2$ by means of the following positions $\alpha_2 = 1, \beta_2 = 0, \alpha_1 = 0$ and $\beta_1 = 1$ we obtain the circuit shown in fig. (4-12) where the subnetworks inside the gray triangle (see fig. (2-18)) are been replaced with suitable version of the termination sections shown in fig. (2-46).

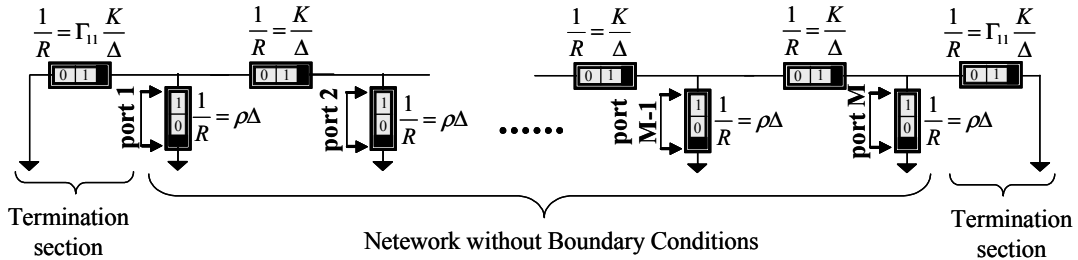


Figure 4-12: One node to one ports $\frac{dF}{dt} \rightarrow \Pi$ synthesis complete network for a second order system.

Now we can use the ports shown in fig. (4-12) in order to derive the \mathbb{Y} matrix of the system. As expected we will find a matrix having the structure shown in fig. (2-44). The corner submatrices taking in count for the BC will depend on the parameter Γ_{11} .

$$\mathbb{Y} = \mathbb{Y}_1 + \mathbb{Y}_2 \quad (4.12)$$

$$\mathbb{Y}_1 = \Delta \rho s \begin{pmatrix} 1 & 0 & 0 & \cdots & 0 & 0 & 0 \\ 0 & 1 & 0 & \cdots & 0 & 0 & 0 \\ 0 & 0 & 1 & \cdots & 0 & 0 & 0 \\ \vdots & \vdots & \vdots & \ddots & \vdots & \vdots & \vdots \\ 0 & 0 & 0 & \cdots & 1 & 0 & 0 \\ 0 & 0 & 0 & \cdots & 0 & 1 & 0 \\ 0 & 0 & 0 & \cdots & 0 & 0 & 1 \end{pmatrix} = \Delta \rho s \mathbb{I} \quad (4.13)$$

$$\mathbb{Y}_2 = \frac{K}{\Delta s} \begin{pmatrix} \Psi_{11} & -1 & 0 & 0 & 0 & 0 & 0 & \cdots & 0 \\ -1 & 2 & -1 & 0 & 0 & 0 & 0 & \cdots & 0 \\ 0 & -1 & 2 & -1 & 0 & 0 & 0 & \cdots & 0 \\ 0 & 0 & -1 & 2 & -1 & 0 & 0 & \cdots & 0 \\ \vdots & \ddots & \ddots & \ddots & \ddots & \ddots & \ddots & \ddots & \vdots \\ 0 & \cdots & 0 & 0 & -1 & 2 & -1 & 0 & 0 \\ 0 & \cdots & 0 & 0 & 0 & -1 & 2 & -1 & 0 \\ 0 & \cdots & 0 & 0 & 0 & 0 & -1 & 2 & -1 \\ 0 & \cdots & 0 & 0 & 0 & 0 & 0 & -1 & \Psi_{MM} \end{pmatrix} \quad (4.14)$$

where

$$\Psi_{11} = \Psi_{MM} = 1 + \Gamma_{11}$$

As we explain in the second chapter we can evaluate the BCs for the one node to one port mapping by equating the Ψ_{ij} obtained in this synthesis technique with the ψ_{ij} obtained for the one node to n port mapping. This procedure brings to the following linear system of one

$((1/2)(1 + 1) = 1)$ equation in one unknown

$$1 + \Gamma_{11} = 1 + \gamma_1 \tag{4.15}$$

Solving this system for Γ_{11} we obtain:

$$\Gamma_{11} = \gamma_1 \tag{4.16}$$

From the table above we are able to evaluate the value of all possible termination conditions.

We summarize those results in the following table:

	type1	type2
γ_1	$(\infty)1$	0
Γ_{11}	2	1

Table 4-6

$\frac{dF}{dt} \rightarrow \Phi$ synthesis

Fixing $n = 1$ and satisfying the constraint $\alpha_2 - \beta_2 - \alpha_1 + \beta_1 = 2$ by means of the following positions $\alpha_2 = 1, \beta_2 = 0, \alpha_1 = 0$ and $\beta_1 = 1$ we obtain the circuit shown in fig. (4-13).

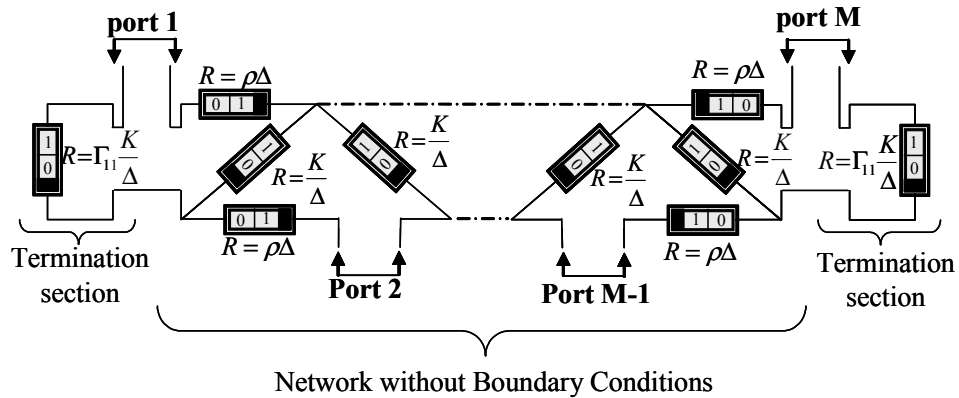


Figure 4-13: One node to one port $\frac{dF}{dt} \rightarrow \Phi$ synthesis complete network for a second order system.

Now we can use the ports shown in fig. (4-13) in order to derive the \mathbb{Z} matrix of the system. As expected we will find a matrix having the structure shown in fig. (2-44). The corner submatrices taking in count for the BC will depend on the parameter Γ_{11} .

$$\mathbb{Z} = \mathbb{Z}_1 + \mathbb{Z}_2 \quad (4.17)$$

$$\mathbb{Z}_1 = \Delta \rho s \begin{pmatrix} 1 & 0 & 0 & \cdots & 0 & 0 & 0 \\ 0 & 1 & 0 & \cdots & 0 & 0 & 0 \\ 0 & 0 & 1 & \cdots & 0 & 0 & 0 \\ \vdots & \vdots & \vdots & \ddots & \vdots & \vdots & \vdots \\ 0 & 0 & 0 & \cdots & 1 & 0 & 0 \\ 0 & 0 & 0 & \cdots & 0 & 1 & 0 \\ 0 & 0 & 0 & \cdots & 0 & 0 & 1 \end{pmatrix} = \Delta \rho s \mathbb{I} \quad (4.18)$$

$$\mathbb{Z}_2 = \frac{K}{\Delta s} \begin{pmatrix} \Xi_{11} & -1 & 0 & 0 & 0 & 0 & 0 & \cdots & 0 \\ -1 & 2 & -1 & 0 & 0 & 0 & 0 & \cdots & 0 \\ 0 & -1 & 2 & -1 & 0 & 0 & 0 & \cdots & 0 \\ 0 & 0 & -1 & 2 & -1 & 0 & 0 & \cdots & 0 \\ \vdots & \ddots & \ddots & \ddots & \ddots & \ddots & \ddots & \ddots & \vdots \\ 0 & \cdots & 0 & 0 & -1 & 2 & -1 & 0 & 0 \\ 0 & \cdots & 0 & 0 & 0 & -1 & 2 & -1 & 0 \\ 0 & \cdots & 0 & 0 & 0 & 0 & -1 & 2 & -1 \\ 0 & \cdots & 0 & 0 & 0 & 0 & 0 & -1 & \Xi_{MM} \end{pmatrix} \quad (4.19)$$

where

$$\Xi_{11} = \Xi_{MM} = 1 + \Gamma_{11}$$

As we explain in the second chapter we can evaluate the BC for the one node to one port mapping by equating the Ξ_{ij} obtained in this synthesis technique with the ζ_{ij} obtained for the one node to n port mapping. This procedure brings to the following linear system of one

$((n/2)(n + 1) = 1)$ equation in one unknown

$$1 + \Gamma_{11} = 1 + \gamma_1 \quad (4.20)$$

Solving this system for Γ_{11} we obtain:

$$\Gamma_{11} = \gamma_1 \quad (4.21)$$

From the table above we are able to evaluate the value of all possible termination condition. We summarize those results in the following table:

	type1	type2
γ_1	$(\infty)1$	0
Ξ_{11}	2	1

Table 4-7

In the following subsection we will give an example of a second order ondulatory phenomena.

4.5 An example of second order network

4.5.1 Extensional vibration on a beam.

The beam theory can be derived by the general second order theory by the following interpretation of the general parameters:

General descriptor	Actual descriptor	Physical meaning
$F(x, t)$	$w(x, t)$	horizontal displacement
K	K_N	extensional stiffness
ρ	λ	mass per unit of length

Table 4-8

Over this condition the equation (4.5) becomes:

$$-w_{k-1}(t) + 2w_k(t) - w_{k+1}(t) + \Delta^2 \frac{\lambda}{K_n} \frac{\partial^2 w_k(t)}{\partial t^2} = 0 \quad (4.22)$$

As well known by the Euler beam theory, the differential descriptor involved in the BC can be physically interpreted as follows:

differential description	short description	Physical meaning
$w(x, t)$	$w(x, t)$	horizontal displacement
$K_N \frac{\partial w(x, t)}{\partial x}$	$N(x, t)$	axial force

(4.23)

Table 4-9 (4.24)

consequently the BC assumes the following form:

$$N_k(t) = 0 \quad \text{or} \quad \delta(w_k(t)) \quad \text{specified} \quad (4.25)$$

Looking at eq. (4.25) it can be easily understand that the two different types of BC assume in this case a precise physical meaning. The graphical symbols and the terminology used for those BC are listed in the following table.



$w_k(t)=0$	$N_k(t)=0$
	
clamp	free

Table 4-10

4.5.2 One node to n port mapping

$\frac{\partial F}{\partial t} \rightarrow \Pi$ synthesis

In this section we will give an actual meaning to the components and the physical quantity governing the evolution of the general second order circuit shown in fig. (4-8). As reported in table (4-9) the scalar field $F(x, t)$ is associated with the horizontal displacement $w(x, t)$ so that the intensive quantity Π_k of the k^{th} node will be associated with the horizontal velocity ϖ_k . Consequently the complementar extensive quantity will be associated with the axial force N_k . Based on those argumentations using table (2-1), it is possible to specify the general circuit, shown in fig. (4-8) for the case of interest as shown in fig (4-14 a). In fig. (4-14 b) it is shown the mechanical model of the basic section.

Figure 4-14: One node to n ports $\frac{dF}{dt} \rightarrow \Pi$ synthesis axial vibration on a beam analogy. a) equivalent circuit, b) mechanical model.

$\frac{\partial F}{\partial t} \rightarrow \Phi$ synthesis

In this section we will give an actual meaning to the components and the physical quantity governing the evolution of the general second order circuit shown in fig. (4-10). As reported in table (4-9) the scalar field $F(x, t)$ is associated with the horizontal displacement $w(x, t)$ so that the extensive quantity Φ_k of the k^{th} node will be associated with the horizontal velocity ϖ_k . Consequently the complementar intensive quantity will be associated with the axial force N_k . Based on those argumentations using table (2-1) it is possible to specify the general circuit, shown in fig. (4-10) for the case of interest as shown in fig (4-15).

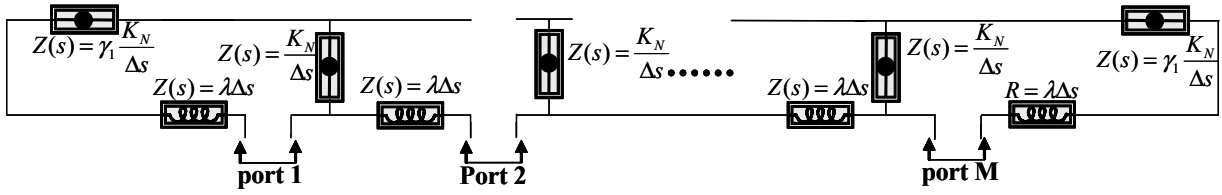


Figure 4-15: One node to n ports $\frac{dF}{dt} \rightarrow \Phi$ synthesis axial vibration on a beam analogy.
Equivalent circuit.

4.5.3 One node to one port mapping

$\frac{\partial F}{\partial t} \rightarrow \Pi$ synthesis

The general circuit derived in the previous section can be now specialized for the case of interest. As reported in table (4-9) the scalar field $F(x, t)$ is associated with the horizontal displacement $w(x, t)$ so that the intensive quantity Π_k of the k^{th} node will be associated with the horizontal velocity ϖ_k . Consequently the complementar extensive quantity will be associated with the axial force N_k . It should be noted that for $n = 1$ the one node to n ports mapping coincide with the one node to one port mapping. The circuit obtained is shown in fig. (4-16 a) while in fig. (4-16 b) it is shown the equivalent mechanical system.

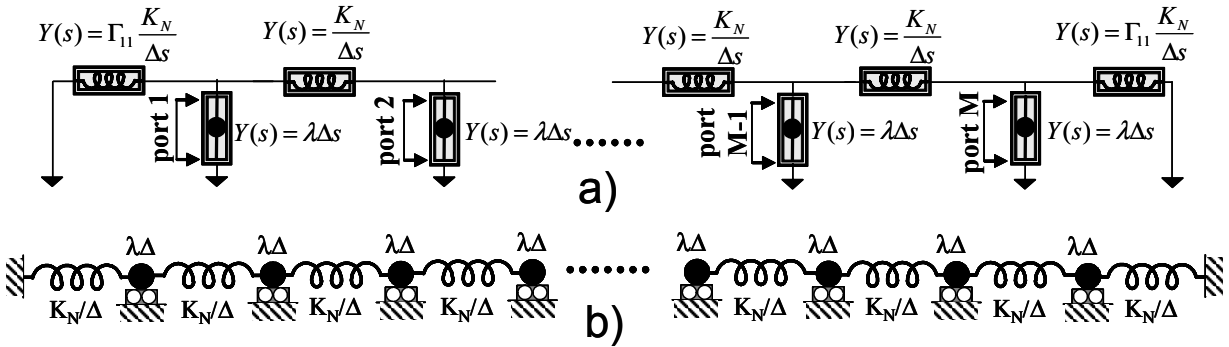


Figure 4-16: One node to one port $\frac{dF}{dt} \rightarrow \Pi$ synthesis axial vibration on a beam analogy. a) equivalent circuit, b) mechanical model.

$\frac{\partial F}{\partial t} \rightarrow \Phi$ synthesis

Similarly the general circuit derived in the previous section shown in fig. (4-13) can be specialized for the case of interest. As reported in table (4-9) the scalar field $F(x, t)$ is associated with the horizontal displacement $w(x, t)$ so that the extensive quantity Φ_k of the k^{th} node will be associated with the horizontal velocity ϖ_k . Consequently the complementar intensive quantity will be associated with the axial force N_k .

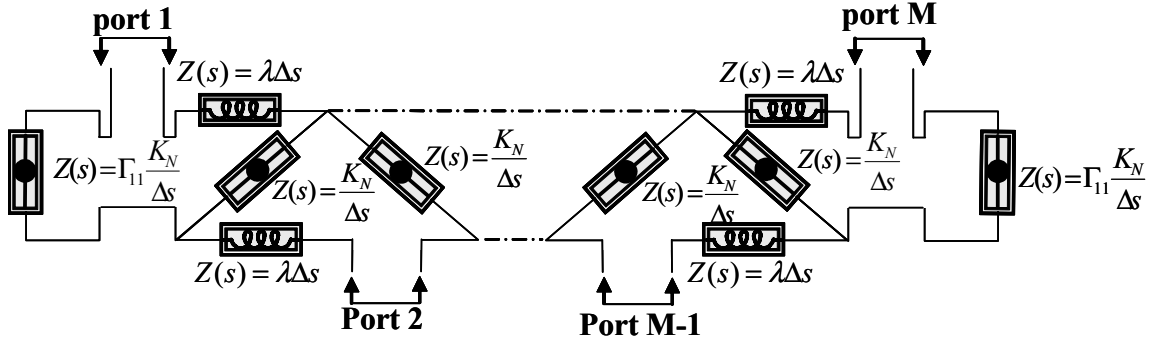


Figure 4-17: One node to one port $\frac{dF}{dt} \rightarrow \Phi$ synthesis axial vibration on a beam analogy. Equivalent circuit.

4.6 Derivation of the fourth order networks.

The equation governing the evolution of a discrete fourth order ondulatory phenomena can be obtained by choosing $n = 2$ in eq. (2.1) that will assume the following form:

$$\sum_{i=-2}^2 (-1)^{i+2} \binom{4}{i+2} F_{k+i}(t) + (-1)^2 \frac{K}{\rho} \Delta^4 \frac{\partial^2 F_k(t)}{\partial t^2} = 0 \quad (4.26)$$

that can be rewritten in extended form as follows:

$$F_{k-2}(t) - 4F_{k-1}(t) + 6F_k(t) - 4F_{k+1}(t) + F_{k+2}(t) + \frac{K}{\rho} \Delta^4 \frac{\partial^2 F_k(t)}{\partial t^2} = 0 \quad (4.27)$$

The previous equation puts in evidence that, when $n = 2$, there exists an interaction between the k^{th} node of the mesh and the previous and the subsequent two nodes, consequently the left (right) termination network taking in count for the BC will interact with the first (last) two nodes. This means that in this case it will be needed to evaluate all the possible termination conditions using the one node to n ports network. Then based on this synthesis we will evaluate the right termination section for all the possible BC for both the $\frac{dF}{dt} \rightarrow \Pi$ and $\frac{dF}{dt} \rightarrow \Phi$ synthesis. As we said before we have in general 2^n different types of BCs, so in this case we will have the four (2^2) different types of BC listed in the following table:

	EBC1=0	NBC1=0
EBC2=0	type1	type3
NBC2=0	type2	type4

Table 4-11

4.6.1 One node to n port synthesis

$\frac{dF}{dt} \rightarrow \Pi$ synthesis

When $n \geq 2$ in the one node to n ports mapping we have different lines associated with signals having different meaning. Consequently, in this case, it is interesting to show the basic section. In fig. (4-18) it is shown the basic section connecting the node k^{th} with the node $(k + 1)^{th}$ including both the constitutive and the geometrical/balancioum subnetwork. Based on the notions given in the previous chapter we can identify the generalized lever acting between two lines characterized by the two different pairs (Π_1, Φ_1) and (Π_2, Φ_2) as an ideal bidirectional transducer.

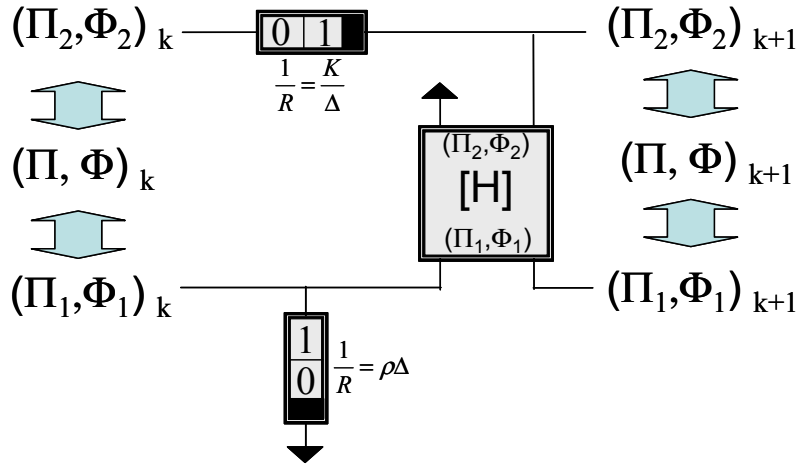


Figure 4-18: One node to n ports $\frac{dF}{dt} \rightarrow \Pi$ synthesis. Basic section of a fourth order system.

As we have said in the second chapter the complete circuit can be obtained by the cascade connection of a number of basic sections large as the number of the nodes of the mesh. Then we need to symmetrize the system including the symmetrization subnetwork. Finally we need to terminate the left and the right side of the whole circuit with two termination section shown in fig (2-41 a). The complete network obtained is shown in fig. (4-19).

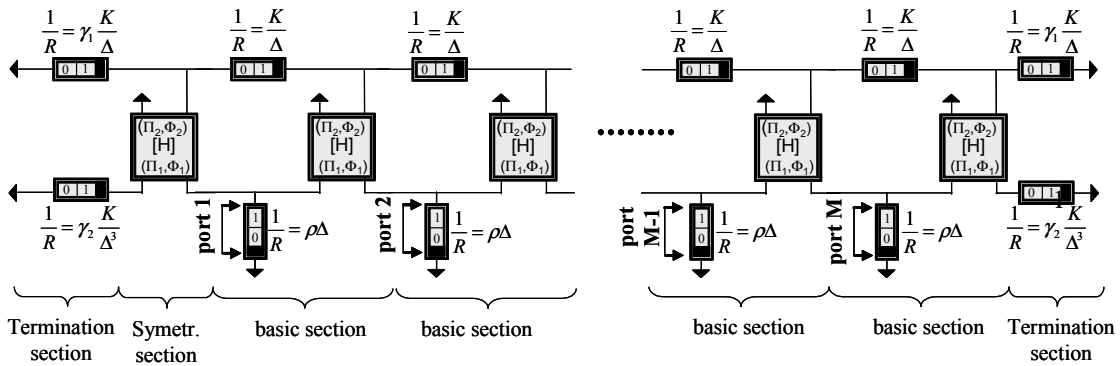


Figure 4-19: One node to n ports $\frac{dF}{dt} \rightarrow \Pi$ synthesis. complete network of a fourth order system.

Now we want to derive an external characterization of the circuit shown in fig.(4-19). In that figure we have explicitly shown the access port of the system. The admittance matrix \mathbb{Y} of this

circuit evaluated from those ports is given below:

$$\mathbb{Y} = \mathbb{Y}_1 + \mathbb{Y}_2 \quad (4.28)$$

$$\mathbb{Y}_1 = \Delta \rho s \begin{pmatrix} 1 & 0 & 0 & \cdots & 0 & 0 & 0 \\ 0 & 1 & 0 & \cdots & 0 & 0 & 0 \\ 0 & 0 & 1 & \cdots & 0 & 0 & 0 \\ \vdots & \vdots & \vdots & \ddots & \vdots & \vdots & \vdots \\ 0 & 0 & 0 & \cdots & 1 & 0 & 0 \\ 0 & 0 & 0 & \cdots & 0 & 1 & 0 \\ 0 & 0 & 0 & \cdots & 0 & 0 & 1 \end{pmatrix} = \Delta \rho s \mathbb{I} \quad (4.29)$$

$$\mathbb{Y}_2 = \frac{K}{\Delta^3 s} \begin{pmatrix} \psi_{11} & -\psi_{12} & 1 & 0 & 0 & 0 & 0 & \cdots & 0 \\ -\psi_{12} & \psi_{22} & -4 & 1 & 0 & 0 & 0 & \cdots & 0 \\ 1 & -4 & 6 & -4 & 1 & 0 & 0 & \cdots & 0 \\ 0 & 1 & -4 & 6 & -4 & 1 & 0 & \cdots & 0 \\ \vdots & \ddots & \ddots & \ddots & \ddots & \ddots & \ddots & \ddots & \vdots \\ 0 & \cdots & 0 & 1 & -4 & 6 & -4 & 1 & 0 \\ 0 & \cdots & 0 & 0 & 1 & -4 & 6 & -4 & 1 \\ 0 & \cdots & 0 & 0 & 0 & 1 & -4 & \psi_{(M-1)(M-1)} & -\psi_{(M-1)M} \\ 0 & \cdots & 0 & 0 & 0 & 0 & 1 & -\psi_{(M-1)M} & \psi_{MM} \end{pmatrix} \quad (4.30)$$

where

$$\psi_{11} = \psi_{MM} = \frac{1 + 2\gamma_1 + 5\gamma_2 + \gamma_1\gamma_2}{1 + \gamma_1 + \gamma_2} \quad (4.31)$$

$$\psi_{12} = \psi_{(M-1)M} = \frac{2 + 3\gamma_1 + 4\gamma_2}{1 + \gamma_1 + \gamma_2} \quad (4.32)$$

$$\psi_{22} = \psi_{(M-1)(M-1)} = \frac{1 + 6\gamma_1 + 6\gamma_2}{1 + \gamma_1 + \gamma_2} \quad (4.33)$$

It can be noted that the matrix \mathbb{Y}_2 takes in count the $(0,1)$ elements and the transducers while the matrix \mathbb{Y}_1 takes in count the $(1,0)$ elements. As we said previously the 2×2 corner submatrices take in count for the termination subnetwork emulating the most general BC. The

terms $\psi_{11}, \psi_{12}, \psi_{22}$ can be specified in order to obtain all the needed BC. The four (2^2) possible types of homogeneous BC are listed in the following table:

	type1	type2	type3	type4
γ_1	$(\infty)1$	0	∞	0
γ_2	∞	∞	0	0
ψ_{11}	6	5	2	1
ψ_{12}	4	4	3	2
ψ_{22}	6	6	6	5

Table 4-12

In the previous table we wrote that the type1 condition is obtained by taking the limit for $\gamma_1 \rightarrow 1$ and $\gamma_2 \rightarrow \infty$ instead of $\gamma_1 \rightarrow \infty$ and $\gamma_2 \rightarrow \infty$ as expected from the theory we described in the previous section. Now we try to explain this fact. When both γ_1 and γ_2 go to infinity both the components of the termination section become generalized short circuit and so the $(1,0)$ element shunted with the first port is connected between two copies of the reference node, and consequently can not be used as a port of the system. This situation requires the definition of a reduced matrix having one port less. In this situation shown in fig.(4-10) the elements in the dashed circle don't give any contribution to the circuit and can be removed.

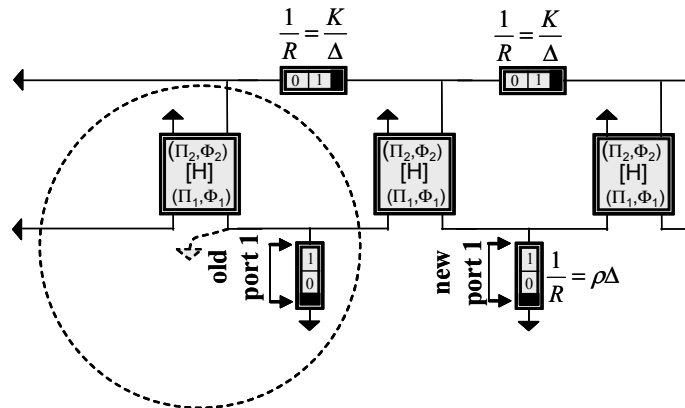


Figure 4-20: One node to n ports $\frac{dF}{dt} \rightarrow \Pi$ synthesis. Type 1 BC of a fourth order system.

The resultant circuit is equivalent to the old one if we consider the first termination component equivalent to one of the element $(0, 1)$ element of the constitutive subnetwork (i.e. $\gamma_1 \rightarrow 1$) and the second one equal to a generalized short circuit (i.e. $\gamma_2 \rightarrow \infty$).

$\frac{dF}{dt} \rightarrow \Phi$ synthesis

As we have done before, first of all we will show in fig. (4-21) the basic section connecting the node k^{th} with the node $(k+1)^{th}$ including both the constitutive and the geometrical/balancioum subnetworks. Based on the notions given in the previous chapter we can identify the generalized lever acting between two lines characterized by the two different pairs (Π_1, Φ_1) and (Π_2, Φ_2) as an ideal bidirectional transducer.

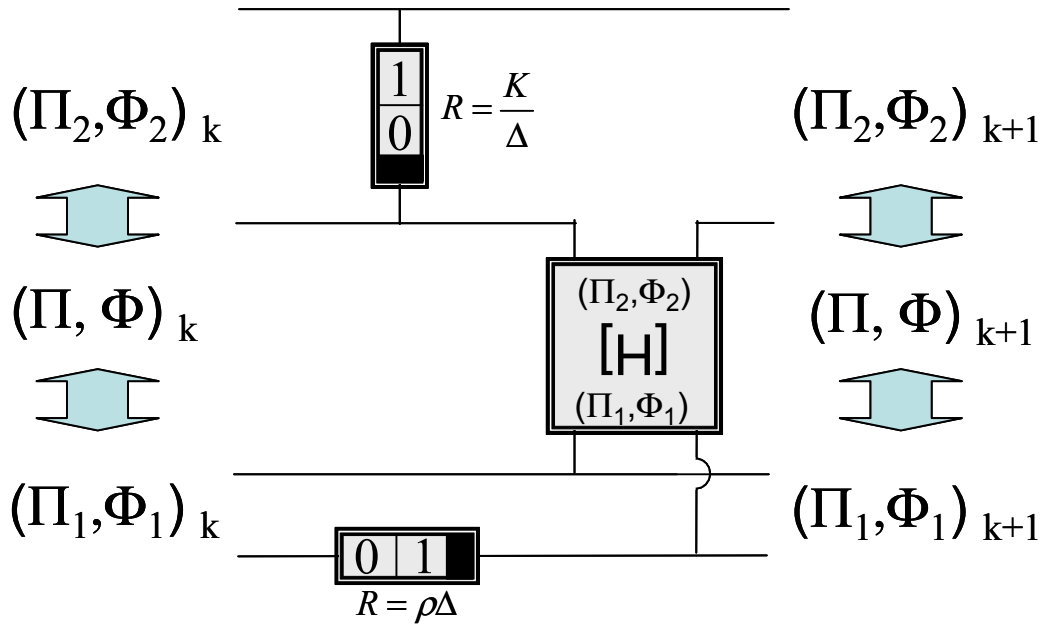


figure 4-21: One node to n ports $\frac{dF}{dt} \rightarrow \Phi$ synthesis. Basic section of a fourth order system.

As we have said in the second chapter the complete circuit can be obtained by the cascade connection of how many basic sections how many are the nodes of the mesh; then we need to symmetrize the system including the symmetrization subnetwork; finally we need to terminate the left and the right side of the whole circuit with two termination sections. The complete network obtained is shown in fig. (4-22).

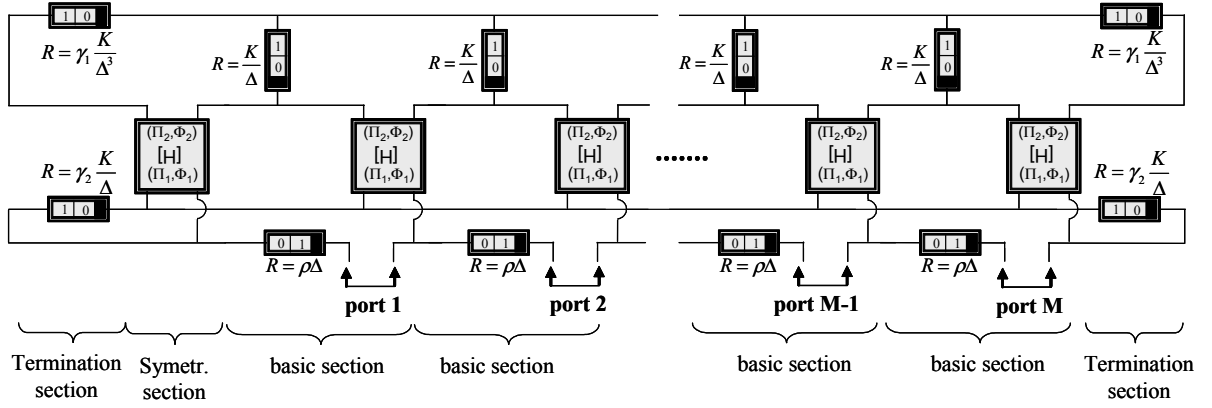


Figure 4-22: One node to n ports $\frac{dF}{dt} \rightarrow \Phi$ synthesis. Complete network of a fourth order system.

Now we want to derive an external characterization of the circuit shown in fig.(4-22). In that figure we have explicitly shown the access port of the system. The impedance matrix \mathbb{Z} of this circuit evaluated from those ports is given below:

$$\mathbb{Z} = \mathbb{Z}_1 + \mathbb{Z}_2 \quad (4.34)$$

$$\mathbb{Z}_1 = \Delta \rho s \begin{pmatrix} 1 & 0 & 0 & \dots & 0 & 0 & 0 \\ 0 & 1 & 0 & \dots & 0 & 0 & 0 \\ 0 & 0 & 1 & \dots & 0 & 0 & 0 \\ \vdots & \vdots & \vdots & \ddots & \vdots & \vdots & \vdots \\ 0 & 0 & 0 & \dots & 1 & 0 & 0 \\ 0 & 0 & 0 & \dots & 0 & 1 & 0 \\ 0 & 0 & 0 & \dots & 0 & 0 & 1 \end{pmatrix} = \Delta \rho s \mathbb{I} \quad (4.35)$$

$$\mathbb{Z}_2 = \frac{K}{\Delta^{3s}} \begin{pmatrix} \xi_{11} & -\xi_{12} & 1 & 0 & 0 & 0 & 0 & \cdots & 0 \\ -\xi_{12} & \xi_{22} & -4 & 1 & 0 & 0 & 0 & \cdots & 0 \\ 1 & -4 & 6 & -4 & 1 & 0 & 0 & \cdots & 0 \\ 0 & 1 & -4 & 6 & -4 & 1 & 0 & \cdots & 0 \\ \vdots & \ddots & \ddots & \ddots & \ddots & \ddots & \ddots & \ddots & \vdots \\ 0 & \cdots & 0 & 1 & -4 & 6 & -4 & 1 & 0 \\ 0 & \cdots & 0 & 0 & 1 & -4 & 6 & -4 & 1 \\ 0 & \cdots & 0 & 0 & 0 & 1 & -4 & \xi_{(M-1)(M-1)} & -\xi_{(M-1)M} \\ 0 & \cdots & 0 & 0 & 0 & 0 & 1 & -\xi_{(M-1)M} & \xi_{MM} \end{pmatrix} \quad (4.36)$$

where

$$\xi_{11} = \xi_{MM} = \frac{1 + 2\gamma_1 + 5\gamma_2 + \gamma_1\gamma_2}{1 + \gamma_1 + \gamma_2} \quad (4.37)$$

$$\xi_{12} = \xi_{(M-1)M} = \frac{2 + 3\gamma_1 + 4\gamma_2}{1 + \gamma_1 + \gamma_2} \quad (4.38)$$

$$\xi_{22} = \xi_{(M-1)(M-1)} = \frac{1 + 6\gamma_1 + 6\gamma_2}{1 + \gamma_1 + \gamma_2} \quad (4.39)$$

It can be noted that the matrix \mathbb{Z}_2 take in count the $(1,0)$ elements and the transducers while the matrix \mathbb{Z}_1 take in count the $(0,1)$ elements. As we said previously the 2×2 corner submatrices take in count for the termination subnetwork emulating the most general BC. The terms $\xi_{11}, \xi_{12}, \xi_{22}$ can be specified in order to obtain all the needed BC. The four (2^2) possible types of homogenous BC are listed in the following table:

	type1	type2	type3	type4
γ_1	$(\infty)1$	0	∞	0
γ_2	∞	∞	0	0
ξ_{11}	6	5	2	1
ξ_{12}	4	4	3	2
ξ_{22}	6	6	6	5

Table 4-12

In the previous table we wrote that the type1 condition is obtained by taking the limit for $\gamma_1 \rightarrow 1$ and $\gamma_2 \rightarrow \infty$ instead of $\gamma_1 \rightarrow \infty$ and $\gamma_2 \rightarrow \infty$ as expected from the theory we described in the previous section. Now we try to explain this fact. When both γ_1 and γ_2 go to infinity both the components of the termination section become generalized open circuit and so the (0,1)element connected in series with the first port is flowed by a zero Φ quantity, and consequently can not be used as a port of the system. This situation requires the definition of a reduced matrix having one port less. In this situation shown in fig.(4-23) the elements in the dashed line don't give any contribution to the circuit and can be removed. The resultant circuit is equivalent to the old one if we consider the first termination component equivalent to one of the element (1,0)element of the constitutive subnetwork (i.e. $\gamma_1 \rightarrow 1$) and the second one equal to a generalized open circuit (i.e. $\gamma_2 \rightarrow \infty$).

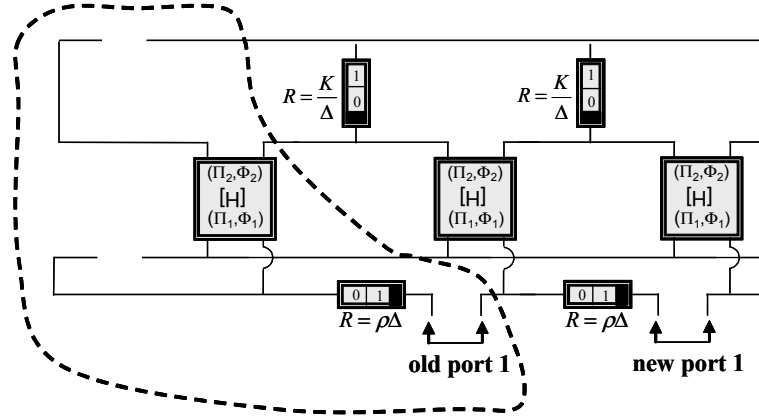


Figure 4-23: One node to n ports $\frac{dF}{dt} \rightarrow \Phi$ synthesis. type 1 BC of a fourth order system.

4.6.2 One node to one port synthesis

$\frac{dF}{dt} \rightarrow \Pi$ synthesis

As we have said in the second chapter the needed circuit can be obtained by means of the circuit shown in fig. (2-18). Fixing $n = 2$ and satisfying the constraint $\alpha_2 - \beta_2 - \alpha_1 + \beta_1 = 2$ by means of the following positions $\alpha_2 = 1, \beta_2 = 0, \alpha_1 = 0$ and $\beta_1 = 1$ we obtain the circuit shown in fig. (4-24) where the subnetworks inside the gray triangle (see fig. (2-18)) are been replaced with the termination sections.

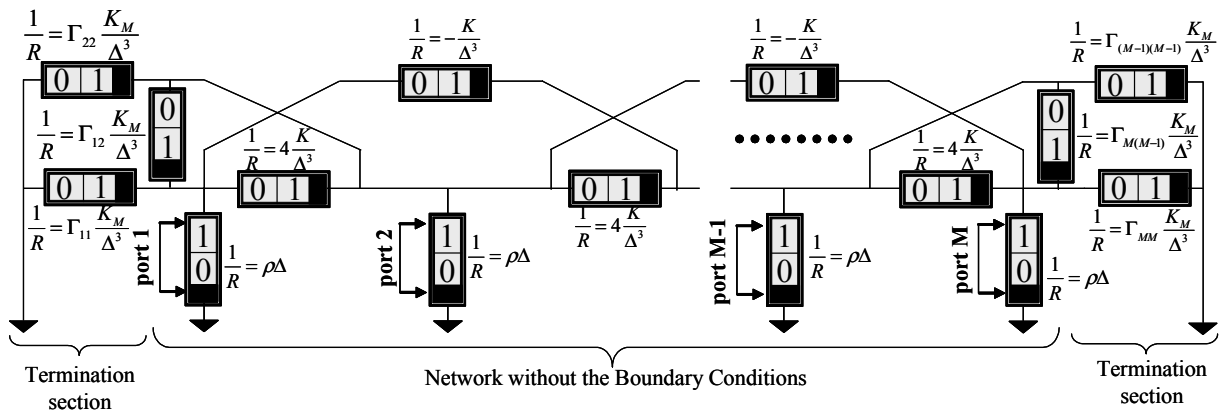


Figure 4-24: One node to one port $\frac{dF}{dt} \rightarrow \Pi$ synthesis. Complete network of a fourth order system.

Now we can use the ports shown in fig. (4-24) in order to derive the \mathbb{Y} matrix of the system. As expected we will find a matrix having the structure shown in fig. (2-44). The corner submatrices taking in count for the BC will depend on the parameters Γ_{11}, Γ_{12} and Γ_{22} .

$$\mathbb{Y} = \mathbb{Y}_1 + \mathbb{Y}_2 \quad (4.40)$$

$$\mathbb{Y}_1 = \Delta \rho s \begin{pmatrix} 1 & 0 & 0 & \cdots & 0 & 0 & 0 \\ 0 & 1 & 0 & \cdots & 0 & 0 & 0 \\ 0 & 0 & 1 & \cdots & 0 & 0 & 0 \\ \vdots & \vdots & \vdots & \ddots & \vdots & \vdots & \vdots \\ 0 & 0 & 0 & \cdots & 1 & 0 & 0 \\ 0 & 0 & 0 & \cdots & 0 & 1 & 0 \\ 0 & 0 & 0 & \cdots & 0 & 0 & 1 \end{pmatrix} = \Delta \rho s \mathbb{I} \quad (4.41)$$

$$\mathbb{Y}_2 = \frac{K}{\Delta^3 s} \begin{pmatrix} \Psi_{11} & -\Psi_{12} & 1 & 0 & 0 & 0 & 0 & \cdots & 0 \\ -\Psi_{12} & \Psi_{22} & -4 & 1 & 0 & 0 & 0 & \cdots & 0 \\ 1 & -4 & 6 & -4 & 1 & 0 & 0 & \cdots & 0 \\ 0 & 1 & -4 & 6 & -4 & 1 & 0 & \cdots & 0 \\ \vdots & \ddots & \ddots & \ddots & \ddots & \ddots & \ddots & \ddots & \vdots \\ 0 & \cdots & 0 & 1 & -4 & 6 & -4 & 1 & 0 \\ 0 & \cdots & 0 & 0 & 1 & -4 & 6 & -4 & 1 \\ 0 & \cdots & 0 & 0 & 0 & 1 & -4 & \Psi_{(M-1)(M-1)} & -\Psi_{(M-1)M} \\ 0 & \cdots & 0 & 0 & 0 & 0 & 1 & -\Psi_{(M-1)M} & \Psi_{MM} \end{pmatrix} \quad (4.42)$$

where

$$\Psi_{11} = \Psi_{MM} = 3 + \Gamma_{11} + \Gamma_{12} \quad (4.43)$$

$$\Psi_{12} = \Psi_{(M-1)M} = 4 + \Gamma_{12} \quad (4.44)$$

$$\Psi_{22} = \Psi_{(M-1)(M-1)} = 7 + \Gamma_{12} + \Gamma_{22} \quad (4.45)$$

As we explain in the second chapter we can evaluate the BCs for the one node to one port

mapping by equating the Ψ_{ij} obtained in this synthesis technique with the ψ_{ij} obtained for the one node to n port mapping. This procedure brings to the following linear system of three $((2/2)(2 + 1) = 3)$ equations in three unknowns

$$\left\{ \begin{array}{l} 3 + \Gamma_{11} + \Gamma_{12} = \frac{1 + 2\gamma_1 + 5\gamma_2 + \gamma_1\gamma_2}{1 + \gamma_1 + \gamma_2} \\ 4 + \Gamma_{12} = \frac{2 + 3\gamma_1 + 4\gamma_2}{1 + \gamma_1 + \gamma_2} \\ 7 + \Gamma_{12} + \Gamma_{22} = \frac{1 + 6\gamma_1 + 6\gamma_2}{1 + \gamma_1 + \gamma_2} \end{array} \right. \quad (4.46)$$

Solving this system for Γ_{11} , Γ_{12} and Γ_{22} we obtain:

$$\begin{aligned} \Gamma_{11} &= \frac{2\gamma_2 + \gamma_1\gamma_2}{1 + \gamma_1 + \gamma_2} \\ \Gamma_{12} &= -\frac{2 + \gamma_1}{1 + \gamma_1 + \gamma_2} \\ \Gamma_{22} &= -\frac{\gamma_2}{1 + \gamma_1 + \gamma_2} \end{aligned} \quad (4.47)$$

From the table above we are able to evaluate the value of all possible termination conditions.

We summarize those results in the following table:

	type1	type2	type3	type4
γ_1	1	0	∞	0
γ_2	∞	∞	0	0
Γ_{11}	3	2	0	0
Γ_{12}	0	0	-1	-2
Γ_{22}	-1	-1	0	0

Table 4-13

$\frac{dF}{dt} \rightarrow \Phi$ synthesis

Fixing $n = 2$ and satisfying the constraint $\alpha_2 - \beta_2 - \alpha_1 + \beta_1 = 2$ by means of the following positions $\alpha_2 = 1, \beta_2 = 0, \alpha_1 = 0$ and $\beta_1 = 1$ we obtain the circuit shown in fig. (4-25) where the subnetworks inside the gray triangle (see fig. (2-18)) are been replaced with the termination sections.

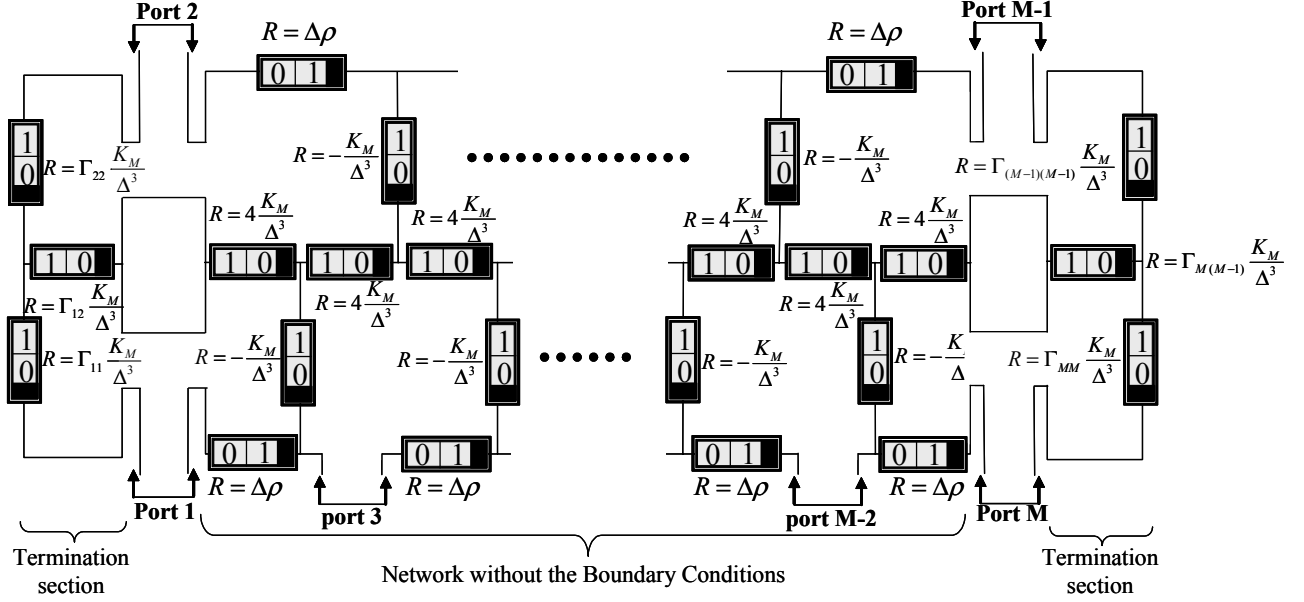


Figure 4-25: One node to one port $\frac{dF}{dt} \rightarrow \Phi$ synthesis. complete network of a fourth order system.

Now we can use the ports shown in fig. (4-24) in order to derive the \mathbb{Z} matrix of the system. As expected we will find a matrix having the structure shown in fig. (2-44). The corner submatrices taking in count for the BC will depend on the parameters Γ_{11}, Γ_{12} and Γ_{22} .

$$\mathbb{Z} = \mathbb{Z}_1 + \mathbb{Z}_2 \quad (4.48)$$

$$\mathbb{Z}_1 = \Delta \rho s \begin{pmatrix} 1 & 0 & 0 & \cdots & 0 & 0 & 0 \\ 0 & 1 & 0 & \cdots & 0 & 0 & 0 \\ 0 & 0 & 1 & \cdots & 0 & 0 & 0 \\ \vdots & \vdots & \vdots & \ddots & \vdots & \vdots & \vdots \\ 0 & 0 & 0 & \cdots & 1 & 0 & 0 \\ 0 & 0 & 0 & \cdots & 0 & 1 & 0 \\ 0 & 0 & 0 & \cdots & 0 & 0 & 1 \end{pmatrix} = \Delta \rho s \mathbb{I} \quad (4.49)$$

$$\mathbb{Z}_2 = \frac{K}{\Delta^3 s} \begin{pmatrix} \Xi_{11} & -\Xi_{12} & 1 & 0 & 0 & 0 & 0 & \cdots & 0 \\ -\Xi_{12} & \Xi_{22} & -4 & 1 & 0 & 0 & 0 & \cdots & 0 \\ 1 & -4 & 6 & -4 & 1 & 0 & 0 & \cdots & 0 \\ 0 & 1 & -4 & 6 & -4 & 1 & 0 & \cdots & 0 \\ \vdots & \ddots & \ddots & \ddots & \ddots & \ddots & \ddots & \ddots & \vdots \\ 0 & \cdots & 0 & 1 & -4 & 6 & -4 & 1 & 0 \\ 0 & \cdots & 0 & 0 & 1 & -4 & 6 & -4 & 1 \\ 0 & \cdots & 0 & 0 & 0 & 1 & -4 & \Xi_{(M-1)(M-1)} & -\Xi_{(M-1)M} \\ 0 & \cdots & 0 & 0 & 0 & 0 & 1 & -\Xi_{(M-1)M} & \Psi_{MM} \end{pmatrix} \quad (4.50)$$

where

$$\Xi_{11} = \Xi_{MM} = 3 + \Gamma_{11} + \Gamma_{12} \quad (4.51)$$

$$\Xi_{12} = \Xi_{(M-1)M} = 4 + \Gamma_{12} \quad (4.52)$$

$$\Xi_{22} = \Xi_{(M-1)(M-1)} = 7 + \Gamma_{12} + \Gamma_{22} \quad (4.53)$$

As we have explained in the second chapter we can evaluate the BCs for the one node to one port mapping by equating the Ξ_{ij} obtained in this synthesis technique with the ζ_{ij} obtained for the one node to n port mapping. This procedure brings to the following linear system of three

$((n/2)(n + 1) = 3)$ equations in three unknowns

$$\left\{ \begin{array}{l} 3 + \Gamma_{11} + \Gamma_{12} = \frac{1 + 2\gamma_1 + 5\gamma_2 + \gamma_1\gamma_2}{1 + \gamma_1 + \gamma_2} \\ 4 + \Gamma_{12} = \frac{2 + 3\gamma_1 + 4\gamma_2}{1 + \gamma_1 + \gamma_2} \\ 7 + \Gamma_{12} + \Gamma_{22} = \frac{1 + 6\gamma_1 + 6\gamma_2}{1 + \gamma_1 + \gamma_2} \end{array} \right. \quad (4.54)$$

Solving this system for Γ_{11} , Γ_{12} and Γ_{22} we obtain:

$$\begin{aligned} \Gamma_{11} &= \frac{2\gamma_2 + \gamma_1\gamma_2}{1 + \gamma_1 + \gamma_2} \\ \Gamma_{12} &= -\frac{2 + \gamma_1}{1 + \gamma_1 + \gamma_2} \\ \Gamma_{22} &= -\frac{\gamma_2}{1 + \gamma_1 + \gamma_2} \end{aligned} \quad (4.55)$$

From the table above we are able to evaluate the value of all possible termination condition. We summarize those results in the following table:

	type1	type2	type3	type4
γ_1	1	0	∞	0
γ_2	∞	∞	0	0
Γ_{11}	3	2	0	0
Γ_{12}	0	0	-1	-2
Γ_{22}	-1	-1	0	0

Table 4-14

In the following subsection we will give an example of a fourth order undulatory phenomena.

4.7 An example of fourth order network

4.7.1 The Euler beam.

The Euler beam theory can be derived by the general fourth order theory by the following interpretation of the general parameters:

General descriptor	Actual descriptor	Physical meaning
$F(x, t)$	$u(x, t)$	vertical displacement
K	K_M	bending stiffness
ρ	λ	mass per unit of length

Table 4-15

Over this condition the equation (4.27) became:

$$u_{k-2}(t) - 4u_{k-1}(t) + 6u_k(t) - 4u_{k+1}(t) + u_{k+2}(t) = \Delta^4 \frac{\lambda}{K_M} \frac{\partial^2 u_k(t)}{\partial t^2} \quad (4.56)$$

As well known by the Euler beam theory the differential descriptor involved in the BC can be physically interpreted as follow:

General descriptor	Actual descriptor	Physical meaning
$u(x, t)$	$u(x, t)$	vertical displacement
$\frac{\partial u(x, t)}{\partial x}$	$\theta(x, t)$	rotation of the transversal section
$K_M \frac{\partial^2 u(x, t)}{\partial x^2}$	$M(x, t)$	bending moment
$K_M \frac{\partial^3 u(x, t)}{\partial x^3}$	$T(x, t)$	transverse shear force

Table 4-16

(4.57)

(4.58)

consequently the BC assumes the following form:

$$M_k(t) = 0 \quad \text{or} \quad \delta(\theta_k(t)) \quad \text{specified} \quad (4.59)$$

$$T_k(t) = 0 \quad \text{or} \quad \delta(u_k(t)) \quad \text{specified}$$

Table 4-16 (4.60)

Looking at eq.4.59 it can be easily understood that the four different types of BC assume in this case a precise physical meaning. The graphical symbols and the terminology used for those BC are listed in the following table.


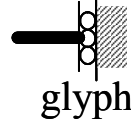


	$u_k(t)=0$	$T_k(t)=0$
$\theta_k(t)=0$	 clamp	 glyph
$M_k(t)=0$	 hing	 free

Table 4-17

4.7.2 One node to n port mapping

$\frac{\partial F}{\partial t} \rightarrow \Pi$ synthesis

In this section we will give an actual meaning to the components and the physical quantity governing the evolution of the general fourth order circuit shown in fig. (4-18). As reported in table (4-15) the scalar field $F(x, t)$ is associated with the vertical displacement $u(x, t)$ so that the intensive quantity Π_k of the k^{th} node will be associated with the vertical velocity v_k . Consequently the complementar extensive quantity will be associated with the transversal force T_k . The generalized lever (pinned rigid link) behaves as a bidirectional ideal transducer.

Changing the pair (v, T) in the pair (ω, M) characterizing the second line of the circuit. Based on those argumentation using table (2-1) it is possible to specify the general circuit, associated with the basic section, shown in fig. (4-18) for the case of interest as shown in fig (4-26 a). In fig. (4-26 b) it is shown the mechanical model of the basic section.

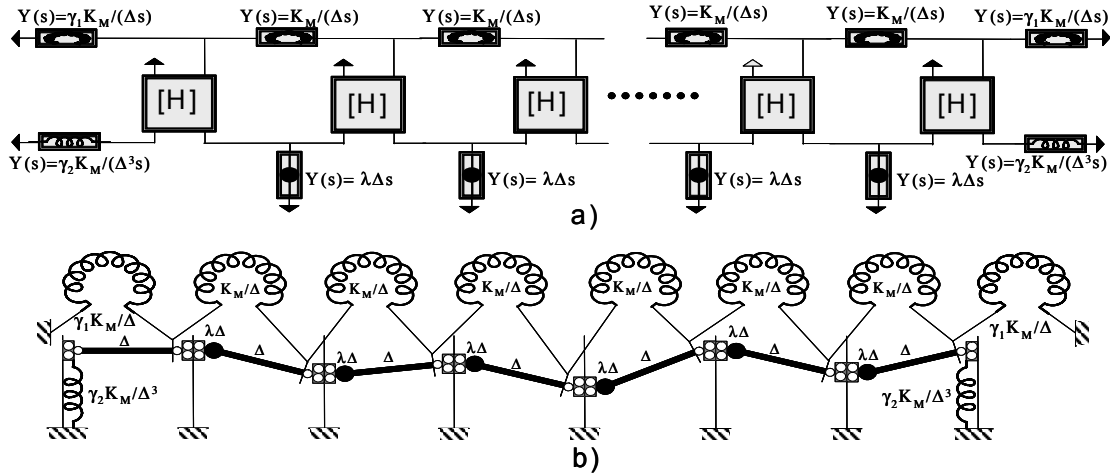


Figure 4-26: One node to n ports $\frac{dF}{dt} \rightarrow \Pi$ synthesis transversal vibration on a beam analogy.

a) equivalent circuit, b) mechanical model.

Similarly the components of the general circuit shown in fig. (4-19) can be specialized once it is known the physical meaning of the pair (Π, Φ) characterizing each line of the circuit. Using table (2-1) we obtain the circuit shown in fig. (4-27 a). In fig. (4-27 b) is shown the mechanical model of the whole beam.

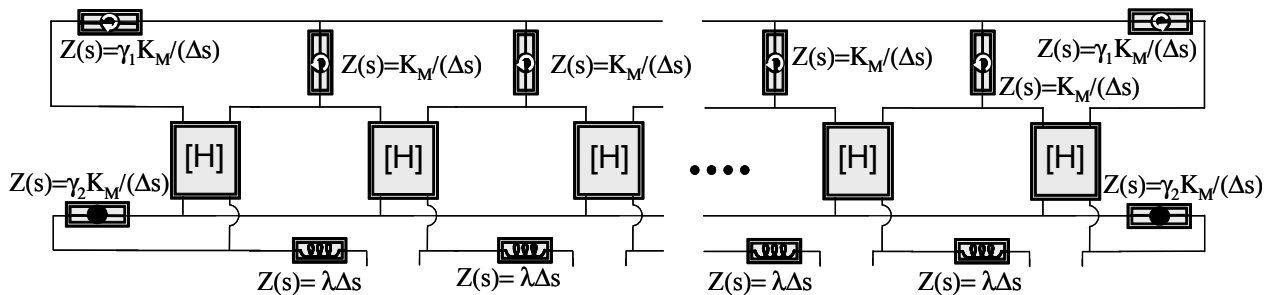


Figure 4-27: One node to n ports $\frac{dF}{dt} \rightarrow \Phi$ synthesis transversal vibration on a beam analogy.

Equivalent circuit.

$\frac{\partial F}{\partial t} \rightarrow \Phi$ synthesis

In this section we will give an actual meaning to the components and the physical quantity governing the evolution of the general fourth order circuit shown in fig. (4-21). As reported in table (4-15) the scalar field $F(x, t)$ is associated with the vertical displacement $u(x, t)$ so that the extensive quantity Φ_k of the k^{th} node will be associated with the vertical velocity v_k . Consequently the complementar intensive quantity will be associated with the transversal force T_k . The generalized lever (pinned rigid link) behaves as a bidirectional ideal transducer. Changing the pair (v, T) in the pair (ω, M) characterizing the second line of the circuit. Based on those argumentation using table (2-1) it is possible to specify the general circuit, associated with the basic section, shown in fig. (4-21) for the case of interest as shown in fig (4-28).

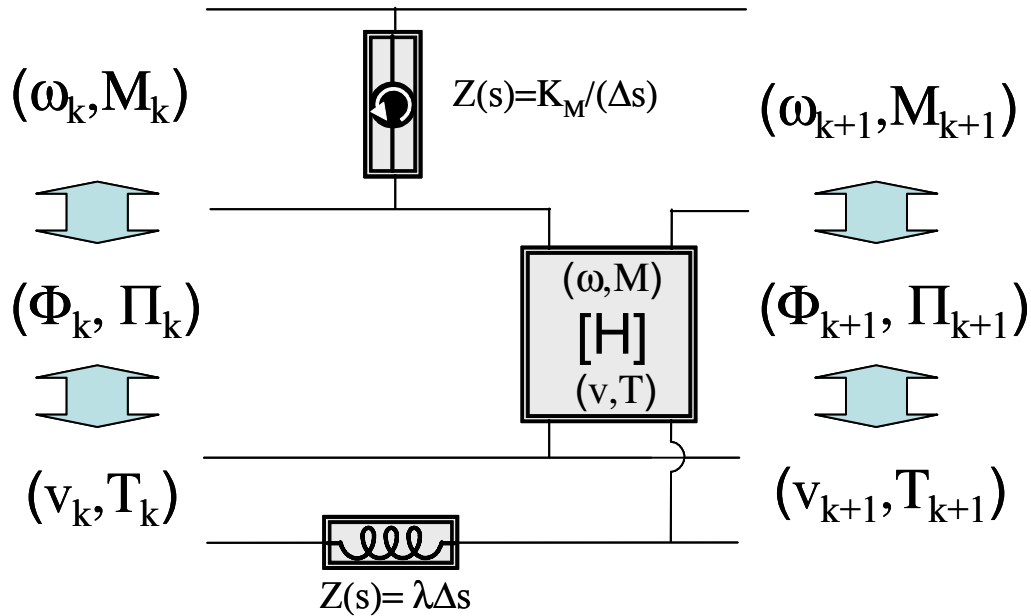


Figure 4-28: One node to n ports $\frac{dF}{dt} \rightarrow \Phi$ synthesis trasversal vibration on a beam analogy.
Basic section.

Similarly the components of the general circuit shown in fig. (4-22) can be specialized once it is known the physical meaning of the pair (Π, Φ) characterizing each line of the circuit. Using table (2-1) we obtain the circuit shown in fig. (4-29).

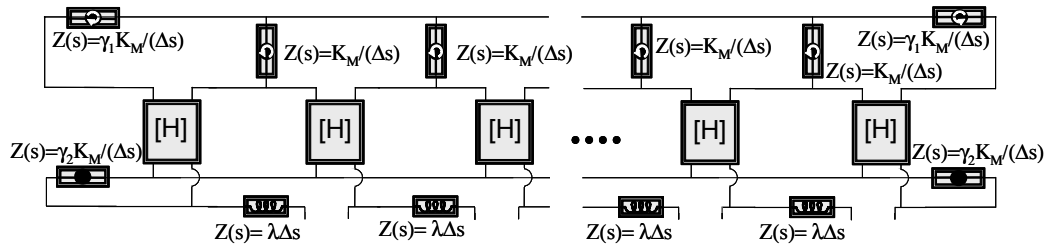


Figure 4-29: One node to n ports $\frac{dF}{dt} \rightarrow \Phi$ synthesis trasversal vibration on a beam analogy.
Complete network.

4.7.3 One node to one port mapping

$\frac{\partial F}{\partial t} \rightarrow \Pi$ synthesis

The general circuit derived in the previous section can be now specialized for the case of interest. The circuital scheme obtained is shown in the fig (4-30), in this figure we have explicitly shown the access port of the system. As reported in table (4-15) the scalar field $F(x, t)$ is associated with the vertical displacement $u(x, t)$ so that the intensive quantity Π_k of the k^{th} node will be associated with the vertical velocity v_k . Consequently the complementar extensive quantity will be associated with the transversal force T_k . Conversely from the one node to n ports mapping in this kind of network there are not any transducers and consequently each node of the network will be characterized by means of the same pair (v, T) . In fig (4-30 a) is shown a replica of the general circuit shown in fig (4-24) where the components are been interpreted for the pair of interest (v, T) . As we did before, we will show in fig. (4-30 b) the mechanical equivalent system where, also if not explicitly shown, the pointwise masses are constrained to move on a purely vertical path.

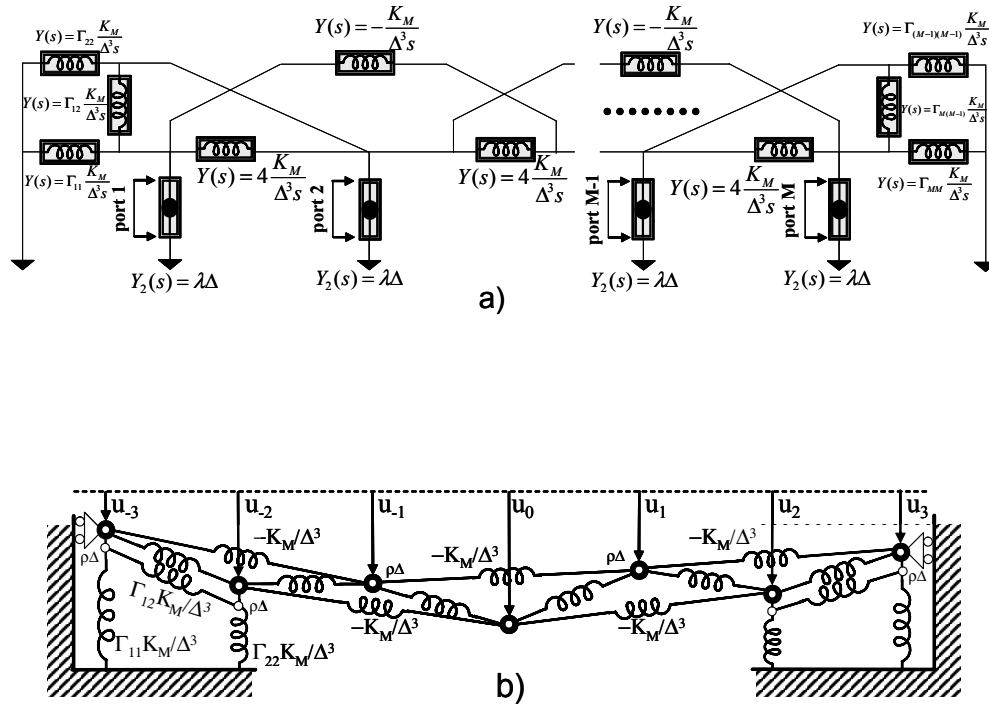


Figure 4-30: One node to one port $\frac{dF}{dt} \rightarrow \Pi$ synthesis trasversal vibration on a beam analogy.

a) equivalent circuit, b) mechanical model.

$\frac{\partial F}{\partial t} \rightarrow \Phi$ synthesis

Similarly the general circuit derived in the previous section can be specialized for the case of interest. The circuitual scheme obtained is shown in the fig (4-31), in this figure we have explicitly shown the access port of the system. As reported in table (4-15) the scalar field $F(x, t)$ is associated with the vertical displacement $u(x, t)$ so that the extensive quantity Φ_k of the k^{th} node will be associated with the vertical velocity v_k . Consequently the complementar intensive quantity will be associated with the transversal force T_k . Conversely from the one node to n ports mapping in this kind of network there are not any transducers and consequently each node of the network will be characterized by means of the same pair (v, T) . In fig (4-31) is shown a replica of the general circuit shown in fig (4-25) where the components are been interpreted for the pair of interest (v, T) .

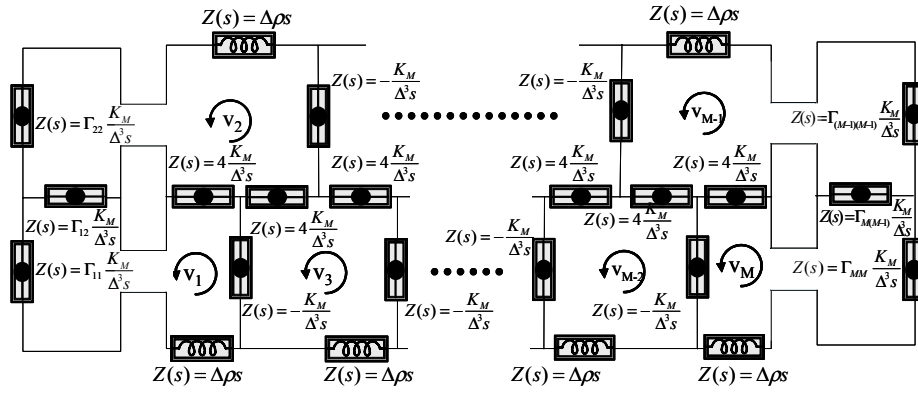


Figure 4-31: One node to one port $\frac{dF}{dt} \rightarrow \Phi$ synthesis trasversal vibration on a beam analogy.
Equivalent circuit.

Chapter 5

Hybrid systems gyroscopically coupled

5.1 Introduction

In this chapter we will introduce the system of equations describing a coupled system. A coupled system can be obtained by interconnecting two different subsystems by means of a transducer. Obviously it is not required for the two systems to have the same nature, the only important point is that the transducers will be able to establish a bidirectional communication between the two different subsystems. This structure, shown in fig. (4-1) will be referred as an hybrid coupled system.

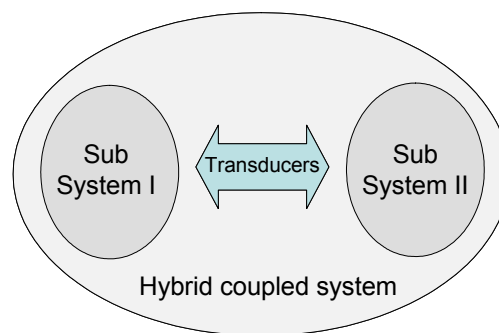


Figure 5-1: A hybrid coupled system as the set of two subsystems having different nature communicating by means of a transducer.

In particular we will assume that each of the two subsystems will be accessible by a certain number of ports. The hybrid coupled system will be obtained by interconnecting one to one the ports of the two subsystems by means of an array of bidirectional transducers, modelled as two ports networks. First of all we will consider a one dimensional system described in the Laplace domain by means of its impedance or its admittance depending on the convenience. Then we will describe the performance of this system and we will compare them with the performance of the same system coupled with a second subsystem by means of a single actuator. Finally we will generalize the results obtained to the n dimensional case.

5.2 One dimensional coupling

5.2.1 Introduction

In this section we will study a system accessible from one port. This system will be described in the Laplace domain by means of its impedance (admittance) and will be coupled to a similar system by means of a bidirectional transducer. As we have shown in the previous chapter a bidirectional transducer can be modeled in four different ways, similarly we can describe a coupled system for each one of the four possible models of a transducer.

5.2.2 The case of ideal transducers

Y coupling

Here we model the first subsystem by means of a bipolar admittance Y_1 , this system is coupled with a second subsystem modeled as a bipolar admittance Y_2 . The coupling is realized through a bidirectional ideal Y transducer characterized by the two pairs (Π_1, Φ_1) and (Π_2, Φ_2) . Finally an independent Φ generator, of value $\hat{\Phi}$ is shunted to the admittance Y_1 in order to give an excitation to the system.

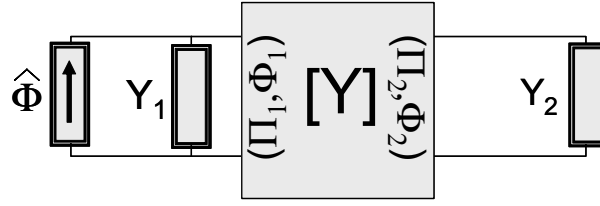


Figure 5-2: One dimensional coupling. Y model.

The coupled system shown in fig. (5-2) can be described by means of the following system of equations:

$$\begin{cases} \hat{\Phi} = Y_1 \Pi_1 + y_{12} \Pi_2 \\ 0 = y_{21} \Pi_1 + Y_2 \Pi_2 \end{cases} \quad (5.1)$$

Z coupling

Here we model the first subsystem by means of a bipolar impedance Z_1 , this system is coupled with a second subsystem modeled as a bipolar impedance Z_2 . The coupling is realized through an ideal bidirectional Z transducer, characterized by the two pairs (Π_1, Φ_1) and (Π_2, Φ_2) . Finally an independent Π generator, of value $\hat{\Pi}$ is connected in series with the impedance Z_1 in order to give an excitation to the system.

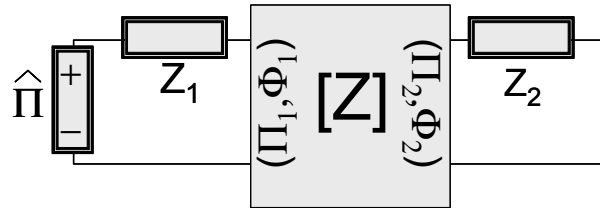


Figure 5-3: One dimensional coupling. Z model.

The complete system, shown in fig. (5-3) can be described by means of the following system of equations:

$$\begin{cases} \hat{\Pi} = Z_1 \Phi_1 + z_{12} \Phi_2 \\ 0 = z_{21} \Phi_1 + Z_2 \Phi_2 \end{cases} \quad (5.2)$$

G coupling

Here we model the first subsystem by means of a bipolar admittance Y_1 , this system is coupled with a second subsystem modeled as a bipolar impedance Z_2 . The coupling is realized through

an ideal bidirectional G transducer, characterized by the two pairs (Π_1, Φ_1) and (Π_2, Φ_2) . Finally an independent Φ generator, of value $\hat{\Phi}$ is shunted to the admittance Y_1 in order to give the same excitation to the system.

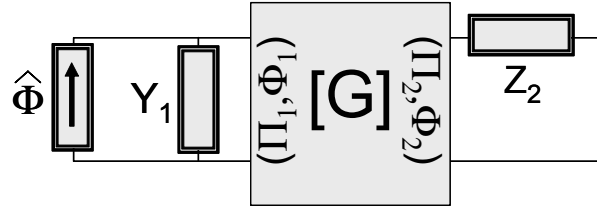


Figure 5-4: One dimensional coupling. G model.

The complete system, shown in fig. (5-4) can be described by means of the following system of equations:

$$\begin{cases} \hat{\Phi} = Y_1 \Pi_1 + g_{12} \Phi_2 \\ 0 = g_{21} \Pi_1 + Z_2 \Phi_2 \end{cases} \quad (5.3)$$

H coupling

Here we model the first subsystem by means of a bipolar impedance Z_1 , this system is coupled with a second subsystem modeled as a bipolar admittance Y_2 . The coupling is realized through an ideal bidirectional Y transducer, characterized by the two pairs (Π_1, Φ_1) and (Π_2, Φ_2) . Finally an independent Π generator, of value $\hat{\Pi}$ is connected in series with the impedance Z_1 in order to give same excitation to the system.

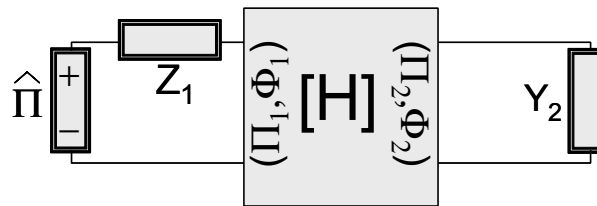


Figure 5-5: One dimensional coupling. H model.

The complete system, shown in fig. (5-5) can be described by means of the following system of equations:

$$\begin{cases} \hat{\Pi} = Z_1 \Phi_1 + h_{12} \Phi_2 \\ 0 = h_{21} \Phi_1 + Y_2 \Phi_2 \end{cases} \quad (5.4)$$

5.2.3 Uncoupled system VS gyroscopically coupled system

Now we want to make a comparison between the uncoupled system and the coupled one. This analysis can be made studying the two network functions obtained by the ratio between the two independent quantities characterizing the transducer model and the impressed quantity. For example, in the case of the Y coupling, the independent quantities are Π_1 and Π_2 while the impressed quantity is $\widehat{\Phi}$. The uncoupled system can be obtained from by eq. (5.1) by avoiding the transducer effect (i.e. $y_{12} = y_{21} = 0$). In this case we obtain:

$$Z_1^0(s) = \left. \frac{\Pi_1(s)}{\widehat{\Phi}(s)} \right|_{y_{12}=y_{21}=0} = \frac{1}{Y_1(s)} = \frac{D_1(s)}{N_1(s)} \quad (5.5)$$

$$Z_2^0(s) = \left. \frac{\Pi_2(s)}{\widehat{\Phi}(s)} \right|_{y_{12}=y_{21}=0} = 0 \quad (5.6)$$

The second case of interest is obtained when the coupling coefficients y_{12} and y_{21} are equal and opposite one to each other (i.e. $y_{12} = -y_{21} = \alpha$). In this situation the coupling is referred as gyroscopic and the two network functions of interest become:

$$Z_1^\alpha(s) = \left. \frac{\Pi_1(s)}{\widehat{\Phi}(s)} \right|_{y_{12}=-y_{21}=\alpha} = \frac{Y_2(s)}{Y_1(s)Y_2(s) + \alpha^2} = \frac{N_2(s)D_1(s)}{N_1(s)N_2(s) + \alpha^2 D_1(s)D_2(s)} \quad (5.7)$$

$$Z_2^\alpha(s) = \left. \frac{\Pi_2(s)}{\widehat{\Phi}(s)} \right|_{y_{12}=-y_{21}=\alpha} = \frac{-\alpha}{Y_1(s)Y_2(s) + \alpha^2} = \frac{-\alpha D_2(s)D_1(s)}{N_1(s)N_2(s) + \alpha^2 D_1(s)D_2(s)} \quad (5.8)$$

In the following we will study the properties of those two network functions in both the frequency and the time domain, comparing them for the coupled and the uncoupled case.

Frequency domain analysis

In order to perform a comparison between a coupled and an uncoupled system we need to specify the form of the admittance $Y_1(s)$ describing the first subsystem. In this work the attention is focused on the ondulatory phenomena. As we have deeply studied in the second chapter a discrete version of those phenomena can be described by means of circuitual network involving $(1, 0)$ elements, $(0, 1)$ element and generalized lever. The simplest case we have studied is given

by a zero order system shown in fig (2-16).The admittance of this system assumes the following form:

$$Y_1(s) = A \frac{(s^2 + s_0^2)}{s} \quad (5.9)$$

it should be noted that (5.9) describes an harmonic oscillator (in the Laplace domain). It is useful for our purpose to define an adimensional version of (5.9). In order to proceed with the adimensionalization process we will make the following position:

$$s = s_0 \bar{s} \quad (5.10)$$

$$Y_0 = A s_0 \quad (5.11)$$

$$\alpha = 2Y_0 \bar{\alpha} \quad (5.12)$$

substituting (5.10) and (5.11) in (5.9) we can define an adimensional admittance $\bar{Y}_1(\bar{s})$ as follows:

$$\bar{Y}_1(\bar{s}) = \frac{\bar{Y}_1(\bar{s})}{Y_0} = \frac{(\bar{s}^2 + 1)}{\bar{s}} \quad (5.13)$$

it should be noted that the adimensionalization parameter has been used in order to normalize to a unit value the natural frequency and the amplitude of the oscillation. Now we need to properly design the second subsystem $Y_2(s)$. In [Vidoli et al.(2000)] it was heuristically proven that in order to guarantee the maximum energy transfer between the first ($Y_1(s)$) and the second system ($Y_2(s)$), they should be governed by the same differential operator this results was expanded in [dell' Isola et al. (2003)]. This request guarantees that they will have equivalent spectral properties, consequently can be established a multimodal resonance. This consideration brings us to assume $Y_2(s) = Y_1(s)$ and consequently $\bar{Y}_2(\bar{s}) = \bar{Y}_1(\bar{s})$. Under this assumption and using (5.13) in (5.5)..(5.8) we obtain:

$$\bar{Z}_1^0(\bar{s}) = Y_0 Z_1^0(\bar{s}) = \frac{1}{\bar{Y}_1(\bar{s})} = \frac{\bar{s}}{\bar{s}^2 + 1} \quad (5.14)$$

$$\bar{Z}_2^0(\bar{s}) = 0 \quad (5.15)$$

$$\bar{Z}_1^\alpha(\bar{s}) = Y_0 Z_1^\alpha(\bar{s}) = Y_0 \frac{Y_0 \bar{Y}_1(\bar{s})}{Y_0 \bar{Y}_1(\bar{s}) Y_0 \bar{Y}_1(\bar{s}) + (2Y_0 \bar{\alpha})^2} = \frac{\bar{s}(\bar{s}^2 + 1)}{1 + (2 + 4\bar{\alpha}^2)\bar{s}^2 + \bar{s}^4} \quad (5.16)$$

$$\bar{Z}_2^\alpha(\bar{s}) = Y_0 \bar{Z}_2^\alpha(\bar{s}) = Y_0 \frac{-2Y_0 \bar{\alpha}}{Y_0 \bar{Y}_1(\bar{s}) Y_0 \bar{Y}_1(\bar{s}) + (2Y_0 \bar{\alpha})^2} = \frac{-2\bar{\alpha} \bar{s}^2}{1 + (2 + 4\bar{\alpha}^2)\bar{s}^2 + \bar{s}^4} \quad (5.17)$$

It is interesting to compare $|\overline{Z}_1^0(\overline{\omega})|$ with the $|\overline{Z}_1^\alpha(\overline{\omega})|$. First of all we need to evaluate those functions.

$$|\overline{Z}_1^0(\overline{\omega})| = \frac{\overline{\omega}}{\overline{\omega}^2 - 1} \quad (5.18)$$

$$|\overline{Z}_1^\alpha(\overline{\omega})| = \frac{\overline{\omega}(\overline{\omega}^2 - 1)}{1 - 2(1 + 2\overline{\alpha})\overline{\omega}^2 + \overline{\omega}^4} \quad (5.19)$$

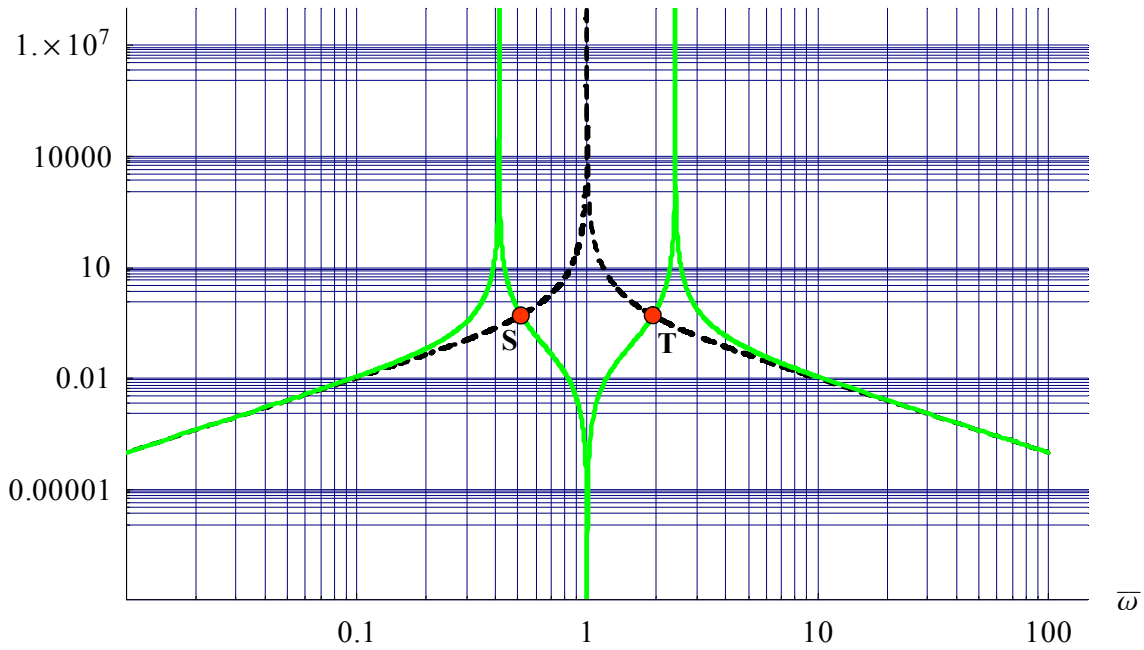


Figure 5-6:

In figure (5-6) are shown the two functions $|\overline{Z}_1^0(\overline{\omega})|$ (dashed) and $|\overline{Z}_1^\alpha(\overline{\omega})|$ (solid); looking at the picture it can be noted that when a logarithmic scale is used the two split poles of $|\overline{Z}_{11}^\alpha(\overline{\omega})|$ are symmetric with respect to the one of $|\overline{Z}_1^0(\overline{\omega})|$, this distinctive feature happens if and only if the resonance frequencies of the system $Y_2(s)$ are exactly equal to the ones of the system $Y_1(s)$. This symmetry can be mathematically analyzed by evaluating the intersection points between $|\overline{Z}_1^0(\overline{\omega})|$ and $|\overline{Z}_1^\alpha(\overline{\omega})|$. Considering positive frequency and neglecting the trivial

solutions we will find:

$$\bar{\omega}_S = \sqrt{1 + \bar{\alpha}^2 - \bar{\alpha}\sqrt{2 + \bar{\alpha}^2}} \quad (5.20)$$

$$\bar{\omega}_T = \sqrt{1 + \bar{\alpha}^2 + \bar{\alpha}\sqrt{2 + \bar{\alpha}^2}} \quad (5.21)$$

substituting (5.20) and (5.21) in (5.18) and (5.19) we will find:

$$\left| \bar{Z}_{11}^0(\bar{\omega}_S) \right| = \left| \bar{Z}_{11}^0(\bar{\omega}_T) \right| = \left| \bar{Z}_{11}^\alpha(\bar{\omega}_S) \right| = \left| \bar{Z}_{11}^\alpha(\bar{\omega}_T) \right| = \frac{1}{\sqrt{2\bar{\alpha}}} \quad (5.22)$$

the property expressed by equation (5.22) gives us a quantitative way to express this symmetry, in fact it can be expressed by saying that the intersection points S and T between $\left| \bar{Z}_1^0(\bar{\omega}) \right|$ and $\left| \bar{Z}_1^\alpha(\bar{\omega}) \right|$ assume the same value. In general when the resonance frequencies of the second system don't match with the ones of the first system this symmetry is lost and the points S and T assume different values as shown in fig. (5-7) and (5-8).

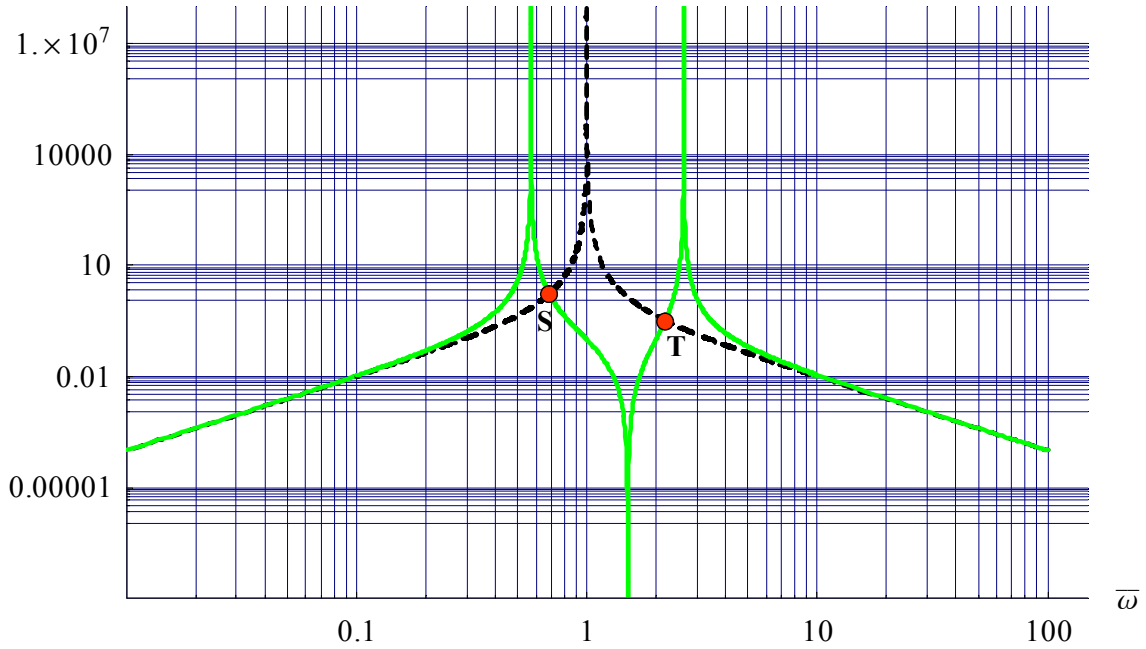


Figure 5-7:

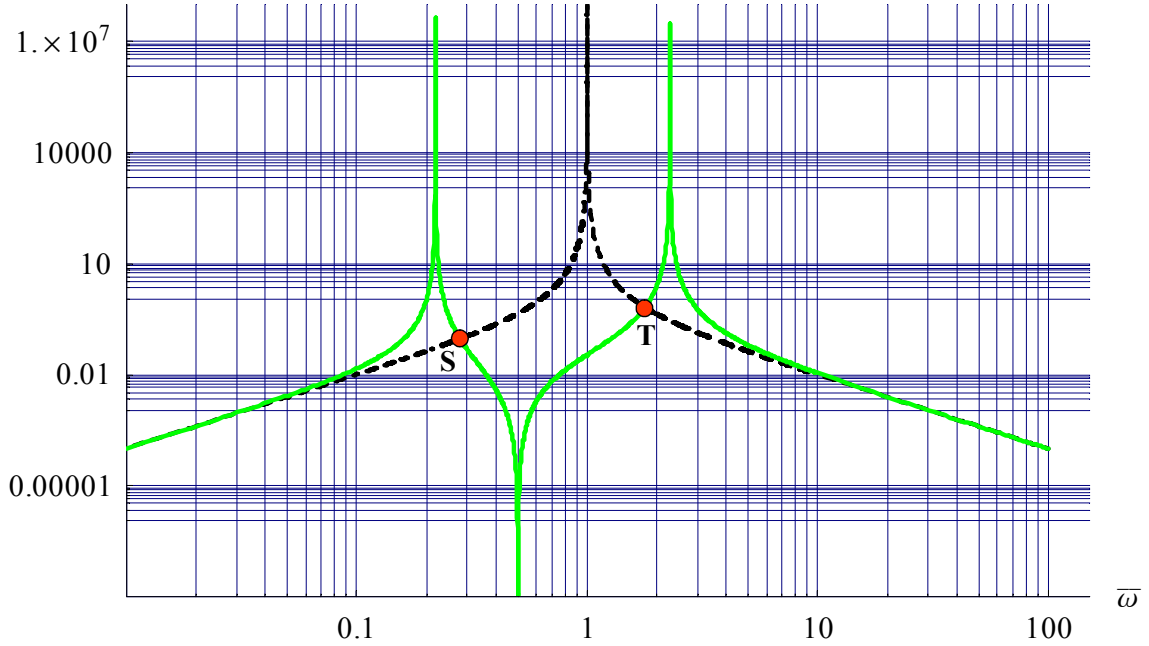


Figure 5-8:

Time evolution

Now it is useful to give some descriptions of the time evolution of the uncoupled and the coupled system. First of all we will derive the impulsive response for the uncoupled system. Having the network function $\bar{Z}_{11}^0(\bar{s})$, the physical meaning of an impedance, the impulsive response associated to it will represent the time evolution $\pi_1^0(t)$ of the Π quantity between the terminals of the first system (i.e. Y_1) when an impulsive Φ quantity of unitary amplitude is applied through the terminals of the same system at $\bar{t} = 0$. Consequently $\pi_1^0(t)$ can be evaluated by computing the inverse Laplace transform of the network function $\bar{Z}_1^0(\bar{s})$. We will find¹:

$$\bar{\pi}_1^0(\bar{t}) = \mathcal{L}^{-1} \left\{ \bar{Z}_1^0(\bar{s}) \right\} = \cos(\bar{t})u_{-1}(\bar{t}) \quad (5.23)$$

¹Where $u_{-1}(\bar{t})$ is the Havisade unit step function defined as follows:

$$u_{-1}(t) = \begin{cases} 1 & t \geq 0 \\ 0 & t < 0 \end{cases}$$

similarly, even if it is trivial, we can define $\pi_2^0(t)$ as follows:

$$\bar{\pi}_2^0(\bar{t}) = \mathcal{L}^{-1} \left\{ \bar{Z}_2^0(\bar{s}) \right\} = 0 \quad (5.24)$$

Comparing those two functions it is possible to note that when the first system is uncoupled from the second one an impulsive excitation given to the first system produces an oscillation of constant amplitude and unitary value in that system while the second one remains at rest. This behavior is pointed out in fig. (5-9).

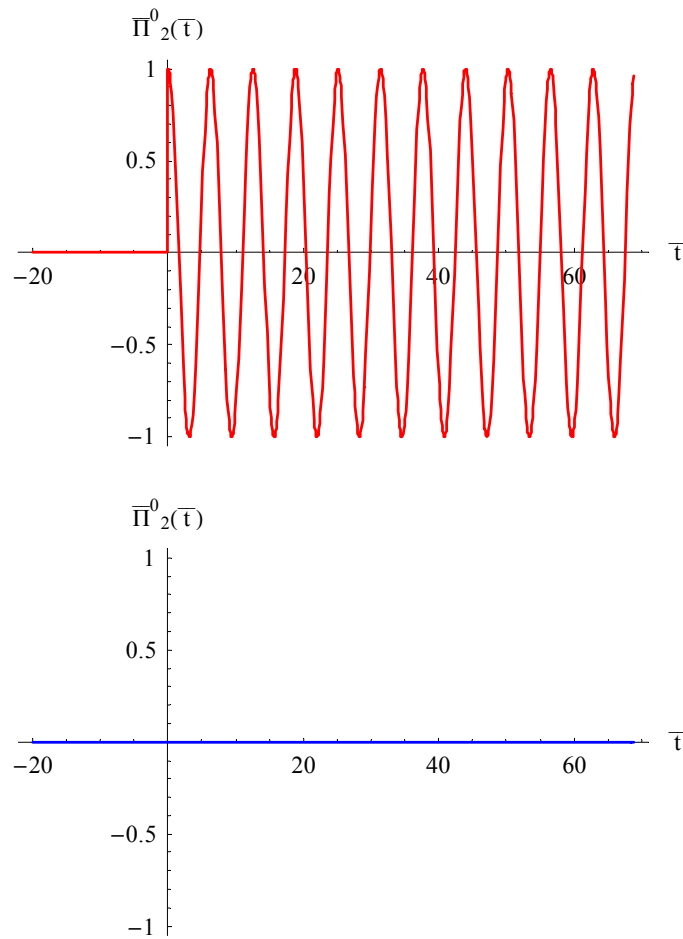


Figure 5-9:

Similarly we can perform the same analysis for the coupled system by considering the functions

$\bar{\pi}_1^\alpha(\bar{t})$ and $\bar{\pi}_2^\alpha(\bar{t})$ defined as follows:

$$\bar{\pi}_1^\alpha(\bar{t}) = \mathcal{L}^{-1} \{ \bar{Z}_1^\alpha(\bar{s}) \} = \left(\cos(\bar{\alpha}\bar{t}) \cos(\sqrt{1 + \bar{\alpha}^2}\bar{t}) - \frac{\bar{\alpha}}{\sqrt{1 + \bar{\alpha}^2}} \sin(\bar{\alpha}\bar{t}) \sin(\sqrt{1 + \bar{\alpha}^2}\bar{t}) \right) \quad (5.25)$$

$$\bar{\pi}_2^\alpha(\bar{t}) = \mathcal{L}^{-1} \{ \bar{Z}_2^\alpha(\bar{s}) \} = \left(-\sin(\bar{\alpha}\bar{t}) \cos(\sqrt{1 + \bar{\alpha}^2}\bar{t}) - \frac{\bar{\alpha}}{\sqrt{1 + \bar{\alpha}^2}} \cos(\bar{\alpha}\bar{t}) \sin(\sqrt{1 + \bar{\alpha}^2}\bar{t}) \right) \quad (5.26)$$

Looking at eq. (5.25) and (5.26) governing the time evolution of the coupled system it can be noted that now both $\bar{\pi}_1^\alpha(\bar{t})$ and $\bar{\pi}_2^\alpha(\bar{t})$ have a non trivial evolution. More precisely we can recognize a shifting of the oscillation frequency from the uncoupled value 1 to the coupled value $\sqrt{1 + \bar{\alpha}^2}$ this means that the coupling produces always an increment of the oscillation frequency.

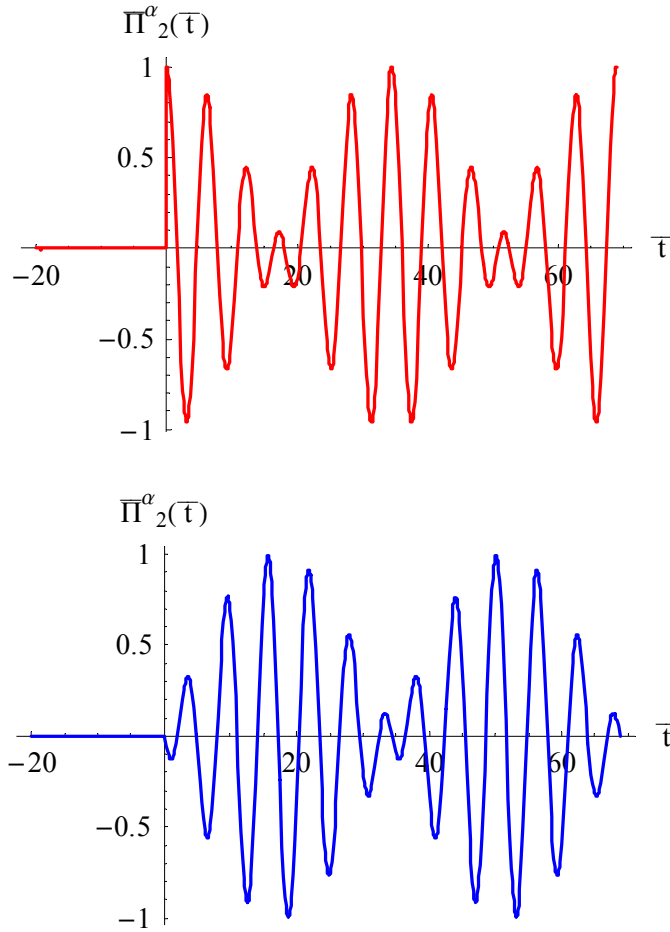


Figure 5-10:

Moreover in the coupled system the amplitude of the fundamental oscillation is modulated with a secondary frequency equal to the coupling coefficient $\bar{\alpha}$. This phenomenon known as beat, is a different interpretation of the poles doubling we had observed in the frequency domain. In fig. (5-10) it is shown the evolution of eq. (??) and (5.26) when $\bar{\alpha} = \frac{1}{3\sqrt{11}}$. This choice is motivated by the fact that it forces the primary frequency to be a multiple of the secondary one.

Energetic consideration

In order to show how the coupling procedure is able to produce a transfer of the energy from the first system to the second one it is crucial to study the time evolution of the energy of the first and the second system for both the coupled and the uncoupled case. First of all we need to derive an analytical form for the energy of a system characterized by the dimensionless admittance (5.13) as a function of the pair (Π, Φ) , characterizing the system. As usual we can express the energy of the system $e(t)$ in the following way:

$$e(t) = \int p(t) dt \quad (5.27)$$

where $p(t)$ is the power absorbed by a given system accessible from a port. As we have said before the power absorbed by a port is given by the product of the quantity characterizing the port, so we have:

$$e(t) = \int \pi(t) \phi(t) dt \quad (5.28)$$

In the previous subsection we derive an analytical form for the function $\pi(t)$ so it can be considered a known quantity. Consequently we need to manipulate expression (5.28) in order to derive an expression depending on this function only. A suitable form of the energy can be obtained by means of the following steps:

$$\begin{aligned} \bar{e}(\bar{t}) &= \int \bar{\pi}(\bar{t}) \mathcal{L}^{-1} \{ \bar{Y}_1(\bar{s}) \bar{\Pi}(\bar{s}) \} d\bar{t} = \int \bar{\pi}(\bar{t}) \mathcal{L}^{-1} \left\{ \frac{\bar{s}^2 + 1}{\bar{s}} \bar{\Pi}(\bar{s}) \right\} d\bar{t} = \\ &= \int \bar{\pi}(\bar{t}) \mathcal{L}^{-1} \left\{ \frac{\bar{\Pi}(\bar{s})}{\bar{s}} + \bar{s} \bar{\Pi}(\bar{s}) \right\} d\bar{t} = \int \bar{\pi}(\bar{t}) \left(\mathcal{L}^{-1} \left\{ \frac{\bar{\Pi}(\bar{s})}{\bar{s}} \right\} + \mathcal{L}^{-1} \{ \bar{s} \bar{\Pi}(\bar{s}) \} \right) d\bar{t} = \\ &= \int \bar{\pi}(\bar{t}) \left(\int \bar{\pi}(\bar{t}) d\bar{t} + \frac{d\bar{\pi}(\bar{t})}{d\bar{t}} \right) d\bar{t} = \int \left(\bar{\pi}(\bar{t}) \left(\int \bar{\pi}(\bar{t}) d\bar{t} \right) + \bar{\pi}(\bar{t}) \left(\frac{d\bar{\pi}(\bar{t})}{d\bar{t}} \right) \right) d\bar{t} = \end{aligned}$$

$$= \frac{1}{2} \left(\int \bar{\pi}(\bar{t}) d\bar{t} \right)^2 + \frac{1}{2} \bar{\pi}(\bar{t})^2 \quad (5.29)$$

We can use expression (5.29) for evaluating the energy of the first and the second system for both the coupled and the uncoupled case. First of all we need to evaluate the time integral of the expressions (5.23)..(5.26).

$$\begin{aligned} \int \bar{\pi}_1^0(\bar{t}) d\bar{t} &= \sin(t) \\ \int \bar{\pi}_2^0(\bar{t}) d\bar{t} &= 0 \\ \int \bar{\pi}_1^\alpha(\bar{t}) d\bar{t} &= \frac{\cos(\bar{\alpha}\bar{t}) \sin(\sqrt{1 + \bar{\alpha}^2}\bar{t})}{\sqrt{1 + \bar{\alpha}^2}} \\ \int \bar{\pi}_2^\alpha(\bar{t}) d\bar{t} &= -\frac{\sin(\bar{\alpha}\bar{t}) \sin(\sqrt{1 + \bar{\alpha}^2}\bar{t})}{\sqrt{1 + \bar{\alpha}^2}} \end{aligned} \quad (5.30)$$

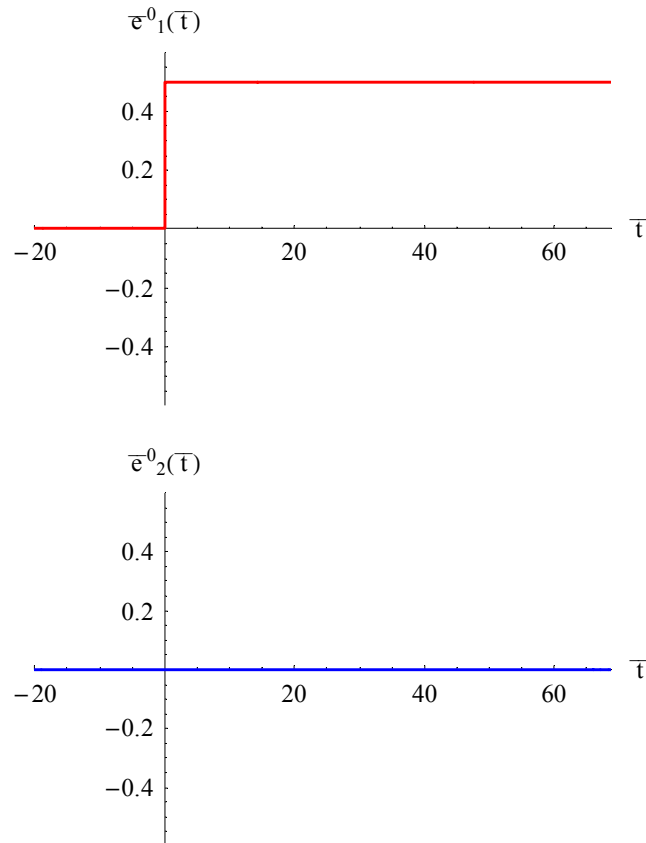


Figure 5-11:

Substituting expressions (5.23) and (5.30) in (5.29) we will find the analytical expression for the energy of the first and the second system. When we consider the uncoupled configuration we obtain the following plots for the time evolution of the energy. Looking at fig.(5-11) it is clear that when we give an impulsive excitation the energy of the first system rises suddenly from zero to 0.5 at $\bar{t} = 0$ and it stays at this constant value, while the energy of the second system is always zero, i.e. there is not energy transfer from the first to the second system. In a similar way it is possible to plot the time evolution of the energy for the coupled configuration. It is illustrated in the following figure.

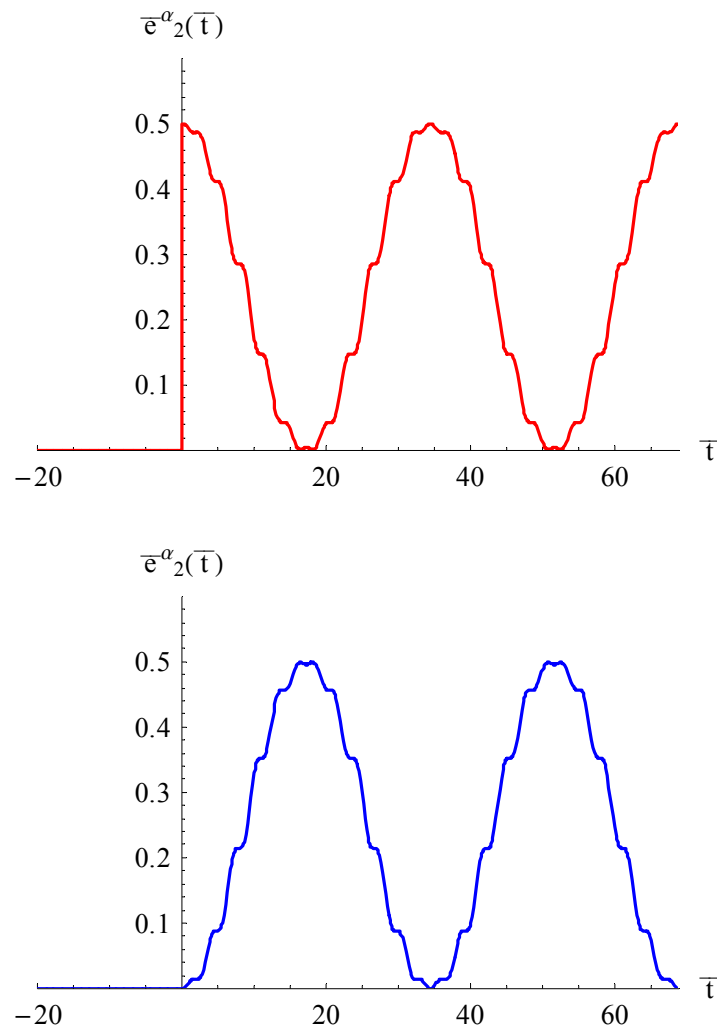


Figure 5-12:

From the fig. (5-12) it is clear that when we consider the coupled configuration the amplitude of the energy of the first system rises suddenly from zero to 0.5 at $\bar{t} = 0$ as well as in the uncoupled case but now its value changes in time oscillating from this maximum value and zero. Simultaneously the second system starts from a zero energy at $\bar{t} = 0$ and increase its energy until it reach the maximum value (i.e. the total energy of the coupled system) in correspondence with the minimum energy of the first system (i.e. zero). At that instant the energy of the first system is completely transferred to the second one. Then the energy starts to come back to the first system until it goes back completely to it. In conclusion we can say that the energy of the system oscillates from the two coupled systems with a given period.

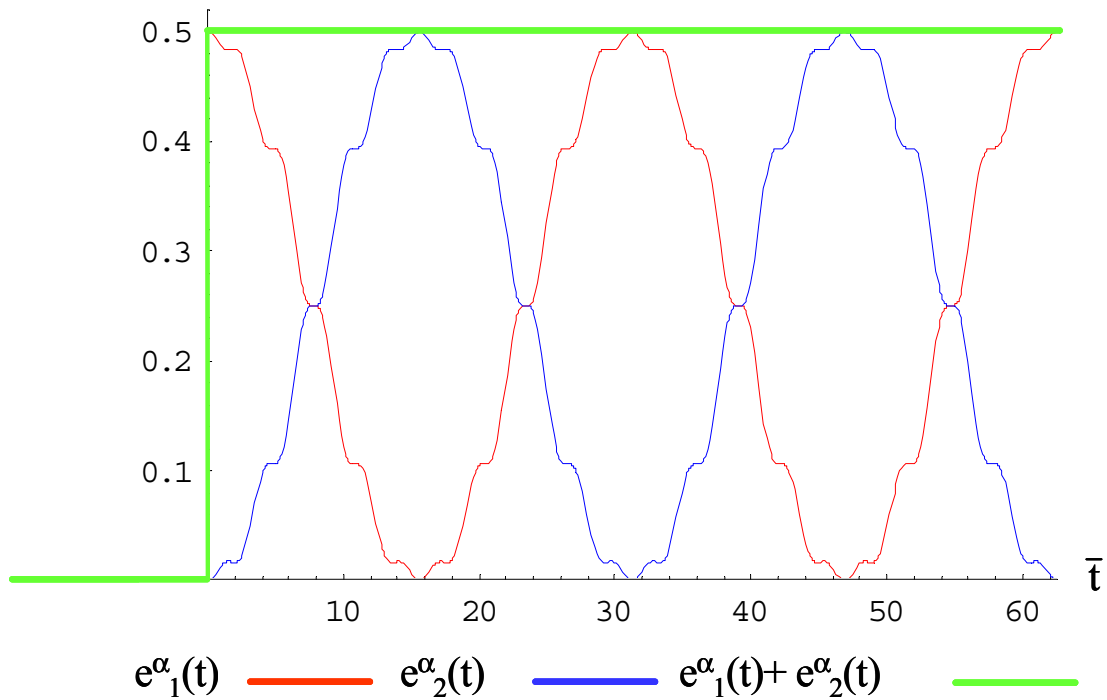


Figure 5-13:

In fig. (5-13) it is shown that, as expected from the conservation of energy, the sum of the energy of the first and the second system is equal to the total energy (i.e. 0.5) instant by instant. It should be noted that the totality of the consideration we have done referring to the Y-coupling can be replicated for the other kind of coupling without any sort of complication.

5.2.4 The case of real transducers

In the previous subsection we have shown that the energy of an oscillating system can be optimally transferred in a second system when the second system is equal to the first one and it is coupled to it by means of an ideal bidirectional transducer. More precisely it should be noted that the second system must be designed taking in count of the model we are using for the coupling. This means that we need to make the admittance of the second system equal to the admittance of the first system for the Y coupling while we need to make the impedance of the second system equal to the admittance of the first system for the G coupling, and so on. Some complications rise when we consider parasite effects of real transducers. In fact those parasite elements break the symmetry of the coupling avoiding the suitable properties we had put in evidence in the previous subsection. By the way in some case this problem can be overpassed by choosing a suitable coupling model. In order to select the right model we need to use the notion of constitutive symmetry we had introduced in the previous chapter. As usual there exist four cases of interest.

Y coupling

If the transducers we are using to couple the two systems is Y symmetrizable we need to use the Y coupling model, in fact comparing fig. (3-13) and fig. (5-2) is easy to verify that by choosing

$$\frac{1}{\overline{R}_{11}} = 0 \quad (5.31)$$

$$\frac{1}{\overline{R}_{22}} = \left(\frac{1}{R_{11}} - \frac{1}{R_{22}} \right) \quad (5.32)$$

$$Y_2 = Y_1 + \frac{s^{\alpha_2 - \beta_2}}{\overline{R}_{22}} \quad (5.33)$$

we obtain a symmetric Y coupled system where the transducers can be thought as ideal and the parasitic element at the first port can be thought to be part of the given system modeled by means of the admittance Y_1 as shown in fig (4-14).

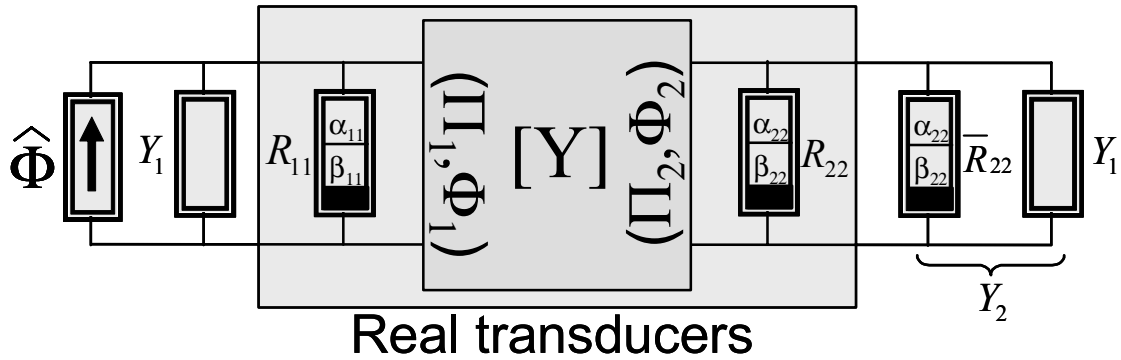


Figure 5-14:

This procedure will result very useful when Y_1 (or at least part of it) will have the same constitutive nature of the term $\frac{s^{\beta_2 - \alpha_2}}{R_{22}}$ in fact in this case this term can be realized by suitably changing the value of some components. This argumentation will be much more clear when we will give some examples in the following section.

Z coupling

If the transducers we are using to couple the two systems is Z symmetrizable we need to use the Z coupling model, in fact comparing fig. (3-14) and fig. (5-3) is easy to verify that by choosing

$$\bar{R}_{11} = 0 \quad (5.34)$$

$$\bar{R}_{22} = (R_{11} - R_{22}) \quad (5.35)$$

$$Z_2 = Z_1 + \bar{R}_{22} s^{\beta_2 - \alpha_2} \quad (5.36)$$

we obtain a symmetric Z coupled system where the transducers can be thought as ideal and the parasitic element at the first port can be thought to be part of the given system modeled by means of the impedance Z_1 as shown in fig (4-15).

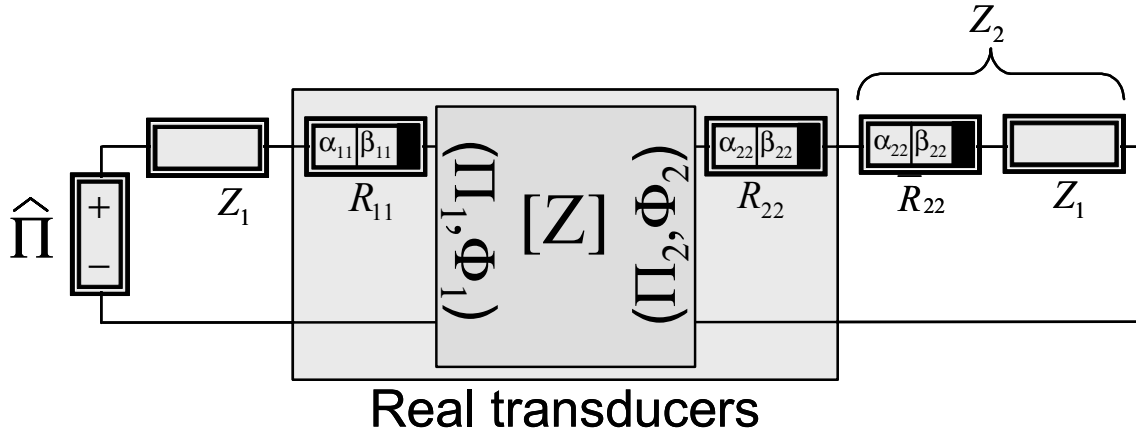


Figure 5-15:

This procedure will result very useful when Z_1 (or at least part of it) will have the same constitutive nature of the term $\bar{R}_{22}s^{\alpha_2-\beta_2}$ in fact in this case this term can be realized by suitably changing the value of some components. This argumentation will be much more clear when we will give some examples in the following section.

G coupling

If the transducers we are using to couple the two systems is G symmetrizable we need to use the G coupling model, in fact comparing fig. (3-15) and fig. (5-4) is easy to verify that by choosing

$$\frac{1}{\bar{R}_{11}} = 0 \quad (5.37)$$

$$\bar{R}_{22} = \left(\frac{1}{R_{11}} - R_{22} \right) \quad (5.38)$$

$$Z_2 = Z_1 + \bar{R}_{22}s^{\beta_2-\alpha_2} \quad (5.39)$$

we obtain a symmetric G coupled system where the transducers can be thought as ideal and the parasitic element at the first port can be thought to be part of the system one modeled by means of the admittance Y_1 as shown in fig. (4-16).

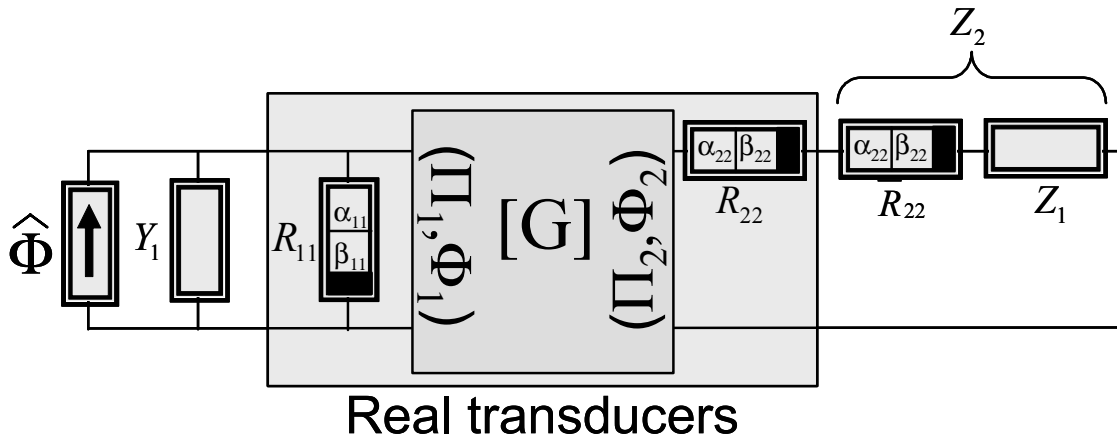


Figure 5-15:

This procedure will result very useful when Z_1 (or at least part of it) will have the same constitutive nature of the term $\overline{R}_{22}s^{\alpha_2-\beta_2}$ in fact in this case this term can be realized by suitably changing the value of some components. This argumentation will be much more clear when we will give some examples in the following section.

H coupling

If the transducers we are using to couple the two systems is H symmetrizable we need to use the H coupling model, in fact comparing fig. (3-15) and fig. (5-5) is easy to verify that by choosing

$$\overline{R}_{11} = 0 \quad (5.40)$$

$$\frac{1}{\overline{R}_{22}} = \left(R_{11} - \frac{1}{R_{22}} \right) \quad (5.41)$$

$$Y_2 = Y_1 + \frac{s^{\alpha_2-\beta_2}}{\overline{R}_{22}} \quad (5.42)$$

we obtain a symmetric H coupled system where the transducers can be thought as ideal and the parasitic element at the first port can be thought to be part of the system one modeled by means of the admittance Z_1 as shown in fig. (4-17).

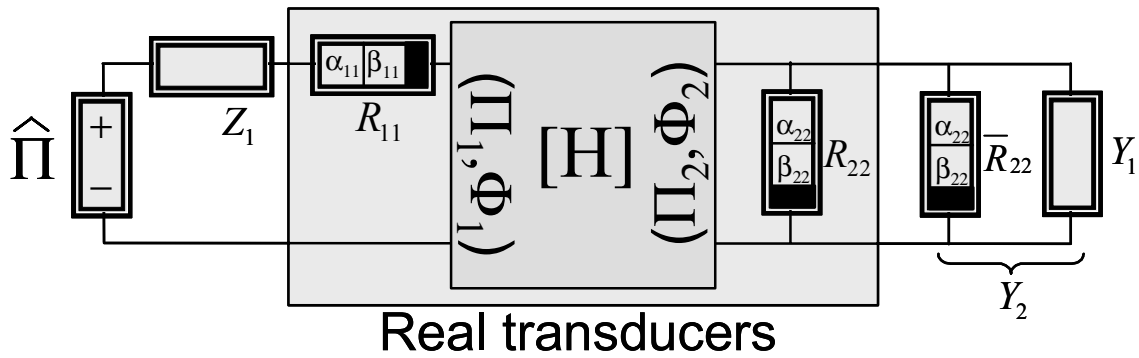


Figure 5-16:

This procedure will result very useful when Y_1 (or at least part of it) will have the same constitutive nature of the term $\frac{s^{\beta_2 - \alpha_2}}{R_{22}}$ in fact in this case this term can be realized by suitably changing the value of same components. This argumentation will be much more clear when we will give some examples in the following section.

5.3 M-dimensional coupling

5.3.1 Introduction

In this section we will study a system accessible from M ports and described in the Laplace domain by means of its open circuit impedance (short circuit admittance) matrix coupled to a similar system by means of an array of bidirectional transducers. As we show in the previous chapter a bidirectional transducers can be modeled in four different way, similarly we can describe a coupled system for each one of the four possible models of a transducers.

5.3.2 The case of ideal transducers

Y coupling

Here we model the first M ports subsystem by means of its admittance matrix \mathbb{Y}_1 , relating the vector Φ_1 with the vector Π_1 this system is coupled with a second M ports subsystem modeled by means of its admittance matrix \mathbb{Y}_2 relating the vector Φ_2 with the vector Π_2 . The coupling is realized through an array of identical ideal bidirectional Y transducers. The j^{th} transducers

will be characterized by the two pairs $\left((\mathbf{\Pi}_1)_j, (\mathbf{\Phi}_1)_j \right)$ and $\left((\mathbf{\Pi}_2)_j, (\mathbf{\Phi}_2)_j \right)$. Finally an array of independent Φ generators, whose value will be given by the components of the vector $\hat{\Phi}$. The j^{th} independent Φ generator is shunted with the j^{th} port of the first subsystem.

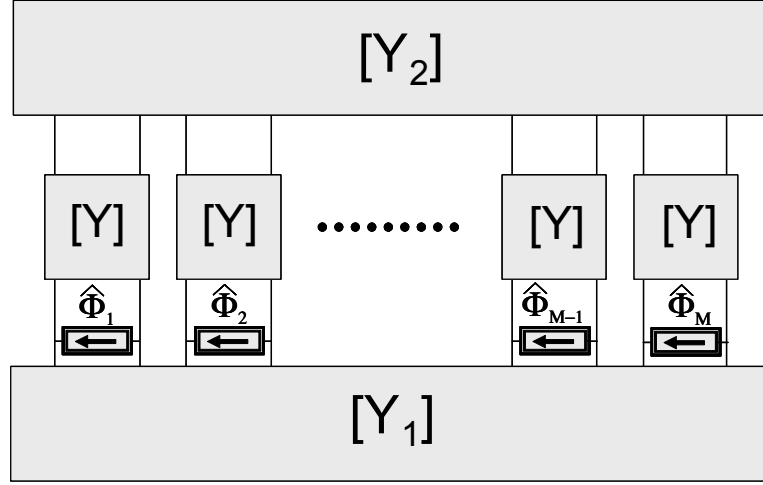


Figure 5-17

The coupled system shown in fig. (5-17) can be described by means of the following system of equations:

$$\begin{cases} \hat{\Phi} = Y_1 \mathbf{\Pi}_1 + y_{12} \mathbf{\Pi}_2 \\ \mathbf{0} = y_{21} \mathbf{\Pi}_1 + Y_2 \mathbf{\Pi}_2 \end{cases} \quad (5.43)$$

Z coupling

Here we model the first M ports subsystem by means of its impedance matrix Z_1 , relating the vector $\mathbf{\Pi}_1$ with the vector $\mathbf{\Phi}_1$ this system is coupled with a second M ports subsystem modeled by means of its impedance matrix Z_2 relating the vector $\mathbf{\Pi}_2$ with the vector $\mathbf{\Phi}_2$. The coupling is realized through an array of identical ideal bidirectional Z transducers. The j^{th} transducers will be characterized by the two pairs $\left((\mathbf{\Pi}_1)_j, (\mathbf{\Phi}_1)_j \right)$ and $\left((\mathbf{\Pi}_2)_j, (\mathbf{\Phi}_2)_j \right)$. Finally an array of independent Π generators, whose value will be given by the components of the vector $\hat{\Pi}$. The j^{th} independent Π generator is connected in series with the j^{th} port of the first subsystem.

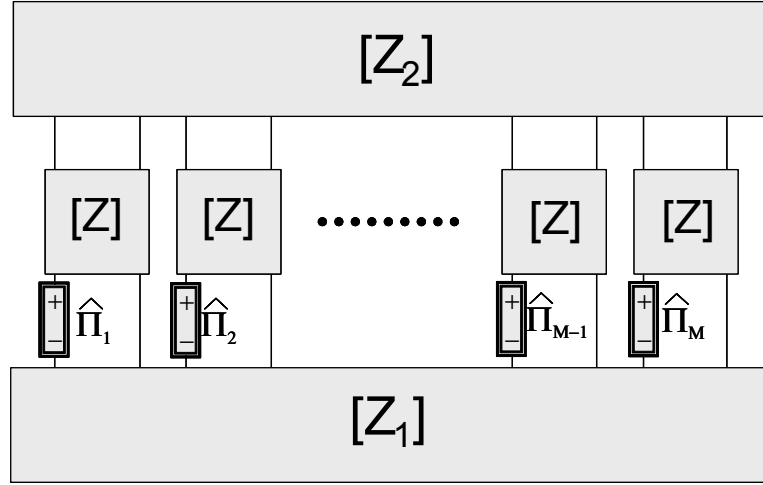


Figure 5-18:

The coupled system shown in fig. (5-18) can be described by means of the following system of equations:

$$\begin{cases} \hat{\Pi} = Z_1 \Phi_1 + z_{12} \mathbb{I} \Phi_2 \\ \mathbf{0} = z_{21} \mathbb{I} \Phi_1 + Z_2 \Phi_2 \end{cases} \quad (5.44)$$

G coupling

Here we model the first M ports subsystem by means of its admittance matrix \mathbb{Y}_1 , relating the vector Φ_1 with the vector Π_1 this system is coupled with a second M ports subsystem modeled by means of its impedance matrix Z_2 relating the vector Π_2 with the vector Φ_2 . The coupling is realized through an array of identical ideal bidirectional G transducers. The j^{th} transducers will be characterized by the two pairs $((\Pi_1)_j, (\Phi_1)_j)$ and $((\Pi_2)_j, (\Phi_2)_j)$. Finally an array of independent Φ generators, whose value will be given by the components of the vector $\hat{\Phi}$. The j^{th} independent Φ generator is shunted with the j^{th} port of the first subsystem.

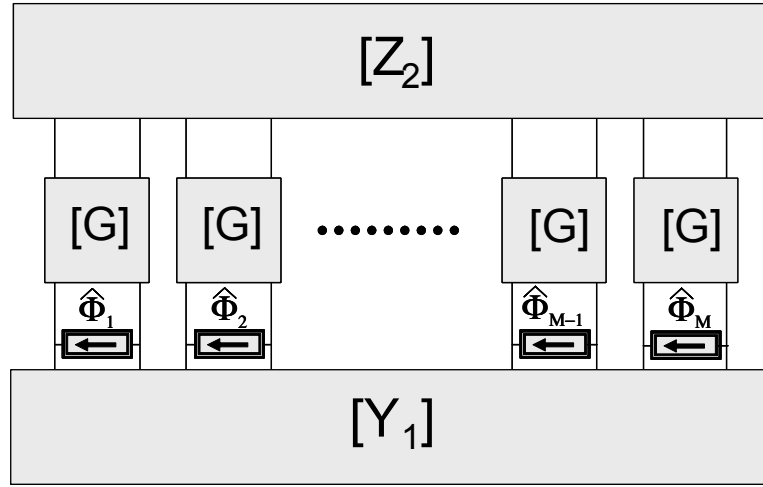


Figure 5-19:

The coupled system shown in fig. (5-19) can be described by means of the following system of equations:

$$\begin{cases} \hat{\Phi} = \mathbb{Y}_1 \mathbf{\Pi}_1 + g_{12} \mathbb{I} \Phi_2 \\ \mathbf{0} = g_{21} \mathbb{I} \mathbf{\Pi}_1 + \mathbb{Z}_2 \Phi_2 \end{cases} \quad (5.45)$$

H coupling

Here we model the first M ports subsystem by means of its impedance matrix \mathbb{Z}_1 , relating the vector $\mathbf{\Pi}_1$ with the vector Φ_1 this system is coupled with a second M ports subsystem modeled by means of its admittance matrix \mathbb{Y}_2 . The coupling is realized through an array of identical ideal bidirectional H transducers. The j^{th} transducers will be characterized by the two pairs $((\mathbf{\Pi}_1)_j, (\Phi_1)_j)$ and $((\mathbf{\Pi}_2)_j, (\Phi_2)_j)$. Finally an array of independent Π generators, whose value will be given by the components of the vector $\hat{\mathbf{\Pi}}$. The j^{th} independent Π generator is connected in series with the j^{th} port of the first subsystem.

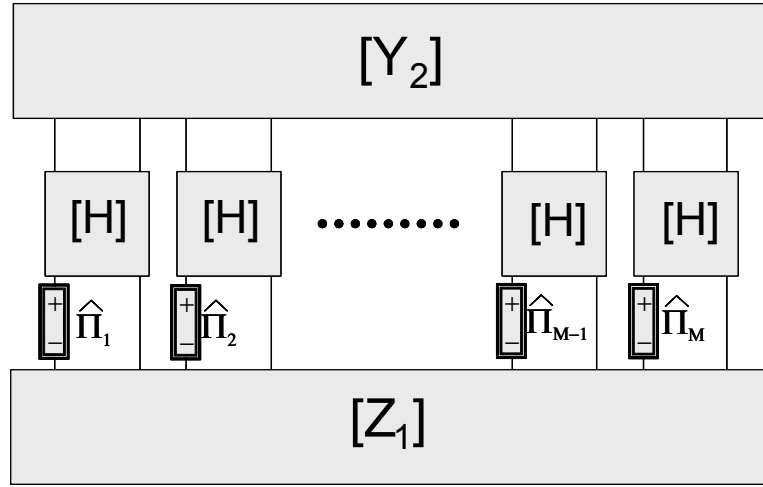


Figure 5-20:

The coupled system shown in fig. (5-18) can be described by means of the following system of equations:

$$\begin{cases} \hat{\Pi} = Z_1 \Phi_1 + h_{12} \mathbb{I} \Pi_2 \\ \mathbf{0} = h_{21} \mathbb{I} \Phi_1 + Y_2 \Pi_2 \end{cases} \quad (5.46)$$

We will omit a complete tractation of the real transducers M dimensional coupling, by the way we will give some example of it basing our tractation on the notion given for the one dimensional case.

5.3.3 Uncouple system VS gyroscopically Coupled system

Now we want to make a comparison between the uncoupled system and the coupled one. This analysis can be made studying the two matrices of network functions relating the independent quantities defining the transducer model. and the impressed quantities. For example in the case of the Y coupling the independent quantities are the vectors Π_1 and Π_2 while the impressed quantity is the vector $\hat{\Phi}$. The uncoupled system can be obtained from the general case described by eq. (5.43) by avoiding the transducer effect (i.e. $y_{12} = y_{21} = 0$). In this case we obtain:

$$\Pi_1(s) = Z_1^0(s) \hat{\Phi}(s) \Rightarrow Z_1^0(s) = Y_1^{-1}(s) \quad (5.47)$$

$$\Pi_2(s) = Z_2^0(s) \hat{\Phi}(s) \Rightarrow Z_2^0(s) = 0 \quad (5.48)$$

The second case of interest is obtained when the coupling coefficients y_{12} and y_{21} are equal and opposite one to each other (i.e. $y_{12} = -y_{21} = \alpha$). In this situation the coupling is referred as gyroscopic and the two matrices of network functions of interest become:

$$\mathbf{\Pi}_1(s) = \mathbf{Z}_1^0(s)\widehat{\mathbf{\Phi}}(s) \Rightarrow \mathbf{Z}_1^\alpha(s) = (\mathbf{Y}_1(s) + \alpha^2\mathbf{Y}_2^{-1}(s))^{-1} \quad (5.49)$$

$$\mathbf{\Pi}_2(s) = \mathbf{Z}_2^0(s)\widehat{\mathbf{\Phi}}(s) \Rightarrow \mathbf{Z}_2^\alpha(s) = -\alpha (\mathbf{Y}_1(s)\mathbf{Y}_2(s) + \alpha^2\mathbf{I})^{-1} \quad (5.50)$$

It is quite easy to understand that similar argumentation can be developed for the other model of coupling. The complexity of the analytical calculations we had performed for the one dimensional rise very quickly with the order of the problem, consequently it is quite unseasonable reproduce those calculations for the general case. By the way we will give same notion about the principal aspect of this work i.e. the energy balancioum of the uncoupled system versus the coupled one when the two coupled system are identical (i.e. $\mathbf{Y}_1(s) = \mathbf{Y}_2(s)$). The energy of a M dimensional system described by means of its admittance matrix $\mathbf{Y}(s)$ can be evaluated when it is known the time evolution of the vector of the independent quantities defining the system by the following expression:

$$e(t) = \int p(t)dt = \int \mathbf{\Pi}^T(t)\mathbf{\Phi}(t)dt = \int \mathbf{\Pi}^T(t)\mathbf{\Phi}(t)dt = \int \mathbf{\Pi}^T(t)\mathcal{L}^{-1}\{\mathbf{Y}\mathbf{\Pi}(t)\} dt \quad (5.51)$$

This equation results in a very tedious calculation so it could be necessary to evaluate it by means of numerical methods. In order to focus the attention on the energy transfer we will give same example of the result of this calculation procedure fore the simplest second order network (i.e. $n = 1$) and the simplest fourth order network (i.e. $n = 2$).

The simples Y model of a second order system is obtained by setting $M = 3$ in equation (4.12). Following an adimensionalization procedure similar to the one described for the one dimensional case we obtain:

$$\mathbf{Y} = \begin{pmatrix} \frac{2}{s} + s & -\frac{1}{s} & 0 \\ -\frac{1}{s} & \frac{2}{s} + s & -\frac{1}{s} \\ 0 & -\frac{1}{s} & \frac{2}{s} + s \end{pmatrix} \quad (5.52)$$

Starting From eq. (5.52) we can evaluate the impedance matrices $\mathbb{Z}_1^0(s)$ for the uncoupled case. It is given by:

$$\mathbb{Z}_1^0(s) = \mathbb{Y}^{-1} = \begin{pmatrix} \frac{s(3+4s^2+s^4)}{4+10s^2+6s^4+s^6} & \frac{s}{(2+4s^2+s^4)} & \frac{s}{4+10s^2+6s^4+s^6} \\ \frac{s}{(2+4s^2+s^4)} & \frac{s(2+s^2)}{(2+4s^2+s^4)} & \frac{s}{(2+4s^2+s^4)} \\ \frac{s}{4+10s^2+6s^4+s^6} & \frac{s}{(2+4s^2+s^4)} & \frac{s(3+4s^2+s^4)}{4+10s^2+6s^4+s^6} \end{pmatrix}$$

Exciting the system by means of an impulsive Φ quantity of unitary amplitude at the second port (i.e. $\widehat{\Phi}(t) = (0, \delta(t), 0)$) we obtain as expected for the total energy of the system the time evolution shown in fig. (5-21). It should be noted that when at $t = 0$ the impulse reach the system its total energy $\bar{e}_1^0(\bar{t})$ rise suddenly from zero to a value equal to 0.5. This value doesn't change in time. Moreover being the matrix $\mathbb{Z}_2^0(s)$ that characterize the second system for the uncoupled situation equal to zero the total energy $\bar{e}_2^0(\bar{t})$ of the second system will be always equal to zero regardless for the impulse $\delta(t)$. This trivial evolution is shown in fig. (5-21)

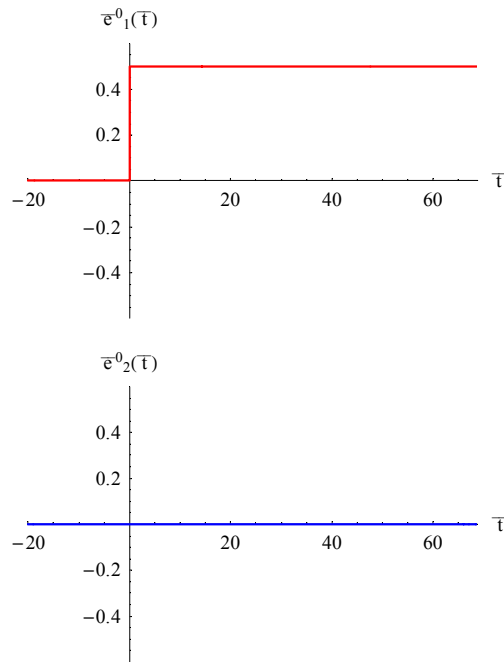


Figure 5-21:

Similarly we can evaluate the matrices $\mathbb{Z}_1^\alpha(s)$ and $\mathbb{Z}_2^\alpha(s)$ for the couple configuration. The

expressions obtained are quite complex and will be omitted. Computing the total energy of the two systems $\bar{e}_1^\alpha(\bar{t})$ and $\bar{e}_2^\alpha(\bar{t})$ for the same value of $\bar{\alpha}$ we use in the one dimensional case (i.e. $1/(3\sqrt{11})$) we obtain the time evolution shown in fig. (5-22). It should be noted that the qualitative behavior of the time evolution is very similar to the one obtained in the one dimensional case. The important point focused by fig. (5-22) is that it is still possible to transfer the energy from the first system to the second one. Moreover the time needed for a complete transfer depend only on the coupling parameter α and not on the order of the system. Finally it should be remarked that the sum of the total energy of the first and the second systems is equal to the total energy 0.5 instant by instant.

(i.e. $n = 2$).

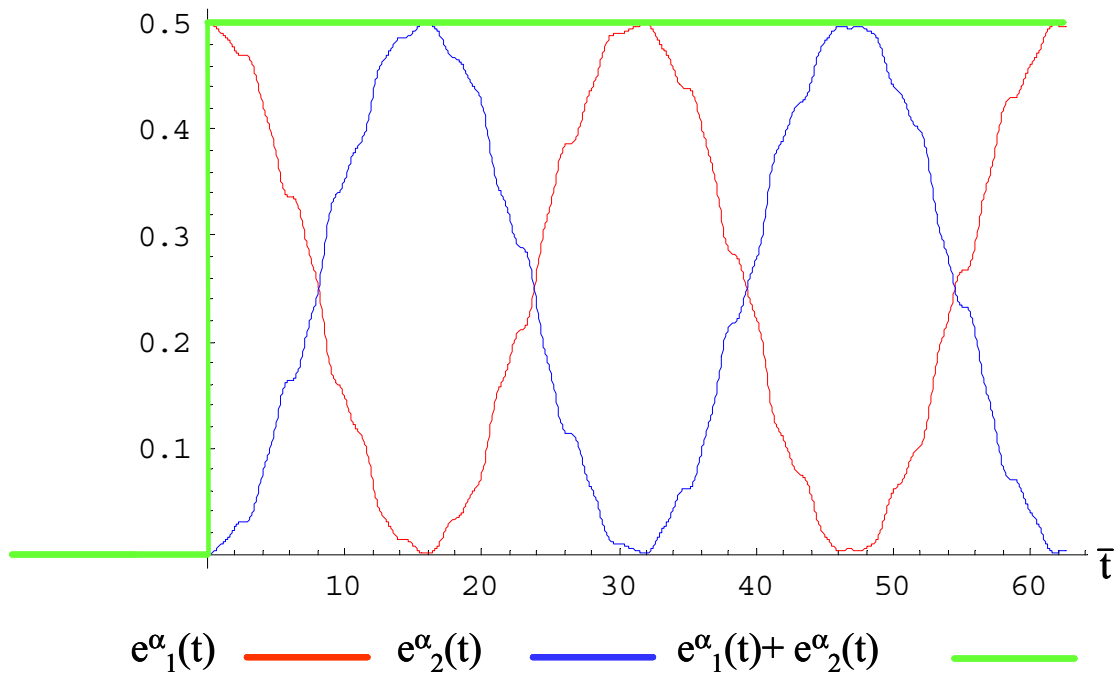


Figure 5-22:

The simple Y model of a fourth order system is obtained by setting $M = 5$ in equation (4.40). Following an adimensionalization procedure similar to the one described for the one dimensional case we can evaluate the impedance matrices $Z_1^0(s)$. The obtained expression is omitted. Exciting the system by means of an impulsive Φ quantity of unitary amplitude at the

third port (i.e. $\widehat{\Phi}(t) = (0, 0, \delta(t), 0, 0)$) we obtain as expected for the total energy of the system the time evolution shown in fig. (5-23). It should be noted that when at $t = 0$ the impulse reach the system its total energy $\bar{e}_1^0(\bar{t})$ rise suddenly from zero to a value equal to 0.5. This value doesn't change in time. Moreover being the matrix $Z_2^0(s)$ that characterize the second system for the uncoupled situation equal to zero the total energy $\bar{e}_2^0(\bar{t})$ of the second system will be always equal to zero regardless for the impulse $\delta(t)$. This trivial evolution is shown in fig. (5-23)

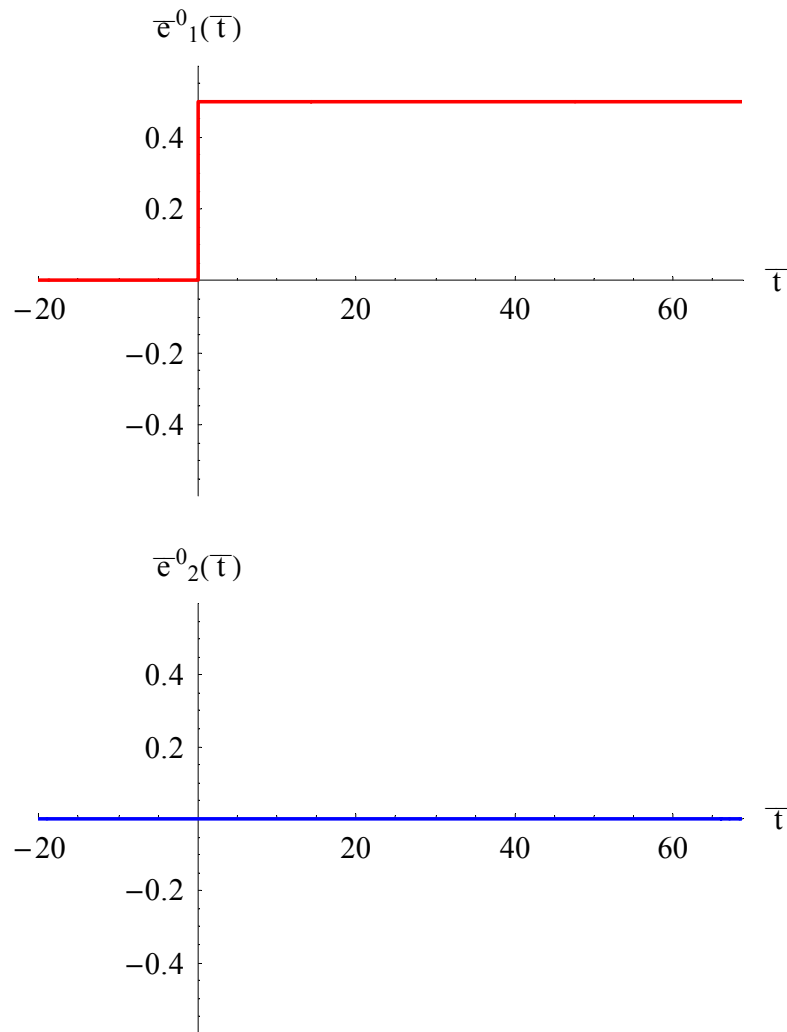


Figure 5-23:

Similarly we can evaluate the matrices $Z_1^\alpha(s)$ and $Z_2^\alpha(s)$ for the couple configuration. The

expressions obtained are quite complex and will be omitted. Computing the total energy of the two systems $\bar{e}_1^\alpha(\bar{t})$ and $\bar{e}_2^\alpha(\bar{t})$ for the same value of $\bar{\alpha}$ we use in the one dimensional case (i.e. $1/(3\sqrt{11})$) we obtain the time evolution shown in fig. (5-24). It should be noted that the qualitative behavior of the time evolution is very similar to the one obtained in the one dimensional case. The important point focused by fig. (5-24) is that it is still possible to transfer the energy from the first system to the second one. Moreover the time needed for a complete transfer depend only on the coupling parameter α and not on the order of the system. Finally it should be remarked that the sum of the total energy of the first and the second systems is equal to the total energy 0.5 instant by instant.

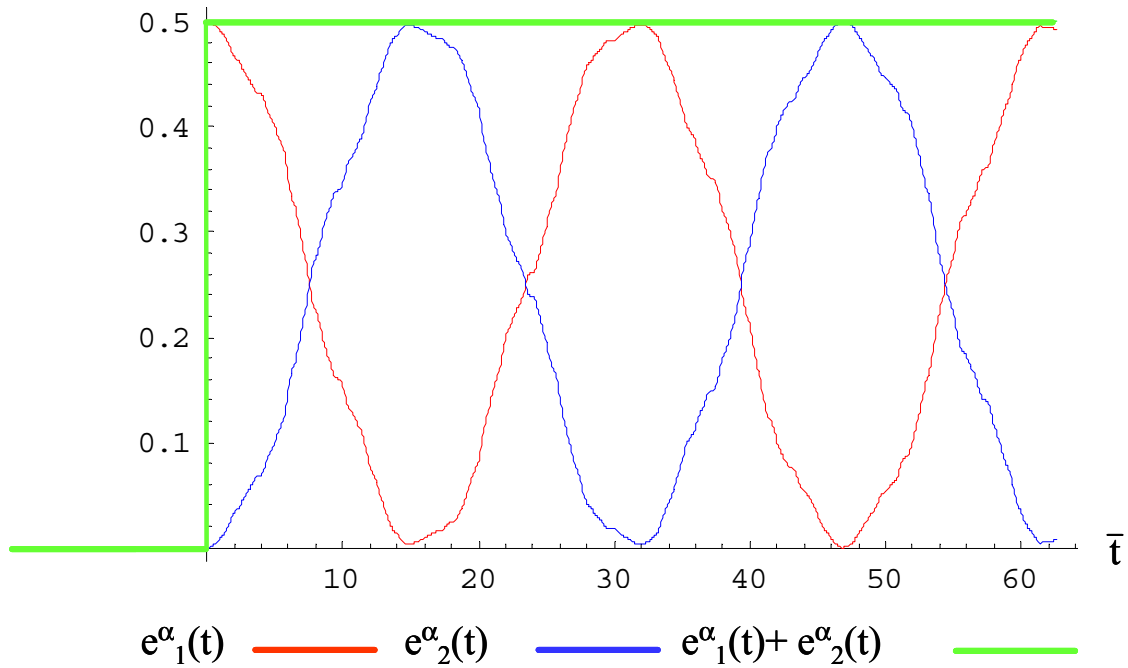


Figure 5-24:

5.3.4 same example of hybrid coupled system

In this section we will give some examples of hybrid coupled systems obtained by design an electrical analogue of a given mechanical system and coupling them by means a piezo transducers. The most of those system are known in the literature on vibration damping even if

they are been derived following a different approach. We will show how using the notion given in this work it is possible to obtain a quite simple methodology able to produce the hybrid system starting from the knowledge of the equation governing the given uncoupled system and the constitutive equation of the transducer. As we did in the previous section we will give an example of zero order system an example of second order system and an example of forth order system.

An example of zero order system hybrid system

In the fourth chapter we propose the mass spring oscillators as an example of zero order system, in the third chapter we describe the extensional piezoelectric transducers as an hybrid two ports network. Now we show how, using the theory developed in this work, it will be possible to design an electrical analogue of mechanical system. Obviously the labels "mechanical" and "electrical" are restricted to this particular example.

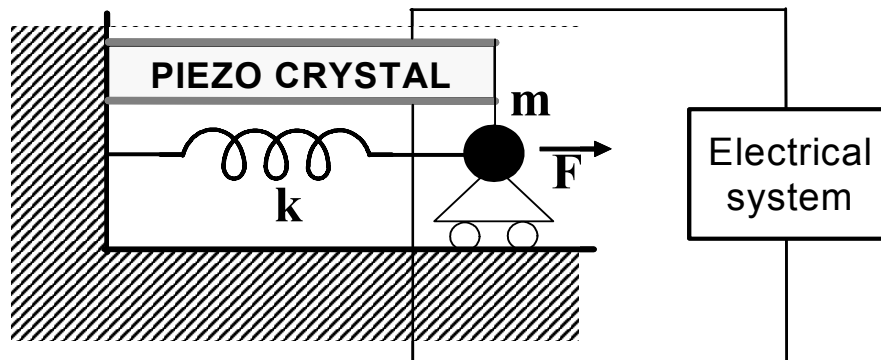


Figure 5-25:

In figure 5-25 we show a realistic representation of the system under exam where one side of a piezo crystal is fixed to the soil while the remaining one is fixed to the point wise mass connected to the soil through an extensional spring. The velocity (Π quantity) of the mass is measured with respect to the soil, being two mechanical access points of the transducer connected between the mass an the soil those two elements are shunted As we said before a couple of metallization on the top and the bottom faces of the crystal realize an electrical port. we will design a suitable electrical system to be connected to this port. The first step we need to walk is to choose the coupling model. As we said before this choice can be made looking at the consecutive symmetry

of the real bidirectional transducer we want to use to realize the coupling. In fig. (3-23) we had shown the equivalent circuit for a extensional piezo transducers and we had highlight that this device can be modeled as an ideal transducer having a extensional spring (i.e. a (0,1) element) as a parasite element on the mechanical port and a capacitor (i.e. a (1,0) element) as a parasite element on the electrical port. It is easy to verify that those elements verify the basic condition for the G and the H symmetrization, in fact they fulfill eq. (3.17) being $\alpha_{11} - \beta_{11} - \alpha_{22} + \beta_{22} = 1 - 0 - 1 + 0 = 0$. We chose to use the G coupling model. Consequently we need to use a Y model for the mechanical system and a Z model for the electrical system. The Y model of a mass spring oscillator has been derived in the previous chapter and it is shown in fig. (4-3) while the equivalent, of the transducers is given in fig (3-23) while the equivalent Z model of a zero order system is shown in fig. (4-1 a). Based on fig. (5-15) and Table (2-1) we can draw the equivalent circuit of the hybrid system as shown in fig. (5-26).

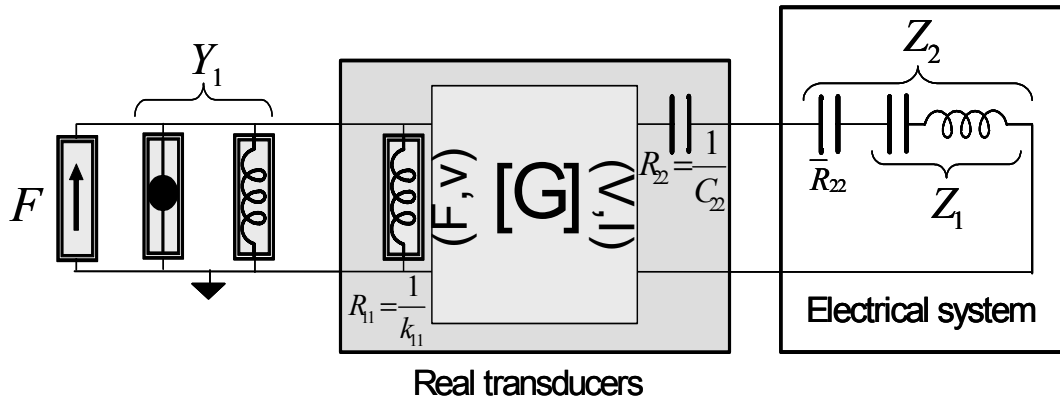


Figure 5-26:

The admittance of the mechanical system can be obtained by taking the Laplace transform of eq. (4.2) and using the definition (2.12) We obtain:

$$Y_1 = ms + \frac{k}{s} = Z_1$$

Looking at the fig. (5-26) and using eq. (5.38) and (5.39) we can write the following relation:

$$\begin{aligned}\bar{R}_{22} &= \frac{1}{R_{11}} - R_{22} = k_{11} - \frac{1}{C_{22}} \\ Z_2 &= Z_1 + \bar{R}_{22}s^{\beta_2 - \alpha_2} = ms + \frac{k}{s} + \left(k_{11} - \frac{1}{C_{22}}\right) \frac{1}{s} = \\ &= ms + \left(k + k_{11} - \frac{1}{C_{22}}\right) \frac{1}{s} = Ls + \frac{1}{Cs}\end{aligned}$$

Summarizing we can say that in order to guarantee the symmetry of the coupled hybrid system we need to design the electrical system by connecting in series an inductor of inductance $L = m$ and a capacitor of capacitance $C = C_{22}/(C_{22}(k + k_{11}) - 1)$. It should be noted that the latter value can assume in same case a negative value.

An example of second order system hybrid system

In the fourth chapter we propose the axial vibrations on a beam as an example of second order system, in the third chapter we describe the extensional piezoelectric transducers as an hybrid two ports network. Now we show how, using the theory developed in this work, it will be possible to coupling this mechanical system with its electrical analogue. Obviously the labels "mechanical" and "electrical" are restricted to this particular example.

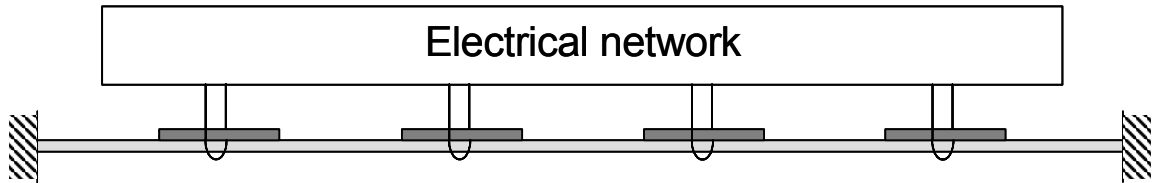


Figure 5-27:

In figure 5-27 we show a realistic representation of the system under exam where an array (four in the example) of a piezoelectric crystal is fixed to an hosting beam forced with axial excitation and clamped at both the ends. Moreover each transducer is connected to a port of the analogue electrical network. As we have seen in the second chapter a discrete version of a beam under axial excitation can be thought as set of point wise masses connected through extensional springs. The horizontal velocity (Π quantity) of the masses is measured with respect to the soil, being the two mechanical access points of each transducer connected between two

adjacent masses the mechanical port of the transducer will result shunted with the extensional spring connecting the two masses, as shown in fig. (5-28)

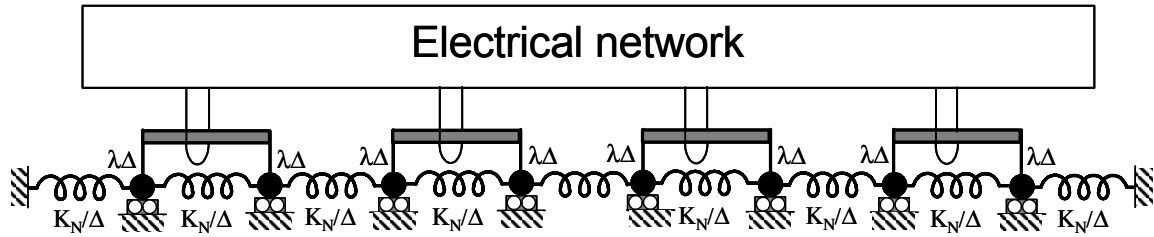


Figure 5-28:

The first step we need to walk in order to design the analogue network is to choose a suitable coupling model. As we said before this choice can be made looking at the consecutive symmetry of the real bidirectional transducer we want to use to realize the coupling. In fig. (3-23) we had shown the equivalent circuit for a extensional piezo transducers and we had highlight that this device can be modeled as an ideal transducer having a extensional spring (i.e. a (0,1) element) as a parasite element on the mechanical port and a capacitor (i.e. a (1,0) element) as a parasite element on the electrical port. It is easy to verify that those elements verify the basic condition for the G and the H symmetrization, in fact they fulfill eq. (3.17) being $\alpha_{11} - \beta_{11} - \alpha_{22} + \beta_{22} = 1 - 0 - 1 + 0 = 0$. We chose to use the G coupling model. Consequently we need to use a Y model for the mechanical system and a Z model for the electrical system. The Y model of a beam excited by axial forces has been derived in the previous chapter and it is shown in fig. (4-16 b) while the equivalent circuit of the transducers is given in fig (3-23). The equivalent Z model of a second order system is shown in fig. (4-10). Based on fig. (5-19) and Table (2-1) we can draw the equivalent circuit of the hybrid system as shown in fig. (5-29).

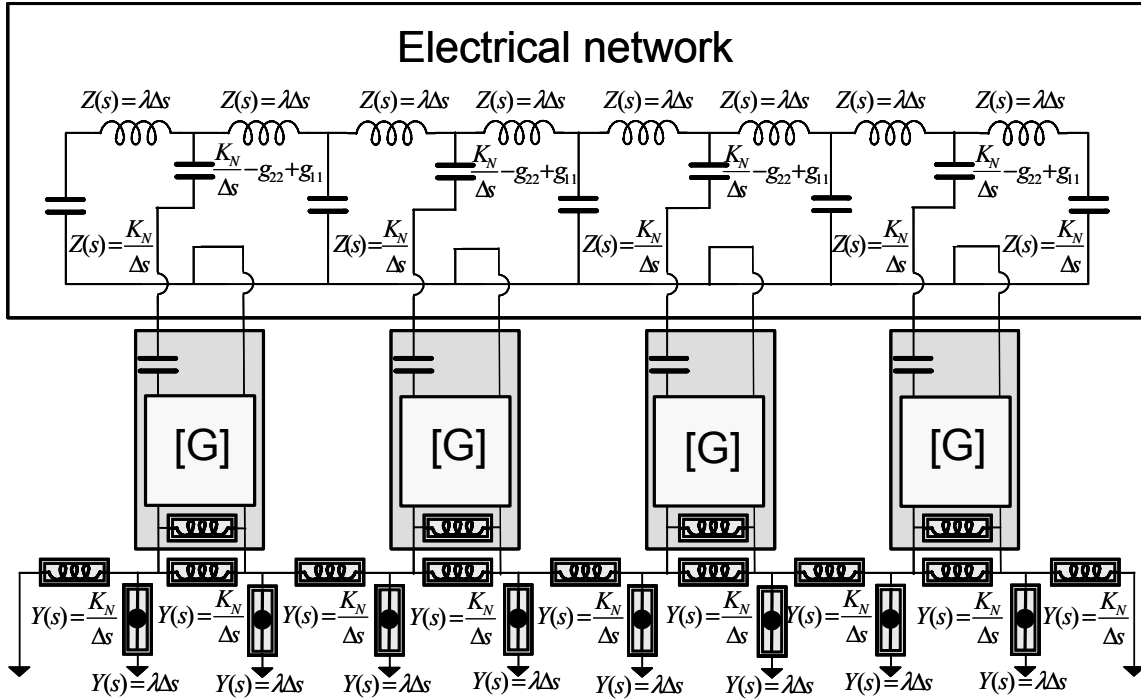


Figure 5-29:

In the figure are shown the value of each component of both the electrical and the mechanical side of the hybrid circuit. It can be noted that as we did before for a zero order system the asymmetry introduced by the real transducer can be eliminated by using a G coupling model.

An example of fourth order system hybrid system

In the fourth chapter we propose the transversal vibrations on a beam as an example of fourth order system, in the third chapter we describe the bending piezoelectric transducers as an hybrid two ports network. Now we show how, using the theory developed in this work, it will be possible to coupling this mechanical system with its electrical analogue. Obviously the labels "mechanical" and "electrical" are restricted to this particular example.

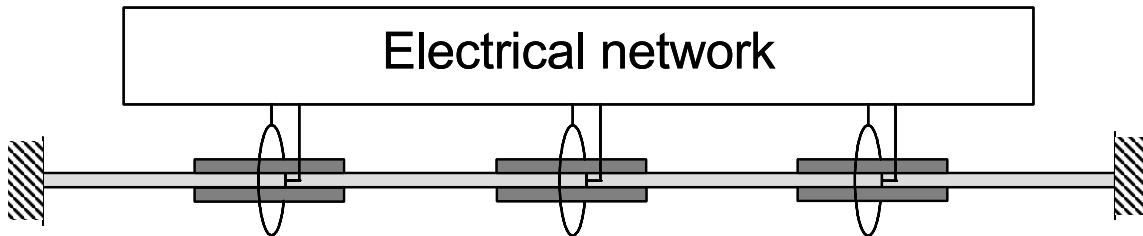


Figure 5-30:

In figure 5-30 we show a realistic representation of the system under exam where an array (four in the example) of a piezoelectric crystal in the bending configuration is fixed to an hosting beam forced with transversal excitation and clamped at both the ends. Moreover each transducer is connected to a port of the analogue electrical network. As we have seen in the second chapter a discrete version of a beam under transversal excitation can be though as set of point wise masses connected through pinned rigid link, moreover the pin of two adjacent rigid links are connected through bending springs. The angular velocity (Π quantity) of the rigid links is measured with respect to the horizontal position, being the two mechanical access points of each transducer connected between two adjacent pins the mechanical port of the transducer will result shunted with the bending spring connecting the two pins, as shown in fig. (5-31)

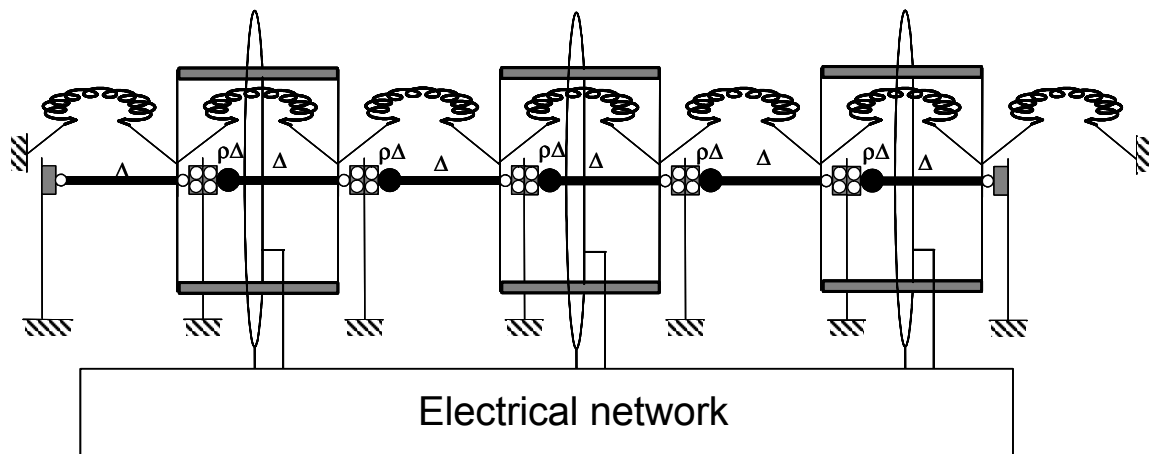


Figure 5-31:

The first step we need to walk in order to design the analogue network is to choose a suitable coupling model. As we said before this choice can be made looking at the constitutive symmetry of the real bidirectional transducer we want to use to realize the coupling. In fig. (3-23) we had shown the equivalent circuit for a extensional piezo transducers and we had highlighted that this device can be modeled as an ideal transducer having a extensional spring (i.e. a $(0, 1)$ element) as a parasite element on the mechanical port and a capacitor (i.e. a $(1, 0)$ element) as a parasite element on the electrical port. It is easy to verify that those elements verify the basic condition for the G and the H symmetrization, in fact they fulfill eq. (3.17) being

$\alpha_{11} - \beta_{11} - \alpha_{22} + \beta_{22} = 1 - 0 - 1 + 0 = 0$. We chose to use the G coupling model. Consequently we need to use a Y model for the mechanical system and a Z model for the electrical system. The Y model of a beam excited by transversal forces has been derived in the previous chapter and it is shown in fig. (4-26 a) while the equivalent circuit of the transducers is given in fig (3-23). The equivalent Z model of a fourth order system is shown in fig. (4-22). Based on fig. (5-19) and Table (2-1) we can draw the equivalent circuit of the hybrid system as shown in fig. (5-32).

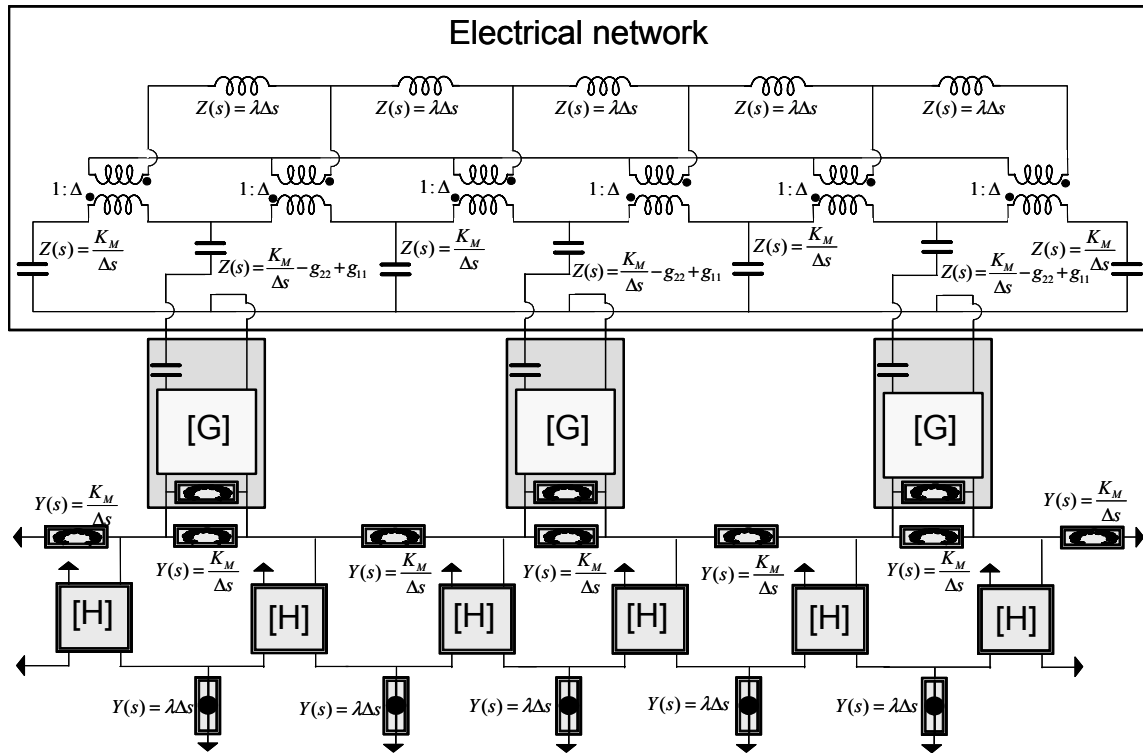


Figure 5-32:

In the figure are shown the value of each component of both the electrical and the mechanical side of the hybrid circuit. It can be noted that as we did before for a zero order system the asymmetry introduced by the real transducer can be eliminated by using a G coupling model.

Chapter 6

RC Active Synthesis of the analogue electrical network

6.1 Introduction

At the end of the previous chapter we have given some example of hybrid coupled systems obtained by interconnecting a given mechanical system with an electric circuit analogue to the mechanical system itself. The communication between the two subsystems is realized by means of an array of piezoelectric transducers that perform a conversion of the mechanical signal into an electrical one. The large knowledge available in the literature on electrical circuit synthesis makes the transduction in the electrical form very suitable. The theory developed in the previous chapters put in evidence how it is possible to obtain the electrical analogue of a system of order $2n$ by properly connecting a certain number of capacitors inductances and ideal transformers. The argumentation given above can convince us that we did the job since the complete circuit can be obtained by connecting those basic elements, unfortunately it is not true. In fact, the ideal transformers are theoretical components and can not be constructed by simply wrapping a wire. Moreover the value of inductance required for the component identification could be very large or even negative. All those argumentations bring us to make a point of the opportunity to design an active circuit whose behavior provides a best simulation of the desired ideal behavior. In this chapter we will initially give an overview at the literature on RC active circuits focusing our attention on the circuital complexity it is needed for the

RC active synthesis of each basic component i.e. floating and grounded positive and negative inductors, floating and grounded negative capacitors and ideal transformers. Once it is clear how to realize each basic component the complete network can be obtained by the straight forward connection of them. The described approach will produce a quite complex structure involving a large number of active components that can effect the stability of the complete network, moreover larger is the number of active components larger is the power needed to supply them. Being the energy transfer the principal aim of this work it is crucial to safe as much power as possible by decreasing the number of active component involved in the circuit. In the final part of this chapter we will propose some new RC active strategy of synthesis resulting in a strongly reduced circuital complexity.

6.2 Straight Forward synthesis

6.2.1 A brief overview on classical synthesis Technique

As we have said in the introduction a first possible approach to the realization of the circuital networks described in the previous chapters is the straight forward synthesis of the basic circuital components i.e. floating and grounded ideal transformers, floating and grounded positive and negative inductors and floating and grounded negative capacitors. The problem of the design of active synthetic active impedances was deeply studied in the past years in order to produce integrated active filters. Consequently there exist a large literature on this topic. In the following of this section we will give a brief overview on the classical solutions historically proposed in order to obtain the needed components. The design of RC synthetic inductor has been simplified when in 1948 a new two ports component named gyrator has been introduced by B. D. H. Tellegen [Tellegen (1948)], in fact this device has the useful properties to produce an inductive impedance at the first port when its second port is closed on a capacitor. More precisely a gyrator is a two ports network described by means of the following constitutive equations:

$$\left\{ \begin{array}{l} I_1 = GV_2 \\ I_2 = -GV_1 \end{array} \right. \quad or \quad \left\{ \begin{array}{l} I_1 = -GV_2 \\ I_2 = GV_1 \end{array} \right. \quad (6.1)$$

Where G is called gyration conductance. The circuital symbol used for this component is shown in fig. (6-1).

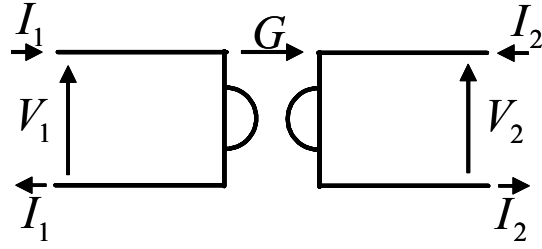


Figure 6-1: Circuital symbol for a gyrator.

As we said above when the second port of this component is chosen on a capacitor (i.e. $V_2 = -I_2/sC$) at the first port we get an inductive impedance equal to Cs/G^2 as can be easily verified by using one of the two set of constitutive eq. (6.1). The gyrator can be even successfully used in order to obtain an ideal transformer in fact the chain connection of two gyrator results in an ideal transformer. This result can be easily proven, first of all we need to derive the chain matrix of a gyrator. By using eq. (6.1) we can write

$$\begin{cases} V_1 = 1/G(-I_2) \\ I_1 = GV_2 \end{cases} \Rightarrow \mathbb{T} = \begin{pmatrix} 0 & \frac{1}{G} \\ G & 0 \end{pmatrix}$$

where T is the chain matrix of a gyrator. As known from the circuit theory the chain matrix describing the chain connection of two ports network is obtained by the multiplication of the two chain matrix describing each subnetwork. By performing the chain connection of two different gyrators we obtain the following relation:

$$\mathbb{T} = \mathbb{T}_1\mathbb{T}_2 = \begin{pmatrix} 0 & \frac{1}{G_1} \\ G_1 & 0 \end{pmatrix} \begin{pmatrix} 0 & \frac{1}{G_2} \\ G_2 & 0 \end{pmatrix} = \begin{pmatrix} 0 & \frac{G_1}{G_2} \\ \frac{G_2}{G_1} & 0 \end{pmatrix} \quad (6.2)$$

This relation can be used in order to write back the constitutive relations of the system obtained by the chain connection of the two gyrators.

$$\mathbb{T} \Rightarrow \begin{cases} V_1 = G_1/G_2(-I_2) \\ I_1 = G_2/G_1V_2 \end{cases} = \begin{cases} V_1 = -G_1/G_2I_2 \\ I_1 = G_2/G_1V_2 \end{cases} \quad (6.3)$$

Making a comparison between the last of (6.3) and (2.10) we can realize that the new system behaves as a generalized lever having $n = G_1/G_2$. Being both the ports of this system characterized by the electrical pair (V, I) by using table 2-1 we can say that this behaves as a ideal transformer¹. The previous argumentations should convince us that most of the components we need to design can be easily obtained once we have are able to synthetize a gyrator. In the following subsection we will show some possible implemetation of gyrators, a more complete overview on this subject can be found in [Kumar et al. 2002] The only renaming problem is related to the synthesis of component having negative nominal value. This task can be solved by introducing an ulterior two ports network known in the literature as negative impedance converter (NIC). The constitutive equation of this network are given below.

$$\begin{cases} V_1 = V_2 \\ I_1 = I_2 \end{cases} \quad (6.4)$$

The circuitual symbol for a NIC is shown in fig. (6-2).

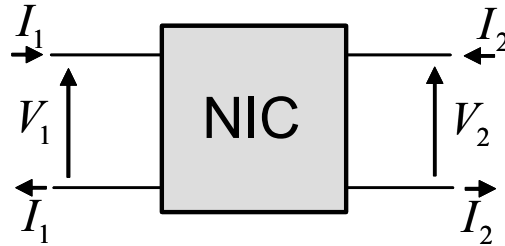


Figure 6-2: Circuitual symbol for a negative impedance converter.

Closing the second port of a NIC on a generic bipolar impedance Z we impose the following relation. $V_2 = -ZI_2$ by using this relation together with eq. (6.4) we obtain at the first port the relation $V_1 = -ZI_1$. This results can be expressed by saying that at the first port of a NIC we obtain the negative of the impedance we are using to close its second port.

Once we have introduced those two fundamental networks, we can restrict our interest on

¹Loking at eq. (6.3) and (6.1) we can recognize the constitutive relations we had used to define an ideal transducer. This fact is not surprising if we look at the result shown in [Premoli et al. (2004)] where it is said that the gyrator and the ideal transformer are the only two networks that can absorb istantaneous power from one port and supply the same amount of istantaneous power from the other port. This means that the Y and Z model of an ideal transducer can be thought as an hybrid ideal transformer while the G and H model of an ideal transducers can be thought as an hybrid gyrator.

the synthesis of those basic section. We will achieve this task in the following sub section.

6.2.2 RC-Active synthesis of a gyrator inductors and a NIC.

As we had said before there exist a lot of possible synthesis techniques in order to design an RC-Active filter. By the way we will restrict our research to the synthesis involving ideal operational amplifiers (OPA) resistors and capacitors only. As well known an operational amplifier is a three terminals network that can be thought as a grounded voltage controlled voltage source having infinite gain. The fact that this voltage source is grounded implies the existence of an intrinsic ground in each circuit containing OPAs. This reason forces us to consider each bipolar element as a two port unbalanced network. For example a RC-Active floating inductor must be thought as the circuit shown in fig (6-3).

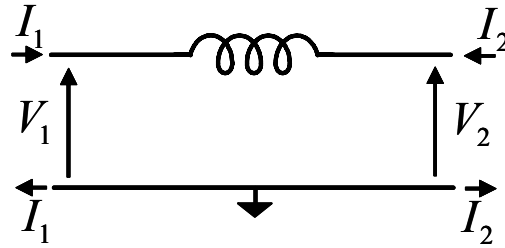


Figure 6-3: Equivalent circuit of an RC-Active floating inductor.

The same argumentation holds each time we want to consider a floating port. For example we need to design an ideal transformer having a balanced port and an unbalanced port. When we are implementing a synthesis of this element by using OPAs we need to consider this element as a three ports unbalanced network as shown in fig. (6-4).

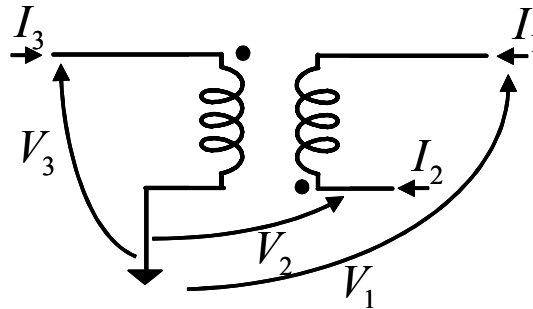


Figure 6-4: Equivalent circuit of an RC-Active ideal transformer having one balanced and one unbalanced port.

As we said in the previous subsection an ideal transformer can be obtained by the chain connection of two gyrators, consequently we are not interested in the synthesis of the circuit shown in fig. 6-4. Conversely we are interested in the synthesis of a four terminals gyrator whose equivalent circuit is shown in fig. 6-5.

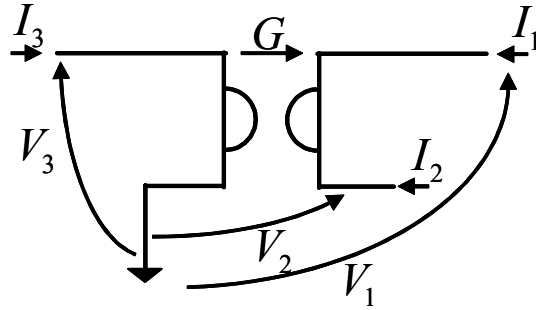


Figure 6-5: Equivalent circuit of an RC-Active gyrator having one balanced and one unbalanced port.

An interesting OPA implementation of the circuitual network shown in fig. (6-5) is due to G. J. Deboo [?]. This circuit is shown in fig.(6-6).

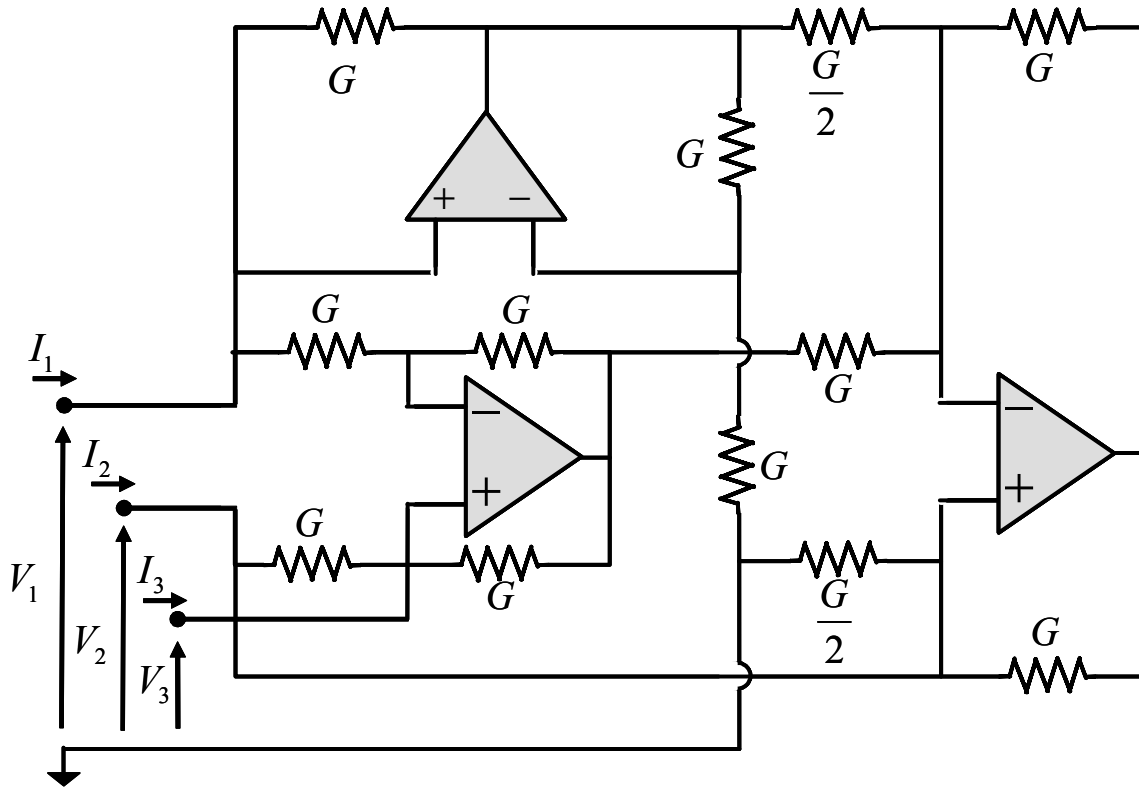


Figure 6-6: Deboo Gyrator-Type circuit.

This circuit is really suitable for our purpose; in fact it can be used to realize all the positive components we need. In fact by connecting a capacitor of nominal value C at the third port of the circuit, we can obtain between the first and the second port a floating inductance of nominal value C/G^2 where G is the conductance of the resistors shown in fig. (6-6). The described circuit allows us to obtain a floating synthetic inductor by means of three OPAs. Alternative circuital solutions involving Three OPAs can be found in [Reddy (1975)], [Senani (1978)] and [Senani (1989)]. In the literature can be found also oldest solutions of active floating inductors synthesized using four OPAs [Riordan (1967)] or, in more recent times solutions involving the use of two OPAs only [Senani (1987)]. There exist also a circuital scheme due to H. J. Orchard and A. N. Willson [Orchard et al. (1974)] involving the use of one OPA only in order to obtain a floating inductor. This scheme, shown in fig. (6-7), is very relevant from a theoretical point of view by the way its high sensitivity to the variation of the components value makes it not suitable for practical use.

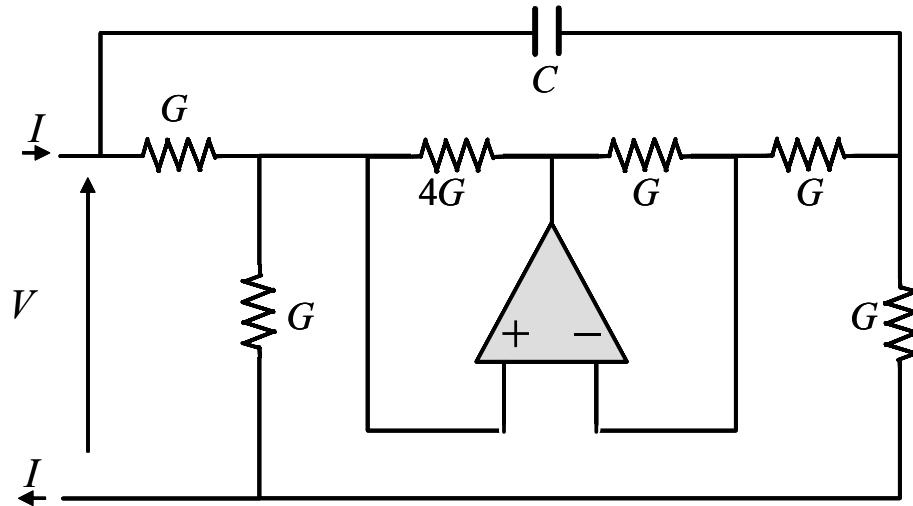


Figure 6-7: Orchard and Willson floating inductor using one OPA only.

Alternatively we can use the Deboo circuit shown in fig. (6-6) in order to obtain a gyrator having both its port grounded by short cutting the first or the second port. In both the cases one of the three OPAs in the circuit together with some resistors becomes redundant and can be removed, so that is possible to obtain a grounded gyrator by means of two OPAs. In [Antoniou (1968-1)] was shown that under certain conditions this circuit can become unstable

and has been proposed some circuitual modifications in order to solve this problem. As we said above in order to obtain a floating ideal transformer whose equivalent circuit is shown in fig. (6-4) we can connect an unbalanced gyrator with a balanced one. The argumentation given above should make clear that this synthesis requires the use of three OPAs. Alternatively a synthesis technique based on the scattering matrix was proposed in [Mussman et al. (1972)] this approach require 3 OPAs for a grounded gyrator and 4 OPAs for a grounded transformer. Another interesting solution able to produce a grounded transformer involving the use of two OPAs only is given in [Yanagisawa et al. (1976)]. The circuitual scheme is given in fig. (6-8).

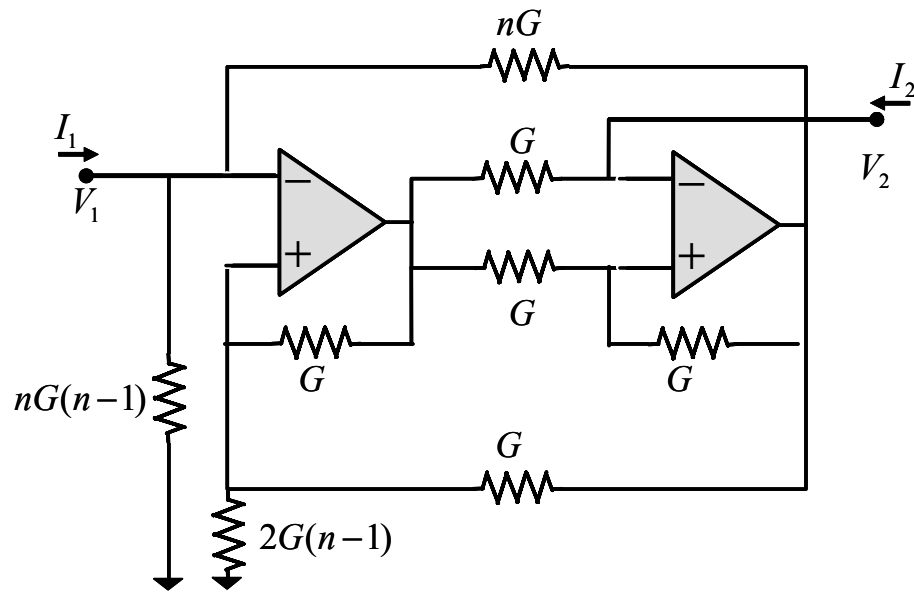


Figure 6-8: Yanagisawa and Bhattacharjee grounded transformer.

In order to complete this brief overview we need to show some possible implementations of a NIC. First of all we want to show a simple circuitual scheme involving the use of one OPA only able to realize a grounded negative impedance. This scheme is shown in fig (6-9).

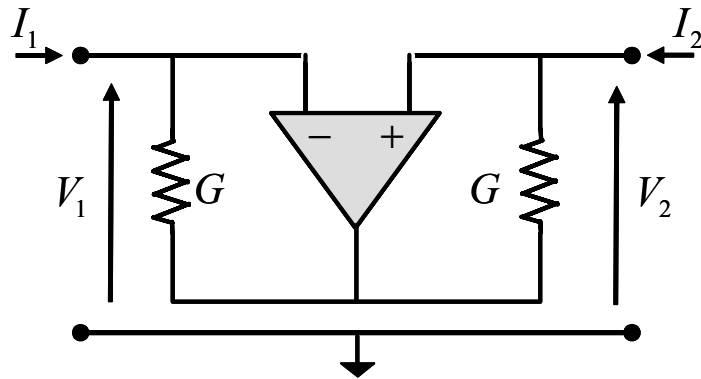


Figure 6-9: Grounded negative impedance converter.

The second scheme we want to show is able to realize a floating negative impedance by using two OPAs. This scheme due to A. Antoniou [Antoniou (1965)] is shown in fig (6-10).

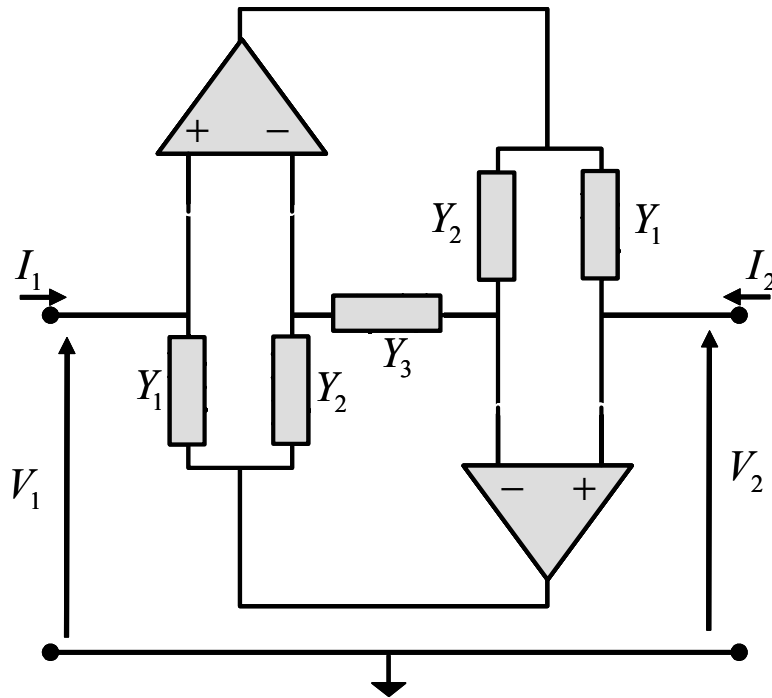


Figure 6-10: A. Antoniou Floating negative impedance converter.

An analysis of the circuitual scheme of fig. (6-10) brings to the following relation:

$$\begin{cases} V_1 - V_2 = -\frac{Y_2}{Y_1 Y_3} I_1 \\ I_1 = -I_2 \end{cases} \quad (6.5)$$

Looking at eq. (6.5) it is easy to realize that a negative floating capacitor can be obtained by choosing Y_1 and Y_2 to be resistors and Y_3 to be a capacitor while a negative floating inductor can be obtained by choosing Y_1 and Y_3 to be resistors and Y_2 to be a capacitor. We have now all we need in order to design each of the circuital element, but before choosing this subsection we like to focus our attention on the number of OPA needed to implement a basic section of the circuital network described in the previous chapters. We will focus our attention on the $\frac{dF}{dt} \rightarrow \Pi$ synthesis because, as we have shown in the second chapter, in this case it is possible to extract a basic section for both the one node to one port synthesis and the one node to n port synthesis. The basic section for the one node to one port synthesis is shown in fig. (2-19) for $n = 6$. For a system of order $2n$ we need n inductors part of them are negative and part of them are positive. Assuming that we can use 2 OPAs for each of them we need to use $2n$ OPAs for each module. Similarly we can consider the basic section of the one node to n ports synthesis whose basic section is shown in fig.(2-35). For a system of order $2n$ we need one floating inductor and $n - 1$ ideal transformers having a floating port and a grounded one. Assuming we need two OPAs for the inductor and five OPAs for the transformer we need $5n - 3$ OPAs for each module. This means that this kind of network requires a larger number of OPAs compared with the previous one. This argumentation suggests to use the one node to one port synthesis and gives a practical motivation to the study of the termination condition for this kind of network.

6.2.3 Some new strategies of synthesis

In the previous subsection we had produced an overview on the historically proposed synthesis devoted to the realization of gyrators inductors and NICs then we had given a rough estimation of the numbers of active components needed in order to obtain a basic section of each one of the circuital network proposed presented in the second chapter. As we have seen this approach results in a very large circuital complexity, moreover it doesn't take care of the modality of interaction of each component with the other ones. This means that the connection of two stable active components can result in an unstable network. In this subsection we propose some novel synthesis devoted to the implementation of a whole basic section considered as a multiports system. As it will be clear in the following of this subsection, this strategy will strongly

reduce the number of active components needed of each module, moreover this remarkable simplification allows us to perform an analytical study of the stability of the system when the active components are modelled including some not ideal features like the finite gain and the finite bandwidth.

Tension Normalized fourth order line

A first solution devoted to the implementation of a basic section of a fourth order line has been proposed in [Panella et al.(2005-1)], in this work a one node to one port network associated with a fourth order line is proposed as the chain connection of a large number of basic section as shown in fig. (6-11).

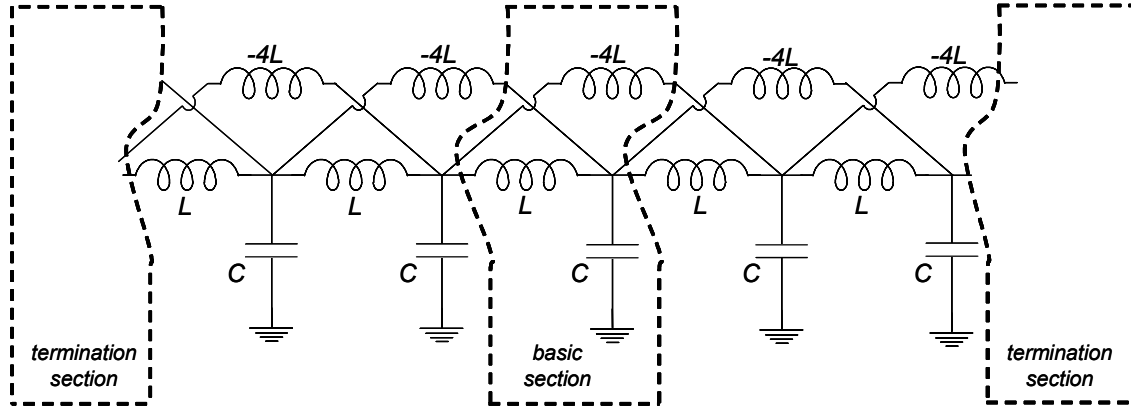


Figure 6-11: A fourth order line as the chain connection of a large number of basic sections.

Focusing our attention on a single module show in fig. (6-12), we can write some relations among the quantities describing this system as follows:

$$\begin{aligned}
 V_i &= (I_{i-1}^C + I_i^B - I_{i+1}^C + I_{i+1}^B) Z_A \\
 I_i^B &= (V_{i-1} - V_i) Y_B \\
 I_i^C &= (V_{i-1} - V_{i+1}) Y_C
 \end{aligned} \tag{6.6}$$

where

$$Z_a = \frac{1}{sC}, Y_B = \frac{1}{sL}, Y_C = -\frac{1}{s4L}$$

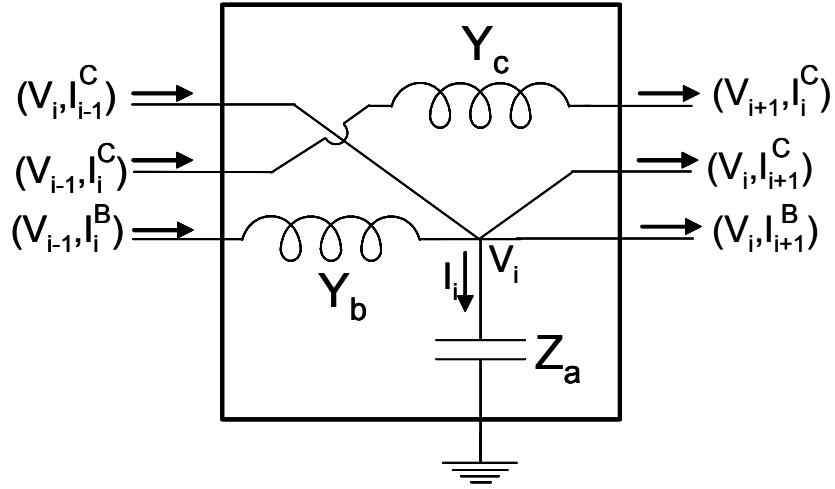


Figure 6-12: Basic section of a fourth order line.

The basic idea of this kind of synthesis is to normalize the current involved in this basic section with respect of the impedance Y_B introducing three new tension lines taking in count for the currents. We put a bar over this virtual tension in order to distinguish them from the real ones. Performing the described normalization eq. (6.6) become:

$$\begin{aligned}
 V_i &= (\bar{V}_{i-1}^C + \bar{V}_i^B - \bar{V}_{i+1}^C + \bar{V}_{i+1}^B)T_A \\
 \bar{V}_i^B &= (V_{i-1} - V_i)T_B \\
 \bar{V}_i^C &= (V_{i-1} - V_{i+1})T_C
 \end{aligned} \tag{6.7}$$

where

$$T_A = \frac{1}{s^2CL}, T_B = 1, T_C = -\frac{1}{4} \tag{6.8}$$

Eq. (6.7) can be interpreted as the relations between blocks having transfer function T_A , T_B and T_C . A blocks diagram able to implement eq. (6.7)

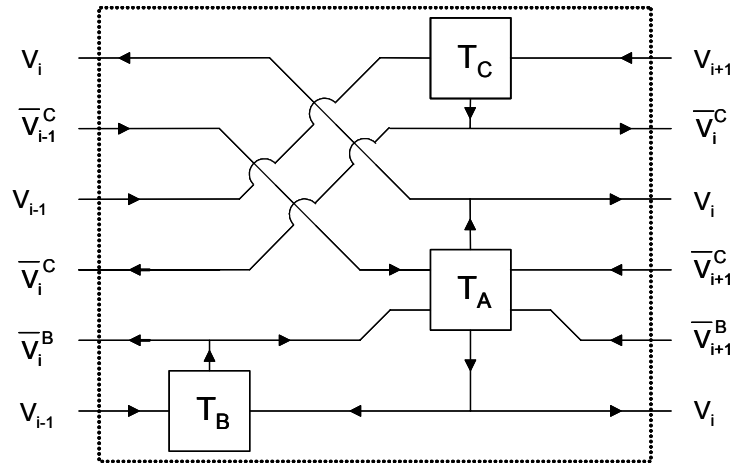


Figure 6-13: Blocks diagram for a tension normalized fourth order line.

It should be noted that in such a circuit a true line characterized by means of the pair (V, I) is splitted in two lines one bringing the real tension signal and the other one bringing a virtual tension proportional to the current. The next step is to show a physical implementation of the transfer functions T_A , T_B and T_C . T_B and T_C are simple gain transfer functions and can be implemented by means of a classical scheme shown in fig. (6-14).

The implementation of T_A is shown in fig. (6-15).

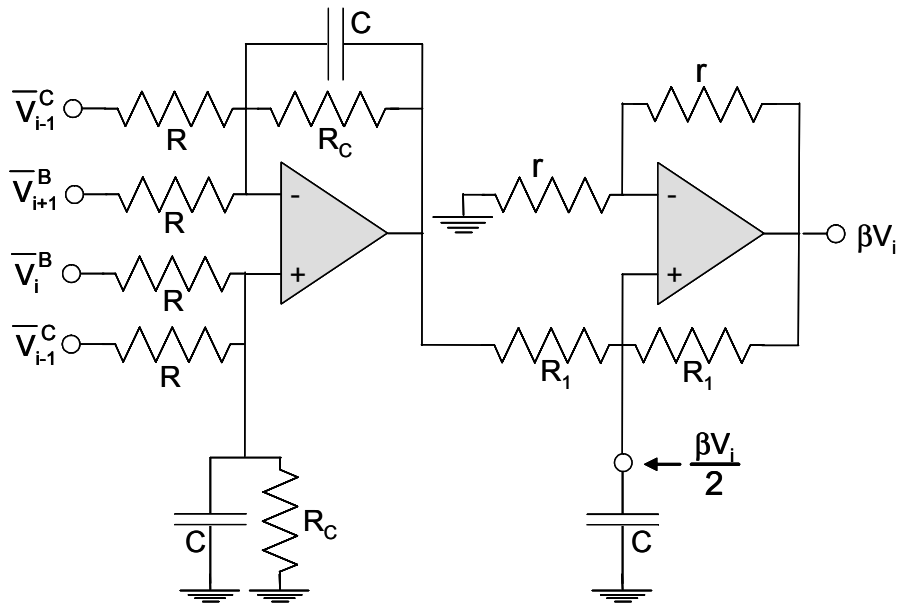


Figure 6-15: Implementation of the transfer function T_A .

A comparison between the performance of the described synthesis with respect to the theoretical network are given in [Panella et al.(2005-1)].

Optimized RC-active synthesis I

An ulterior improvement to the synthesis of the network under exam can be obtained by making a different choice for the coefficients $\alpha_2, \beta_2, \alpha_1$ and β_1 of the basic section shown in fig. (2-17). As we explain in the second chapter we need to fulfill the following relation $\alpha_2 - \beta_2 - \alpha_1 + \beta_1 = 2$. The choice we did in the previous chapter was $\alpha_2 = 1, \beta_2 = 0, \alpha_1 = 0$ and $\beta_1 = 1$. Here we show how a different choice of those parameters can make the RC-active synthesis much more simple. In fact by choosing $\alpha_2 = 2, \beta_2 = 0, \alpha_1 = 0$ and $\beta_1 = 0$ all the (α_1, β_1) elements become $(0, 0)$ elements i.e. resistor of positive and negative value. It is quite simple to understand that the positive resistors don't require any active synthesis while the negative one require the use of a NIC. On the other side the (α_2, β_2) elements become super capacitor and can be implemented by the chain connection of an integrator having a transfer function $T = 1/s$ and a normal capacitor. An optimized solution can be obtained by splitting the transfer function T in the following way:

$$T = T_1 T_2 = \left(-\frac{1}{s}\right)(-1) = \frac{1}{s}$$

This trick allows us to access to a negative copy of the "integrated node" so that connecting positive resistors to it they will appear as negative ones. a schematic implementation of this technique for a fourth order system is shown in fig. (6-16).

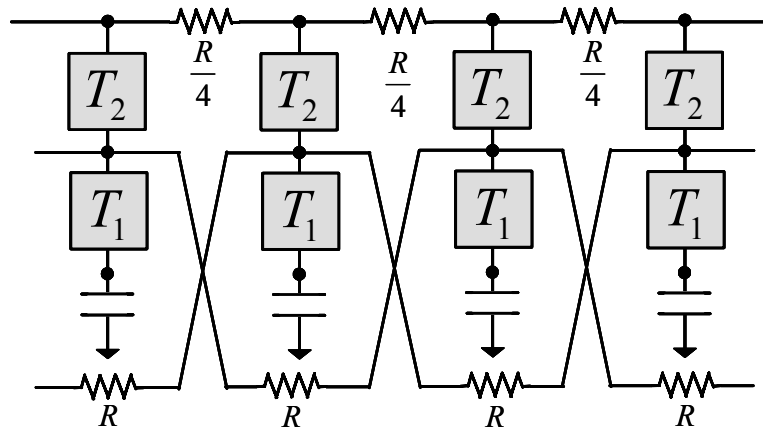


Figure 6-16: Optimized RC-active synthesis of a fourth order line.

It should be noted that in this kind of synthesis the number of required active components is constant and does not depend on the order of the system. The last thing we need to mention before to close this section is to give an implementation of the transfer function T_1 and T_2 . T_1 is a NIC and it can be implemented by using the one OPA scheme shown in fig (6-9) T_2 can be obtained by the same scheme by interchanging the resistor closer to the first port with a capacitor. The circuit obtained in this way derives the current instead of integrating the voltage, but from a practical point of view those two operations are equivalent. Concluding we can say that the Optimized RC-active synthesis (ORCSI) require the use of two OPAs for each module, moreover a single capacitor is used to realize all the positive and the negative inductor so that it is possible to realize proportional value of inductance by using proportional resistors. The consideration expressed in this section are collected in [Panella et al. (2005-2)].

Optimized RC-active synthesis II

The ORCSI synthesis proposed in the previous section produces the needed ideal network when the OPAs are considered ideal, but what happens when we include in the model some not ideal feature? In [Paschero et al. (2006)] the stability of the ORCSI circuit was investigated considering for the gain of the OPAs a dominant pole model. More precisely we assume the gain of each OPA to assume the following form:

$$A(s) = \frac{A_0}{(1 + \tau s)}$$

where

$$\tau = \frac{1}{2\pi f_c}$$

The stability of the system is investigated by plotting the roots locus for a fixed value of the parameter f_c and using A_0 as varying parameter. The root locus that the ORCS I produces for a wide range of variation of the parameter f_c (0 Hz to 3000 Hz)² is shown in fig. (6-17).

²For $f_c > 3000$ Hz the system can be made stable.

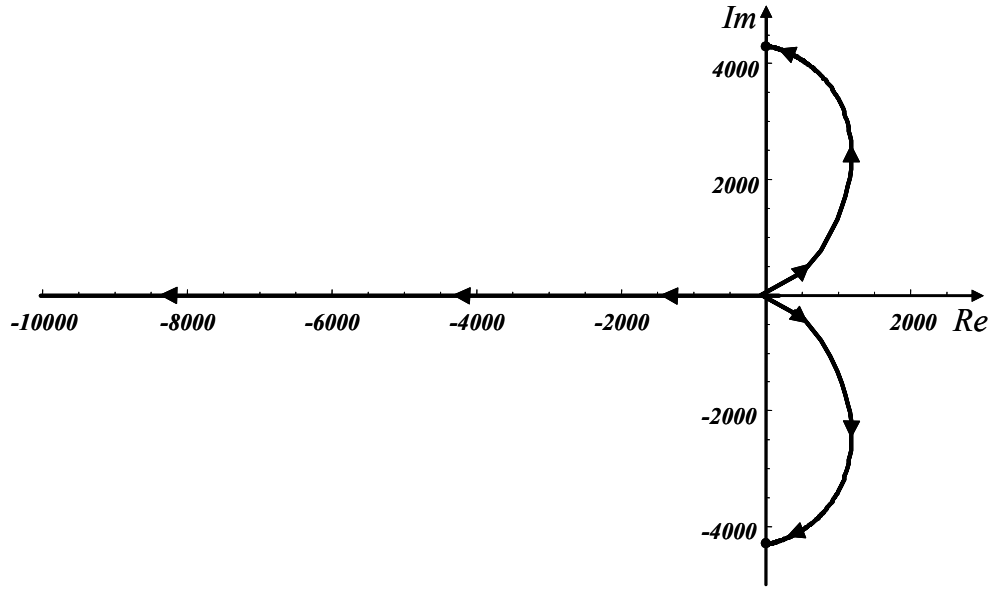


Figure 6-17: Root locus for the ORCSI synthesis.

Looking at the figure it is possible to note that the poles of the system converge to the expected value on the imaginary axis from values having positive real part. This means that the system must be considered unstable for finite values of the gain A_0 . The system can be made stable by increasing the bandwidth over some kHz by the way the real components commercially available do not have a so good bandwidth making this system not usable in the practice. This problem can be solved in two different ways. The first one has been proposed in [Paschero et al. (2006)] and it is based on a different circuitual scheme of comparable complexity. This new scheme is shown if fig. (6-18).

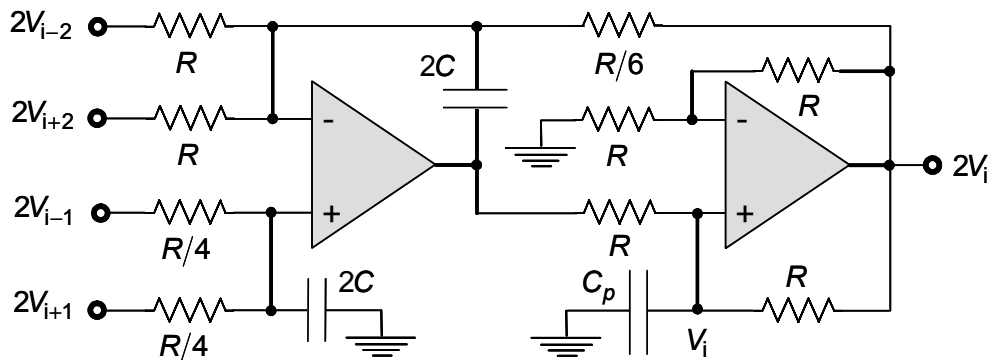


Figure 6-18: Circuitual scheme for the ORCSII synthesis.

Performing a stability analysis of this new scheme we obtain the root locus shown in fig. 6-19.

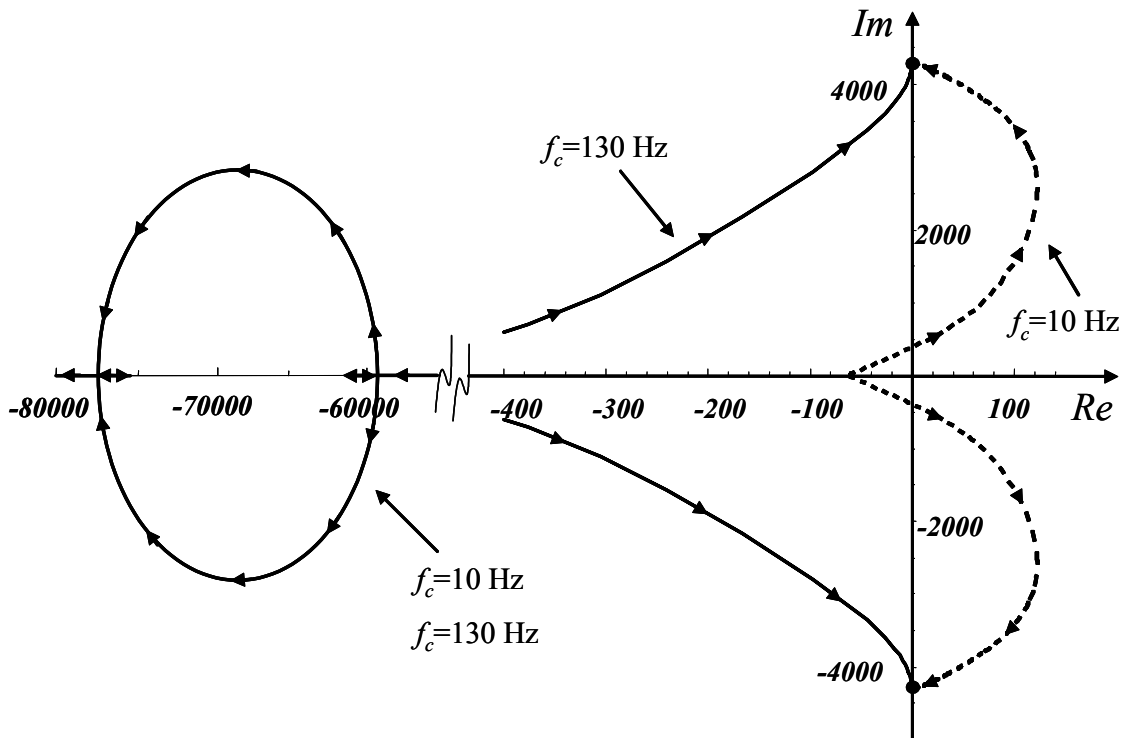


Figure 6-19: Root locus for the ORCSII synthesis.

Looking at the picture it is clear that the poles of the system converge to the ideal value for values having negative real part when the cut frequency f_c is greater than 130 Hz³. This means that the this system can be considered stable when the ideal component are replaced with the real ones. A useful inspiration for finding a different solution to the stability problem of ORCSI synthesis can be found in [Senani (1989)]. The basic ideal is to replace each OPA with the pair nullator norator and to apply some circuitual transformation involving those bipolar elements. A nullators norators model of ORCSI is shown in fig. 6-20.

³This value has to be considered indicative. In fact it depend on the coiche of the componets and the frequency of the poles we need to obtain. By the way the fact that under similar condition the ORCSII synthesis can be made stable for smaller values of f_c with respect ot the ORCSI solution can be considered a general result.

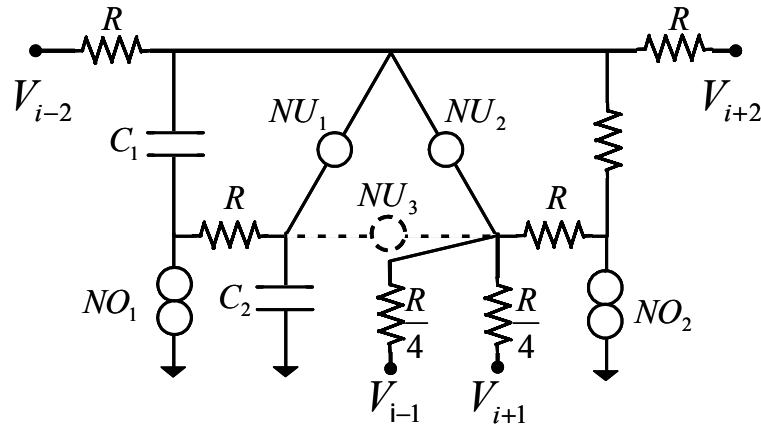
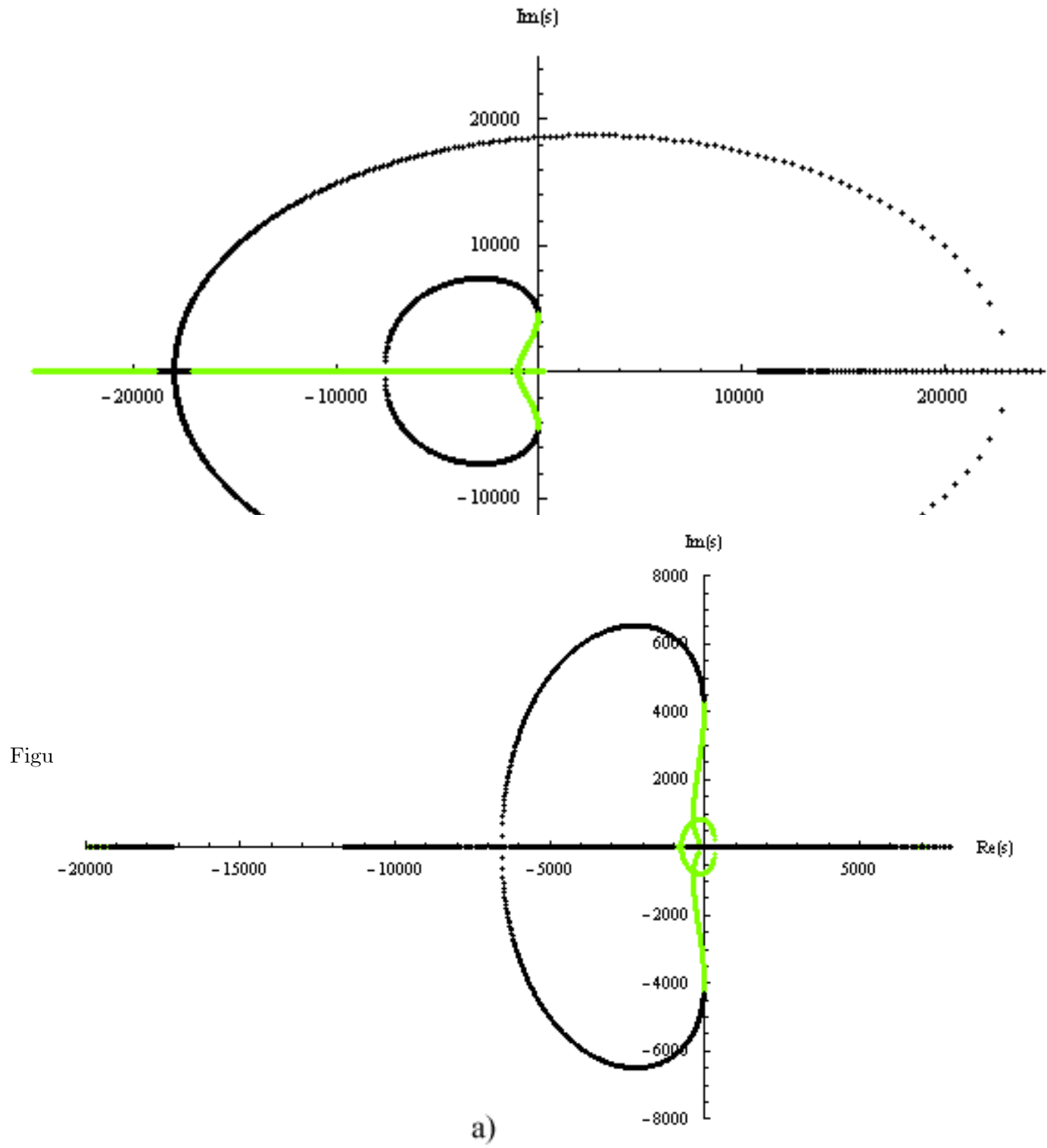


Figure 6-20: Nullators and Norators model of ORCSI.

Looking at the figure it is clear that a third nullator labeled with NU_3 can be connected in the circuit without producing any side effects. Now we can come back to OPAs by pairing each norator with a nullator and removing the redundant nullator. It is quite easy to realize that we can produce six different configurations, moreover if we consider real OPAs we can make a distinction between the inverting and the not inverting terminals. Having two OPAs we have four different ways to choose the sign. This additional degree of freedom let the possible configurations rise to twentyfour. Performing the stability analysis trough the examination of the root locus we can realize if there exist a configuration performing better than the original version of ORCSI. In the table (6-1) we list the six fundamental configurations.

	OPA1		OPA2	
Configuration 1	NO1	NU1	NO2	NU2
Configuration 2	NO2	NU1	NO1	NU2
Configuration 3	NO1	NU1	NO2	NU3
Configuration 4	NO2	NU1	NO1	NU3
Configuration 5	NO1	NU2	NO2	NU3
Configuration 6	NU2	NO2	NO1	NU3

Table 6-1



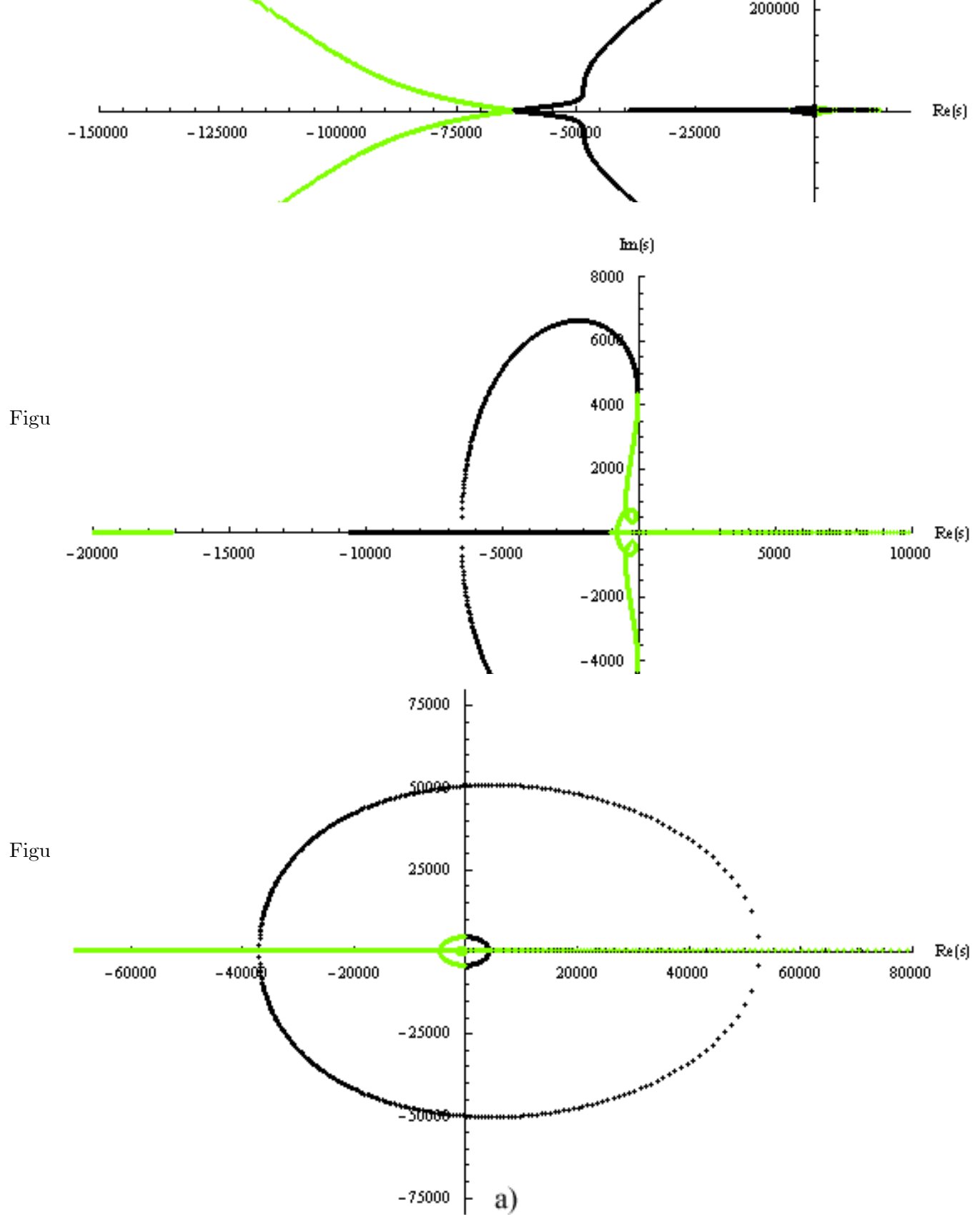


Figure 6-25: ORCSI root locus configuration 5. a) ++ in green (light gray) and -- in black.
 b) +- in green (light gray) and -+ in black.

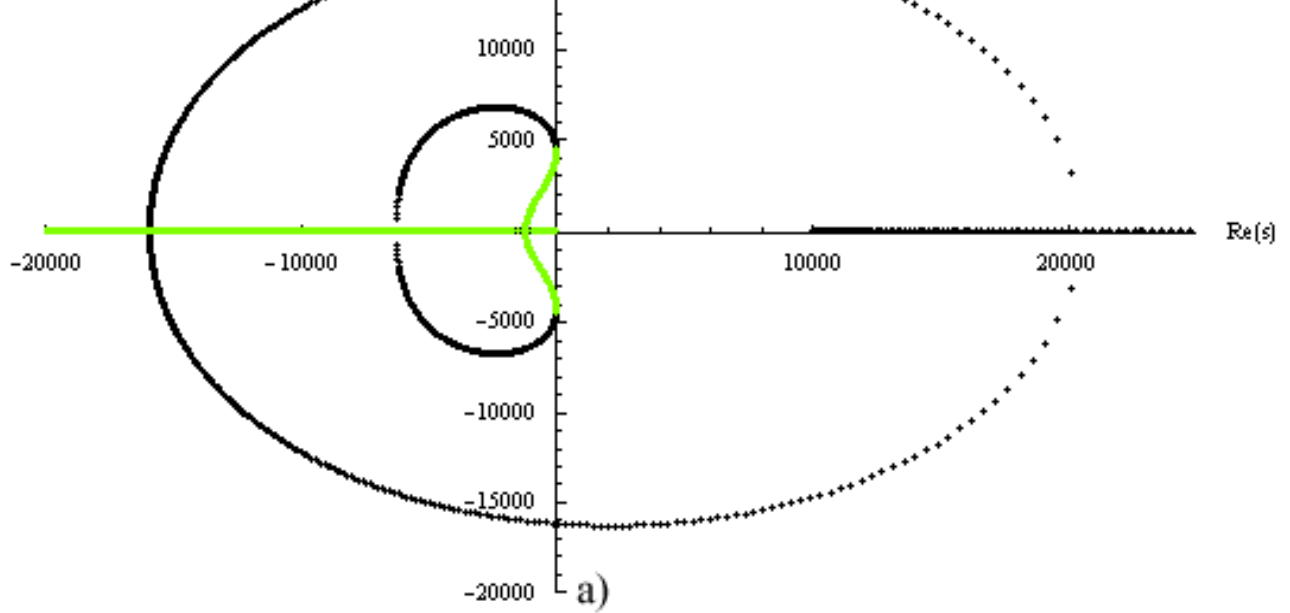


Figure 6-26: ORCSI root locus configuration6. a) ++ in green (ligh gray) and -- in black.
 b) +- in green (ligh gray) and -+ in black.

A visual inspection of those root loci can give us some qualitative information on the behavior of the totality of the possible configurations. It is found that the configuration 1 can be made stable by choosing the ++ subconfiguration while it is unstable for all the other subconfigurations. The configuration 2 can be made stable by choosing the -+ subconfiguration while it is unstable for all the other subconfigurations. The configuration 3 is unstable for all the possible subconfigurations. The configuration 4 can be made stable by choosing the -+ subconfiguration while it is unstable for all the other subconfigurations. The configuration 4 can be made stable by choosing the +- subconfiguration while it is unstable for all the other subconfigurations. Finally the configuration 6 can be made stable by choosing the ++ subconfiguration while it is unstable for all the other subconfigurations. Those argumentations make clear that there exist only four configurations among the twentyfour ones that can be made stable depending on the position of the cut frequency of the OPAs gain. A quantitative measure, even if indicative, of the critical bandwidth can be numerically evaluated. Using for the component the same values we choose before we can obtain results comparable with the previous ones. Those results are

listed in table (6-2).

	++	+-	-+	--
Configuration 1	$f_c > 3000$	X	X	X
Configuration 2	X	X	$f_c > 150$	X
Configuration 3	X	X	X	X
Configuration 4	X	X	$f_c > 165$	X
Configuration 5	X	$f_c > 0$	X	X
Configuration 6	$f_c > 2360$	X	X	X

Table 6-2

Looking at table (6-2) it can be noted that among the five stable configurations the fifth one is independent from the cut frequency and must be considered the most interesting one. Two of them are comparable with the ORCSII synthesis and can be considered still valuable while the remaining two are not usable in the practice.

Chapter 7

Concluding remarks

7.1 Conclusions

In this work we have shown how it is possible to obtain a circuit analogue of a differential operator able to describe a large number of physical phenomena. We describe two different synthesis techniques. The problem of deriving a suitable network able to realize the most general boundary condition has been studied and completely solved for both the described synthesis. One of this technique has to be considered general and can be applied in order to find a circuit analogue to a different differential operator. The notion of circuit is extended to a very general contest. This means that the same circuit can assume a different physical meaning once the general quantity defining each port are specified.

In this work the transducers are modeled as hybrid two ports networks, where the word hybrid is used to put in evidence that the two ports are in general characterized by quantities having different physical unit. Some simple physical device has been described using this approach.

A circuital model of a multidimensional coupled system is given and is used in order to show some possible example.

In the last part of the work it is given an overview on the classical synthesis technique and are been proposed some new RC active circuit including a reduced number of active components.

7.2 Recommendations for future works

The circuital approach used in this work brings to a pure algebrical formulation. This description is very suitable in order to realize a digital elaboration on this kind of system. This elaboration can be devoted to a large number of application, among them we can highlight the vibration damping from whom this work take the inspiration. Another problems of great interest are the harvesting the damage detection, the insonorization ecc. This work doesn't not look into those application but can be fruitfully used in order to explore those and a lot of other problems.

Bibliography

- [Alessandroni et al. (2002)] S. Alessandroni, F. dell' Isola and M. Porfiri, "A revival of electric analogs for vibrating mechanical systems aimed to their efficient control by PZT actuators", *International Journal of Solids and Structures*, vol. 39, 5295–5324, 2002.
- [Andreus et al. (2004)] U. Andreus, F. dell' Isola and M. Porfiri, "Piezoelectric Passive Distributed Controllers for Beam Flexural Vibrations", *Journal of Vibration and Control*, vol. 10 625-659, 2004.
- [Antoniou (1965)] A. Antoniou, "Negative impedance convertors using operational amplifiers", *IEE Electronics Letters*, vol. 1, June 1965.
- [Antoniou (1967)] A. Antoniou, "Gyrators Using Operational Amplifiers", *IEE Electronics Letters*, vol. 3 n. 8, Aug 1967.
- [Antoniou (1968-1)] A. Antoniou, "3-Terminal Gyrator Circuits Using Operational Amplifiers", *IEE Electronics Letters*, vol. 4 n. 26, Dec. 1968.
- [Antoniou (1968-2)] A. Antoniou, "New Gyrator Circuits Obtained by Using Nullors" *IEE Electronics Letters*, vol. 4 n. 5, Mar 1968.
- [Antoniou (1972)] A. Antoniou, "Floating Negative-Impedance Converters", *IEEE Transactions on Circuit Theory*, 209-212, Mar. 1972.
- [Bendik (1967)] J. Bendik, "Equivalent Gyrator Networks with Nullators and Norators", *IEEE Transactions on Circuit Theory*, 88, Mar. 1967.

- [Chua (2003)] L. O. Chua, "Nonlinear Circuit Foundations for Nanodevices, Part I: The Four-Element Torus", Proceedings of the IEEE-Invited paper, vol. 91, n. 11, 1830-1859, Nov. 2003.
- [Cox et al (1971)] N. W. Cox, K. L. Su and Woodward, "A Floating Three-Terminal Nullor and the Universal Impedance Converter", IEEE Transactions on Circuit Theory (Correspondence), 399-400, May 1971.
- [Crawley et al. (1987)] E. F. Crawley and J. de Luis, "Use of Piezoelectric actuators as Elements of Intelligent Structures", AIAA J. vol. 25, num. 10, 1373-1385, 1987.
- [G.J. Deboo (1967)] G.J. Deboo, "Application of a Gyrator-Type Circuit to Realize Ungrounded Inductors", IEEE Transaction on Circuit Theory (Correspondence), 101-102, Mar.
- [dell'Isola et al. (1998-1)] F. dell'Isola, S. Vidoli, "Continuum modelling of piezoelectromechanical truss beams: an application to vibration damping", Archive of Applied Mechanics, vol. 68, 1-19, 1998.
- [dell'Isola et al. (1998-2)] F. dell'Isola and S. Vidoli, "Damping of bending waves in truss beams by electrical transmission lines with PZT actuators", Archive of Applied Mechanics, vol. 68, 626-636, 1998.
- [dell'Isola et al. (2003)] F. dell'Isola, E. G. Henneke and M. Porfiri, "Piezoelectromechanical structures: a survey of basic concepts and methodologies", Proceedings of SPIE Smart Structures and Materials, Smart structures and Integrated Systems, vol.5052, 392-402, San Diego, USA, 2003.
- [dell'Isola et al. (2004)] F. dell'Isola, C. Maurini and M. Porfiri, "Passive damping of beam vibrations through distributed electric networks and piezoelectric transducers: prototype design and experimental validation", Smart Materials and Structures. vol. 13, 299-308, 2004.

- [Erwing (1985)] G. M. Erwin, "Calculus of Variations with applications", Dover, 1985.
- [Escher (2001)] M. C. Escher "The Graphic Work", Taschen 2001.
- [IEEE (1987)] IEEE std. 176-1987, IEEE Standard on Piezoelectricity, The institute of Electrical and Electronic Engineers.
- [Hagood et al. (1991)] N.W Hagood and, A.H von Flotow, "Damping of structural vibrations with piezoelectric materials and passive electrical networks",. Journal of Sound and Vibrations,. vol. 146, n.2, 243-368,.1991.
- [Hanagud et al. (1992)] S. Hanagud, M.W. Obal and A.J.Calise , "Optimal Vibration Control by the use of Piezoceramic Sensors and Actuators", Journal of. Guid. Control Dynamics,.vol. 15, n. 5, 1199-1206,.1992.
- [Kumar et al. 2002] Kumar P. and Senani R., "Bibliography on Nullors and Their Applications in Circuit Analysis, Synthesis and Design", Analog Integrated Circuits and Signal Processing, 33, 65–76, Nov. 2002.
- [Lesiutre (1998)] G. A. Leisutre, "Vibration Damping and Control Using shunted piezoelectric materials, The Shock and Vibrations Digest, vol. 30, n. 3, 187-195, 1998."
- [Marshall (1994)] W. Marshall Leach, "Controlled-Source Analogous Circuits and SPICE Models for Piezoelectric Transducers", IEEE Transactions on Ultrasonics, Ferroelectrics, and Frequency Control, vol. 41, n. 1, Jan. 1994.
- [Meirovitch (2000)] L. Meirovitch, "Fundamental of vibrations", McGraw-Hill, Boston, 2000.
- [Mussman et al. (1972)] H. E. Mussman and S. L. Hakimi, "A Scattering Matrix Synthesis Technique for Transformers, Circulator and Gytrators"

- IEEE transaction on Circuit Theory-Correspondance, 382-383, Jul. 1972.
- [Niezrecki et al. (2001)] C. Niezrecki, D. Brei, S. Balakrishnan and A. Moskalik, "Piezo-electric Actuation: State of the Art", The Shock and Vibration Digest, vol. 33, n. 4, 269-280, Jul. 2001.
- [Orchard et al. (1974)] H. J. Orchard and A. N. Willson Jun., "New Active-Gyrator Circuit" IEE Electronics Letters, vol. 10 n. 13, Mar 1974.
- [Panella et al.(2005-1)] M. Panella, M. Paschero and F. M. Frattale Mascioli, "A Modular RC-Active Network for Vibration Damping in Piezo-Electro-Mechanical Beams", Proc. of IEEE International Symposium on Circuits and Systems (ISCAS 2005), 5393-5396, Kobe, Japan, May 2005.
- [Panella et al. (2005-2)] M. Panella, M. Paschero and F.M. Frattale Mascioli, "Optimised RC-active Synthesis of PEM Networks", IEE Electronics Letters, vol. 41, issue 19,1041 – 1043, Sep. 2005.
- [Panella et al. (2006)] M. Panella, M. Paschero and F.M. Frattale Mascioli, "Symbolic Analysis and Optimization of Piezo-Electromechanical Systems", Proc. of IEEE International Symposium on Circuits and Systems (ISCAS 2006), pp.633-636, Kos, Greece, May 2006.
- [Paschero et al. (2006)] M.Paschero, M.Panella, and F.M. Frattale Mascioli, "Stability analysis of optimal PEM networks", IEE Electronics Letters, vol. 42, issue 17,.961-962, Aug 2006.
- [Patranabis et al. (1979)] D. Panatrabis, M.P. Tripathi and S.B. Roy, "A New Approach for Lossless Floating Inductor Realization" IEEE Transaction on Circuit and Systems, vol. cas-26,.n.10, Oct. 1979.
- [Porfiri et al. (2004)] M. Porfiri, F. dell'Isola and F. M. Frattale Mascioli, "Circuit analog of a beam and its application to multimodal vibration

- damping, using piezoelectric transducers", *International Journal of Circuit Theory and Applications*. vol. 32, 167–198, 2004.
- [Porfiri et al. (2005)] M. Porfiri, F. dell' Isola and E. Santini, Modelling and design of passive electric networks interconnecting piezoelectric transducers for distributed vibration control, *International Journal of Applied Electromagnetics and Mechanics* vol. 21, n. 2, 69-87, 2005.
- [Premoli et al. (2004)] A. Premoli and M. Stora, "Two-Port Ideal Transferors: A Unified Introduction to ideal transformer and Gyrator", *IEEE Transactions on circuits and Systems- II: Express Briefs*, vol. 51, n.8, Aug. 2004.
- [Reddy (1975)] M.A. Reddy, "Some New Operational-Amplifier Circuits for the Realization of the Floating Inductance", *IEEE Transaction on Circuits and Systems-Letters to the Editor*, Mar. 1976.
- [Riordan (1967)] R. H. S Riordan, "Simulated inductors using differential amplifiers", *IEE Electronics Letters*, vol. 3 n. 2, Feb 1967.
- [Schattschneider et al. (1990)] D. Schattschneider and W. Walker, "M. C. Escher Kaleidocicli", Taschen 1990.
- [Senani et al. (1978)] R. Senani and R. N. Tiwari, "New Canonic Active RC Realizations of Grounded and Floating Inductors" *Proc. of IEEE Proceedings Letters*, 803-804, Jul. 1978.
- [Senani (1978)] R. Senani, "Realization of single-Resistance-Controlled Lossless Floating Inductance" *IEE Electronics Letters*, vol. 14 n. 25, Dec. 1978.
- [Senani (1987)] R. Senani, "Generation of new Two-Amplifiers synthetic Floating Inductors" *IEE Electronics Letters*, vol. ?? n. ??, Jul. 1987.

- [Senani (1988)] R. Senani, "Floating immittance Realization: A nular Approach", IEE Electronics Letters, vol. 24 n. 7, Mar 1988.
- [Senani (1989)] R. Senani, "Three Op Amp Floating Immitance Simulators: A Retrospection", IEEE Transaction on Circuit and Systems, vol. 36,.n.11, Nov. 1989.
- [Soundararajan et al. (1975)] K. Soundararajan and K. Ramakrishna, "Nonideal Negative Resistors and Capacitors Using an Operational Amplifier", IEEE Transactions on Circuit and Systems (Letters to the Editor), Set. 1975.
- [Tellegen (1948)] B. D. H. Tellegen, "The Gyrator a New Ectric Network Element", Philips Research Reports, vol.3, 81-101, Apr 1948.
- [Vidoli et al.(2000)] S. Vidoli and F. dell'Isola, "Modal coupling in one-dimensional electro-electromechanical structured continua", Acta Mechanica, vol.141, 37-50, 2000.
- [Yanagisawa et al. (1976)] T. Yanagisawa and G. BhattaCharjee, "Realizzation of a Generalized Active Transformer" IEE Electronics Letters, vol. 12 n. 12, Jun. 1976.